Structural Basis for Rap1-Rif1-Rif2 Assembly:

Insights into Budding Yeast

Telomere Architecture and Functions

Inauguraldissertation

Zur

Erlangung der Würde eines Doktors der Philosophie

Vorgelegt der

Philosophisch-Naturwissenschaftlichen Fakultät

der Universität Basel

von

Tianlai Shi

Aus Shanghai, China

Basel 2012

Genehmigt von der Philosophisch-Naturwissenschaftlichen Falkultät

auf Antrag von

Prof. Dr. Susan M. Gasser

Prof. Dr. Joachim Lingner

Dr. Nicolas H. Thomä

Basel, den 16. 10.2012

Prof. Dr. Jörg Schibler

Dekan

Table of contents

Acknowledgements

First of all, I owe my gratitude to my PhD supervisor Dr. Nicolas Thomä for providing me the opportunity to work on this fascinating project and encouraging me to perform my PhD in crystallography. His help and advice allowed me to develop as a young scientist.

I would also like to acknowlege the members of my PhD thesis committee, Professor Dr. Susan Gasser and Professor Dr. Joachim Lingner for their advice and time for thesis committee meetings. Susan, thank you for all the suggestions in your mini group meetings!

I am very grateful to our former lab member Dr. Andrea Scrima for spending enormous time to teach me how to solve structures step by step. In addition, I also want to thank Andrea for all the great encouragement at times when the project did not seem so promising. Also Mahamadou Faty, thank you for many protein purifications in my PhD project.

Dr. Ulrich Rass, thank you very much for performing radioactive experiments and teaching me the skills of doing those experiments. I apprecied that Uli always took extensive time to disccuss experimental results with me, and offered great help in the process of the manuscript.

I want to give a big thank to Cyril Ribeyre, David Shore and Stefano Mattarocci for great collaboration and exchange of scientific ideas.

Kenji Shimada, Monika Tsai and Stephanie Kueng, thank you for providing helpful advice and teaching me all the yeast techniques.

I also would like to thank Dr. Heinz Gut from the Protein Structure Facility, Dominique Klein and Dr. Daniel Hess from the Protein Analysis Facility. Heinz supported me with scientific advice in crystallography and drove me to many SLS trips. Dominique and Daniel were always helpful and friendly in the mass spectrometry service.

Luis Moreton Achsel and Kerstin Böhm, thank you for correcting my PhD thesis.

Finally, I am deeply indebted to my family and the guest family Moreton from Germany for all kinds of help and support during my entire education.

Summary

Telomeres form the ends of eukaryotic linear chromosomes and are composed of specialized nucleoprotein complexes. They have been the subject of intense investigation over several decades, as telomere dysfunction has been associated with genome instability and the development of cancer. Yeast (*Saccharomyces cerevisiae*) telomeric DNA is comprised of irregular TG_{1-3} repeats, bound in a sequence-specific manner by multiple copies of Rap1, forming Rap1 arrays. Together with its telomere binding proteins Rif1 and Rif2, arrays of Rap1, Rif1 and Rif2 form a protective proteinaceous cap that regulates telomere length, modulates Sir-mediated transcriptional silencing, and prevents unwanted DNA-repair events. As a general transcription regulator in budding yeast, about 90% of cellular Rap1 is found in promoters or silencers, whereas Rif1 and Rif2 can only be detected at telomeres.

The following questions remain unresolved for the major telomere capping proteins Rap1, Rif1, and Rif2. What determines the exclusive telomeric localization of Rif1 and Rif2, and their absence elsewhere in the genome, given that the association of Rif1 and Rif2 at telomeres is solely dependent on the Rap1 C-terminal domain ($Rap1_{RCT}$)? What is the molecular basis behind the competition between Rif and Sir proteins at telomeres? How do the telomere-associated proteins Rap1, Rif1, and Rif2 influence telomerase activities? And, of central importance to genome stability, what are the roles of Rif1 and Rif2 in damping DNA repair at telomeres?

To address these questions, I determined the structures of Rif2, Rif2-$Rap1_{RCT}$, Rif1-$Rap1_{RCT}$, and the outermost Rif1 C-terminal domain, $Rif1_{CTD}$, using x-ray crystallography. Structural studies, combined with *in vitro* reconstitution and cellular assays, demonstrated that Rif1 and Rif2 are the long-sought elements that interlink Rap1 units cooperatively. The long- and short-range protein interactions from Rif1 and Rif2, the multimerization module present in $Rif1_{CTD}$, and the *trans* interaction between Rap1 and Rif2 provide a network of Rap1-Rif1-Rif2 complexes. This protein network allows the formation of higher-order structures at telomeres. The organizing principle that controls Rap1-Rif1-Rif2 assembly relies on the presence of arrays of Rap1-binding sites, which are exclusively found in telomeric regions. This explains why Rif1 and Rif2 are restricted to telomeric regions, and are not localized to the other ~300 single/double Rap1-binding sites at promoters or silencers within the *S. cerevisiae* genome.

In addition, I was able to provide the molecular basis for Rif1- and Rif2-modulated silencing at telomeres and *HMR*. Structural studies, combined with *in vivo* analysis, allowed me to identify the interaction domains within Rif1 (Rif1$_{RBM}$) and Rif2 (Rif2$_{RBM}$), which block the transcriptional repressor Sir3 from accessing the common binding cleft on Rap1. Thus, Rif1 and Rif2 directly compete with Sir3 for the RBM binding groove on Rap1. This protein-binding groove therefore enables Rap1 to integrate opposing cues coming from the Sir3 and Rif1/Rif2 RBMs into a composite silencing response. The partially redundant assembly of Rif1 and Rif2 on Rap1 also elucidates the reported synergistic function of Rif1 and Rif2 in modulating transcriptional silencing at telomeres and *HMR*.

In this study, I could demonstrate that the Rif2-mediated anti-checkpoint function is dependent on its telomeric localization through the protein interaction with Rap1. I further identified a novel function of Rif1 as a direct DNA-binding protein for protecting resected telomeres from being accidentally recognized as DNA double-strand breaks. Both *in vivo* and *in vitro* studies illustrate the remarkable ability of Rif1 to directly outcompete the yeast RPA complex from single-stranded DNA next to single-/double-stranded DNA junctions. The architecture of Rap1-Rif1-Rif2 assemblies favors Rif1 binding the resected telomeric DNA, once the telomere capping function is compromised. Notably, the structure-function studies of Rif1$_{CTD}$ and the Rif1 N-terminus (Rif1$_{NTD}$) provide strong evidence for applying the principle of inhibiting checkpoint activation from yeast to human.

The work presented here details how the yeast shelterin complex Rap1-Rif1-Rif2 directly influences transcriptional silencing, telomere length regulation, and telomere protection against inadvertent DNA-damage checkpoint activation.

Introduction

1 End-replication problem and discovery of telomeres and telomerase

In the 1930s, Hermann Muller first noted that the ends of the chromosomes had unique properties, and named these ends telomeres (from the Greek words *telo*, meaning "end", and *mere*, meaning "part") (Muller, 1938). In classic mutagenesis experiments with *Drosophila*, X-ray irradiation generates various chromosome aberations, many of which involve chromosome breakage and fusion cycles. At that time, he was surprised to discover that the ends of the chromosomes are strangely resistant to the chromosome fusion events. About 20 years later, Watson and Crick discovered the double helix structure of DNA (Watson and Crick, 1953), and in subsequent years (early 1970s) clarified the mechanism of semi-conservative DNA-replication. James Watson realized that the 3' end of a linear DNA could not be synthesized by the DNA polymerase (Watson, 1972). During the DNA replication process, DNA polymerases require a 3'-OH group as the site for *de novo* nucleotide addition, using short RNA molecules as primers to carry out re-synthesis in the 5' to 3' direction. Primers need to be subsequently removed and the resulting gaps are then filled by the DNA polymerase. Duplication of a circular template does not confer this challenge, as the 8-12 nt gaps left after removal of the primers from the lagging strand can be closed by extending a preceding Okazaki fragment (a short, newly synthesized DNA fragment on the lagging strand). However, the last primer from the lagging strand on a linear chromosome is terminal and its removal cannot be replaced by DNA. This causes a problem in semi-conservative replication when a linear DNA molecule has to be fully replicated. In this way, every round of DNA replication results in loss of sequence and subsequent shortening of chromosome ends. This dilemma is referred to as the "end-replication problem" (**Figure 1)** (Olovnikov, 1973; Watson, 1972).

Without any compensatory events, chromosomes loose terminal sequences at a rate of 3-5 bp/cell-cycle in fungi, flies and mosquitos (Levis et al., 1993; Lundblad and Szostak, 1989; Walter et al., 2001), and at faster rate about 50-150 bp/cycle in human and mouse (Harley et al., 1990; Niida et al., 1998). To overcome end-replication problems, linear chromosomes have evolved the special DNA region called "telomeres" at both ends. The presence of telomeres and their length homeostasis offers a solution to counteract chromosome attrition, ensuring long-term proliferation of all eukaryotic cells, including germline cells. In

1985, the discovery of a novel enzymatic activity in the extracts from *Tetrahymena*, a unicellular ciliate organism (Greider and Blackburn, 1987), led to the proposal of a enzymatic mechanism to overcome the end-replication problem. The subsequent works identified telomerase, a reverse transcriptase, utilizing its integral RNA subunit as a template for extending the 3' end of the G-rich telomere strand (Greider and Blackburn, 1989; Lingner et al., 1997b).
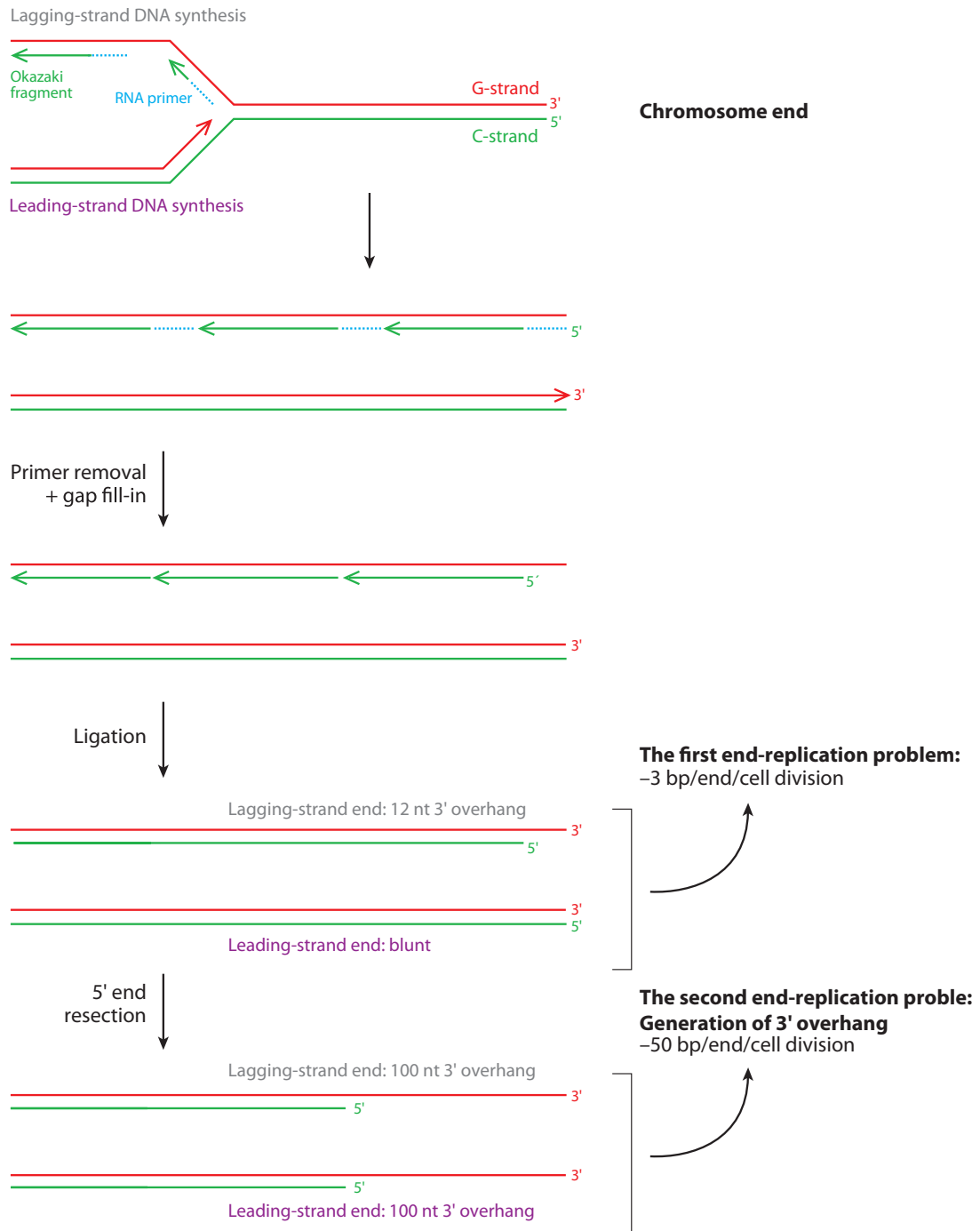
Figure 1. Illustration of the two "end-replication problems" on eukaryotic linear chromosomes. The loss of terminal sequence after each around of replication represents the first "end-replication problem". The challenge to generate the 3' overhang on the blunt-ended leading strand DNA after replication leads to the second "end-replication problem" (as discussed below). Adapted and modified from Palm and de Lange, 2008.

2 Sequence and organization of telomeres

Telomeres confer genome stability through protecting chromosome ends against cellular exonucleases and non-homologous end joining (NHEJ). As chromosome ends resemble one half of a DNA double-strand break (DSB), the presence of telomeres allows cells to distinguish natural DNA ends from normal DSBs. In nearly all eukaroytes, the terminal telomeric DNA comprises tandem repeats of a short sequence (2-50 kb TTAGGG repeats in metazoans, 300-350 bp $(TG)_{1-4}G_{2-3}$ repeats in *S. cerevisiae*) (reviewed in Wihelm and de Lange, 2008; Cohn et al., 1998; Wang and Zakian, 1990). The telomeric DNA is coated with its associated proteins called the "shelterin" complex in mammals (de Lange 2005), forming a protective nucleoprotein complex at chromosome ends. In budding yeast, the "shelterin" like complex can be devided into the Rap1-Rif1-Rif2 complex, the Ku70-Ku80 complex and the Cdc13-Stn1-Ten1 complex (**Figure 2**). The Rap1-Rif1-Rif2 complex provides the major telomere-binding proteins at double-stranded telomeres, maintaining telomeres in their correct length. In the following chapters, detailed disscusions will show our current knowledge about how Rap1, Rif1 and Rif2 associate at teomeres, and thereby (i) regulate telomere length, (ii) protect telomeres from all aspects of the DNA damage response, and (iii) modulate telomeric silencing.
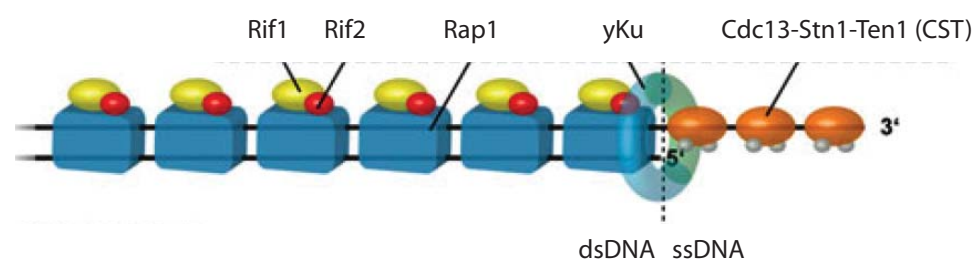
Figure 2. The "shelterin" complex in *S. cerevisiae*. The telomeric dsDNA is bound by the sequence-specific DNA-binding protein Rap1, which recruits its interaction partners Rif1 and Rif2. Cdc13 binds to the telomeric ssDNA and interacts with Stn1 and Ten1 to form the CST complex at the end of telomeres. The yKu complex, a component of the DNA damage repair, is localized at the transition between dsDNA and ssDNA, where it plays a protective role at telomeres. Adapted and modified from Dewar and Lydall, 2012.

2.1 Sub-telomeric region

Telomere regions can be divided into a sub-telomeric domain, a double-stranded terminal region and the distal 3' G-rich single-stranded tail. Like most organisms, yeast sub-telomeric regions contain repetitive TAS elements (<u>t</u>elomere <u>a</u>ssociated <u>s</u>equence). X and Y' are the two classes of TAS found in *S. cerevisiae*. Sub-telomeric regions can be classified into XY' and X-only. Depending on its size, the Y' element can be further subdivided into Y' long (6.7 kb) and Y' short (5.2 kb) (Chan and Tye, 1983). The X element is more heterogeneous in both sequence and size. X and Y' have recently been shown to contain binding sites for various transcription factors (Mak et al., 2009). Due to the sequence heterogeneity of sub-telomeric regions and the associated factors, individual telomeres exhibit distinctive behaviors.

Despite the heterochromatic state of telomeres, earlier reports indicate the presence of transcriptional activity at telomeres in many eukaryotes (Morcillo et al., 1988; Solovei et al., 1994). Recently, a new class of large non-coding RNA TERRA (<u>te</u>lomeric <u>r</u>epeat-containing <u>R</u>NA) has been identified oringinating from the sub-telomeric region (Azzalin et al., 2007; Luke et al., 2008; Schoeftner and Blasco, 2008). TERRA is transcribed by RNA polymerase II (Schoeftner and Blasco, 2008). The majority of TERRA transcriptions stems from the sub-telomeric region, with its 3' end transcribed from telomeric sequences. The size of TERRA ranges from 100 to 9000 nt in mammals (Azzain et al., 2007). *S. cerevisiae* TERRA has an average length of 380 nt (Luke et al., 2008). Several findings indicate that TERRA probably regulates telomere length by inhibiting telomerase activity, as mutation in the *rat1* gene (a 5'-3' exonuclease in budding yeast) increases TERRA levels, leading to short telomeres (Luke et al. 2008). Moreover, recent analysis suggests that TERRAs transcribed from X-telomeres are regulated by Rap1 and the Sir complex, whereas TERRAs originating from XY' telomeres are under the control of double-stranded telomere associated proteins Rap1 and Rif1/Rif2 (Iglesias et al., 2011). The discovery of TERRA and its functions at telomeres offer a new

dimension for telomerase regulation. Importantly, the wide spread evolutionary conservation of TERRA from yeasts to plants and mammals suggests a conserved function in telomere regulation.

2.2 Single-stranded telomere region

The actual terminus of eukaryotes is not blunt-ended, but rather consists of a 3' G-rich single-stranded overhang. The presence of this single-stranded portion provides a second "end replication problem" to the cells, as the leading strand DNA synthesis results in a blunt-ended DNA terminus (**Figure 1**). This problem is circumvented by the C-strand (5'-end) nucleolytic degradation (Wellinger et al., 1996). Degradation has two important biological impacts: firstly, it creates the potential substrate for telomerase, which cannot act on blunt-ended DNA molecules; secondly, it provides accommodation for the telomere-dedicated single-stranded binding protein Cdc13. The mammalian 3' G-strand varies between 50 and 500 nt (Makarov et al., 1997; McElligott and Wellinger, 1997), while the budding yeast 3' overhang is around 12-15 nt throughout most of the cell cycle (Larrivee et al., 2004). However, during telomere replication in late S and G2 phases, the G-tail in *S. cerevisiae* is temporarily extended up to 100 nt (Wellinger et al., 1993a).

Cdc13 is the major telomeric 3'-overhang binding protein
In vitro, Cdc13 tightly binds to telomeric ssDNA in a sequence-specific manner with excess of 11 nt (**Figure 2**) (Hughes et al., 2000; Lin and Zakian, 1996). *CDC13* was first identified as a cell division cycle mutant (Garvik et al., 1995). In parallel, it was also found as *EST4* (ever short telomeres gene 4, renamed later as *cdc13-2*) in an independent screen for genes, whose mutations result in short telomeres (Lendvay et al., 1996). The NMR structure of the Cdc13 DNA-binding domain (DBD) bound to a telomeric G-tail revealed that Cdc13 DBD has an OB-fold. Through hydrophobic interactions between aromatic protein residues of this DBD domain and nucleotide bases, Cdc13 binds to the telomeric 3'-overhang with high affinity and specificity (Mitton-Fry et al., 2002). Cdc13 has been shown to interact with Est1, a subunit of telomerase, *in vitro* (Wu and Zakian, 2011), implying a role of Cdc13 in recruiting telomerase in the process of telomere elongation. In addition, the telomere-lengthening defect of the *cdc13-2* mutant can be compensated by a specific mutation in the *EST1*, which further supports this model (Pennock et al., 2001).

10

Stn1 and Ten1, together with Cdc13 form a CST complex at the telomeric overhang

Besides Cdc13, two other essential proteins Stn1 and Ten1 also have the potential to associate directly with the telomeric G-tail. Stn1 and Ten1 serve as interacting partners of Cdc13 (Gao et al., 2007; Pennock et al., 2001). Together, the three proteins form a complex of Cdc13-Stn1-Ten1 that is generally referred to as the CST complex. Loss of Cdc13 function in a *cdc13-1* temperature sensitive strain results in C-strand degradation and subsequent cell cycle arrest due to DNA-damage response activation (Vodenicharov and Wellinger, 2006; Garvik et al., 1995). Mutations in either *STN1* or *TEN1* show similar phenotypes (Grandin et al., 1997; Grandin et al., 2001). The N-terminus of Stn1 interacts with Ten1, while its C-terminus binds to both Cdc13 and Pol12 (Grossi et al., 2004; Puglisi et al., 2008), a subunit of the DNA polymerase α primase complex. Interestingly, Cdc13 interacts with the catalytic subunit of the same complex (Qi and Zakian, 2000), indicating the connection between the CST function and the priming of the telomeric C-strand. It is therefore unclear whether a telomeric ssDNA excess present in the *CDC13* mutants is due to failure in preventing nuclease activities, or because it favors the interaction between Stn1 and Pol12, promoting polα-primase dependent C-strand synthesis.

2.3 Double-stranded telomere terminal region

The double-stranded telomere terminal region of *S. cerevisiae* chromosomes consists of about 300-350 bp of $(TG)_{1-4}G_{2-3}$-repeats that are coated with telomere-associate proteins Rap1, Rif1, Rif2 and the Ku complex (Cohn et al., 1998; Wang and Zakian, 1990). Unlike most of the eukaryotes including human, that contain a variable number of the TTAGGG-like repeats, the sequence of *S. cereivisae* telomeric repeats is heterogeneous in nature. This heterogeneity originates from the combinational effect of abortive reverse transcription events and redundant alignment possibilities between telomeres and the template RNA (Forstemann and Lingner, 2001). Sequencing of the same telomere driven from a given colony shows that the internal half has an identical sequence, while the distal portion of the telomere exhibits great sequence-diversity (Wang and Zakian 1990). This indicates that mostly the terminal region of the telomere is more susceptible to recombination, degradation or telomerase lengthening.

The Ku complex is located at the transition between double- and single-stranded telomeres

The yeast heterodimer Ku complex (yKu), composed of Ku70 and Ku80, is present at the double-stranded to single-stranded telomeric junctions (**Figure 2**) (Boulton and Jackson, 1996; Gravel et al., 1998). Ku is an evolutionary conserved complex, involved in NHEJ of DNA double-strand breaks (DSBs). Conserved from yeast to human, it associates at the DNA ends (DSBs or telomeric ends) in a sequence-unspecific manner (Walker et al., 2001). Although the association of yKu at telomeres, which are protected from NHEJ, is counterintuitive, it is critical for proper telomere functioning (Pfingsten et al., 2012). It has been suggested that yKu performs two functions at telomeres. One is to positively regulate telomere length by facilitating the recruitment of telomerase through its interaction with a conserved stem loop of the telomerase RNA TLC1 (Peterson et al., 2001; Stellwagen et al., 2003). The yKu-TLC1 interaction appears essential for the Est2 association at telomeres in G1 phase. The same interaction is also required for Est2 and Est1 telomere binding in late S phase (Fisher et al., 2004), indicating that yKu participates directly in telomerase recruitment for telomere lengthening. The other function of yKu is to prevent excessive resection of the C-strand, and thereby contributing to the telomere capping function (Gravel et al., 1998; Polotnianka et al., 1998). In accordance with these findings, *yKu* deletion mutants have short telomeres with long overhangs (Gravel et al., 1998). Despite intensive studies on yKu function, it still remains unclear how yKu associates at telomeres (Walker et al., 2001). Nevertheless, a "two-face" model is suggested, in which Ku70 provides the NHEJ-specific interface, whereas the Ku80 surface is required for the association with telomeric ends (Ribes-Zamora et al., 2007).

The multifunctional protein Rap1 binds directly to the telomeric DNA and recruits its interacting partners

In budding yeast, the double-stranded telomeric region contains arrays of high-affinity Rap1-binding sites (Repressor Activator Protein 1) with irregular spacing (Shore and Nasmyth, 1987). *RAP1* is an essential gene in *S. cerevisiae*, as it fulfills transcription regulation at promoters and gene silencing at silencers besides its essential role at telomeres. Rap1 is an abundant nuclear protein with only about 10% of Rap1 molecules located at telomeres. The remainder Rap1 targets 5% of the yeast genes as a promoter-binding protein, which accounts for 37% of total mRNA initiation events (Lieb et al., 2001). In contrast, at the silent-mating type loci *HML* and *HMR*, it acts as transcriptional repressor (Kurtz and Shore, 1991).
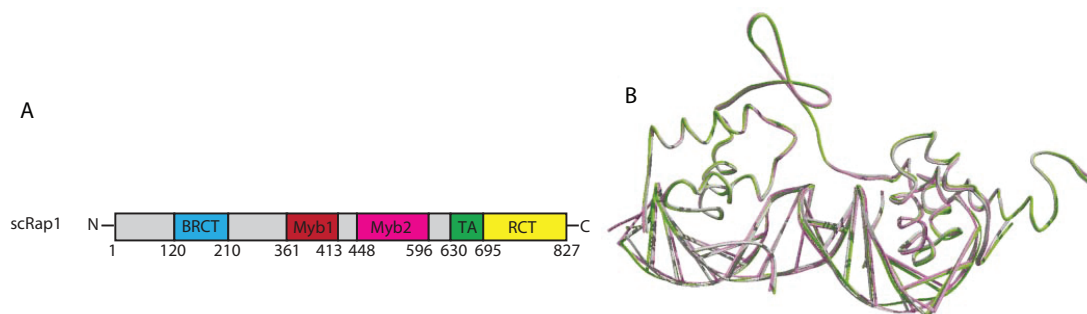
Figure 3. *S. cerevisiae* **Rap1 DBD domain binds to various DNA substrates with the same overall structure.** (A) Domain organization of Rap1. The DBD domain contains two Myb-like folds. (B) Structure superposition of scRap1 DBD domain bound to three different DNA substrates: Rap1-TeloA (grey), Rap1-TeloS (green), and Rap1-HMRE (lilac). Adapted and modified from Taylor et al., 2000.

Despite extensive biochemical and genetic studies, not all the functional domains for Rap1 are completely defined. For example, the first 279 residues at the N-terminus, including the BRCT domain (**Figure 3A**), are largely dispensable for all known biological functions of Rap1, both *in vitro* and *in vivo* (Gilson et al., 1993; Graham et al., 1999; Moretti et al., 1994). However, it is clear that the central Myb DNA-binding domain of Rap1 (minimal boundary residues 361-596, Henry et al., 1990), is essential for all Rap1 functions, and loss of this domain causes lethality (Graham et al., 1999). The importance of the essential Myb-domain is also demonstrated by the fact that overexpression of the DNA-binding domain together with an adjacent C-terminal sequence leads to toxicity and growth inhibition (Freeman et al., 1995). Rap1 has been shown to tolerate many sequence variations in its recognition sites without compromising the overall binding affinity (Idrissi et al., 1998; Vignais et al., 1990). To understand how Rap1 fulfills various cellular functions at different DNA elements, crystal structures of Rap1 Myb-domain bound to three different DNA substrates are determined using: (i) the canonical telomeric sequence (TeloA) (Konig et al., 1996), (ii) a modified version of the telomeric repeat (TeloS), and (iii) a binding site found at the *HMR* locus (HMRE) (Taylor et al., 2000). Comparison of these structures reveals no significant changes in the protein structure (**Figure 3B**). However, a detailed examination of the structures indicates that the recognition of different binding sites is through side-chain rearrangements, adapted to different hydrogen bonding contacts (**Figure 4**) (Taylor et al., 2000).
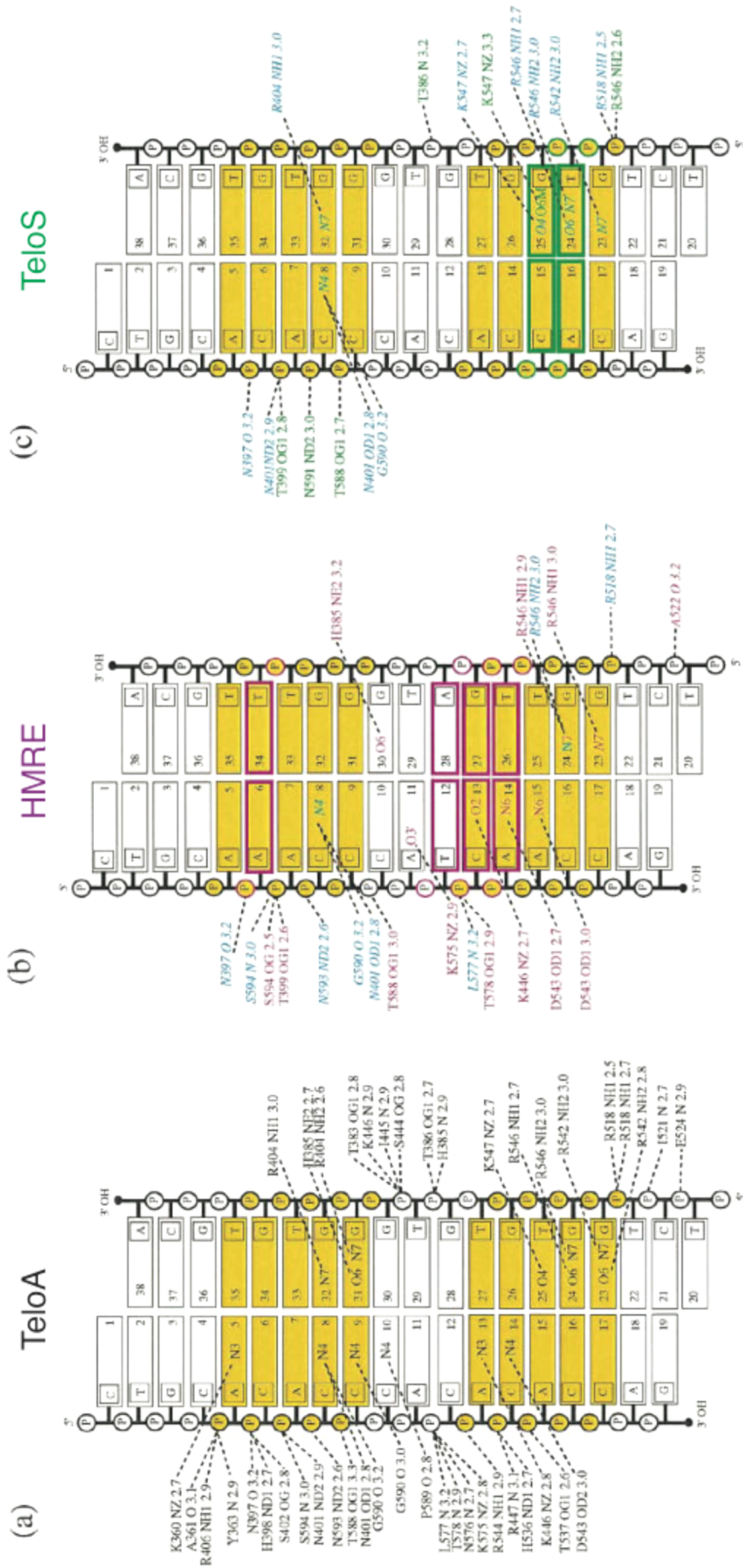
Figure 4. Comparison of the hydrogen bonding interactions observed in the Rap1-TeloA, Rap1-HMRE and Rap1-TeloS complexes. Hydrogen bonding interactions that are abolished (blue), or formed (magenta) in the HMRE complex and (green) in the TeloS complex as compared to the TeloA complex are shown in (b) and (c), respectively. Adapted from Taylor et al., 2000.

Among all the DNA-binding transcription factors, consensus sequences for Rap1 DNA-binding have been published most extensively (Lieb et al., 2001; Graham and Chambers, 1994). Consistent with its role as an essential yeast telomeric protein, telomeric TG_{1-3} repeats reveal the highest affinity binding sites for Rap1. *In vitro*, Rap1 binds to telomeres with a frequency of about one per 18 bp telomeric DNA (Gilson et al., 1993; Ray and Runge, 1999). Thus, telomeres with ~300 +/- 75 bp length could in principle accommodate 14-20 Rap1 molecules.

A transcriptional activation domain is located between residues 630 and 695 of Rap1, partially overlapping with the C-terminal protein interaction domain (residues 672-827, referred as to $Rap1_{RCT}$) (**Figure 3A**) (Buck and Shore, 1995; Hardy et al., 1992). Although *S. pombe* and human Rap1 lost their DNA-binding ability, their telomeric associations are dependent on Taz1 and Trf2. Like scRap1, both spRap1 and hRap1 utilize their $Rap1_{RCT}$ domains to recruit other proteins. Despite great changes in the composition for telomere-associated proteins during evolution, Rap1 is conserved from yeast to human. The first structure of the $Rap1_{RCT}$ domain from *S. cerevisiae* was solved by Feeser and Wolberger in 2008. It revealed an all-helical fold with no structural homolog. Structures of the protein interaction module in *S. pombe* and human Rap1 resemble that of scRap1 (Chen et al., 2011), further supporting Rap1 functional and structural conservations. In *S. cerevisiae*, the $Rap1_{RCT}$ domain is crucial for its telomere functions and gene silencing through recruitment of Rif1/Rif2 and Sir3/Sir4 (Buk and Shore 1995; Hardy et al., 1992; Wotton and Shore, 1997; Moretti et al., 1994).

Rif1 and Rif2 bind to Rap1, providing the major proteinaceous complexes at double-stranded telomeres

RIF1 and *RIF2* were identified in yeast two-hybrid (Y2H) experiments as direct Rap1 interaction factors 1 and 2, which also show binding to each other (Hardy et al., 1992; Wotton and Shore 1997). Unlike the higher eukaryotes genome, only about 5% of the genes

in *S. cerevisiae* contain introns. The sequence of *RIF1* indicates a single large open reading frame that encodes a protein of 1916 amino acids. The absence of the intron in *RIF1* was confirmed by the northern analysis of both total and poly(A)-detected RNA (Hardy et al., 1992). In other organisms including human, Rif1 orthologs were identified based on low sequence similarity to scRif1 (Adams and McLaren, 2004; Kanoh and Ishikawa, 2001). In general, all the Rif1 proteins share low sequence conservation to known protein domains. Nevertheless, Rif1 proteins were reported to possess a conserved N-terminal domain with HEAT-like or Armadillo-type repeats fold (Silverman et al., 2004; Xu et al., 2010) (**Figure 5**). The C-terminal domain of Rif1 is thought to be only conserved in vertebrates, whereas it is completely absent in yeast (Xu et al., 2010). Although higher eukaryotes have conserved Rap1 protein at telomeres, the interaction between Rap1 and Rif1 is only observed in *S. cerevisiae.* The Rap1-interaction domain of Rif1 is mapped to its C-terminal fragment (residues 1614-1916) (Hardy et al., 1992). As an independent method to assess the interaction of Rap1 and Rif1, different laboratories demonstrated the co-localization of Rif1 and Rap1 foci at telomeres using immunofluorescence (Mishra and Shore, 1999; Smith et al., 2003).
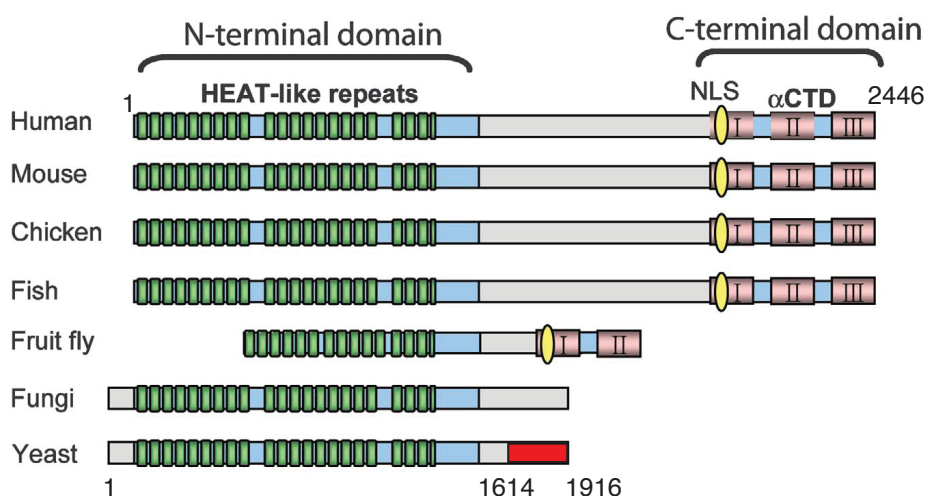
Figure 5. Schematic representation of Rif1 domain organization in different eukaryotic species. The HEAT-like repeats are indicated by the green blocks. The three conserved C-terminal subdomains I-III are marked by red boxes. The potential nuclear localization signal (NLS) is shown by yellow ovals. The Rap1-binding domain of budding yeast Rif1 is shown by the dark red box. Adapted and modified from Xu et al., 2010.

While homologues of *RIF1* with low sequence similarity could be identified from budding yeast to higher eukaryotes including human, no ortholog for *RIF2* was found beyond closely

related yeast species. Using sequence comparison of the genome between *S. cerevisiae* and *Kulyveromyces polysporus*, *RIF2* was found syntenic to *ORC4* (Scannell et al., 2007). Orc4 is a subunit of the conserved origin recognition complex (ORC), which contains an AAA+ ATPase fold followed by a C-terminal DNA-binding winged-helix domain. Due to the low sequence similarity between *RIF2* and *ORC4*, sequence alignment of Rif2 and Orc4 proteins from different species was demonstrated by Marcand and colleagues using very sensitive sequence analysis methods (Marcand et al., 2008). Based on the sequence alignments, Rif2 was predicted to possess the same overall AAA+ ATPase fold as Orc4 with the absence of a winged-helix domain. The authors indicated that in Rif2, the Walker A lysine is substituted by a histidine and the Walker B aspartate is exchanged by a glutamic acid. These two motifs are responsible for the ATPase activity of the AAA+ module and are highly degenerated in Rif2 compared to Orc4. As a consequence, Rif2 likely lacks any ATPase activity.

By a one-hybrid assay and chromatin immunoprecipitation, Rif1 and Rif2 were demonstrated to localize to yeast telomeres (Bourns et al., 1998; Lieb et al., 2001; Smith et al., 2003). Both Rif1 and Rif2 are among the few telomeric proteins that localize only in telomeric regions and nowhere else in the genome. Unlike Rap1, which directly binds to telomeric DNA, the association of Rif1 and Rif2 at telomere is thought to be Rap1-dependent. Together, Rap1, Rif1 and Rif2 form the major complexes, coating the double-stranded telomeric region of budding yeast telomere.

3 Telomere maintenance

3.1 Homologous recombination (HR) mediated telomere maintenance

In most of the eukaryotes, including yeast, telomere lengthening is carried out by telomerase, which uses its internal RNA component as a template for the extension of the chromosome ends (as discussed below). However, this is not the only mechanism that cells possess to maintain telomeric DNA. For example: in *Drosophila*, retrotransposon-mediated telomere-specific transposition is the major pathway of telomere maintenance (reviewed in Biessmann and Mason, 1997). Or in green alga Chlorela, both telomerase and transposition contribute to the maintenance of telomeric DNA (Higashiyama et al., 1997). Although most cells in *S. cerevisiae*, *S. pombe* or *Kluyveromyces Lactis* undergo progressive shortening of

telomeres and subsequently take senescence when telomerase is lost, a small cell population continues to divide (Lundblad and Blackburn, 1993; McEachern and Blackburn, 1996; Nakamura et al., 1997). These survivors do not arise when *RAD52* or both *RAD50* and *RAD51*, the three major proteins responsible for the homologous recombination in yeast, are deleted. The replication protein Pol32 appears indispensable as well (Lydeard et al., 2007), suggesting that replication accompanies recombination to maintain telomeric DNA.

Type I survivors

Most of the cells that survive in the absence of telomerase have multiple tandem repeats of the subtelomeric Y' elements followed by very short tracts of TG_{1-3} DNA (Lundblad and Blackburn 1993; Teng and Zakian, 1999). Type I survivors are dependent on the Rad51-mediated HR pathway, which is a RecA-like recombinase that acts in concert with Rad54, Rad55 and Rad57. Type I survivors grow faster than the type II survivors and therefore usually take over liquid culture. However, type I survivors are not stable and can convert to type II cells.

Type II survivors

The frequency of type II survivors is only about 10% of the total survivors. These cells carry long and very heterogeneous telomere length with terminal TG_{1-3} tracts to 12 kb or longer (Teng and Zakian, 1999). This pattern is similar to the long telomeres observed in human tumor cells (Bryan et al., 1997) or immortal culture cells (Bryan et al., 1995), which maintain their telomeric DNA by the telomerase-independent alternative lengthening of telomeres (ALT) pathway. The type II survivor pathway is mediated by Rad50-dependent HR in complex with Mre11 and Xrs2, and requires Rad59 and Sgs1 (Teng and Zakian 1999; Tsai et al., 2006). In cells lacking *TLC1*, deletion of either *RIF1* or especially *RIF2* results in significantly increased type II survivors (Teng et al., 2000), indicating that both Rif1 and Rif2 are negative regulators for Rad50-mediated HR. In agreement, Rif2, but not Rif1 is an effective inhibitor for the NHEJ repair pathway at telomeres (Marcand et al., 2008). The common feature of Rad50-mediated type II survivors, NHEJ at telomeres, and telomere lengthening is the involvement of the Mre11-Rad50-Xrs2 (MRX) complex. It is possible that Rif2 negatively regulates all these three events through inhibiting the MRX complex by preventing the association of Tel1 at telomeres (discussed below). In addition, Rif1 and Sgs1, the yeast homolog of human BLM helicase, seem to have opposing effects on the telomerase-independent survival pathway. While lack of *sgs1* decreases type II survivors, in line with the

known negative effect of Sgs1/BLM on Rad51, deletion of *RIF1* in an *sgs1Δ* strain restores the appearance of type II survivors (Tsai et al., 2006).

3.2 Telomerease-dependent length regulation

The telomerase holoenzyme is thought to consist of a two-component ribonucleoprotein complex harbouring a highly conserved reverse transcriptase subunit (Est2/hTERT) (Lingner et al., 1997a; Lundblad and Szostak, 1989; Nakamura et al., 1997) and a template RNA (TLC1/hTERC) (Greider and Blackburn, 1989; Hughes et al., 2000; Singer and Gottschling, 1994). Like other reverse transcriptases, telomerase extends the 3' end of the DNA rather than that of the RNA primer end. During telomere elongation, the 3' end of the chromosome serves as the primer for telomerase and is positioned adjacent to the short (often 6 nt) template sequence within TLC1/hTERC. Each extension round of the telomere terminus leads to the addition of one telomeric repeat. The repeated alignment, extension and translocation steps then endow the chromosome ends with telomere repeats.

In *S. cerevisiae*, Est2 (e̲ver s̲hort t̲elomere 2) is the catalytic subunit of telomerase (Lingner et al., 1997b). Est2 binds to the RNA template TLC1, forming the core components of telomerase (Lingner et al., 1997a). *In vivo*, the telomerase holoenzyme often contains additional factors that are not required for catalysis *per se*. The two accessory factors Est1 and Est3 were identified in the same screen as Est2, whose mutation leads to an *est* phenotype (Lendvay et al., 1996), which is known for progressive loss of telomere, chromosome instability and cell death (Lundblad and Szostak 1989). Est1 binds to Est3 and to a stem loop in TLC1 (Hughes et al., 2000). Although both Est1 and Est3 are required for the telomerase activity *in vivo*, they are dispensable for the telomerase activity *in vitro*. So far, *EST1*, *EST2*, *EST3*, *TLC1* and *CDC13* are the only genes, whose single deletion or mutation results in an *est* phenotype. However, double mutations of other genes can give rise to est-like telomerase null phenotype, as seen for the *tel1Δmec1Δ* double mutant (Ritchie et al., 1999) or the *mrxΔyKuΔ* double mutant (DuBois et al., 2002).

In most unicellular organisms, the core components of telomerase are consitutively expressed, having a housekeeping function. In contrast, telomerase is mostly suppressed in human somatic cells. Similarly to primary cells, tumor cells require a telomere maintenance mechanism. In many cases, upregulation of hTERT is sufficient to allow cells for long-term proliferation (reviewed in Cong et al., 2002). Although hTERT alone is not an oncogene and

telomerase activity does not induce cell transformation (Hahn et al., 1999; Morales et al., 1999), the progressive proliferation of adult human cancers is associated with disturbed telomerase activity (Hiyama et al., 1995).

3.2.1 Cell cycle dependent telomerase activity

Several studies using different approaches have demonstrated that telomerase action is cell cycle dependent, with telomere elongation occuring in the late S/G2 phase only. Although the catalytic subunit of telomerase Est2 is found at telomeres throughout most of the cell cycle, including during G1 and S phase, no telomerase activity is detected *in vivo* (Taggart et al., 2002). Furthermore, Est2 binding at telomeres is not constitutive, as evident in a second peak of Est2 association observed in the late S/G2 phase (Smith et al., 2003). In contrast, the *EST1* expression level is cell cycle dependent with its expression peaking in the late S/G2 phase (Taggart et al., 2002). Since the Est3 telomeric binding relies on Est1, the cell cycle dependence of Est1 indirectly determines the presence of Est3 at telomeres. Although Est1 and Est3 are dispensable *in vitro*, they are essential for the *in vivo* activity of telomerase. Thus, telomerase action is restricted to the late S/G2 phase, at least partially due to the lack of binding of its accessory factors Est1/Est3. Besides the cell cycle dependent association of telomerase subunits at telomeres, other possibilities may also contribute to cell cycle dependent telomerase activity. For example: telomeres structural change that is dependent on the cell cycle might control the access of telomerase to telomeres, or Cdk1-dependent C-strand degradation occuring only in the late S phase could furthet determine the cell cycle dependent telomerase action.

3.2.2 The CST complex positively regulates telomerase-dependent telomere length control

The current model for Cdc13 as a positive regulator for telomere lengthening is based on the interaction between Cdc13 and the telomerase subunit Est1, recruiting telomerase to the chromosome ends. Consistent with this proposal, the *cdc13-2* mutant (also identified as *EST4*) that displays a typical *est* phenotype can be rescued by a compensatory mutation in *EST1* (the *est1-60* allele) (Pennock et al., 2001). A charge swap of a Glu to Lys mutation in the *cdc13-2* is suppressed by the reverse Lys to Glu mutation in *est1-60*. The idea of Cdc13 recruiting telomerase through the Cdc13-Est1 interaction is in line with gene fusion studies, in which Cdc13 or its DBD were fused to Est1, Est2 or Est3 (Pennock et al., 2001; Evans and

Lundblad, 1999). The resulting fusion proteins could efficiently suppress the telomere maintenance defects of *cdc13-2* or *est1-60* alleles.

Since the Cdc13-Est1 interaction is crucial for telomerase action, one hypothesis for telomerase regulation is that Cdc13 would preferentially bind to short telomeres. However, Cdc13 binds at short and wild type length telomeres to similar extent (Bianchi and Shore, 2007; Sabourin et al., 2007), arguing against the above proposal. The cell cycle dependent modification of Cdc13 offers additional possibilities for how telomerase activity is regulated. For example: Binding of the telomerase subunit Est1 and telomere length are both reduced in the absence of Cdc13 phosphorylation by Cdk1 (Li et al., 2009). Sumoylation of Cdc13 in the S phase, which limits telomerase activity by increasing competitive binding of Stn1 to Cdc13 (Hang et al., 2011), would in principle also offer a possible means of telomerase regulation.

Numerous analyses revealed that both Cdc13 and Stn1 have complex roles in telomere length maintenance. Besides their function as positive regulators of telomerase and their role in capping telomere ends (discussed below), Cdc13 and Stn1 are also implicated in negative regulation of telomere elongation. Stn1 appears to limit telomerase activity by competing with Est1 for Cdc13 binding (Chandra et al., 2001; Puglisi et al., 2008). Consistently, *STN1* mutants show a telomere elongation phenotype (Grandin et al., 1997). Deletion of the C-terminal domain of Cdc13 leads to extensive telomere elongation, as a result of impaired ability to facilitate C-strand replication, which limits G-strand synthesis by telomerase (Chandra et al., 2001). Mutations in *TEN1* similarly display elongated telomeres (Xu et al., 2009). However, the mechanism underlying elongation phenotypes in *CDC13* and *TEN1* mutants is so far unclear.

3.2.3   Negative regulators for the telomere length maintenance

The helicase Pif1 negatively regulates telomere length
After intensive genetic studies in yeast telomeres, many genes that affect telomere maintenance have been identified. Only few genes, whose mutations lead to elongated telomeres, act as negative regulators of telomerase. In addition to the most dominant negative regulators Rap1, Rif1 and Rif2 (discussed below), Pif1 emerges as another negative regulator for telomere length. Pif1 is a 5' to 3' helicase in *S. cerevisiae*. Deletion of *PIF1*

increases telomere length while overexpression of the protein leads to short telomeres. Furthermore, the inhibitory effect of Pif1 requires its enzymatic activity (Zhou et al., 2000). It has been shown that Pif1 inhibits the telomere lengthening process by destabilizing the telomerase RNA-DNA hybridization (Boule et al., 2005). Pif1 also appears to participate in preferential lengthening of short telomeres. In the absence of Pif1, Est2 binds equally to short and wild type length telomeres (Li et al., 2009; McGee et al., 2010). However, the exact mechanism underlying the negative regulation effect of Pif1 on telomere length remains unresolved.

Tbf1 and Reb1 provide a backup counting mechanism

The subtelomeric proteins Tbf1 and Reb1 serve as transcription factors in budding yeast. They also have been shown to negatively regulate telomere length. Telomeres shorten proportionally to the number of tethered Tbf1 or Reb1 in *tel1Δ* cells, but not in wild type cells, as Tel1 antagonizes the effect of Tbf1/Reb1 (Berthiau et al., 2006). At an artificial telomere lacking the subtelomeric region, *tel1Δ* cells no longer retain a preference for the elongation of short telomeres. Tethering Tbf1 to the artificial telomeres, however, restores preferential telomeric DNA addition at short telomeres in *tel1Δ* cells (Arneric and Lingner, 2007). These findings suggest that subtelomeric binding proteins Tbf1 and Reb1 provide a backup counting mechanism in case of an accidental loss of terminal telomeric DNA, whose length is under the control of the primary counting module provided by Rap1, Rif1 and Rif2.

Telomere length is reciprocal proportional to telomere bound Rap1, Rif1 and Rif2 proteins

Telomere length regulation involves a negative feedback loop that creates a stochastic process, keeping telomeres within a broad size range. The reason for such a feedback loop is that the newly synthesized telomeric repeats serve as binding sites for the negative regulators of telomerase. In *S. cerevisiae*, the most important negative regulators for the telomere length are the Rap1, Rif1 and Rif2 proteins, which provide the major proteinaceous complexes at the double-stranded telomere region. Overexpression studies of *RAP1* in conjunction with *RAP1* temperature-sensitive mutants underline its important role in the negative telomere length regulation (Conrad et al., 1990; Lustig et al., 1990). The $Rap1_{RCT}$ domain serves as the protein interaction domain, crucial for telomere length regulation and gene silencing. Deletion of this protein interaction domain is dispensable for viability, but results in the deregulation of telomere size, chromosome stability and cellular dysfunctions in yeast (Kyrion et al., 1993). Loss of Rap1 interaction partners Rif1 or Rif2, which bind to the

Rap1$_{RCT}$ domain, causes elongated telomeres with the overall lengthening being moderate in size. Conversely, combinational deletion of both *RIF1* and *RIF2* results in a dramatic increase in the telomere length, similar to that seen with the Rap1$_{RCT}$ deletion mutant (Hardy et al., 1992; Wotton and Shore 1997). In tethering studies with the Rap1$_{RCT}$ domain fused to a DNA-binding domain of Gal4, the number of telomere-bound Rap1 molecules serves as a gauge for the length of telomeric tracts. This established a protein-counting model for the telomere length homeostasis (Marcand et al., 1997). In a later study, telomere tethered Rif1 and Rif2 proteins maintain the regulation of telomeric tracts despite the absence of the Rap1$_{RCT}$ domain. In addition, the previous published counting effect of the tethered Rap1$_{RCT}$ domain is dependent on Rif proteins (Levy and Blackburn, 2004). Therefore, Rap1 counting was in fact Rif proteins counting, and the number of the telomere associated Rif proteins function as sensors for telomere length.

3.2.4   The DNA-damage response factors in telomere length regulation

The replication protein A (RPA) complex has a positive effect on telomere elongation
RPA is a highly conserved heterotrimer single-strand binding complex composed of Rpa1, Rpa2 and Rpa3. Each of the subunit is essential in yeast (Brill and Stillman, 1991; Heyer et al., 1990). RPA is required for various processes in DNA metabolism, including replication, recombination and repair. It was also detected transiently at telomeres in late S phase (McGee et al., 2010; Schramke et al., 2004). The likely explanation for this is its association with a newly synthesized daughter strand during semi-conservative replication (McGee et al., 2010). However, mutant alleles of *RPA* result in shorter telomeres (Smith et al., 2000; Mallory et al., 2003; Ono et al., 2003), suggesting a positive influence of RPA on telomere length. Recently, Luciano and colleagues showed by co-immunoprecipitation that RPA is part of the transient complex in the late S phase comprised of RPA, yKu, Cdc13 and telomerase. The interaction of RPA and telomerase in this complex dependents on yKu and Est1. In the same study, the authors proposed that RPA could facilitate telomerase activity, as *RPA* mutations impair the interaction with yKu and telomerase, counteracting the dramatic telomere lengthening phenotype of *rif1Δrif2Δ* cells (Luciano et al., 2012).

Telomere maintenance requires checkpoint kinases Tel1 and Mec1

Telomere maintenance also depends on the checkpoint kinases Tel1 and Mec1, which are members of the phosphoinositide-3-kinase (PI3 kinase) family and orthologs of human ATM/ATR. Yeast cells lacking Tel1 show short but stable telomeres, whereas loss of Mec1 function yields only a moderate telomere shortening (Greenwell et al., 1995; Ritchie et al., 1999). Double mutation of *tel1Δ*/*mec1Δ* results in a progressive telomere shortening and subsequent senescence, a typical *est* phenotype (Ritchie et al., 1999). This suggests that Tel1 appears to be the main PI3 kinase at telomeres, while Mec1 has a less pronounced but nevertheless biological important role in the regulation of telomerase activity. Despite the crucial roles of Tel1 and Mec1 in the telomere length regulation, the exact mechanisms of regulation remains largely unresolved. The function of Tel1 at telomeres requires its kinase activity, as *TEL1* kinase inactive mutant has short telomeres (Greenwell et al., 1995). It has been proposed that Tel1 positively regulates telomerase activity by phosphorylating Cdc13, and thus promoting the Cdc13-Est1 interaction (Tseng et al., 2006). This model has been questioned recently by Gao and colleagues: firstly, the Cdc13 phosphorylation pattern is not altered upon *TEL1* deletion; secondly, the Ser255 phosphorylation important for the interaction between Cdc13 and Est1 is Tel1-independent; and thirdly, elimination of all the potential Tel1 phosphorylation sites in Cdc13 still confers wild type telomere length (Gao et al., 2010). Interestingly, a recent report demonstrates that upon DSB induction, Cdc13 Ser306 is phosphorylated mainly by Mec1, instead of by Tel1. This posttranslational modification of Cdc13 appears to inhibit the accumulation of Cdc13 at telomeric DSB, thereby preventing telomere addition. However, the Cdc13 Ser306 phosphorylation can be antagonized by the yeast protein phosphatase PP4 (Pph3) together with its regulatory protein Rrd1. Both Pph3 and Rrd1 are necessary for the efficient association of Cdc13 at telomeric DSBs (Zhang and Durocher, 2010).

The Mre11-Rad50-Xrs2 (MRX) complex is required for the telomeric end resection

The MRX complex and Sae2 have been shown to participate in the telomere length regulation. Telomere G-tail generation from blunt ends of leading-strand telomeres is carried out by MRX/Sae2, with MRX playing a major role in this process (Bornetti et al., 2009; Larrivee et al., 2004). Null mutants of *MRE11*, *RAD50*, or *XRS2* are characterized by short telomeres besides other DNA damage phenotypes (Haber, 1998). Epistasis analysis shows that Tel1 acts together with the MRX complex in telomere maintenance (Nugent et al., 1998; Ritchie and Petes, 2000). In agreement with these findings, the telomeric

localization of Tel1 is dependent on MRX (Nakada et al., 2003), and the interaction of MRX-Tel1 increases the telomeric association of MRX (Hirano et al., 2009). In addition, Tel1 regulates telomere nucleolytic processing by promoting the MRX activity (Martina et al., 2012).

The interplay between DNA-damage response factors and Rap1, Rif1 and Rif2 in telomere length regulation

Currently, one of the biggest challenges in telomere research is to understand the mechanism by which the negative regulators exert their control on telomerase. Several labs have suggested a model where Rap1, Rif1 and Rif2 act through MRX/Tel1 in length regulation. *In vitro,* Rif2 has been shown to physically interact with the Xrs2 C-terminus, counteracting the Xrs2-Tel1 binding (Hirano et al., 2009). Abolising the Xrs2-Tel1 interaction reduces the telomeric association of MRX and telomere nucleolytic processing. Lack of Rif2 proteins therefore increases the level of telomere bound MRX/Tel1 and MRX-dependent 5'-end resection (Bonetti et al., 2010; Bonetti et al., 2009; Hirano et al., 2009). In contrast, tethering of Rif2 at telomeres only inhibits telomeric association of Tel1 or Mec1, but not that of MRX (Hirano et al., 2009). This indicates that the primary role of Rif2 is to counteract the telomeric association of Tel1, but not MRX. It has been reported that Rap1 can inhibit MRX binding to telomeres independent on Rif1 and Rif2 when *TEL1* is deleted (Hirano et al., 2009). This suggests a Rif-independent effect of Rap1 on telomere length regulation in the absence of Tel1. But how exactly Rap1 prevents MRX binding once Tel1 is not associated at telomeres still remains to be uncovered. The current model is that Rif2 competes with Tel1 for the Xrs2 binding. This inhibits the telomere association of Tel1, which allows Rap1 to effectively prevent MRX action at telomeres. Although deletion of *RIF1* was shown to favor telomeric binding of MRX/Tel1 and Mec1 (Hirano et al., 2009), no interaction between Rif1 and Xrs2 or other components of the MRX has been reported. The mechanism, by which Rif1 prevents Tel1 or Mec1 and negatively regulates telomere length, is still not understood.

The research to elucidate the interplay between Tel1/Mec1 and Rif1/Rif2 is complicated as Rif1 and Rif2 were shown to inhibit Tel1/Mec1 binding to telomeres, placing both Rif1 and Rif2 upstream of Tel1 in the telomere length control. However, some of the data provide the possibility for Rif1 and Rif2 being targets of Tel1 or Mec1 signaling, explaining why telomere maintenance defects in the absence of Tel1 and Mec1 can be suppressed by the deletion of *RIF1* and *RIF2* (Chan et al., 2001). A recent study reported that human Rif1 is regulated by ATM (mammal ortholog of Tel1) and p53BP1, which favors the interpretation of Rif1 being a

target of ATM (Silverman et al., 2004). Although in *S. cerevisiae,* Rif1 has 14 potential Tel1/Mec1 phosphorylation S/TQ sites, Rif2 does not contain any canonical sites, arguing against its direct regulation by Tel1/Mec1. Further studies are required to provide the mechanism, by which Rif1 and Rif2 influence the activity of Tel1 and Mec1 at telomeres.

4   Similarities and differences between uncapped telomeres and DSBs

The ends of linear chromosomes resemble one half of a DNA double-strand break (DSB) and have the potential to be recognized and processed as a form of DNA-damage. In yeast, a single DSB can cause robust cell cycle arrest (Sandell and Zakian, 1993), which provides cells time to carry out DNA repair. In general, DSBs can either be processed by nucleases, which generate ssDNA and lead to repair through HR, or be repaired by NHEJ in the absence of ssDNA generation (reviewed in Harrison and Haber, 2006).

During S and G2 phases, the choice between the two repair pathways is largely dependent on whether ssDNA generation occurs, or not. The initial nucleases that function at DSBs are the MRX complex and the nuclease Sae2. Together, Sae2/MRX generate 50-100 nucleotide 3' ssDNA overhangs (Ivanov et al., 1994; Mimitou and Symington, 2008). The subsequent process to generate many kilobases of 3' ssDNA is taken over by the nuclease Exo1 (Mimitou and Symington, 2008). Parallel to the Sae2/MRX and Exo1 pathways, additional nuclease activity is provided by the helicase Sgs1 and the helicase-nuclease Dna2 (Bonetti et al., 2009; Gravel et al., 2008).

Resected 3' ssDNA is coated by RPA, which recruits the Mec1-Ddc2 heterodimer and the 9-1-1 complex, thereby initiating the checkpoint response (Lisby et al., 2004; Sanchez et al., 1999). Ddc2 contains its own ssDNA-binding domain. This domain is essential for a functional DNA damage response (Rouse and Jackson, 2002). No other checkpoint proteins are required for the recruitment of Mec1-Ddc2 to sites of DNA damage, demonstrating that RPA-coated ssDNA is the signal that triggers the checkpoint activation. Similarly, RPA is also required for the interaction between the ATR/ATRIP complex and ssDNA in human cells *in vitro* (Zou and Elledge, 2003). The subsequent phosphorylation of histone H2A by Mec1 at the site of DNA damage recruits Rad9 (Hammet et al., 2007). Rad9 then acts as a mediator to promote Mec1 to activate effector kinases Rad53 and Chk1, which in turn activate the downstream checkpoint cascade (Sanchez et al., 1999; Sun et al., 1998). At the same time,

checkpoint components Mec1, Rad53 and Rad9 have been shown to limit the generation of further ssDNA (Lazzaro et al., 2008; Lydall and Weinert, 1995). At blunt or minimally processed DSBs, MRX remains stably associated with breaks and recruits the kinase Tel1 through the C-terminus of Xrs2 (Nakada et al., 2003). Tel1 functions similarly to Mec1 in recruiting Rad9, activating the downstream cascades. Unlike Mec1-Ddc2, neither Tel1 nor MRX requires RPA or any other checkpoint protein to interact with the damage site.

In yeast, a single DSB causes a 12-14 h G2/M arrest (Lee et al., 1998), which corresponds to the time needed of several unperturbed cell cycles. Telomeres therefore have to be strictly protected ("capped") from DNA-damage recognition, in order to prevent unwanted cell cycle arrest or chromosome fusion events. In *S. cerevisiae*, the telomere capping proteins are the CST complex, the yKu complex and Rap1-Rif1-Rif2. Inactivation of any of these complexes leads to telomere uncapping and initiates a DNA-damage response.

The yKu complex as telomere capping proteins

yKu inhibits Exo1 mediated resection at telomeres, just as yKu prevents resection by Exo1 at DSBs (Bonetti et al., 2010; Mimitou and Symington, 2008). It has been shown that the telomeric ssDNA overhang is increased upon inactivation of *yKu*, and the increased ssDNA levels persist throughout the cell cycle (Gravel et al., 1998). In addition, cells lacking *yKu* proteins display a temperature-sensitive growth defect, accompanied by cell cycle arrest and loss of viability (Maringele and Lydall, 2002). Although *yKu* mutants undergo Mec1-dependent checkpoint activation, the 9-1-1 complex appears to be dispensable in the checkpoint activation following telomere uncapping in *yKu* mutants (Maringele and Lydall 2002). Interstingly, the MRX complex is shown to inhibit resection at uncapped telomeres lacking yKu, as increased amount of ssDNA is detected in *yKu70Δmre11Δ* (Foster et al., 2006).

The CST complex prevents checkpoint activation by inhibiting telomeric resection

Using the temperature sensitive allele *cdc13-1*, the CST complex can be inactivated, leading to telomere "uncapping". Cdc13 inactivation gives rise to extensive tracts of ssDNA that cause Mec1-dependent checkpoint activation, which ends in loss of viability (Garvik et al., 1995; Jia et al., 2004). Based on the structural similarity between CST and RPA, the capping function of CST is believed to prevent processing of telomeres as normal DSBs by outcompeting RPA for telomeric ssDNA (Gao et al., 2007). Similarly as seen in *yKu* cells, MRX does not promote resection, but rather inhibits resection at uncapped telomeres lacking

Cdc13 (Foster et al., 2006). In contrast to yKu, Cdc13 has been demonstrated to inhibit 9-1-1 promoted resection at telomeres (Zubko et al., 2004). As mentioned above, Sgs1/Dna2 are involved in the resection of genome-wide DSBs. Sgs1 also plays a role in the resection of uncapped telomeres in the *cdc13-1* mutant (Ngo and Lydall, 2010). While the helicase Pif1 does not appear to participate in the resection at DSBs, it has a critical role in the resection of uncapped telomeres, once Cdc13 function is compromised (Zhou et al., 2000). Exo1 is likely the major nuclease that acts at *cdc13-1* uncapped telomeres (Maringele and Lydall 2002). The essential role of Cdc13 in telomere capping is to prevent Pif1- and Exo1-dependent resection, as elimination of both Pif1 and Exo1 also counteracts the requirement of Cdc13 for telomere capping (Dewar and Lydall, 2010).

Rap1, Rif1 and Rif2 cap telomeres from the DNA-damage response by distinct mechanisms
Inactivation of Rap1 using a conditional *rap1-td* allele leads to Exo1-dependent telomere resection, which does not trigger Mec1-mediated checkpoint activation and instead results in cell arrest in G1 (Vodenicharov et al., 2010). However, deletion of the Rap1 C-terminus, which leads to the loss of Rif1 and Rif2, increases the accumulation of telomeric ssDNA in an MRX-dependent manner (Bonetti et al., 2010), accompanied by the cell cycle arrest at G2/M phases (Ribeyre and Shore, 2012). Consistently, deletion of *RIF2* causes significant increase of ssDNA at telomeres (Ribeyre and Shore, 2012; Xue et al., 2011). The capping function of Rif2 is believed to attenuate Tel1 at telomeres, which regulates end resection by promoting MRX activity (Martina et al., 2012). Given that Rap1 and Rif2, and to a lesser extend Rif1, inhibit telomeric resection, inactivation of these proteins is expected to favor NHEJ at uncapped telomeres. Paradoxically, Rap1 and Rif2 are required for inhibiting NHEJ at telomeres (Marcand et al., 2008). Further studies are required to elucidate their roles in the DNA-damage repair at telomeres. Rif1 in *S. cerevisiae* was thought not be involved in the DNA-damage repair. However, according to recent studies, Rif1 inhibits the checkpoint activation at uncapped telomeres by preventing the association of DNA damage repair factors like Rad9, Ddc1, Ddc2, RPA and Mec1 (Xue et al., 2011; Ribeyre and Shore, 2012). In addition, deletion of Rif1 causes a dramatic reduction in cell viability of the *cdc13-1* or *cdc13-5* mutant, demonstrated by enhanced DNA damage checkpoint activation. These studies suggest a role for Rif1 in assisting the CST complex in telomere capping (Anbalagan et al., 2011).

5   Silencing

Transcriptional silencing involves the formation of a specialized chromatin structure that blocks the expression of most genes within the silenced region. This process is mediated by regulatory sites known as silencers that act at some distance from the targeted genes. In contrast, gene-specific repression is mediated by operators at, or near the site of transcription initiation. In *S. cerevisiae*, Sir proteins, known as <u>s</u>ilent <u>i</u>nformation <u>r</u>egulators, are the structural proteins of silenced chromatin. Silenced domains are characterized by continuously distributed Sir proteins and hypoacetylated nucleosomes (Hecht et al., 1996; Lieb et al., 2001). Therefore, silenced domains are restricted to transcriptions, nucleases and DNA methylases (Gottschling, 1992; Singh and Klar, 1992).

Genetic studies have identified the mating type loci, the telomeres, and the rRNA-encoding DNA (rDNA) as the three targets of transcriptional silencing in *S. cerevisiae*. In addition to the mating type locus *MAT*, *S. cerevisiae* has unexpressed copies of mating type genes at the *HML* and the *HMR* loci. Although the *HM* loci contain complete structural genes and promoter sequences, these two loci are generally not transcribed due to the flanking silencers (reviewed in Laurenson and Rine, 1992). Reporter genes placed in the vicinity to telomeres are silenced by a process known as <u>t</u>elomere <u>p</u>osition <u>e</u>ffect (TPE). Telomeric silencing utilizes most of the genes (*SIR2*, *SIR3* and *SIR4*) required for silencing of the *HM* loci, with the exception of Sir1 and the <u>o</u>rigin <u>r</u>ecognition <u>c</u>omplex (ORC) genes (Aparicio et al., 1991). However, TPE differs from *HM* silencing, in that it is inherently unstable. This instability can be explained by the lack of Sir1 in silencing (Chien et al., 1993). Sir1 promotes the establishment of silencing by facilitating the assembly of other Sir protiens at the silencer (Rusche et al., 2002). Silencing of genes in rDNA requires Sir2, an NAD$^+$-dependent histone deacetylase, while other *SIR* genes are dispensable for this process. Thus, rDNA silencing reveals a fundamental difference compared to *HM* silencing and TPE.

The four Sir proteins were identified by mutagenesis that activated the silent mating type genes (*MATα* and *MATa*). *SIR2*, *SIR3* and *SIR4* are essential for silencing, with Sir2 and Sir4 forming a stable complex (Moazed et al., 1997). The histone deacetylase Sir2 modifies H3 and H4 tails to enhance the binding for Sir3 and Sir4 (Landry et al., 2000; Hecht et al., 1995). Unlike the other three *SIR* genes, *SIR1* contributes to silencing, but is not essential for this event. It rather plays a role in the establishment of silencing.

Silencing at *HM* loci requires two flanking silencer elements called E and I. The *HMR-E* silencer is the most thoroughly studied silencer and has three partially redundant regulatory elements called A, E, and B (Brand et al., 1987). The A element is an ARS consensus sequence (ACS), recognized by the ORC complex (Bell and Stillman, 1992), which is required for the initiation of DNA replication in general. The E and B sites are bound by two abundant and essential regulatory proteins Rap1 and ABF1, respectively (Shore and Nasmyth 1987). Both Rap1 and ABF1 also bind to promoters of a large number of genes, where they often function as transcriptional regulators. Mutations in any two of the three binding sites are required to achieve complete loss of silencing (Brand et al., 1987).

The only known sequence-specific DNA-binding protein for TPE is Rap1 (Kyrion et al., 1993), which binds to TG_{1-3}-repeats at telomeres. Therefore, instead of being regulated by discrete silencer elements as at *HM* loci, TPE is though to be mediated by long TG_{1-3} tracts to which multiple copies of Rap1 are bound. Mutational studies indicate that the carboxyl terminus of Rap1 is crucial for both *HM* silencing and TPE, as it is the interaction domain for both Sir3 and Sir4 (Sussel and Shore, 1991). Deletion of the Rap1 C-terminus results in a complete loss of TPE and *HML* silencing, while full derepression at *HMR* can only be achieved when the ORC binding site A is mutated (*hmrΔA*) (Kyrion et al., 1993; Moretti et al., 1994). In addition, genetic studies suggest that yeast is restricted in the total amount of the Sir proteins that can form silenced chromatin. This limitation leads to the shift in the balance between silencing at *HMR* and telomeres, which is regulated by the telomere length and the interplay between Rap1 and Sir proteins (Buck and Shore, 1995). Both Rif1 and Rif2 regulate telomere length, affecting the number of Rap1-binding sites. Additionally, the same Rap1 carboxyl terminus ($Rap1_{RCT}$) that recruits Sir3 and Sir4 is also essential for the interaction with Rif1 and Rif2. As consequence, Rif1 and Rif2 have been shown to compete with Sir3 and Sir4 for binding to $Rap1_{RCT}$ at telomeres. Thereby, both Rif1 and Rif2 can modulate TPE by interfering the protein interaction between Rap1 and Sir proteins. As mentioned above, yeast is restricted in the total amount of the Sir proteins that can form silenced chromatin. The telomeric competition between Rif proteins and Sir proteins thus allows Rif1 and Rif2 to affect the balance between telomeric and *HM* locus silencing (Wotton and Shore, 1997). Despite numerous genetic experiments studying the interplay between Rif and Sir proteins on binding to Rap1, the molecular basis describing how the competition takes place still remains to be clarified.

Aims of this work

Yeast pioneered the research in telomere biology and numerous genetic studies have explored the functions of telomere-associated proteins Rap1, Rif1 and Rif2 over the past years. Yet, so far, neither biochemical characterization, nor structural information of Rif1 and Rif2 are available. From previous publications, most of the telomere functions of Rif1 and Rif2, and even their telomeric localization, appear to rely on their association with Rap1. Thus, the mechanism by which Rap1, Rif1 and Rif2 govern telomere properties cannot be assessed without knowing how these proteins interact with each other. One aim of this work is to elucidate how the major telomere binding proteins Rap1, Rif1 and Rif2 form complexes on telomeric tracts. This was done by structural and functional analysis of the sub-complexes Rap1-Rif1 and Rap1-Rif2. Structural information was then used in differentiating individual roles of Rap1, Rif1 and Rif2 at telomeres.

In yeast, Rif1 is an extraordinary large protein, which complicates its purification from yeast or other host organisms. This obstructs the *in vitro* characterization and structure determination of Rif1. We set out to establish Rif1 biochemical and structural studies in an effort to assess how Rif1 exerts its telomere function. In addition, these approaches allow us to explore new functions of Rif1 at telomeres.

Chapter 1

Rif1 and Rif2 shape telomere function and architecture through multivalent Rap1 and DNA interactions

Authors: Tianlai Shi[1], Richard Bunker[1*], Cyril Ribeyre[2,3*], Stefano Mattarocci[2], Mahamadou Faty[1], Heinz Gut[1], Andrea Scrima[1,4], Ulrich Rass[1], David Shore[2] and Nicolas H. Thomä[†1]

[1] Friedrich Miescher Institute for Biomedical Research, Maulbeerstrasse 66, CH-4058 Basel, Switzerland.

[2] Department of Molecular Biology and NCCR "Frontiers in Genetics" program, 30 quai Ernest-Ansermet, CH-1211 Geneva, Switzerland.

[3] Current address: Institute of Human Genetics, Centre National de la Recherche Scientifique UPR1142, Montpellier, France.

[4] Current address: Helmholtz-Centre for Infection Research, Inhoffenstrasse 7, D-38124 Braunschweig, Germany.

* both authors contributed equally

† to whom correspondence should be addressed: nicolas.thoma@fmi.ch

Key words: telomeres, genome stability, DNA-repair, arrays of genomic DNA-binding sites, higher-order chromatin structures

This work is currently in preparation for submission in *Cell*.

Authors on this manuscript contributed to the following:

- Tianlai Shi purified and solved the structures of Rif2, Rif2-Rap1, Rif1-Rap1 in Figures 2, 3, 6, S2, S3, S4 and S6, performed experimental work for the Rif1$_{CTD}$ structure in Figure 4B and S5C, EMSA assays (Figures 1, 5D, 5F, S1, S5D-5J), yeast-two hybrid experiments, silencing assays including yeast strains generation, and contributed to the writing of the manuscript.
- Richard Bunker performed data analysis and structure determination of the Rif1$_{CTD}$ structure in Figures 4B and S5C.
- Cyril Ribeyre generated yeast strains for G2/M assays and telomere length assays, and performed those assays (Table 1 and Figures S2F, S2G, S3E, S4F, S5A, S6C and S6D).
- Stefano Mattarocci performed western blots (Figure S4B), chromatin immunoprecipitation (Figures 3F, 5A, 5B and S4C).
- Mahamadou Faty performed many protein purifications used in the structural and biochemical assays.
- Heinz Gut helped in the initial molecular replacement for the Rif2-Rap1 structure.
- Andrea Scrima supervised me in the structure determination process of Rif2 and Rif2-Rap1
- Uli Rass performed EMSA assays (Figures 5B, 5E and S5B) and contributed to the writing of the manuscript.
- David Shore contributed to the writing of the manuscript.
- Nicolas Thomä contributed to experimental designs and to the writing of the manuscript.

1 Summary

Yeast telomeres comprise irregular TG_{1-3} DNA repeats bound by the general transcription factor Rap1. Rif1 and Rif2 are also found at telomeres, and together with Rap1 form a proteinaceous protective cap that inhibits telomerase, SIR-complex mediated transcriptional silencing, and inadvertent DNA-repair. We present the structures of Rif1 and Rif2 bound to the Rap1 C-terminal domain, demonstrating that Rif1, Rif2 and Rap1 bind *Saccharomyces cerevisiae* telomeres in a cooperative manner. Multivalent short- and long-range protein-protein interactions drive a Rap1-Rif1-Rif2 higher-order architecture, conferring telomere-specific function: in silencing, Rif1 and Rif2 compete with Sir3 for binding the same cleft on Rap1; to prevent a DNA damage response, we find that Rif1 specifically binds single/double-stranded DNA junctions where it outcompetes RPA, explaining how resected telomeres avoid recognition as DNA double-strand breaks. By defining the intermolecular scaffold at yeast telomeres, we exemplify how arrays of common transcription factors can be organized into domains of novel function.

2 Introduction

The *Saccharomyces cerevisiae* Repressor-activator protein 1 (Rap1) serves as a general transcriptional activator at about 300 genomic loci (Lieb et al., 2001; Shore and Nasmyth, 1987; Yarragudi et al., 2007), while at the same time participating in repression (gene silencing) at the two *HM* silent mating-type loci and at sub-telomeric regions (Rusche et al., 2002). Indeed, approximately 15% of total cellular Rap1 is found at telomeres, where it binds directly to the telomeric DNA repeats and assembles the proteinaceous telomere 'cap', together with its interaction partners Rif1 and Rif2. We herein examine how telomere-specific properties emerge once multiple repeats of Rap1-binding sites are present (referred to as Rap1 arrays).

In nearly all eukaryotes, telomeric DNA comprises a short sequence (T_2AG_3 in metazoans, TG_{1-3} in *S. cerevisiae*) repeated multiple times (~1,000 repeats at human telomeres). Because telomeres resemble one half of a DNA double-strand break (DSB), they require protection from the DNA-repair machinery, that would otherwise drive chromosome fusion-breakage cycles, as well as from DNA damage checkpoint mechanisms, that would lead to cell-cycle arrest (de Lange, 2009; Dewar and Lydall, 2012). This protective function, referred to as telomere 'capping', is provided by a set of proteins that assemble on the telomeric DNA repeats, called the 'shelterin' complex in mammals (de Lange, 2005). The mechanisms by which shelterin, or its yeast equivalent, achieve telomere capping are still incompletely understood.

In yeast, Rap1 (whose mammalian ortholog is also a shelterin component) binds directly to the TG_{1-3} repeats and participates in telomere capping together with the Rif1 and Rif2 proteins, which are recruited in a Rap1-dependent manner (Hardy et al., 1992; Wotton and Shore, 1997). Two other protein complexes contribute to telomere capping: Cdc13-Stn1-Ten1 (CST), an RPA-like heterotrimer (Gao et al., 2007) that binds to telomeric single-stranded ends and prevents their degradation during S phase (Vodenicharov and Wellinger, 2006), and the yeast Ku70/80 complex, a ubiquitous DNA end-binding factor that protects telomeres from resection in non-dividing cells (Vodenicharov et al., 2010). Rap1 itself plays a critical role in capping outside of S phase, by

inhibiting end resection, and by blocking both checkpoint activation and telomere fusion (Marcand et al., 2008; Negrini et al., 2007). The Rap1-interacting proteins Rif1 and Rif2 play largely non-overlapping roles in capping. Rif2 serves to inhibit MRX/Tel1 binding and resection of telomeric 5' ends (Bonetti et al., 2010; Hirano et al., 2009; Ribeyre and Shore, 2012). Thus, tethering Rif2 to a DSB blocks Tel1 recruitment and checkpoint activation. Rif1 on the other hand appears to play a direct role in protecting telomeric single-stranded DNA and preventing it from triggering a G2/M checkpoint arrest (Xue et al., 2011; Ribeyre and Shore, 2012). Moreover, Rif1 limits resection and checkpoint activation when Cdc13 function is compromised (Addinall et al., 2011; Anbalagan et al., 2011).

Budding yeast telomere repeats are on average around 300 bp in length, and are thought to be maintained by a feedback mechanism that controls telomerase action through an inhibitory signal whose strength is proportional to the amount of bound Rap1, Rif1 and Rif2 molecules (Marcand et al., 1999; Marcand et al., 1997). This mechanism ensures that telomerase acts more frequently on short telomeres (Bianchi and Shore, 2007; Sabourin et al., 2007; Teixeira et al., 2004). Rif1 and Rif2 work synergistically to influence the frequency of these lengthening events. Wild-type telomeres bind around 15-20 Rap1 molecules (Gilson et al., 1993; Williams et al., 2010). Consistent with the 'counting' model for telomere length regulation (Bianchi and Shore, 2008), shortened telomeres lose Rap1 as well as Rif2 (McGee et al., 2010). However, Rif1 levels remain constant at shortened telomeres (McGee et al., 2010; Sabourin et al., 2007). How Rif1 is recruited to shortened telomeres in what is presumably a Rap1-independent mechanism is unclear at present.

RNA polymerase II-mediated transcription of genes placed in proximity to telomeres is repressed (Gottschling et al., 1990) through a chromatin-mediated 'telomere position effect' (TPE) silencing mechanism that requires the SIR complex (composed of Sir2, Sir3 and Sir4) (Aparicio et al., 1991). The SIRs are recruited to telomeres, in part, through interactions between Rap1 and both Sir3 and Sir4 (Moretti et al., 1994; Moretti and Shore, 2001). Interestingly, the Rap1 C-terminal domain (Rap1$_{RCT}$) used for recruiting Sir3 and Sir4 also binds Rif1 and Rif2. Yeast two-hybrid (Y2H)

experiments suggest that Rif proteins compete with SIRs for binding to the $Rap1_{RCT}$, consistent with the observation that mutations in either *RIF1* or *RIF2* lead to increased telomeric silencing. The biochemical basis of the competition for Rap1 has remained elusive.

In vivo, Rap1 confers telomeric properties to TG_{1-3} arrays once approximately 4-5 binding sites are present. Yet, *in vitro*, Rap1 molecules bind TG_{1-3} repeats in an independent fashion with no obvious interaction between the individual Rap1 proteins, as evident by the lack of apparent cooperativity (Williams et al., 2010). What then allows arrays of Rap1-binding sites to assume telomere-like properties not observed at single or double sites? We focused on the two candidate proteins, Rif1 and Rif2, the major components of the double-stranded yeast telomeric cap. By combining structural studies of the *S. cerevisiae* Rap1-Rif1-Rif2 assembly with *in vitro* reconstitution and cellular assays, we investigated how arrays of Rap1-Rif1-Rif2 organize telomeric TG_{1-3} repeats into domains of specialized structure and function, how they counteract silencing and how Rif1 and Rif2 are recruited in order to inhibit the DNA damage checkpoint. The structures of Rif2, Rif2-$Rap1_{RCT}$, Rif1 (1752-1772)-$Rap1_{RCT}$ and that of the outermost Rif1 C-terminal domain (1857-1916), which we identify as a tetramerization domain, reveal the detailed molecular architecture at telomeres and provide a molecular rationale for understanding Rap1-Rif1-Rif2 assembly and function in arrays.

3 Results

Rap1-Rif1-Rif2 binds to telomeric TG$_{1-3}$ repeats in a cooperative manner

We first characterized the interactions of Rif1, Rif2, and Rap1 in solution. Rif1 did not interact with Rif2, but both proteins were found to bind Rap1 independently (**Figure S1A**). No evidence for a stable stoichiometric Rap1-Rif1-Rif2 complex was observed in solution (**Figure S1A** and data not shown). We then tested whether Rif1-Rap1 and Rif2-Rap1 units interact when juxtaposed on Rap1-DNA arrays. Tel80, a naturally occurring telomeric sequence harboring five Rap1-binding sites (Gilson et al., 1993), was pre-incubated with Rap1 and titrated with increasing amounts of Rif1, Rif2, or Rif1 and Rif2 in the presence of a non-specific competitor DNA, which was added to quench any unspecific Rif1/Rif2 DNA-binding (**Figure 1A**). A unique, slow migrating protein-DNA species emerged when both Rif1 and Rif2 were present (**Figure 1A**, lane 14), which appeared significantly more compact than either the Rif1-Rap1-DNA (**Figure 1A**, lane 10) or the Rif2-Rap1-DNA species (**Figure 1A**, lane 6). The Rap1 BRCT domain (residues 1 to 351) and the N-terminal domain of Rif1 (residues 100-1322, hereafter referred to as Rif1_N) were dispensable for this binding behavior (**Figure S1B** and **S1C**), and were omitted from subsequent studies. The finding that Rif1 and Rif2 can simultaneously bind Rap1 on DNA was also observed using a shorter 31 bp duplex containing two juxtaposed Rap1 sites (**Figure S1D**).

While Rif1 and Rif2, in the absence of Rap1 (**Figure 1B**, lanes 10-13) were readily competed from the Tel80 by non-specific competitor DNA, they remained stably anchored to the array in the presence of Rap1 (**Figure 1B**, compare lanes 2-5 and lanes 6-9). We then competed complexes of Rif1-Rap1, Rif2-Rap1 and Rif1-Rif2-Rap1 with an unlabeled 19 bp DNA containing a single telomeric Rap1-binding site (Tel19) to assess whether the three proteins interact and stabilize each other through cooperative interactions (**Figure 1C**). Tel80 was incubated with Rap1, Rap1 and Rif1, Rap1 and Rif2, or Rap1, Rif1 and Rif2 in the presence of non-specific competitor for one hour allowing pre-equilibration. Subsequent challenge with Tel19 displaced Rap1 from Tel80 as indicated by loss of multiply Rap1-bound Tel80 species and the emergence of free Tel80. Rif1, and in particular Rif2,

stabilized Rap1 on Tel80 (**Figure 1C**, compare lanes 2-4 with 5-7 and 8-10; see **Figure 1E** for quantitation). The greatest stabilization of Rap1-DNA complexes was observed when both Rif1 and Rif2 were present (**Figure 1C**, lanes 11-13). In fine titrations (**Figure 1D** and **1F**), we observed that 80% of Rap1 was displaced from Tel80 by Tel19 at a 4-fold molar excess (after 18 h), while a 64-fold molar excess of competitor DNA was required to observe 40% Rap1 displacement in the presence of Rif1 and Rif2. We note that near complete displacement of Rap1 (>80%) was only detected following longer incubation times (greater than 18 h) indicating that cooperativity, under our experimental conditions, has a clear, but likely minor kinetic component (**Figure S1E** and **S1F**). Together these results suggest that whereas Rif1-Rap1 and Rif2-Rap1 units operate independently of one another in solution, they become cooperatively interlinked when juxtaposed on DNA.

Rif2 interacts through distinct epitopes with two adjacent Rap1$_{RCT}$ domains

The binding between Rif1, Rif2 and Rap1 has previously been shown in Y2H assays to involve the Rap1$_{RCT}$ domain (Hardy et al., 1992; Wotton and Shore, 1997). Structural analysis of Rif1 and Rif2 has been elusive, prompting us to examine the molecular basis of Rif1 and Rif2 binding to Rap1$_{RCT}$. The structures of Rif2 (residues 66-380) alone and full-length Rif2 (1-395) in complex with Rap1$_{RCT}$ were solved by X-ray crystallography and refined at 2.55 Å and 3.1 Å resolution, respectively (**Figure 2A** and **2B**). We found that Rif2 is a member of the AAA+ initiator sub-family (**Figure S2A**) and is monomeric in solution (**Figure S2B**). The Rif2 structure consists of two lobes (**Figure 2A**); an α-helical domain composed of six helices (α0, α6-α10), and an <u>a</u>dditional <u>s</u>trand <u>c</u>onserved <u>E</u> family (ASCE) αβα-domain found as an insertion between α0 and α6. The Rif2 C-terminus (residues 371-395, referred to as Rif2$_{CTD}$) is generally unstructured, but was stabilized by crystal packing interactions provided in the Rif2 lattice. Upon Rap1-binding, the Rif2$_{CTD}$ is sandwiched between the α-helical and the αβα-domain (**Figure 2B** and **Figure S2C**). The ATP binding site within this AAA+ domain is degenerate and isolated Rif2 shows no measurable ATP hydrolysis. We can currently not rule out that the site is important for Rif2 folding or ligand binding, as mutations in this nucleotide-binding

groove exhibit mild phenotypes *in vivo* (**Figure S2D-S2G**). The Rif2$_{CTD}$ combined with the α-helical

bundle of the AAA+ fold forms the major Rap1-binding interface (**Figure 2A** and **2B**) (subsequently

referred to as Rif2$_{AAA+}$) comprising a surface area of about 1280 Å^2. In line with this observation,

deletion of Rif2$_{CTD}$ also diminishes Rap1-binding *in vitro* (**Figure 2F,** see **Figure S3A** for loading

controls). The Rif2$_{AAA+}$-Rap1 interaction is directed towards the N-terminal face of Rap1$_{RCT}$ and is

largely hydrophobic in nature. Rap1 residues Phe708, Phe705, Leu706 and Rif2 residues Leu79,

Phe342, Val350, Leu384 participate in extended hydrophobic interactions (**Figure 2C** and **2D**).

Hydrogen bonding interactions were observed between Rif2 Leu386, Gln382, Ala375 and Rap1

Gln715, Asp742, Arg747 (**Figure 2C** and **2D**). A pronounced salt bridge is formed between Rif2

Glu347 and Rap1 Arg747. The interfaces between Rap1 His709 and Rif2 Thr346; Rap1 Arg747 and

Rif2 Glu347 are consistent with previous mapping attempts (Feeser and Wolberger, 2008). No

significant conformational changes in the core of Rap1 or Rif2 are found following complex

formation.

The Rif2-Rap1$_{RCT}$ structure revealed a second Rap1 molecule bound *in trans* through the Rif2

N-terminus (residues 1 to 60). This R̲ap1$_{RCT}$ b̲inding m̲otif (RBM), comprising Rif2 residues 36-48

(referred to as Rif2$_{RBM}$), is helical and attaches to a surface cleft in Rap1$_{RCT}$ involving helices α3 to α6

(**Figure 2B**). Rif2$_{RBM}$ residues Leu42 and Leu44 bind to the Rap1 hydrophobic cleft provided by Rap1

residues Leu736, Leu755, Leu762 and Ala733 (**Figure 2E**). Further stabilization of the interaction

between Rif2$_{RBM}$ and Rap1 is achieved through backbone hydrogen bonds formed between Rif2

Val45 amide and Rap1 Gly760 carbonyl. The Rif2$_{RBM}$ epitope cannot be donated intra-molecularly by

the same Rif2 molecule (*in cis*), since the observed intermolecular distance between Rif2$_{RBM}$ and the

first visible residue of the Rif2-AAA+ fold (Pro61) spans more than 60 Å, while the rms end-to-end

distance of the 14-residue linker (residues 48-61) only extends to about 42 Å (Miller and Goebel,

1968). We find that the Rif2$_{RBM}$ epitope likely originates from a second Rif2 molecule in the crystal

lattice located *ca*. 24 Å away (**Figure 2G**, see **Figure S3B-D** for sequence assignment and validation of

the origin of Rif2$_{RBM}$ in the structure). In line with this finding, an isolated Rif2$_{RBM}$ segment was

sufficient for binding Rap1 *in vitro* (**Figure 2H**, lane 1). Furthermore, a N-terminal fragment encompassing Rif2$_{RBM}$ (residues 1-60) displayed robust binding to Rap1$_{RCT}$ *in vivo* (in a Y2H assay), while mutations in the Rap1 RBM-binding groove (Gly760Arg or Ala733Arg) abolished this interaction (**Figure 2I**).

To evaluate the possible *in vivo* function of these two separate Rap1$_{RCT}$ interaction modules, we generated strains in which three different *rif2$_{AAA+}$* mutant alleles or the *rif2$_{RBM}$* mutant allele replaced the wild-type copy of *RIF2* at its endogenous locus. Each of these mutants exhibited a partial telomere elongation phenotype (**Table 1** and **Figure S3E**), suggesting that the two Rap1-interacting modules make independent contributions to telomere length control by Rif2. As shown in **Table 1**, and discussed in more detail below, each of these modules was also required for the capping function of Rif2 at telomeric DSBs.

Taken together, the data described above suggest that a single Rif2 molecule is able to bind one Rap1 molecule *in cis* (through Rif2$_{AAA+}$) while holding a second Rap1 *in trans* (through Rif2$_{RBM}$), with both interactions contributing to Rif2 function *in vivo*.

A short Rif1 peptide binds the same Rap1$_{RCT}$ cleft as does Rif2

Rif1 recognizes the Rap1$_{RCT}$ domain independently of Rif2 (Hardy et al., 1992). Using Y2H assays, we identified a Rif1 fragment comprising residues 1709-1916, which retained the ability to bind Rap1$_{RCT}$ (**Figure 3A**). Examination of the Rif1 sequence from diverse yeast species revealed a conserved 20 amino acid motif (residues 1752-1772; **Figure S4A**) with sequence similarity to the Rif2$_{RBM}$ motif identified above (**Figure 3B**). An additional conserved region was observed at the very C-terminus of Rif1 (residues 1850-1916) (**Figure 4D**, see below for details). A Rif1-derived peptide containing residues 1752-1772 (referred to as Rif1$_{RBM}$) was co-crystallized with Rap1$_{RCT}$, and allowed structural analysis of the Rif1$_{RBM}$-Rap1$_{RCT}$ complex at 1.6 Å resolution. In the crystal, Rif1$_{RBM}$ binds Rap1$_{RCT}$ as a linear peptide, at a location identical to that of Rif2$_{RBM}$ (**Figure 3C-E**). Rif1$_{RBM}$ forms extended hydrophobic interactions with Rap1$_{RCT}$ through residues Ile1760, Ile1762, Ile1764 and Phe1765

(**Figure 3C**). In accordance with the structure, individual mutations (Ile1760Arg, Ile1762Arg or Ile1764Arg) within Rif1$_{RBM}$ abolished Rap1$_{RCT}$ binding in Y2H assays (**Figure 3A**). We then asked if the Rif1$_{RBM}$ mutant is indeed absent at telomeres *in vivo* due to the loss of Rap1 binding detected by the Y2H assay. Chromatin immunoprecipitation (ChIP) of Myc-tagged wild-type Rif1 showed clear binding at two native telomeres (on chromosomes VI-R and XV-L). The Rif1$_{RBM}$ mutant, in contrast, was not found at either locus under these conditions (**Figure 3F)**, while its expression was clearly detectable by western blot (**Figure S4B**). Comparable Rap1 levels at both telomeres were found in the wild-type and the *rif1$_{RBM}$* mutant strain (**Figure S4C**). Consistent with these findings, mutations of complementary positions in the Rap1 RBM-binding groove (Gly760Arg or Ala733Arg) impaired Rap1 binding to both Rif1$_{RBM}$ and Rif2$_{RBM}$ (**Figure 3A** and **Figure 2I**). The Rap1 RBM-binding groove has previously been observed to interact with a Sir3 peptide (Chen et al., 2011). The binding sites for all three proteins within the Rap1 RBM-binding groove completely overlap imposing mutual exclusivity on the interaction (**Figure 3D** and **3E**). Surprisingly, however, the secondary structure motifs used for Rap1 binding by Rif1, Rif2 and Sir3, as well as the directionality of the protein chains, differ (**Figure 3B**, see **Figure S4D** and **S4E** for detailed discussion).

Rif1$_{RBM}$ and Rif2$_{RBM}$ modulate the balance between telomeric and *HM* locus silencing

Previous Y2H studies have indicated that Rif1 and Rif2 compete with the SIR complex for binding to Rap1 (Buck and Shore, 1995; Moretti et al., 1994; Wotton and Shore, 1997). Consistent with this, both Rif1 and Rif2 appear to be inhibitors of TPE, since *RIF1* deletion and to a lesser extent deletion of *RIF2*, lead to increased telomeric silencing (Kyrion et al., 1993; Wotton and Shore, 1997). Remarkably, these *RIF* deletions, as well as certain mutations in Rap1 that decrease Rif1 binding, lead to a weakening of silencing at the *HMR* silent mating-type locus, pointing to a possible competition between telomeres and *HM* loci for a limited pool of SIR proteins (Buck and Shore, 1995).

To ask whether Rif1$_{RBM}$ and Rif2$_{RBM}$ play a direct role in regulating the balance between TPE and *HM* silencing, we used standard reporter genes placed at a truncated telomere (*telVII-L::URA3*) and at the *HMR* locus (*HMRΔA::TRP1*)(**Figure 3G** and **Table 1**; see **Supplemental experimental procedures** for detailed description). At the telomere, a 100-fold increase in *URA3* repression was observed in the *rif1$_{RBM}$* mutant strain (*rif1$_{RBM}$*: Ile1762Arg-Ile1764Arg), as indicated by growth on the counter-selective drug 5-FOA, an effect similar to that seen in a *rif1Δ* strain. Mutations in the RBM motif of Rif2 (*rif2$_{RBM}$*: Leu44Arg-Val45Glu) gave rise to a TPE phenotype comparable to that of *rif2Δ* cells. The *rif1$_{RBM}$/rif2$_{RBM}$* double mutant showed a greater than additive increase in *URA3* repression (*ca*. 10^3-fold), indicating that Rif1$_{RBM}$ and Rif2$_{RBM}$ synergistically antagonize telomeric silencing. The level of silencing at *HMR* was significantly decreased in the *rif1$_{RBM}$* mutant, as seen by facilitated growth on medium lacking tryptophan. No clear *HMR* silencing phenotype was detected in the *rif2$_{RBM}$* mutant. The *rif1$_{RBM}$/rif2$_{RBM}$* double mutant, however, again led to further de-repression at *HMR* (10-fold) compared to the *rif1$_{RBM}$* mutant alone.

Rif1 and Rif2 negatively regulate telomere length in a telomerase dependent manner (Levy and Blackburn, 2004; Wotton and Shore, 1997). We therefore assessed whether Rif1$_{RBM}$ and Rif2$_{RBM}$ mutations indirectly triggered TPE through telomere elongation, which had previously been shown to increase TPE in otherwise wild-type cells (Kyrion et al., 1993). We observed that the *rif1$_{RBM}$* and *rif2$_{RBM}$* mutants showed only slight telomere elongation phenotypes (**Table 1**, **Figure S4F** and **S3E**). The increased silencing observed in the *rif1* and *rif2* RBM mutants was similar (**Figure 3G** and **Table 1**) to that seen in *rif1Δ* and *rif2Δ* strains, respectively. Telomeres in the *rif1* and *rif2* RBM mutants, on the other hand, were significantly shorter than those from *rif1* or *rif2* deletion strains. Furthermore, telomere elongation beyond 600 bp was required to impact silencing (Kyrion et al., 1993), while length changes triggered by mutations in Rif1$_{RBM}$ and Rif2$_{RBM}$ were significantly below this threshold. We therefore conclude that the increase in silencing observed in *rif1$_{RBM}$* and *rif2$_{RBM}$* mutants *in vivo* is not caused by telomere elongation and is thus likely to result from increased availability of the Rap1 RBM-binding groove for Sir3 binding. Taken together, our results suggest that Rif1 and Rif2 directly

compete with Sir3 for binding to the same RBM-binding groove in Rap1$_{RCT}$. Rap1, using a single mutually exclusive binding site in the Rap1$_{RCT}$ domain, is thus able to integrate opposing cues coming from the RBMs of Sir3 and Rif1/Rif2 into a composite silencing response.

The Rif1$_{CTD}$ serves as a Rap1 binding and tetramerization module

A *rif1* allele encoding a Glu1906Lys mutation, located in the conserved Rif1 C-terminal region (referred to as Rif1$_{CTD}$) *ca.* 100 amino acid residues downstream of Rif1$_{RBM}$ (**Figure 4A**), had previously been shown to abolish binding of Rif1 to Rap1$_{RCT}$ in Y2H assays (Hardy et al., 1992), hinting at the presence of an additional, second Rap1-binding site in Rif1$_{CTD}$. Using limited proteolysis, we were able to map the Rif1$_{CTD}$ domain to residues 1857 to 1916 (data not shown). We subsequently crystallized Rif1$_{CTD}$ and determined its structure using *ab initio* methods at 1.94 Å resolution (**Figure 4B**). Rif1$_{CTD}$ is composed of two anti-parallel Rif1-dimers tetramerizing along the axis of the helix and with pseudo-twofold symmetry. Multi-angle light scattering confirmed that Rif1 is a tetramer in solution (**Figure 4G**), with each Rif1 molecule contributing a helix-loop-helix fold. Intra-dimer packing proceeds in canonical knobs-into-holes fashion, largely driven by internal hydrophobic interactions (Leu1883, Ile1886, Leu1894, Leu1898 and Leu1905) and surface salt bridges (Lys1867-Asp1882, Arg1876-Glu1897) between helices α2, α3 and α4 (**Figure 4C**). The two dimers tetramerize through interactions involving four salt-bridges formed by residues Arg1895 and Glu1906 from the opposing helix α4 (**Figure 4C**). The loops connecting the helices and the residues pointing away from the dimer/tetramer interfaces are hydrophilic in nature.

The isolated Rif1$_{CTD}$ domain alone, in contrast to Rif1$_{RBM}$, failed to co-immunoprecipitate Rap1 in solution, and showed no Rap1 binding in Y2H assays (data not shown). Yet a fragment containing both Rif1$_{RBM}$ and Rif1$_{CTD}$ showed reduced binding in Y2H upon introduction of a Rif1$_{CTD}$ dimer-dimer interface mutation (Leu1905Arg) (**Figure 4E** and **4F**), indicating that Rif1$_{CTD}$ directly contributes to the Rif1-Rap1 interaction. Moreover, the Glu1906Lys mutation in Rif1$_{CTD}$ has previously been shown to be rescued by a compensatory Asp727Ala mutation in Rap1 (identified as

the *rap1-12* allele) (Hardy et al., 1992). Such behavior strongly suggests a direct interaction between Rif1$_{CTD}$ Glu1906 and Rap1$_{RCT}$ Asp727. We observed that the mutation of an additional residue located at the tetramer interface (Arg1895Glu) also impaired Rap1 binding in the Y2H assay (**Figure 4F**). Residues Glu1906 and Arg1895 are therefore most likely at, or at least in proximity to the Rap1-binding site. The exact molecular mechanism by which this low affinity Rif1$_{CTD}$ binding module contributes to Rap1 binding and the number of Rap1 molecules that can be bound by the Rif1$_{CTD}$-tetramer remains to be determined.

Rif2, but not Rif1 RBM mutations, impair the G2/M checkpoint

Defects in replication, repair, or telomere capping result in excess RPA-coated single-stranded DNA (ssDNA), which in turn triggers the G2/M checkpoint response (Lisby and Rothstein, 2004). To address the effect of Rif1 and Rif2 mutations on checkpoint activation, we used a single-cell assay based on *de novo* telomere formation at HO endonuclease-induced DSBs (Michelson et al., 2005), flanked by short (80 bp) telomere repeat tracts (TG80; **Table 1** and **Figure S5A**). In this experimental set-up, wild-type Rif1 and Rif2 are required to prevent short TG80 telomeric tracts from initiating a DNA damage response (Ribeyre and Shore, 2012). Thus, compared to wild-type cells, *rif1Δ* or *rif2Δ* mutants give rise to a transient cell-cycle delay of about 1 h, following HO cutting. We found that mutation of the major Rif2-Rap1 interface Rif2$_{AAA+}$ (Glu347Arg) caused a cell-cycle arrest (~1 h) comparable to that seen in the *rif2Δ* strain (**Table 1**). Mutations in the Rif2-Rap1 *trans*-binding interface Rif2$_{RBM}$ similarly led to a comparable G2/M arrest phenotype (**Table 1**). Rif2-mediated checkpoint inhibition is therefore dependent on Rap1 binding *in cis* (Rif2$_{AAA+}$) and *in trans* (Rif2$_{RBM}$). In a surprising contrast, the Rif1$_{RBM}$ mutant protein, which fails to bind Rap1 in Y2H assays (**Figure 3A**) and is not detectably recruited at native telomeres (**Figure 3F**), conferred no significant cell-cycle arrest phenotype (**Table 1**). We then examined whether the Rif1$_{RBM}$ mutant protein is recruited to telomeric DSBs in order to maintain its anticheckpoint function, as indicated by the *in vivo* G2/M arrest assay. In the absence of an HO-mediated DSB formation at TG80, Rif1$_{RBM}$ was not detectable

at TG80 tracks (**Figure 5A**), similar to what was observed at wild-type telomeres (**Figure 3F**). Following HO cut, wild-type Rif1 is recruited to TG80. Remarkably, Rif1$_{RBM}$ was also readily detectable at the TG80 ends (**Figure 5A**), albeit at lower levels compared to the Rif1 wild-type protein. We therefore conclude that Rif1 is recruited to undamaged native telomeres in a Rap1 dependent manner, whereas direct Rap1 interactions are not essential for the recruitment of Rif1 to TG80 DSBs, and its anticheckpoint function therefore appears largely Rap1 independent.

The Rif1 N-terminus specifically binds to single-stranded/double-stranded junctions

To date, no DNA-binding activity has been reported for *S. cerevisiae* Rif1. Given that we observed Rap1 independent recruitment of Rif1 to TG80 DSBs, we tested by electrophoretic mobility shift assay (EMSA) whether Rif1 might be recruited by binding to telomeric DNA or intermediates formed during its replication and resection. The C-terminus of human Rif1 has previously been reported to bind to a range of DNA substrates, with a preference for branched structures such as Holliday junctions (Xu et al., 2010). Our structure-based sequence alignment of Rif1 orthologs from yeast, other fungi and those of various metazoans, including humans, indicates that the C-termini of *S. cerevisiae* and human Rif1 C-terminal domain II (h-Rif1 C-II) are conserved and share a similar fold (**Figure 4D**). Human Rif1 therefore also likely tetramerizes (whilst having no obvious RBM and thus not localizing to telomeres). Oligomerization of h-Rif1 C-terminus has in fact been observed previously (Xu et al., 2010). We thus assayed the ability of the *S. cerevisiae* Rif1 C-terminus (residues 1709-1916, referred to as Rif1_C, see **Figure 4A**) to bind different DNA structures. Analogously to h-Rif1 C-II, *S. cerevisiae* Rif1_C bound double-stranded DNA (dsDNA) substrates with structural features such as 3' flaps, 5' flaps, replication forks (RF), and Holliday junctions (HJ) (**Figure S5B** and **S5C**). No binding to ssDNA, or linear dsDNA was observed under our experimental conditions.

We next investigated the ability of the Rif1 N-terminus (residues 100-1322, hereafter referred to as Rif1_N, (see **Figure 4A**) to bind linear and branched DNA intermediates. Strikingly, Rif1_N bound a greater range of substrates (**Figure 5C** and **Figure S5D**) than Rif1_C and exhibited a

much higher affinity towards DNA (around 25-fold higher on the substrates bound by Rif1_C). The highest apparent affinity (in the low nano-molar range) was observed for Rif1_N and ssDNA (**Figure 5C,** lanes 1-4). In contrast, binding to dsDNA was 2- to 4-fold reduced (lanes 5-8 and see **Figure S5E** for quantitation), and was only observed at higher protein concentrations. Preferential binding of Rif1_N to branched structures containing ssDNA and dsDNA features, such as 5'-overhangs (lanes 9-12), splayed arm intermediates (SA; lanes 13-16), 3' flaps (lanes 17-20), or 5' flaps (lanes 21-24) over fully double-stranded RF (lanes 25-28) and HJ substrates (lanes 29-32) was also apparent.

Having observed Rif1_N binding to single- and double-stranded DNA, we next determined the substrate length dependency of binding (**Figure 5D**). Rif1_N bound dsDNA weakly when the substrate was 30 bp in length (lanes 13-16), gradually showing more prominent binding once the length of the duplex was increased to 40 bp (lanes 17-20) and 50 bp (lanes 21-24). In contrast, no binding was observed with Rif1_N on a 30 nt (**Figure 5D**, lanes 1-4) or 40 nt (lanes 5-8) ssDNA substrate. A drastic increase in affinity, however, was observed when the oligonucleotide length was extended to 50 nt (lanes 9-12). Comparing the results of ssDNA and dsDNA length dependence, we noted that the 30 nt ssDNA alone was not a substrate (**Figure 5D**, lanes 1-4), and the 30 bp dsDNA was bound only weakly (lanes 13-16). Strikingly, though, combination of the two into a 3'- (or 5')-overhang ssDNA/dsDNA junction molecule gave rise to strong binding (**Figure 5C**, lanes 33-36 and 9-12; see quantitation in **Figure S5D**). The inability of Rif1_N to form stable complexes with a 30 nt ssDNA, in conjunction with the high affinity for 30 nt ssDNA moieties within flap and overhang substrates, suggests that Rif1_N possesses specificity for structural features inherent to ssDNA/dsDNA junctions.

Rif1 displaces RPA at ssDNA/dsDNA junctions

At functional telomeres, the single-stranded G-rich 3'-overhang is bound and protected by the yeast CST complex. Inactivation of Cdc13 leads to telomere uncapping and subsequent DNA end resection in G2/M, allowing RPA to bind the nascent single-stranded region and subsequently trigger a

Mec1/Ddc2-dependent checkpoint response (Dewar and Lydall, 2012; Enomoto et al., 2002). Previous studies demonstrated that Rif1 dampens the checkpoint response (anticheckpoint function) and that deletion of *RIF1* leads to increased RPA recruitment to telomeric DSBs (Ribeyre and Shore, 2012; Xue et al., 2011). These observations imply a functional antagonism between Rif1 and RPA. The anticheckpoint activity of Rif1 could reside in the N-terminus, as the Rif1_N construct (a protein devoid of both Rif1$_{RBM}$ and Rif1$_{CTD}$) has been shown to retain its localization to resected sub-telomeric regions and its anticheckpoint properties (Xue et al., 2011). The molecular mechanism by which this is mediated is currently unknown.

We thus set out to test the idea that the DNA-binding activity we observed for Rif1_N may mediate anticheckpoint activity, and that Rif1 may compete for binding to ssDNA with RPA, the high affinity single-strand binding protein complex found in all eukaryotes. When comparing ssDNA and dsDNA-binding by Rif1_N and RPA side-by-side (**Figure 5E**), we observed that they bound ssDNA with similar apparent affinities, while RPA, as expected, displayed no dsDNA-binding activity. We next performed competitive DNA-binding reactions (**Figure 5F**). Having observed binding of Rif1_N to ssDNA and the 3'-overhang substrate, we thus asked whether Rif1_N and RPA directly crosstalk on ssDNA. We found that RPA avidly bound the ssDNA substrate (lanes 2-4) and that subsequent addition of Rif1_N did not result in disruption of RPA-DNA complexes (lanes 5-7). Pre-bound Rif1_N (lane 8) on ssDNA, on the other hand, was readily displaced by incoming RPA (lanes 9-11). We then used a 3'-overhang instead of ssDNA as substrate, given the observed Rif1_N specificity for ssDNA/dsDNA junctions demonstrated above. Remarkably, incoming Rif1_N (lanes 16-18) effectively displaced RPA, which itself forms stable complexes with the ssDNA moiety of this substrate (lanes 12-15). Complete displacement of RPA on the ssDNA moiety of the junction was observed when Rif1_N and RPA were present at approximately equimolar concentration (lane 17). Addition of RPA to pre-bound Rif1_N-DNA junctions, on the other hand, did not result in removal of Rif1_N (lanes 19-22). These findings demonstrate that Rif1_N cannot outcompete RPA on a 60 nt ssDNA, but that Rif1_N can effectively outcompete and dissociate RPA from ssDNA near ssDNA/dsDNA junctions,

such as those found at naturally occurring telomeres and resected DSBs. This is consistent with the notion that the Rif1$_{RBM}$ mutant protein, which fails to bind Rap1 and is not detectably recruited at native telomeres (**Figure 3F**), was readily detectable at TG80 DSBs (**Figure 5A**). Such a model would further predict that, *in vivo*, RPA at TG80 DSBs is displaced by Rif1 in a Rap1-independent manner. Indeed, we observe that, while RPA strongly accumulates at TG80 DSBs in the absence of Rif1, very little accumulation above wild-type levels is seen in the presence of the Rif1$_{RBM}$ mutant protein (**Figure 5B**). Taken together, these and other data (Ribeyre and Shore, 2012; Xue et al., 2011) strongly support the idea that Rif1 directly competes with RPA for binding ssDNA at ssDNA/dsDNA junctions *in vivo* to exert its anticheckpoint function*.*

Since Rif2 is also implicated in the anticheckpoint response at short telomeres (Ribeyre and Shore, 2012), we addressed the capacity of Rif2 to bind DNA. We found weak binding of full-length Rif2 to dsDNA, but no clear binding to ssDNA (**Figure S5F**), which makes any direct competition between Rif2 and RPA unlikely. Binding of Rif1 and Rif2 to dsDNA was sequence independent and was not enhanced by the presence of Rap1-binding sites within the DNA substrate (**Figure S5G-J**).

4   Discussion

The structural, biochemical and cell biological data presented here allow us to define the molecular basis of Rap1-Rif1-Rif2 architecture at telomeric arrays and illustrate how these components contribute to telomeric silencing and the inhibition of checkpoint activation at telomeres or telomere-like DSBs.

Directed assembly of Rif1, Rif2 and Rap1 at telomeres

Arrays of Rap1-binding sites are required for telomere homeostasis, yet Rap1 binds these sites, *in vitro*, in an independent and non-cooperative manner. How repeats of Rap1-binding sites, by themselves, give rise to domains of specialized structure and function at telomeres and how Rif1 and Rif2 assemble at these Rap1 arrays, but not elsewhere, has been difficult to reconcile. We find that Rif1-Rap1 and Rif2-Rap1 serve as the principal structural units in solution, and that they cooperatively interact once juxtaposed on Rap1-binding site arrays. Through Rif1 oligomerization and Rap1 binding, Rif2 binding to Rap1 both *in cis* and *in trans*, in conjunction with other potential interfaces on Rif2 (see **Figure S6A-S6D**), the Rap1-Rif1-Rif2 complex assembles in a cooperative fashion on Rap1 arrays. This behavior results in preferential stabilization of Rap1 by Rif1 and Rif2 on DNA repeats by a factor of more than 16-fold when compared to Rap1 alone (compare lanes 9 and 11 in **Figure 1D**; quantitation in **Figure 1F**). Such cooperativity is expected to increase with increasing numbers of Rap1-binding sites, hence being less favorable for the single and double binding sites found at promoters. Moreover, single-particle electron-microscopy studies localized Rap1 deeply buried within TFIID and TFIID-TFIIA complexes at promoters (Papai et al., 2010), likely providing further spatial constraints for Rif1/Rif2 interactions. Rif1/Rif2 do not bind to these genomic sites, instead they cooperatively bind telomeric Rap1 arrays, providing a mechanistic rationale for Rap1-Rif1-Rif2 recruitment and spreading along telomeres, which then confers telomeric function.

Redundancy of Rif1 and Rif2 assembly and function at telomeres

Rif1 and Rif2 show functional redundancy *in vivo*. We find this redundancy mirrored in the protein architecture: both Rif1 and Rif2 possess an RBM epitope and a second, non-overlapping, Rap1-binding site (Rif1$_{CTD}$ and Rif2$_{AAA+}$). The flexible linkers connecting each RBM epitope with a multimerization domain allow Rif1 and Rif2 to bind Rap1 molecules over large distances (Rif1:110 Å linker; Rif2:42 Å linker). Rif1 mediates multimerization by the Rif1$_{CTD}$ domain and Rif2 through the ability of binding two Rap1 molecules (*in cis* and *trans*). The structural, biochemical and *in vivo* characterization presented herein suggests that Rif1 and Rif2 act synergistically in silencing and telomere length regulation and are able to compensate partially for the respective loss of the other. Because Rif1 and Rif2 target the same Rap1 RBM-binding groove, which is also the binding site for Sir3, each one of them is individually able to compete with Sir3 for Rap1 over long distances. Our finding thereby provides a molecular basis for the modulation of telomeric silencing by Rif1 and Rif2. Interestingly, Sir4 binds to a distal epitope N-terminal to the Rap1$_{RCT}$ (Moretti et al., 1994) and may thus *co*-exist with Sir3 or Rif1/Rif2, regardless of which protein occupies the Rap1 RBM-binding groove. The redundant presence of a long-range RBM coupled to a multimerization module is also expected to assemble higher-order structures at telomeres (see below), which will similarly persist even if either Rif1 or Rif2 were absent.

Model for Rap1-Rif1-Rif2 binding to telomeric duplex arrays

The available structures of the Rap1-DNA complex (Konig et al., 1996; Matot et al., 2012; Taylor et al., 2000) and that of the Rif1-Rap1 and Rif2-Rap1 complexes determined in this study allow us to build a three-dimensional model of the major telomeric protein assembly at budding yeast TG$_{1-3}$ duplex repeats (**Figure 6**), addressing architecture and unifying functional and structural data. Small angle X-ray scattering (SAXS) studies of full-length Rap1 showed reorientation of Rap1$_{RCT}$ with respect to the Rap1 DNA-binding domain (Rap1$_{Myb}$) following DNA recognition (**Figure 6A**) (Matot et al., 2012). Superposition of the Rif2-Rap1$_{RCT}$ structure onto this Rap1-DNA SAXS model sandwiches

Rif2 between $Rap1_{Myb}$ and $Rap1_{RCT}$ (**Figure 6B**), placing the Rif2 AAA+ domain in direct proximity to DNA. This is in agreement with unspecific DNA-binding observed for Rif2 (**Figure S5I**) and the DNA-binding mode observed in existing AAA+ protein-DNA *co*-complex structures (Duderstadt et al., 2011; Dueber et al., 2007; Gaudier et al., 2007). Both $Rif2_{RBM}$ and $Rif2_{AAA+}$ contribute to Rap1 binding *in vitro*, and mutations in both domains exhibited *in vivo* phenotypes. As Rif2 is unable to bind the same Rap1 molecule through its AAA+ and RBM interface simultaneously, a heterogeneous binding mode has to be considered where Rap1 is bound to either the $Rif2_{RBM}$ or the $Rif2_{AAA+}$ interface (**Figure 6B**: Rap1[#1] depicted as bound by $Rif2_{RBM}$, while Rap1[#5] is held by $Rif2_{AAA+}$). The Rap1 RCT and Myb domains are connected through a 70 amino acid linker, with a predicted *intra*-molecular distance between the two domains up to of 90 Å. Under these conditions, closely positioned, neighboring Rap1 molecules can be interlinked by Rif2 *in cis* (via $Rif2_{AAA+}$) and *trans* (via $Rif2_{RBM}$), resulting in the formation of dimers of Rif2-Rap1 units (referred to as *trans-dimer*), as well as further oligomers of Rif2-Rap1 *trans*-dimers. Such a *trans*-dimeric/oligomeric model with Rap1-binding sites spaced 19 bp apart is shown in **Figure 6B** (see linking neighboring units Rap1[#2,3,4]). Due to the length restriction of the flexible linker, the formation of Rif2-Rap1 *trans*-dimers is dependent on the DNA spacing and the radial orientation between Rap1-binding sites. We estimate that Rap1-binding sites spaced more than 30 bp apart would likely preclude the formation of such Rap1-Rif2 *trans*-dimers, in the absence of large distortions of the DNA.

A Rif2-Rap1 *trans-dimer* composed of two Rap1 molecules involves two $Rif2_{AAA+}$ domains and only one $Rif2_{RBM}$, hence leaving one Rap1 RBM-binding groove unoccupied (due to the inability of Rif2 to bind the same Rap1 *in cis* and *trans*, see **Figure 6B** Rap1[#2]). A free Rap1 RBM-site next to a DNA gap too large to be bridged by Rif2 *in trans*, is a principal binding site for Rif1 (**Figure 6B,** see Rap1[#2] having an unoccupied RBM-binding groove which is closed by $Rif1_{RBM}$ in **Figure 6C** and **6D**). Rif1 has the necessary structural and biochemical properties to bind to unoccupied Rap1 RBM-binding grooves near these large gaps: through its long linker Rif1 can contact Rap1 molecules up to 110 Å away (**Figure 6C**); while the Rif1 N-terminus through its double-stranded DNA-binding activity

can directly bind DNA gaps free of Rap1 or Rif2 (**Figure 5D,** lanes 13-24). Our results suggest that, at undamaged telomeres, Rif1 recruitment is mediated largely by protein-protein interactions between Rif1$_{RBM}$ and Rap1$_{RCT}$, while at resected telomere junctions our results are consistent with DNA-dependent recruitment (see below).

The molecular basis of G2/M checkpoint inhibition by Rif1 and Rif2

We find a pronounced effect of Rif2 on the G2/M checkpoint response, which is Rap1 dependent and mediated by the Rif2$_{RBM}$-Rap1 and Rif2$_{AAA+}$-Rap1 interfaces. The Rif1$_{RBM}$ mutant retains is anticheckpoint activity while being absent at normal telomeres. Our Rif1 *in vitro* studies provide a biochemical rationale for this *in vivo* behavior. We observe very pronounced affinity of Rif1_N for a wide range of DNA substrates, especially to ssDNA in excess of 50 nt. Rif1_N specifically recognizes substrates containing a ssDNA/dsDNA junction: the isolated Rif1_N is unable to compete with RPA for ssDNA-binding, but can effectively prevent RPA from binding to ssDNA when juxtaposed to a ssDNA/dsDNA junction. The Rif1_N is capable of displacing tightly bound RPA from the single-stranded moiety of the junction. Due to the extraordinary affinity of RPA for ssDNA of K_d = 25 nM (Dickson et al., 2009), we suggest that additional DNA repair factors are similarly outcompeted by Rif1 at the junction of resected DSBs *in vivo*. In accordance with this, Rif1 has also been shown to attenuate the arrival of Rad24 at *de novo* telomeres *in vivo* (Ribeyre and Shore, 2012). As the N-terminus of Rif1, which is able to bind ca. 50 nt ssDNA, can tetramerize through the Rif1$_{CTD}$ domain, the full-length Rif1 assembly may bind >200 nt of ssDNA. These biochemical findings show that Rif1 is equipped with the necessary attributes to bind resected telomeres independently of Rap1, to occupy the telomeric ssDNA/dsDNA junction and to exclude DNA-repair factors such as RPA (**Figure 6E**).

It is tempting to speculate that, besides its likely contribution to telomere architecture (**Figure 6C**), the Rif1 N-terminus may help to prevent unscheduled DNA damage responses at telomeres in the normal cell-cycle. Outside late S/G2 phase, the telomeric G-overhang is typically *ca.*

12-15 nt in length (Larrivee et al., 2004), too short for Rif1 single-stranded binding given the observed length restriction (greater than 50 nt). Instead, the G-rich overhang is held by CST in a sequence-specific fashion (Lin and Zakian, 1996; Mitton-Fry et al., 2002). In S/G2 phase, however, when Rif1 protein levels peak (Smith et al., 2003) and the length of G-overhangs temporarily increases to 100 nt (Wellinger et al., 1993b), Rif1 is ideally situated to bind to the extended telomeric single-stranded overhang. It could thereby assist in CST-mediated telomere capping once CST becomes limiting, serving to prevent inadvertent checkpoint activation by the G-rich 3'-overhang.

We established Rif1 as a junction binding protein able to antagonize RPA *in vitro* and *in vivo*, providing a framework for Rif1 function in cells (Ribeyre and Shore, 2012; Xue et al., 2011). Further work is needed to define the precise role of Rif1 at resected junctions and its interplay with the DNA-repair machinery at yeast telomeres. It is of note that Rif1 is also present in metazoans, where it is not considered a telomere protein (Buonomo et al., 2009; Xu and Blackburn, 2004). We find that the Rif1$_{CTD}$ tetramerization domain (**Figure 4D**) and the Rif1_N domain (Xu et al., 2010, data not shown) are structurally conserved between yeast and humans. The metazoan protein has acquired additional domains through which is seems to be able to associate with the TopIIIα-BLM-RMI1 complex (Xu et al., 2010; Xue et al., 2011) instead of Rap1, as in yeasts. In light of this structural conservation in Rif1_N and Rif1_C, it is tempting to speculate that metazoan Rif1 similarly serves to block the recruitment of DNA-repair factors, creating a comparable exclusion zone for repair protein assembly near junctions, thereby counteracting checkpoint activation.

The multivalent binding interfaces present in Rif1 and Rif2, in conjunction with the ability to bind Rap1 through long- and short-range linkers, provide a model for the molecular "Velcro" that organizes Rap1 arrays at telomeres. The ability to interlink distant Rap1-Rif1-Rif2 complexes (up to 110 Å apart), possibly even on neighboring chromosomes, may additionally offer ways to stabilize telomeric fold-back structures, or drive telomeric clustering at the nuclear periphery *in vivo* (**Figure S6E**). Should telomere capping be compromised, the Velcro serves a dual purpose as "Band-Aid",

detecting resected junctions and dampening the checkpoint response until telomeres become critically short.

Understanding repeats in the genome, what makes these DNA arrays 'special'?

Our data provide a molecular and conceptual framework to explain how DNA repeats binding common transcription factors such as Rap1 can be converted into domains of specialized structure and function. We identify an underlying system of cooperative binding coupled to multivalent long- and short-range interactions that gives rise to novel functional properties that are more than the sum of their parts. These architectural principles are expected to extend to other DNA arrays of binding factors in metazoan cells, at telomeres and beyond.

5   Experimental Procedures

Protein expression and purification

S. cerevisiae Rif2 (residues 66-380) and full-length Rif2 (residues 1-395) constructs carried N-terminal GST tags, Rif1_C (residues 1709-1916) a N-terminal $(His)_6$-tag. These constructs were expressed from pGEX-derived vectors in *Escherichia coli* BL21(DE3) pLysS. $Rap1_{\Delta BRCT}$ (residues 353-827), $Rap1_{RCT}$ (residues 672-827), full-length Rap1 (residues 1-827), and Rif1_N (residues 100-1322) were produced in High Five insect cells (Invitrogen) as cleavable N-terminal Strep-tag fusions. Cells were lysed by sonication and proteins isolated by affinity chromatography utilizing their respective tags. Tags were removed with TEV protease and the resultant protein purified by ion exchange chromatography followed by size exclusion chromatography. Purification procedures are described in detail in the **supplemental experimental procedures**. Yeast RPA (a kind gift from Dr Petr Cejka) was purified as outlined in (Alani et al., 1992).

Crystallization and structure determination

Crystallization conditions, data collection, structural determination methods and refinement statistics are given in **Table S1** and described in the **supplemental experimental procedures**.

Yeast two-hybrid studies

Y2H assays were carried out as described (James et. al, 1996). Mutations in plasmids pGAD-Rif1(1709-1916) and pGBD-Rap1(672-827) were introduced using the QuikChange II site-directed mutagenesis kit (Stratagene). Chromosomal *RIF2* (strain Y88) or *RIF1* (strain Y87) was deleted for studies mapping the protein-protein interactions between Rif1 and Rap1, and Rif2 and Rap1, respectively.

Silencing assay

Transcriptional silencing was assayed in derivatives of strain YG16 (listed in **Table S2**) with a *TRP1* reporter gene positioned at a modified *HMR* locus carrying an A-site deletion (*HMRΔA*). Telomeric silencing was studied in the same strains, but using a *URA3* reporter at a telomeric position on chromosome VII.

Telomere blots

Genomic DNA from overnight yeast cultures of the indicated strains listed in **Table S2** was prepared and analyzed as described (Puglisi et al., 2008).

G2/M assay and Chromatin immunoprecipitation (ChIP)

The G2/M cell-cycle arrest assay and ChIP were performed as described (Ribeyre and Shore, 2012) using the indicated strains listed in **Table S2**, which contain a single HO endonuclease cleavage site flanked by short (80 bp) telomeric repeats.

DNA substrates

DNA substrates were prepared by annealing the synthetic oligonucleotides listed in **Table S3**. One oligonucleotide was 5'-labeled with Cy5 for duplex Tel19 (oligos 1 and 2) and Tel31 (oligos 3 and 4). Non-specific competitor duplex contained unlabeled oligos 5 and 6. The Tel80 substrate was prepared by PCR with 5'-Cy5-labeled oligonucleotides 14 and unlabeled oligo 15 on plasmid pYTCA-1x and purified using anion-exchange chromatograph (Source15Q; GE Healthcare), followed by DNA precipitation. ^{32}P-labeled DNA substrates were prepared as described (Rass et al., 2010) by annealing the following component oligonucleotides: HJ, oligos 7-10; dsDNA, oligos 7 and 11; SA, oligos 7 and 10; 3' flap, oligos 7, 10 and 12; 5' flap, oligos 7, 10 and 13; RF, oligos 7, 10, 12 and 13; 5'-overhang, oligos 7 and 13; 3'-overhang, oligos 7 and 21; ss_50 nt, oligo 16; ss_40 nt, oligo 18; ss_30 nt, oligo 20; ds_50 bp, oligos 16 and 17; ds_40 bp, oligos 18 and 19; ds_30 bp, oligos 20 and 21.

Electrophoretic mobility shift assay (EMSA)

Reactions with Cy5-labeled DNA (15 μl) were performed in 20 mM Tris-HCl pH 7.5, 10 mM MgCl$_2$, 50 mM KCl, 50 mM NaCl, 1 mM TCEP, 0.5 mM spermidine, 100 ug/ml BSA, 10% glycerol, 0.1% NP40, with the indicated amounts of protein and DNA. EMSAs with ^{32}P-labeled DNA (10 μl) were performed in 20 mM mM Tris-HCl pH 7.5, 5 mM MgCl$_2$, 100 mM NaCl, 100 ug/ml BSA, 5% glycerol. Incubation was performed on ice for 30 min unless stated otherwise. Non-specific competitor DNA was incubated with protein for 10 min prior to addition of labeled DNA substrates. Electrophoresis was performed at 4°C using 4-20% or 6% PAA gels (Invitrogen) for Tel31 and Rif1_C substrates, respectively. Reactions containing Tel80 or Rif1_N were resolved using 1% or 1.2% agarose gels, respectively. Cy5-labeled DNA substrates were detected using a TYPHOON 940 imaging system, ^{32}P-labeled DNA was analyzed by autoradiography and phosphorimaging.

6 Acknowledgments

7 References

Addinall, S.G., Holstein, E.M., Lawless, C., Yu, M., Chapman, K., Banks, A.P., Ngo, H.P., Maringele, L., Taschuk, M., Young, A.*, et al.* (2011). Quantitative fitness analysis shows that NMD proteins and many other protein complexes suppress or enhance distinct telomere cap defects. PLoS Genet *7*, e1001362.

Alani, E., Thresher, R., Griffith, J.D., and Kolodner, R.D. (1992). Characterization of DNA-binding and strand-exchange stimulation properties of y-RPA, a yeast single-strand-DNA-binding protein. J Mol Biol 227, 54-71.

Anbalagan, S., Bonetti, D., Lucchini, G., and Longhese, M.P. (2011). Rif1 supports the function of the CST complex in yeast telomere capping. PLoS Genet *7*, e1002024.

Aparicio, O.M., Billington, B.L., and Gottschling, D.E. (1991). Modifiers of position effect are shared between telomeric and silent mating-type loci in S. cerevisiae. Cell *66*, 1279-1287.

Bianchi, A., and Shore, D. (2007). Increased association of telomerase with short telomeres in yeast. Genes & Development *21*, 1726-1730.

Bianchi, A., and Shore, D. (2008). Molecular biology. Refined view of the ends. Science *320*, 1301-1302.

Bonetti, D., Clerici, M., Manfrini, N., Lucchini, G., and Longhese, M.P. (2010). The MRX complex plays multiple functions in resection of Yku- and Rif2-protected DNA ends. PLoS One *5*, e14142.

Buck, S.W., and Shore, D. (1995). Action of a RAP1 carboxy-terminal silencing domain reveals an underlying competition between HMR and telomeres in yeast. Genes & Development *9*, 370-384.

Buonomo, S.B., Wu, Y., Ferguson, D., and de Lange, T. (2009). Mammalian Rif1 contributes to replication stress survival and homology-directed repair. J Cell Biol *187*, 385-398.

Chen, Y., Rai, R., Zhou, Z.R., Kanoh, J., Ribeyre, C., Yang, Y., Zheng, H., Damay, P., Wang, F., Tsujii, H.*, et al.* (2011). A conserved motif within RAP1 has diversified roles in telomere protection and regulation in different organisms. Nat Struct Mol Biol *18*, 213-221.

de Lange, T. (2005). Shelterin: the protein complex that shapes and safeguards human telomeres. Genes & Development *19*, 2100-2110.

de Lange, T. (2009). How telomeres solve the end-protection problem. Science *326*, 948-952.

Dewar, J.M., and Lydall, D. (2012). Similarities and differences between "uncapped" telomeres and DNA double-strand breaks. Chromosoma *121*, 117-130.

Dickson, A.M., Krasikova, Y., Pestryakov, P., Lavrik, O., and Wold, M.S. (2009). Essential functions of the 32 kDa subunit of yeast replication protein A. Nucleic Acids Res *37*, 2313-2326.

Dubrana, K., van Attikum, H., Hediger, F., and Gasser, S.M. (2007). The processing of double-strand breaks and binding of single-strand-binding proteins RPA and Rad51 modulate the formation of ATR-kinase foci in yeast. J Cell Sci 120, 4209-4220.

Duderstadt, K.E., Chuang, K., and Berger, J.M. (2011). DNA stretching by bacterial initiators promotes replication origin opening. Nature *478*, 209-213.

Dueber, E.L., Corn, J.E., Bell, S.D., and Berger, J.M. (2007). Replication origin recognition and deformation by a heterodimeric archaeal Orc1 complex. Science *317*, 1210-1213.

Feeser, E.A., and Wolberger, C. (2008). Structural and functional studies of the Rap1 C-terminus reveal novel separation-of-function mutants. J Mol Biol *380*, 520-531.

Gao, H., Cervantes, R.B., Mandell, E.K., Otero, J.H., and Lundblad, V. (2007). RPA-like proteins mediate yeast telomere function. Nat Struct Mol Biol *14*, 208-214.

Gaudier, M., Schuwirth, B.S., Westcott, S.L., and Wigley, D.B. (2007). Structural basis of DNA replication origin recognition by an ORC protein. Science *317*, 1213-1216.

Gilson, E., Roberge, M., Giraldo, R., Rhodes, D., and Gasser, S.M. (1993). Distortion of the DNA double helix by RAP1 at silencers and multiple telomeric binding sites. J Mol Biol *231*, 293-310.

Gottschling, D.E., Aparicio, O.M., Billington, B.L., and Zakian, V.A. (1990). Position effect at S. cerevisiae telomeres: reversible repression of Pol II transcription. Cell *63*, 751-762.

Hardy, C.F., Sussel, L., and Shore, D. (1992). A RAP1-interacting protein involved in transcriptional silencing and telomere length regulation. Genes & Development *6*, 801-814.

Hirano, Y., Fukunaga, K., and Sugimoto, K. (2009). Rif1 and Rif2 inhibit localization of Tel1 to DNA ends. Mol Cell *33*, 312-322.

Konig, P., Giraldo, R., Chapman, L., and Rhodes, D. (1996). The crystal structure of the DNA-binding domain of yeast RAP1 in complex with telomeric DNA. Cell *85*, 125-136.

Kyrion, G., Liu, K., Liu, C., and Lustig, A.J. (1993). RAP1 and telomere structure regulate telomere position effects in Saccharomyces cerevisiae. Genes & Development *7*, 1146-1159.

Larrivee, M., LeBel, C., and Wellinger, R.J. (2004). The generation of proper constitutive G-tails on yeast telomeres is dependent on the MRX complex. Genes & Development *18*, 1391-1396.

Levy, D.L., and Blackburn, E.H. (2004). Counting of Rif1p and Rif2p on Saccharomyces cerevisiae telomeres regulates telomere length. Mol Cell Biol *24*, 10857-10867.

Lieb, J.D., Liu, X., Botstein, D., and Brown, P.O. (2001). Promoter-specific binding of Rap1 revealed by genome-wide maps of protein-DNA association. Nat Genet *28*, 327-334.

Lin, J.J., and Zakian, V.A. (1996). The Saccharomyces CDC13 protein is a single-strand TG1-3 telomeric DNA-binding protein in vitro that affects telomere behavior in vivo. Proc Natl Acad Sci U S A *93*, 13760-13765.

Lisby, M., and Rothstein, R. (2004). DNA damage checkpoint and repair centers. Curr Opin Cell Biol *16*, 328-334.

Marcand, S., Brevet, V., and Gilson, E. (1999). Progressive cis-inhibition of telomerase upon telomere elongation. Embo J *18*, 3509-3519.

Marcand, S., Gilson, E., and Shore, D. (1997). A protein-counting mechanism for telomere length regulation in yeast. Science *275*, 986-990.

Marcand, S., Pardo, B., Gratias, A., Cahun, S., and Callebaut, I. (2008). Multiple pathways inhibit NHEJ at telomeres. Genes & Development *22*, 1153-1158.

Matot, B., Le Bihan, Y.V., Lescasse, R., Perez, J., Miron, S., David, G., Castaing, B., Weber, P., Raynal, B., Zinn-Justin, S.*, et al.* (2012). The orientation of the C-terminal domain of the Saccharomyces cerevisiae Rap1 protein is determined by its binding to DNA. Nucleic Acids Res *40*, 3197-3207.

McGee, J.S., Phillips, J.A., Chan, A., Sabourin, M., Paeschke, K., and Zakian, V.A. (2010). Reduced Rif2 and lack of Mec1 target short telomeres for elongation rather than double-strand break repair. Nat Struct Mol Biol *17*, 1438-1445.

Michelson, R.J., Rosenstein, S., and Weinert, T. (2005). A telomeric repeat sequence adjacent to a DNA double-stranded break produces an anticheckpoint. Genes & Development *19*, 2546-2559.

Miller, W.G., and Goebel, C.V. (1968). Dimensions of protein random coils. Biochemistry *7*, 3925-3935.

Mitton-Fry, R.M., Anderson, E.M., Hughes, T.R., Lundblad, V., and Wuttke, D.S. (2002). Conserved structure for single-stranded telomeric DNA recognition. Science *296*, 145-147.

Moretti, P., Freeman, K., Coodly, L., and Shore, D. (1994). Evidence that a complex of SIR proteins interacts with the silencer and telomere-binding protein RAP1. Genes & Development *8*, 2257-2269.

Moretti, P., and Shore, D. (2001). Multiple interactions in Sir protein recruitment by Rap1p at silencers and telomeres in yeast. Mol Cell Biol *21*, 8082-8094.

Negrini, S., Ribaud, V., Bianchi, A., and Shore, D. (2007). DNA breaks are masked by multiple Rap1 binding in yeast: implications for telomere capping and telomerase regulation. Genes & Development *21*, 292-302.

Papai, G., Tripathi, M.K., Ruhlmann, C., Layer, J.H., Weil, P.A., and Schultz, P. (2010). TFIIA and the transactivator Rap1 cooperate to commit TFIID for transcription initiation. Nature *465*, 956-960.

Puglisi, A., Bianchi, A., Lemmens, L., Damay, P., and Shore, D. (2008). Distinct roles for yeast Stn1 in telomere capping and telomerase inhibition. Embo J *27*, 2328-2339.

Rass, U., Compton, S.A., Matos, J., Singleton, M.R., Ip, S.C., Blanco, M.G., Griffith, J.D., and West, S.C. (2010). Mechanism of Holliday junction resolution by the human GEN1 protein. Genes & Development *24*, 1559-1569.

Ribeyre, C., and Shore, D. (2012). Anticheckpoint pathways at telomeres in yeast. Nat Struct Mol Biol *19*, 307-313.

Rusche, L.N., Kirchmaier, A.L., and Rine, J. (2002). Ordered nucleation and spreading of silenced chromatin in Saccharomyces cerevisiae. Mol Biol Cell 13, 2207-2222.

Sabourin, M., Tuzon, C.T., and Zakian, V.A. (2007). Telomerase and Tel1p preferentially associate with short telomeres in S. cerevisiae. Mol Cell *27*, 550-561.

Shore, D., and Nasmyth, K. (1987). Purification and cloning of a DNA binding protein from yeast that binds to both silencer and activator elements. Cell *51*, 721-732.

Smith, C.D., Smith, D.L., DeRisi, J.L., and Blackburn, E.H. (2003). Telomeric protein distributions and remodeling through the cell cycle in Saccharomyces cerevisiae. Mol Biol Cell *14*, 556-570.

Taylor, H.O., O'Reilly, M., Leslie, A.G., and Rhodes, D. (2000). How the multifunctional yeast Rap1p discriminates between DNA target sites: a crystallographic analysis. J Mol Biol *303*, 693-707.

Teixeira, M.T., Arneric, M., Sperisen, P., and Lingner, J. (2004). Telomere length homeostasis is achieved via a switch between telomerase- extendible and -nonextendible states. Cell *117*, 323-335.

Vodenicharov, M.D., Laterreur, N., and Wellinger, R.J. (2010). Telomere capping in non-dividing yeast cells requires Yku and Rap1. Embo J *29*, 3007-3019.

Vodenicharov, M.D., and Wellinger, R.J. (2006). DNA degradation at unprotected telomeres in yeast is regulated by the CDK1 (Cdc28/Clb) cell-cycle kinase. Mol Cell *24*, 127-137.

Wellinger, R.J., Wolf, A.J., and Zakian, V.A. (1993). Saccharomyces telomeres acquire single-strand TG1-3 tails late in S phase. Cell *72*, 51-60.

Williams, T.L., Levy, D.L., Maki-Yonekura, S., Yonekura, K., and Blackburn, E.H. (2010). Characterization of the yeast telomere nucleoprotein core: Rap1 binds independently to each recognition site. J Biol Chem *285*, 35814-35824.

Wotton, D., and Shore, D. (1997). A novel Rap1p-interacting factor, Rif2p, cooperates with Rif1p to regulate telomere length in Saccharomyces cerevisiae. Genes & Development *11*, 748-760.

Xu, D., Muniandy, P., Leo, E., Yin, J., Thangavel, S., Shen, X., Ii, M., Agama, K., Guo, R., Fox, D., 3rd, *et al.* (2010). Rif1 provides a new DNA-binding interface for the Bloom syndrome complex to maintain normal replication. Embo J *29*, 3140-3155.

Xu, L., and Blackburn, E.H. (2004). Human Rif1 protein binds aberrant telomeres and aligns along anaphase midzone microtubules. J Cell Biol *167*, 819-830.

Xue, Y., Rushton, M.D., and Maringele, L. (2011). A novel checkpoint and RPA inhibitory pathway regulated by Rif1. PLoS Genet *7*, e1002417.

Yarragudi, A., Parfrey, L.W., and Morse, R.H. (2007). Genome-wide analysis of transcriptional dependence and probable target sites for Abf1 and Rap1 in Saccharomyces cerevisiae. Nucleic Acids Res *35*, 193-202.

8 Figure legends

Figure 1. Cooperative binding of Rif1, Rif2 and Rap1 to telomeric repeats

EMSA assays were performed with purified Rap1 (353-827), Rif1 (1709-1916) and Rif2 (1-395), and Cy5-labeled Tel80 DNA (67 nM) containing five Rap1-binding sites. Tel80 was pre-incubated with Rap1 for 10 min on ice before adding Rif1 and/or Rif2.

(A) Rif1, Rif2 and Rap1 form ternary complexes on Rap1-DNA arrays. Tel80 bound with Rap1 was titrated with Rif1, Rif2 or Rif1 and Rif2 in the presence of a 10-fold nucleotide excess of competitor DNA with a non-telomeric, random sequence. Reactions contained 83 nM Rap1 and were titrated with 83, 167, 333, and 667 nM of Rif1 and/or Rif2.

(B) Rap1-Rif1-Rif2 ternary complexes on Rap1-DNA arrays are mediated by protein-protein interactions. Protein-DNA complexes on Tel80 were titrated with unspecific competitor DNA (2-, 4-, and 10-fold nucleotide excess). In the absence of Rap1, Rif1 and Rif2 dissociated from Tel80 in the presence of increasing amounts of competitor DNA, while the ternary Rap1-Rif1-Rif2 complexes remained stable on Tel80. Rap1, Rif1, and Rif2 were used at protein concentrations of 267, 333, and 333 nM, respectively.

(C) Rif1, Rif2, and Rap1 bind to telomeric repeats in a cooperative manner. Proteins were pre-incubated with Tel80 for 30 min in the presence of a 10-fold nucleotide excess of unspecific competitor DNA. After adding sequence-specific competitor DNA (Tel19) containing a single Rap1-binding site, incubation was continued for 1 h. Tel19 associated Rap1-binding sites were in 1- and 2.5-fold excess over Tel80 associated sites. Protein concentrations were as in (B). Rap1 dissociation from telomeric repeats was prevented by the presence of Rif1, Rif2, or Rif1 and Rif2, indicative of cooperative binding.

(D) Quantitative titration of Rap1 on Tel80 in the presence of sequence-specific competitor DNA Tel19. The reactions were performed as in (C) with 4-, 22- and 64-fold molar excess of Tel19-based Rap1-binding sites and overnight incubation.

(E) Quantitation of the EMSA experiments shown in (C). Relative release of Rap1 from Tel80 is shown as the ratio of the additive signal from free Tel80 and Rap1-Tel80 complex 1 to total substrate signal. Release in the presence of Rap1 alone is set to 100% release.

(F) Quantitation of the EMSA experiments shown in (D). Release of Rap1 from Tel80 is shown as the ratio of the additive signal from free Tel80 and Rap1-Tel80 complex 1 to total substrate signal.

Figure 2. Crystal structure and functional analysis of Rif2 and the full-length Rif2-Rap1$_{RCT}$ complex

(A) Ribbon representation of the Rif2 (66-380) structure and schematic representation of full-length Rif2 with domain boundaries. The α-bundle domain (helices α0 and α6-10) is shown in blue, the $\alpha\beta\alpha$ ASCE-domain in green and the C-terminal domain (CTD) in gray.

(B) Ribbon representation of the full-length Rif2-Rap1$_{RCT}$ complex. Rap1$_{RCT}$ is colored in yellow; Rif2-ASCE in green; Rif2 α-bundle in blue; Rif2-RBM in red; Rif2-CTD in gray.

(C-E) Close up views illustrating the interfaces between Rap1$_{RCT}$ and (C) the Rif2-CTD, (D) the Rif2 α-bundle and (E) the Rif2-RBM domains.

(F) Rif2 utilizes multiple domains to interact with Rap1. Strep-pulldown of Rap1$_{RCT}$ in the presence of GST-Rif2ΔNTD (residues 66-395), GST-Rif2ΔCTD (residues 1-380), GST-Rif2 full-length, and GST-Rif2ΔNTDΔCTD (66-380). Deletion of the N- or C-terminus of Rif2 reduced binding to Rap1, while combined deletion abolished any interaction between these proteins (see **Figure S3A** for the loading and pulldown controls).

(G) The Rif2-RBM domain bound to Rap1$_{RCT}$ is donated *in trans* through a neighboring Rif2 molecule. Rap1$_{RCT}$ and Rif2 molecules are shown in the same colors as in (A). The last amino acid of the Rif2-RBM domain (Lys48) visible in the electron density map is marked in red and the first amino acid of the Rif2-AAA+ fold (Pro61) in blue for the *trans*-binding Rif2 molecule, and in gray for the *cis*-binding Rif2 molecule. Dotted lines indicate the two possibilities for the origin of Rif2-RBM: *in trans*-binding

in blue and *in cis*-binding in gray. Due to the limited length of the linker between the RBM and the

AAA+ domains of Rif2, binding between Rap1$_{RCT}$ and Rif2$_{RBM}$ must occur *in trans*.

(H) Reciprocal pulldown of Strep-Rap1$_{RCT}$ and GST-Rif2$_{RBM}$ (residues 1-60) in the presence or absence

of His-Rif2ΔNTD (residues 65-395). Proteins were expressed individually in *E. coli* and lysates were

mixed as indicated. The left panel shows direct interaction between Rif2$_{RBM}$ and Rap1$_{RCT}$. The right

panel demonstrates that Rif2$_{RBM}$ and the remainder of the Rif2 molecule (Rif2ΔNTD) can bind to

Rap1 independently.

(I) Yeast two-hybrid mapping of interactions between Rif2 and Rap1. Full-length Rif2 (residues 1-395)

and Rif2$_{RBM}$ (residues 1-60) were used to create Gal4 activation domain (GAD) fusion proteins that

were tested against a Gal4 DNA-binding domain (GBD) bait protein fusion with Rap1 (residues 672-

827) or two mutant derivatives (Gly760Arg or Ala733Arg) of the RBM-binding cleft, as indicated.

Tenfold serial dilutions of cells transformed with the indicated constructs were spotted onto the

indicated drop-out media. Growth on plates lacking histidine (SC-Leu-Trp-His) reveals a positive

interaction, whereas growth on the SC-Leu-Trp control plates selects for cells containing both the

bait and prey plasmids. A *rif1Δ* reporter strain (Y87, **Table S2**) was used as the experimental

background to eliminate competition by endogenous Rif1. Control experiments using the empty

pGAD or pGBD vectors showed no reporter gene activation for any of the constructs used here (data

not shown).

Figure 3. Crystal structure and *in vivo* analysis of the Rif1$_{RBM}$-Rap1$_{RCT}$ complex

(A) Yeast two-hybrid mapping of interactions between Rif1 and Rap1. A C-terminal fragment of Rif1

(Rif1_WT; residues 1710-1916) or three different Rif1$_{RBM}$ mutant derivatives (Ile1764Arg, Ile1762Arg

or Ile1760Arg) were fused to GAD and tested with a GBD-Rap1 (residues 672-827) fusion protein as

bait. For these experiments, a *rif2Δ* reporter strain (Y88, **Table S2**) was used. Assays were performed

as described in **Figure 2I**.

(B) Structure-based sequence alignment of Rif1$_{RBM}$, Rif2$_{RBM}$ and Sir3$_{RBM}$. Secondary structures of the peptides are indicated above the amino acid sequences. The interactions of the three peptides with Rap1$_{RCT}$ involve hydrophobic residues at equivalent positions in Rif1$_{RBM}$ (I1760, I1762, I1764, F1765), Rif2$_{RBM}$ (L39, L42, L44, V45) and Sir3$_{RBM}$ (L471, L468, I463, M462) are highlighted in red.

(C) Cartoon representation of the Rap1$_{RCT}$-Rif1$_{RBM}$ complex. Rap1$_{RCT}$ is shown in yellow, the Rif1$_{RBM}$ peptide as stick representation in cyan. The interaction residues between Rap1 and Rif1 are shown in the close up view on top.

(D) Ribbon representation of Rif2$_{RBM}$-Rap1$_{RCT}$ and Sir3$_{RBM}$-Rap1$_{RCT}$ in the same orientation as in (C). The Rif2 peptide is shown in red and the Sir3 peptide in gray.

(E) Superposition of Rap1$_{RCT}$–Rif1$_{RBM}$, Rap1$_{RCT}$-Rif2$_{RBM}$ and Rap1$_{RCT}$-Sir3$_{RBM}$ structures shows mutual exclusive binding behavior of the three peptides in the Rap1 RBM-binding groove. Proteins color coded as in (C) and (D). Sir3$_{RBM}$ is bound in the reverse orientation in respect to Rif1$_{RBM}$ and Rif2$_{RBM}$ binding.

(F) Chromatin immunoprecipitation (ChIP) analysis of Rif1 recruitment at undamaged native telomeres in the wild-type (YSM53-2) and the *rif1$_{RBM}$* (YSM54-2) mutant strains. Wild-type Rif1 and the Rif1$_{RBM}$ mutant protein were Myc-tagged. Results are reported as average fold enrichment and s.d. relative to an internal control sequence within the *PDI1* gene on chromosome III (see **experimental procedures**).

(G) Telomeric and *HMR*-mediated transcriptional silencing was assayed using *telVII::URA3* and *hmrΔA::TRP1* reporter constructs in strains YG16 (*RIF1 RIF2*) and its derivatives Y103 (*rif1Δ RIF2*), Y104 (*RIF1 rif2Δ*), Y105 (*rif1Δ rif2Δ)* Y96 (*rif1$_{RBM}$, RIF2*), Y98 (*RIF1 rif2$_{RBM}$*), and Y102 (*rif1$_{RBM}$ rif2$_{RBM}$*) listed in **Table S2**. Growth on medium containing 5-FOA indicates increased telomeric silencing, while growth on medium lacking Trp indicates a decrease in *HMR*-mediated silencing. Mutations in Rif1$_{RBM}$ (I1762R/I1764R), Rif2$_{RBM}$ (L42K/L44R/V45E) or Rif1$_{RBM}$ and Rif2$_{RBM}$ lead to silencing phenotypes similar to those observed after deletion of *RIF1*, *RIF2 or RIF1* and *RIF2*, respectively.

Figure 4. Crystal structure of the Rif1$_{CTD}$ tetramer

(A) Schematic representation of full-length *S. cerevisiae* Rif1 with domain boundaries.

(B) Top and side view of the Rif1$_{CTD}$-tetramer with protomers colored in cyan, magenta, pale cyan, and light pink. The pseudo-twofold symmetry axes are indicated by the x- and y-axes.

(C) Close up views illustrating the Rif1$_{CTD}$ dimer (intradimer) and tetramer (interdimer) interfaces. The top panel depicts the hydrophobic interactions located at the inner side of the intradimer interface. The middle panel shows the two surface salt bridge interactions at the dimer interface. Salt bridge interactions (Arg1895-Glu1906) originating from the tetramer interface are represented in the bottom panel. Due to the pseudo-twofold symmetry, the intradimer and interdimer interactions are found twice along the non-crystallographic symmetry axes.

(D) Structure-based sequence alignment of *S. cerevisiae* Rif1$_{CTD}$ with metazoan Rif1 C-II domains shows Rif1$_{CTD}$ conservation across species. The secondary structure of *S. cerevisiae* Rif1$_{CTD}$ is indicated on top. Conserved residues are colored in shades of yellow.

(E) Analytical size exclusive chromatography of the Rif1 C-terminal domain. Purified Rif1_WT protein (residues 1709-1916) elutes from a Superdex 200 column at a higher apparent molecular weight (about 440 kDa) than Rif1 mutant L1905R (approximate 75 kDa) according to the GE calibration kit, indicating that oligomerization is disrupted by the mutation.

(F) Rif1 utilizes the RBM and the CTD domains to interact with Rap1. The yeast two-hybrid assay was performed as described for **Figure 2I**, with Rif1 (1709-1916) and Rap1 (672-827) as GAD and GBD fusions. Rif1$_{RBM}$ mutation I1760R abolished the binding to Rap1. Both dimer (L1905R) and tetramer (R1895E) interface mutations in the CTD domain impaired interactions between Rif1 and Rap1, indicating a direct effect of Rif1$_{CTD}$ on Rif1 and Rap1 interaction.

(G) Rif1 is a tetramer in solution. Analysis of the Rif1 molecular weight by size exclusion chromatography multi-angle light scattering (SEC-MALS) using a wild-type Rif1 fragment containing Rif1$_{CTD}$ (residues 1709-1916).

Figure 5. Rif1 binds DNA and competes with RPA at ssDNA/dsDNA junctions

(A) The Rif1$_{RBM}$ mutant protein is recruited to telomeric DSBs. ChIP analysis of Rif1 recruitment following HO cleavage at TG80 telomeric tracts. Wild-type (YCR263) and *rif1$_{RBM}$* mutant (YSM52-2) strains are Myc-tagged. The calculations were performed as in **Figure 3F**.

(B) The Rif1$_{RBM}$ mutant protein is able to inhibit RPA recruitment at resected TG80 telomeric tracts. ChIP analysis of RPA before and after cut in wild-type (YCR263), *rif1Δ* (YCR201) and *rif1$_{RBM}$* (YSM52-2) mutant strains. Immunoprecipitation of RPA was performed with a specific antibody (Pierce Biotechnology, PA1-10301). Enrichments were measured as in **Figure 3F**.

(C-F) The interactions of Rif1_N (residues 100-1322) and DNA were studied by electromobility shift assays (EMSAs) using a range of 5'-^{32}P labeled DNA substrates. Protein-DNA complexes were resolved by neutral agarose gel electrophoresis and visualized by autoradiography and phosphorimaging.

(C) Interactions of Rif1_N (0, 10, 20, and 40 nM) with a set of linear and branched DNA substrates (1 nM), as indicated above. A quantitation of this experiment is shown in **Figure S5D**.

(D) Length-dependent DNA-binding of Rif1_N was assessed by incubating increasing amounts of protein (0, 20, 40, and 80 nM) with ssDNA and dsDNA substrates (5 nM) of 30, 40, and 50 nucleotides or base pairs, respectively.

(E) Side-by-side analysis of Rif1_N (10, 20, 40, 80, 160, 320 nM) and purified yeast RPA complex (5, 10, 20, 40, 80, 160 nM) bound with ssDNA and dsDNA (2 nM) of 60 nt and 60 bp, respectively.

(F) Rif1_N displaces RPA from ssDNA/dsDNA junctions but not from ssDNA. A ssDNA substrate of 60 nt or a 3'-overhang substrate consisting of a 30 nt ssDNA and a 30 bp dsDNA components (40 nM) were pre-incubated with 80 nM RPA (lanes 5-7 and 16-18) or 80 nM Rif1_N (lanes 8-11 and 19-22) on ice for 30 min. Increasing amounts of Rif1_N (20, 80, 320 nM) or RPA (20, 40, 80 nM) were then added to pre-formed RPA-DNA or Rif1_N-DNA complexes, respectively, and incubation was continued for 30 min. Lanes 1 and 12 contain the mock treated substrates without protein; lanes 2-4

and 13-15 show reactions containing only RPA (20, 40, 80 nM), and lanes 8 and 19 reactions with only Rif1_N (80 nM).

Figure 6. Model of Rap1-Rif1-Rif2 assembly at telomeres

(A) Cartoon illustration of Rap1 bound to telomeres depicting five Rap1 molecules in complex with their cognate target sites. Rap1[#2,3,4] are spaced 19 bp apart. The Rap1 double Myb domains are shown in orange; the Rap1 RCT domain is depicted in yellow. The Rap1(Myb) and the Rap1(RCT) domains are connected by flexible linkers shown as dotted line. The Rap1 BRCT domain was omitted for clarity.

(B) Cartoon illustration of Rif2 bound to Rap1 arrays on telomere with $Rif2_{AAA+}$ shown in green and $Rif2_{RBM}$ in red. The flexible linker between $Rif1_{RBM}$ and $Rif2_{AAA+}$ spanning up to *ca*. 42 Å is shown as red dotted line. The three closely positioned Rap1 molecules (#2 to #4) are interlinked by the $Rif2_{AAA+}$ and the $Rif2_{RBM}$ domains *in trans*.

(C) Cartoon illustration of Rif1 and Rif2 bound to Rap1 telomeric arrays. Rap1 and Rif2 are presented the same as in (B). The $Rif1_{CTD}$, $Rif1_{RBM}$ and Rif1_N domains are colored in blue. The long flexible linker is shown as dotted line between $Rif1_{CTD}$ and $Rif1_{RBM}$ spanning up to ca. 110 Å.

(D) Structural model of the telosome based on the color scheme in (C). DNA, $Rif1_{RBM}$ and $Rif2_{RBM}$ are shown as surface representation with other protein domains shown as ribbons.

(E) Cartoon illustration of Rif1_N localization at resected telomeres. Rif1_N is shown in blue, the double-stranded telomere in dark gray and the resected single strand in light gray.

9 Table

Table 1. Summary of the *in vivo* assays of Rif1 and Rif2 mutants.

| | Genotype | G2/M arrest assay | | Telomere length | Silencing deficiency (TPE/HMR) |
		Average restart time (hrs)	Phenotype similar to (WT/Δ)		
Controls	WT	4.1	WT	WT	WT/WT
	rif2Δ	5.1	Δ	++	++/WT
Rif2$_{AAA+}$-Rap1 Interface	*rif2-F342A*	4.6	Δ	+	n.d.
	rif2-T346A	4.7	Δ	+	n.d.
	rif2-E347R	5.1	Δ	+	n.d.
Rif2$_{RBM}$-Rap1 Interface	*rif2-L44R-V45E*	4.7	Δ	+	++/WT
Controls	WT	4.1	WT	WT	WT/WT
	rif1Δ	4.9	Δ	+++	+++/---
Rif1$_{RBM}$-Rap1 interface	*rif1-I1762R-I1764R*	4.3	WT	+	+++/---

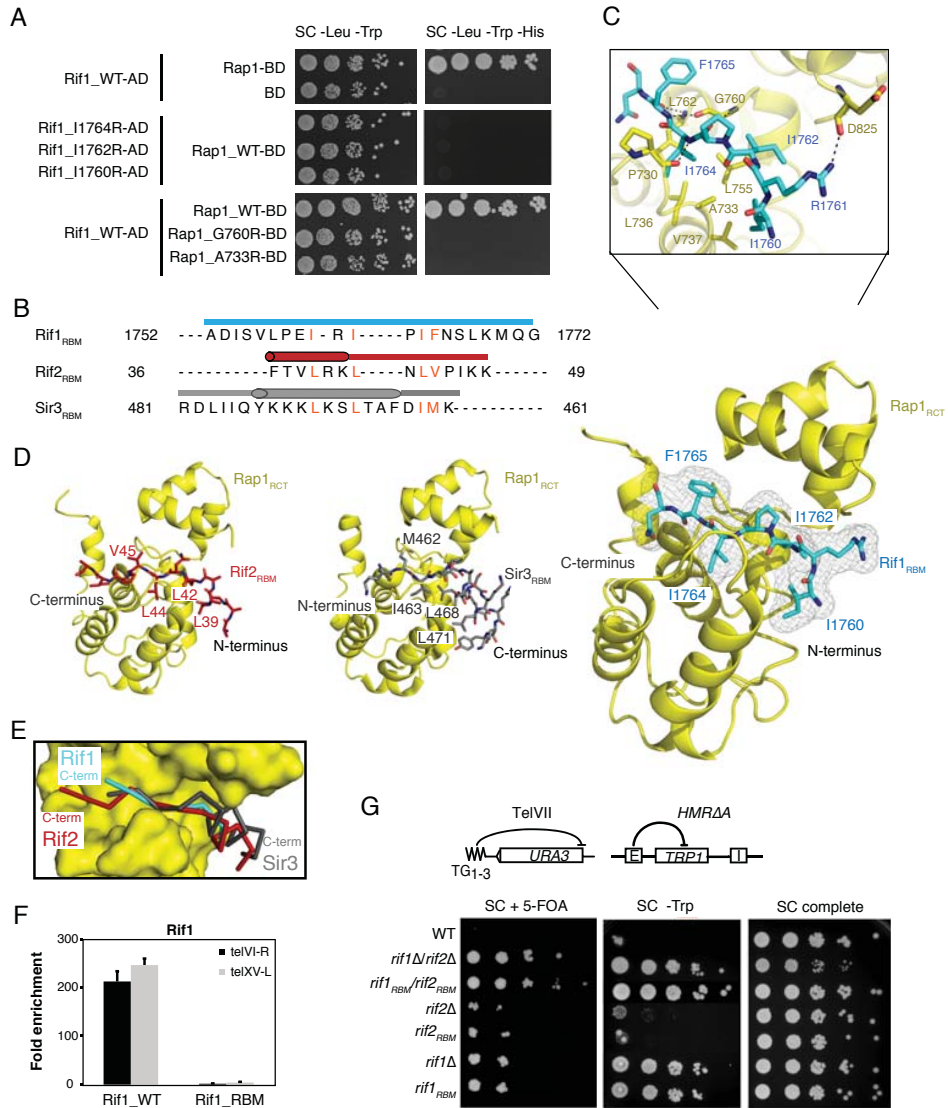"+" Indicates increase; "-" indicates decrease
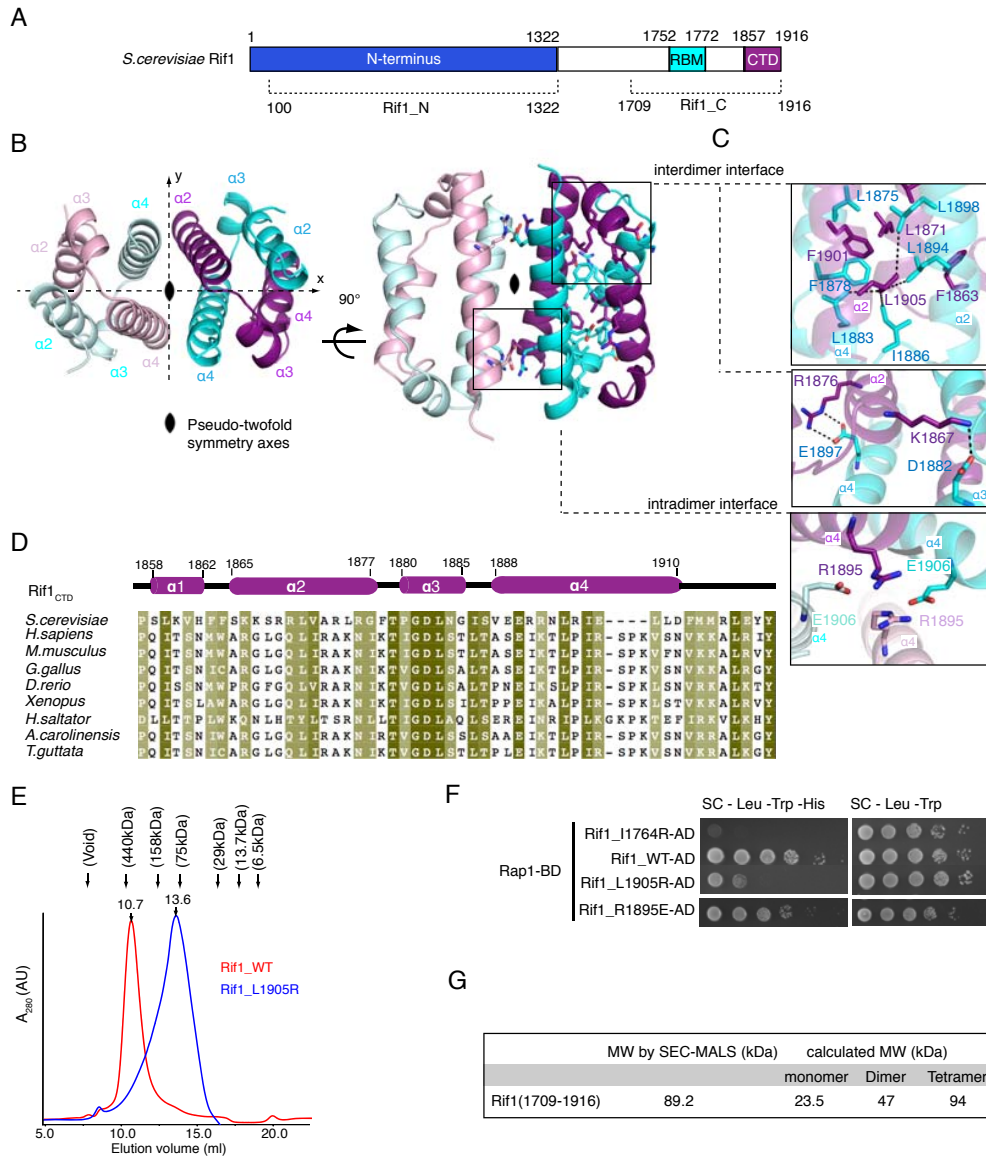
10 Figures

Figure 1
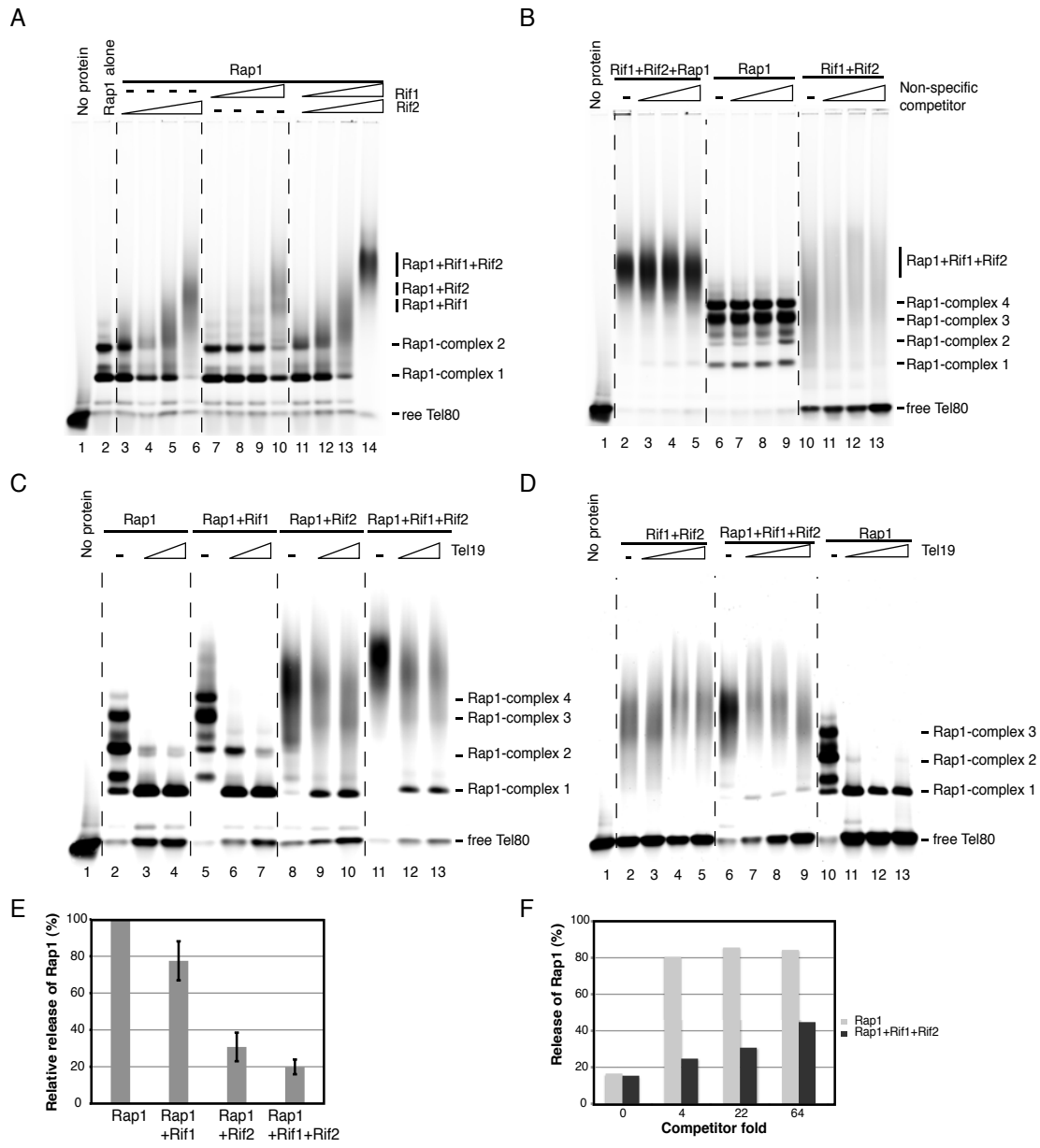
Figure 2
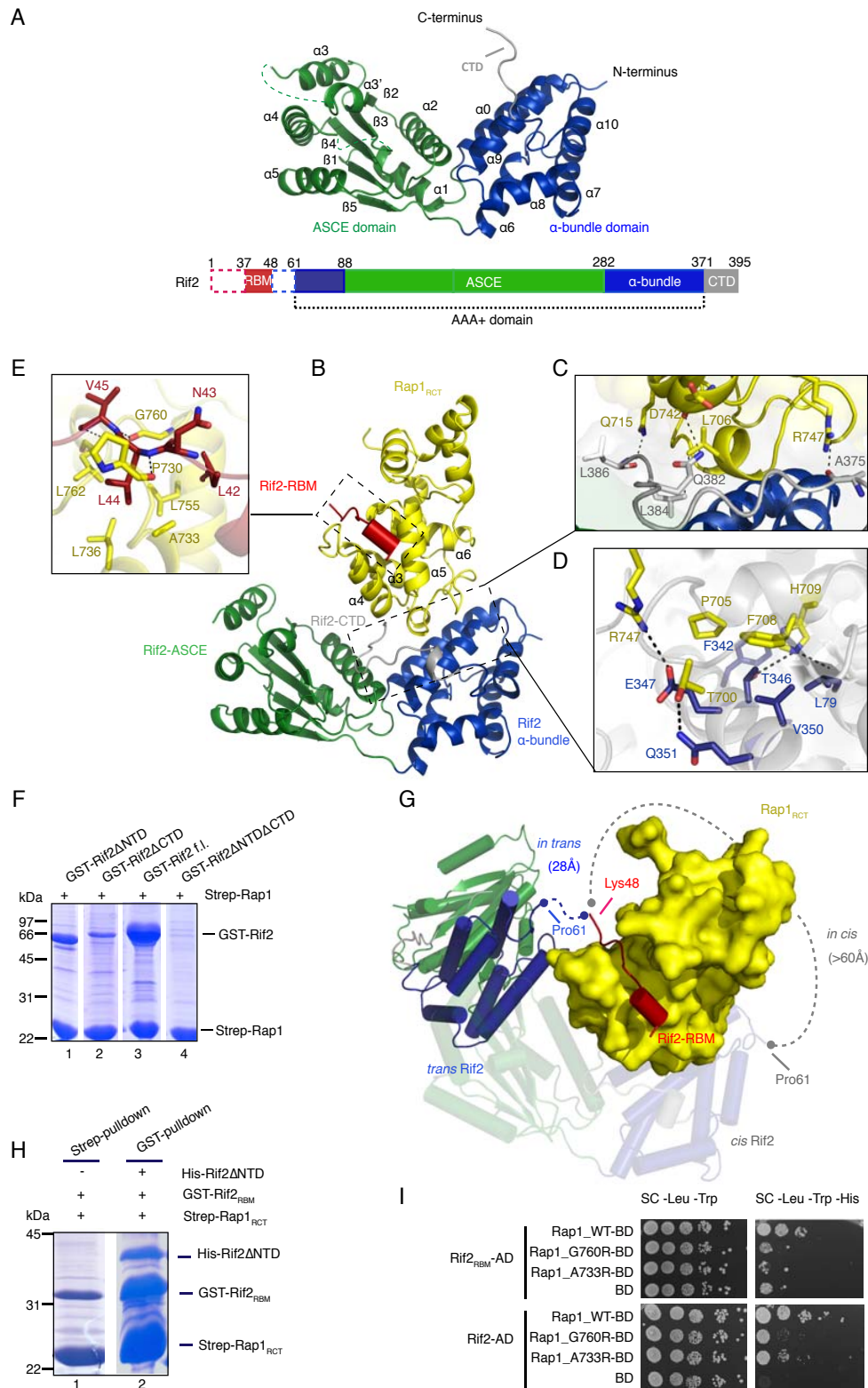
Figure 3

Figure 4

Figure 5

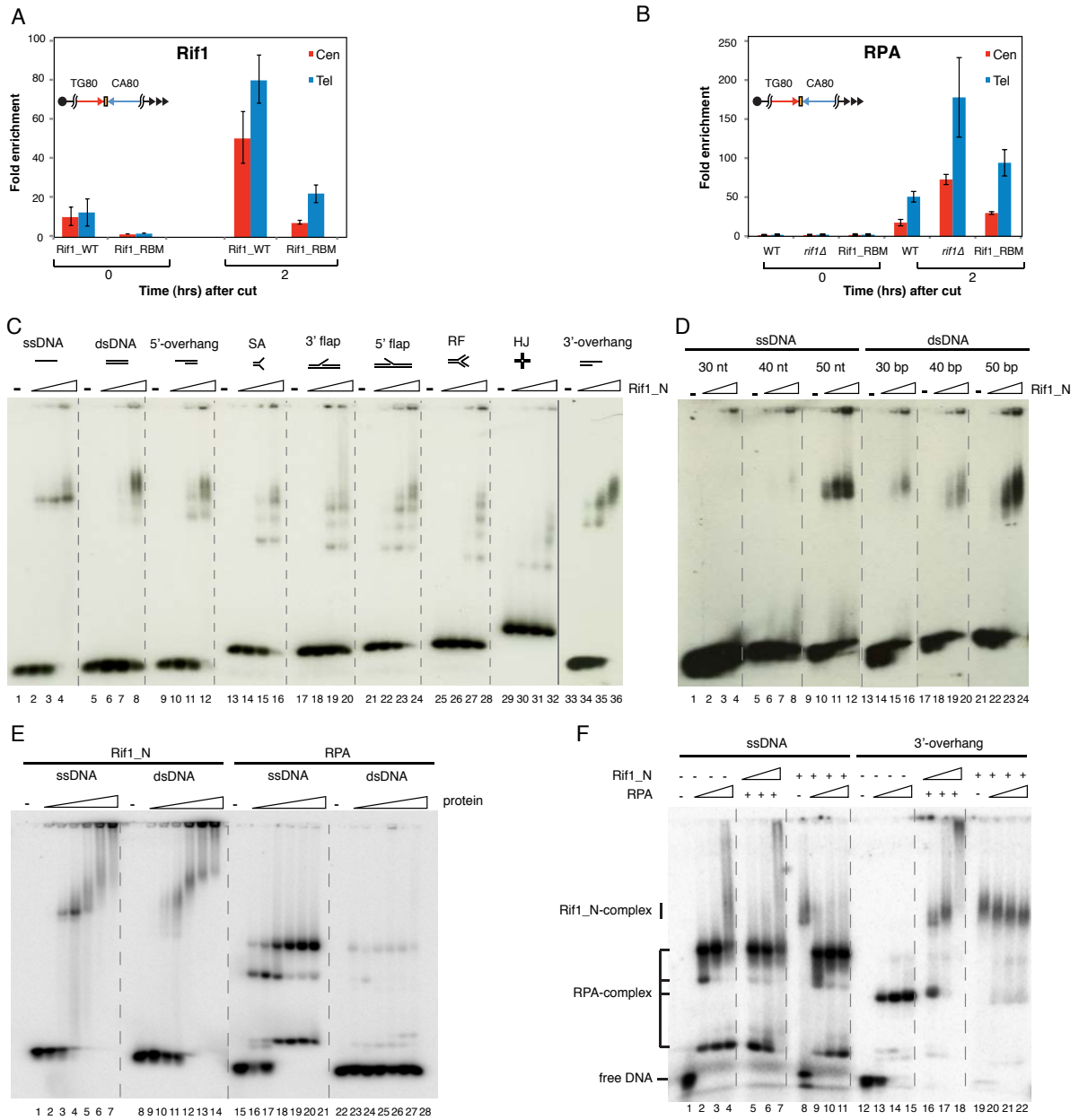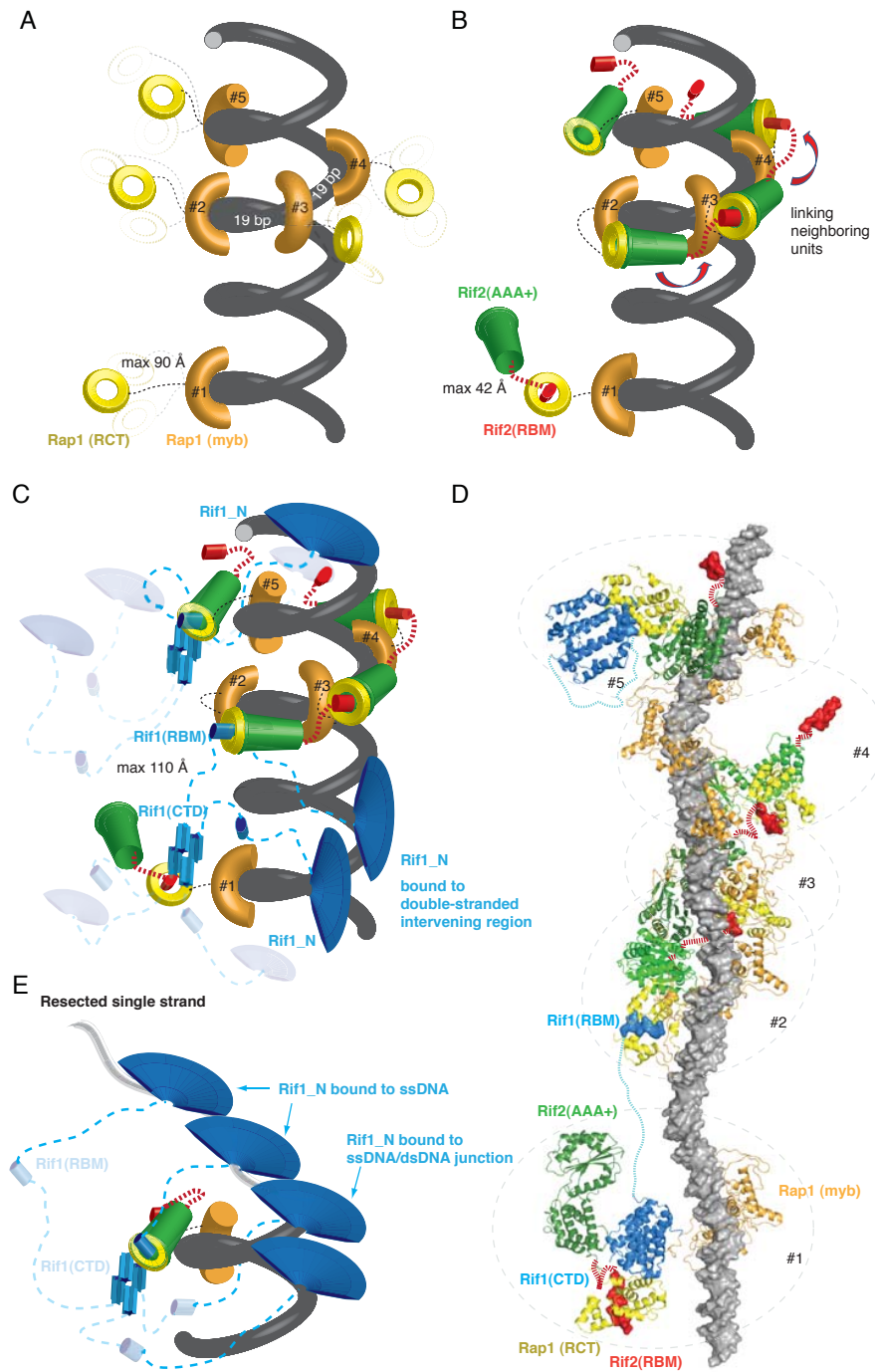Figure 6

11 SUPPLEMENTAL DATA

Figure S1. Rap1, Rif1 and Rif2 form a ternary complex on DNA. Related to Figure 1

(A) To confirm the interactions between Rap1, Rif1, and Rif2 observed in Y2H studies, we performed Strep-pulldown experiments with recombinant Rap1 (672-827), Rif1 (1709-1916), and full-length Rif2. Rif1 and Rif2 could be co-precipitated by Strep-Rap1 from cell lysates, either separately or simultaneously (lanes 2, 3 and 5), demonstrating direct Rap1-Rif1 and Rap1-Rif2 interactions in solution. In contrast, Step-Rif2 failed to co-precipitate Rif1 (lane 4), even in the presence of Rap1, where only trace amounts of Rif1 were detected (lane 6), indicating that Rif1 and Rif2 do not interact directly and that no stable Rap1-Rif1-Rif2 ternary complex exists in solution. Protein bands marked by an asterisk contain non-specific contaminants as confirmed by mass spectrometry.

(B and C) The Rif1 N-terminus and the Rap1 BRCT-domain are dispensable for Rap1-Rif1-Rif2 ternary complex formation on DNA. (B) To investigate the effect of the Rif1 N-terminus (residues 100-1322, Rif1_N) on the recruitment of Rif1 or Rif2 to DNA-bound Rap1, we performed titrations of Rif2 and Rif1_C (residues 1709-1916) (0.17, 0.33, 0.83 μM each) in the presence of constant amounts of Rap1ΔBRCT (267 nM) and Tel80 (67 nM), while adding Rif1_N *in trans* (0.17, 0.33, 0.83 μM). Reactions contained a 10-fold molar excess of non-specific competitor DNA with random sequence. No pronounced difference in ternary complex formation was observed in the presence or absence of Rif1_N (compare lanes 1-3 and 4-6). Note that full-length Rif1 is not available for testing at present.

(C) Full-length Rap1, or Rap1ΔBRCT, were incubated with increasing amounts of Rif1 plus Rif2 in the presence of a 10-fold molar excess of non-specific competitor DNA. Protein and DNA amounts as in (B). The presence of BRCT domain in full-length Rap1 did not improve the Rif recruitment as evident by the absence of an EMSA shift of Rap1 at lower concentration of Rif1 and Rif2 (compare lanes 1-4 and lanes 5-8).

(D) Binding of Rif1, Rif2, and Rap1 to a 31 bp duplex DNA containing two Rap1-binding sites (Tel31). Reactions contained 100 nM Cy5-labled DNA, 267 nM Rap1, 2 μM Rif1, and 0.33 μM Rif2. Tel31 was pre-incubated with Rap1 for 10 minutes in the presence or absence of competitor DNA before Rif1 or Rif2 were added. Characteristic electrophoretic mobility shifts of Rap1-coated Tel31 in the presence of Rif1 (lane 3), Rif2 (lane 4), or Rif1 and Rif2 (lane 5) indicate the formation of a ternary Rap1-Rif1-Rif2 complex on Tel31. This complex was stable in the presence of a 10-fold molar excess of competitor DNA with an unrelated nucleotide sequence (lane 8). While stable Rap1-Rif1 (lane 11) and Rap1-Rif2 (lane 12) complexes were also observed in the presence of a 60-fold molar excess of poly(d(I-C)), no ternary Rap1-Rif1-Rif2 complex could be detected under these conditions (lane 13). Due to intrinsic, sequence-independent DNA-binding activity, Rif1 and Rif2 do not remain associated with Tel31 in the presence of excess competitor when Rap1 is absent (lanes 9, 10, 14 and 15).

(E-F) Release of Rif1, Rif2 and Rap1 from TG_{1-3} arrays is in part kinetically limited (kinetic cooperativity). EMSA reactions contained 67 nM Cy5-labled Tel80 and 267 nM Rap1. (E) Tel80 and specific competitor Tel19 harboring a single Rap1-binding site (at 1-, 11- and 22-fold Rap1-binding site excess), were added at different times during the total 1 h incubation. Rap1 was most effectively displaced from Tel80 when competitor Tel19 was added prior to (lanes 12-14 and 6-8), or at the same time as Tel80 (lanes 3-5). When Tel19 was added after Tel80, Rap1 displacement was only partial (lanes 9-11). Rap1 displacement from DNA is therefore slow. The high affinity of Rap1 (K_d of Rap1 = 13 pM (Vignais et al., 1990)) coupled with slow dissociation apparently gives rise to equilibration on the time scale of hours. Therefore, protein-DNA complexes in (F) were incubated with competitor DNA for 1 h and overnight.

(F) For the analysis of Rap1-Rif1-Rif2, both Rif1 and Rif2 were used at protein concentrations of 83, 167, 333, and 667 nM in the presence of a 1-, 5- or 20-fold Rap1-binding sites excess of competitor Tel19. Cooperativity was observed in both instances (compare lanes 6-9 and lanes 10-13), whereas Rap1-Rif1-Rif2 was more effectively displaced after overnight incubation (compare lanes 7-9 from 1 h and overnight incubation). This suggests that the observed cooperativity is in part due to (small <20%) kinetic effects in addition to the observed equilibrium effects. As the doubling time of yeast cells is in the range of 1.25-2 h, the kinetic component can be expected to be of biological relevance.

Figure S2. Rif2 belongs to AAA+ family. Related to Figure 2

(A) Comparison of the Rif2 structure with different subgroups of the AAA+ family identified Rif2 as a member of the initiator clade. A schematic representation of protein topology shows the characteristic insertion of a long helix (highlighted in red) inserted between β2 and α2 of the ASCE domain colored in green. This insertion comprises residues 146-186 in Rif2, with residues 152-186 disordered in the structure. Alignment of Rif2 and the replication initiation protein DnaA (a member of the initiator clade, PDB code 2Z4R) gave a Z score of 7.4 with rmsd of 3.5 Å and 162 aligned C_α residues by the DALI server (Holm and Rosenstrom, 2010). Comparison with Orc1 (PDB code 2QBY), a functional homologue of DnaA, gave a Z score of 7.5 with 4.2 Å and 180 aligned C_α residues.

(B) Isolated full-length Rif2 is a monomer in solution. Injection of 50 μl sample of full-length Rif2 at a concentration of 10 mg/ml onto a 25 ml Superdex 200 column followed by multi-angle light-scattering (MALS) analysis yielded a molecular weight of 44.5 ±0.4 kDa (see **Supplemental experimental procedure** for detailed description). This is very close to the predicted molecular weight of monomeric Rif2 of 45.6 kDa, in line with the monomeric state of other initiator clade AAA+ proteins.

(C) The C-terminus of Rif2 (Rif2-CTD; residues 371-395; shown in grey) undergoes conformational change upon Rap1 binding. In isolated Rif2, the CTD domain is visible, and interacts with a symmetry-related molecule in the crystal lattice. However, in the Rif2-Rap1 complex, the CTD domain undergoes an approx. 90° rotation and becomes sandwiched between the two Rif2 lobes, thereby contributing to the Rap1 interface (surface area: 834.6 Å^2). In this conformation, Rif2-CTD runs along Rap1 helix α2 (residues 705 to 709).

(D and E) Rif2 contains a non-functional ATP-binding pocket. (D) Amino acid sequence alignment of the ASCE domain of Rif2, DnaA, Cdc6, and Orc4 from different species. The secondary structure elements of Rif2 are presented above the alignment and are based on the structures determined in this study. Positions of the motifs involved in ATP binding or hydrolysis (Walker A, Walker B and Sensor I) are marked in red. The Walker A motif (consensus sequence G-x-x-x-x-GKT/S) between β1 and α2 of Rif2 is highly degenerated with the conserved lysine substituted by a histidine. Residues vaguely reminiscent of an h-h-h-h-DE Walker B motif (h=hydrophobic residues) are present in Rif2 (Glu213 and Gln214 in β3), as is a residue that matches the consensus for the Sensor-I motif (N, D, T and H), namely Asn254 at the apex of β4.

(E) Structure alignment of Rif2 and DnaA bound with ATP (PDB code: 2Z4R); Rif2 is colored in green (ASCE domain) and in blue (α-bundle domain), DnaA in grey, ATP is shown in stick representation in orange, and Mg^{2+} as a yellow sphere. On the basis of the current information of the conformation and length of helix α2 in Rif2, ATP binding cannot be modeled due to large steric clashes. We

assessed the ability of Rif2 to catalyze ATP hydrolysis *in vitro*. No such activity was measured by HPLC after incubation of purified Rif2 (10 µM) in a buffer containing 50 mM HEPES, pH 7.4, 200 mM NaCl, 10 mM MgCl$_2$, 10 mM ATP and 1 mM TCEP for 10, 30, and 60 min (data not shown).

(F) Assessment of telomere length and (G) G2/M cell-cycle arrest phenotypes in yeast strains harboring mutations within the Walker B motif of endogenous Rif2 protein (E213A or E213K). The indicated mutant strains (listed in **Table S2**) exhibited normal telomere length, but, surprisingly, a distinct G2/M arrest phenotype. Based on the poor amino acid sequence conservation within the Walker A motif, the incompatibility of the Rif2 structure with known ATP binding sites, and the lack of ATP hydrolysis *in vitro*, loss of an intrinsic ATPase activity is unlikely the cause for the G2/M arrest phenotype in the *rif2* mutant strains. However, other small molecular weight ligands or interacting proteins may bind to the (non-functional) ATP-binding pocket. Alternatively, the mutations may change the relative orientation of the two Rif2 lobes, possibly triggering more global changes in telomere architecture, which may be responsible for the checkpoint defect. Further work will be required to characterize these mutants.

Figure S3. Rif2 utilizes multivalent binding domains to interact with Rap1. Related to Figure 2

Despite extensive crystallization trials, we were unable to obtain crystals of full-length Rif2 construct in the absence of Rap1. Crystals were obtained, however, for a truncated form of Rif2 lacking the first 65 amino acid residues. The Rif2-Rap1$_{RCT}$ complex, on the other hand, crystallized using full-length Rif2. In the complex structure, electron density was found for the Rif2 N-terminus where the Rap1 moiety contacts Rif2 directly (Rif2$_{RBM}$ residues 36 to 48). Residues 49 to 60 connecting this epitope to the remainder of the AAA+ core were found disordered in the structure. We observed that a Rif2 N-terminal deletion up to residue 35 did not reduce the Rif2 binding affinity to Rap1, while further deletion to residue 48 led to decreased interactions with Rap1 (data not shown). The Rif2 construct spanning residues 35-395 crystallized bound to Rap1 under the same conditions as full-length Rif2 (**Table S1**), and the electron density map was identical with respect to Rif2$_{RBM}$ (data not shown).

(A) Strep-pulldown of Rap1$_{RCT}$ in the presence of GST-Rif2ΔNTD (residues 66-395), GST-Rif2ΔCTD (residues 1-380), GST-Rif2 full-length, and GST-Rif2ΔNTDΔCTD (66-380). GST- and Strep-pulldown of different GST-Rif2 constructs from the same lysate performed and in the absence of Strep-Rap1 as a control. Deletion of the N- or C-terminus of Rif2 reduced binding to Rap1, whereas combined deletion abolished any detectable interaction between the two proteins.

(B-D) Assignment and validation of Rif2$_{RBM}$ in the Rif2-Rap1$_{RCT}$ structure.

(B) Full-length Rif2-Rap1$_{RCT}$ crystals were washed in the mother liquor, dissolved in water and run on an 18% SDS-polyacrylamide gel. A Coomassie blue stained gel showed two protein bands corresponding to full-length Rif2 with a molecular weight of 44.5 kDa and Rap1$_{RCT}$ (MW: 17.2 kDa).

(C) Strep-pulldown using Rap1$_{RCT}$ as bait and full-length Rif2 (wild-type or L42M mutant) as prey. Rif2 was expressed as GST-fusion protein in *E. coli* and Rap1 as Strep-fusion protein in insect cells. Wild-type and mutant Rif2 bind Rap1 with similar apparent affinity.

(D) Ribbon representation of the Rif2-Rap1$_{RCT}$ complex highlighting experimental SeMet sites as yellow mesh. Anomalous difference map contoured at 4.0 σ is shown in yellow. Rif2$_{RBM}$ is presented as stick in blue. In order to confirm the peptide observed bound to Rap1 originates from Rif2, and to facilitate sequence assignment, a selenomethionine-substituted Rif2 L42M mutant was constructed and its structure solved bound to Rap1$_{RCT}$ (**Table S1**). Binding of this Rif2 L42M mutant to Rap1$_{RCT}$ was indistinguishable from that of wild-type Rif2. Mutant crystals grew under similar conditions as the wild-type crystals and diffracted to 3.5 Å resolution. The anomalous difference maps identified 11 out of 12 SeMet sites. The one missing site is located in the disordered region between residues 152-186. Ten SeMet sites matched previous methionine locations in wild-type Rif2. The peak for SeMet_42 corresponds to Leu42 in the wild-type Rif2 structure. The possibility that Rif2$_{RBM}$ was a

proteolytic product of full-length Rif2 was excluded by gel analysis as shown in (B). Rif2$_{RBM}$ thereby binds Rap1 *in trans*.

(E) Telomere length in strains harboring the indicated Rif2$_{AAA+}$ and Rif2$_{RBM}$ (Leu44Arg, Val45Glu) mutations. Genomic DNA was isolated from strains with the indicated genotypes (listed in **Table S2**), digested with *Xho*I and assessed by Southern blotting using a probe that recognizes the telomeric TG$_{1-3}$ repeats. The observed phenotypes are summarized in **Table 1**.

Figure S4. Detailed comparison of Rif1$_{RBM}$, Rfi2$_{RBM}$ and Sir3$_{RBM}$ bound on Rap1$_{RCT}$. Related to Figure 3

(A) Sequence alignment of Rif1$_{RBM}$ across yeast species. The RBM boundary for *S. cerevisiae* Rif1 is shown on top. Residues involved in Rap1 binding are indicated by blue dots.

(B) The Rif1$_{RBM}$ mutant protein was expressed at the same level as the wild-type protein (determined by western blotting). Both wild-type Rif1 and Rif1$_{RBM}$ were Myc-tagged. Western blotting against Actin was performed from the same lysates as loading control.

(C) Chromatin immunoprecipitation (ChIP) analysis of Rap1 recruitment at undamaged native telomeres in the wild-type (YSM53-2) and the *rif1$_{RBM}$* (YSM54-2) mutant strains using polyclonal rabbit anti-Rap1 antiserum. Results are reported as average fold enrichment and s.d. relative to an internal control sequence within the *PDI1* gene on chromosome III.

(D) Structure-based sequence alignment of Rif1$_{RBM}$, Rif2$_{RBM}$ and Sir3$_{RBM}$. Secondary structure elements and numbering schemes are shown on top, with residues contacting Rap1 shown in red. While both Rif2$_{RBM}$ and Sir3$_{RBM}$ contain α-helical RBM elements, no discernible helix was observed within Rif1$_{RBM}$. The directionality of the peptide is found inverted for Sir3$_{RBM}$ respective to Rif1$_{RBM}$ and Rif2$_{RBM}$.

(E) Ribbon representation of Rap1$_{RCT}$-Rif1$_{RBM}$, Rap1$_{RCT}$-Rif2$_{RBM}$ and Rap1$_{RCT}$-Sir3$_{RBM}$ structures with a close-up view illustrating the interaction between Rif1$_{RBM}$ and the Rap1 RBM-binding groove. Rif1$_{RBM}$ is colored in blue, Rif2$_{RBM}$ in red and Sir3$_{RBM}$ in grey. Despite the low sequence and secondary structure similarities found amongst the three Rap1 peptides, all the three use similar residues (Rif1: Ile1764, Ile1762; Rif2: Lue44, Lue42; Sir3: Ile463, Lue468 at position 0 and +5) to bind to the hydrophobic Rap1 RBM-binding groove provided by Rap1 residues Leu755, Ala733 and Leu736. At the same time, backbone amides of residues at position 0 form hydrogen bonds to the backbone carbonyl of Rap1 Pro730. Rap1 Leu736 delimits the size of possible peptide side chains at position 0. Leu or Ile residues at position +8 (Rif1 Ile1760, Rif2 Leu39 and Sir3 Leu471) clamp the peptides to the side of the Rap1 RBM-binding groove through a hydrophobic interaction with Rap1 Val737. Residues at position -1 (Rif1 Phe1765, Rif2 Val45 and Sir3 Met469) further stabilize the peptides by forming hydrogen bonds with their backbone amide to the Rap1 Gly760 carbonyl and Leu762 amide.

(F) Telomere length in strains harboring the *RIF1* deletion and *rif1$_{RBM}$* mutations. Genomic DNA was isolated from strains with the indicated genotypes (listed in **Table S2**), digested with *Xho*I and assessed by Southern blotting using a probe that recognizes the telomeric TG$_{1-3}$ repeats. The observed phenotypes are summarized in **Table 1**.

Figure S5. DNA-binding activities of Rif1, Rif2, and Rap1. Related to Figure 5

(A) Rif2-, but not Rif1-mediated anticheckpoint response in G2/M arrest assay is dependent on its interaction with Rap1. Short telomeric tracts (TG80) were flanked at both sites of the inducible DSB. Percentage of large-budded cells (G2/M arrested) after HO cleavage in indicated strains (listed in **Table S2**) is plotted against cell-cycle progression. The average restart time for each construct (indicated in parentheses, together with the number of cells measured) was estimated using a Kaplan-Meier survival analysis and summarized in **Table 1**.

(B) EMSA assays of Rif1_C show preferred binding to flapped and branched double-stranded DNA substrates. Reactions contained the indicated ^{32}P-labeled substrates at a concentration of 1 nM and increasing amounts of protein (0, 75, 125, 250, 500, and 1000 nM).

(C) Mapping of the mutant A and mutant C sites described for the hRif1 C-II domain (Xu et. al, 2010) onto analogous residues in the yeast Rif1$_{CTD}$ structure. The site analogous to mutant C (Glu1897) is colored in blue and located at the surface of helix α4. Sites corresponding to mutant A (Val1872, Ala1873, Leu1875 and Phe1878, colored in yellow) and those which showed significantly reduced DNA-binding activity upon mutation in human Rif1$_{CTD}$, are found primarily at the dimerization interface of yeast Rif1$_{CTD}$.

(D) Rif1_N prefers DNA substrates with a ssDNA component. Quantitation of the Rif1_N EMSA shown in **Figure 5C**. The ratio of bound DNA to total substrate (% shift) signal is plotted against protein concentration. Substrates containing single-stranded regions are shown in red (ssDNA, 5'-overhang, SA, and 5' flap) and in blue (3' flap). All fully double-stranded substrates are in green.

(E) Rif1_N binds ssDNA with 2- to 4-fold higher affinity than dsDNA. EMSA experiments similar to those in **Figure 5D** using a 60 nt ssDNA or a 60 bp dsDNA substrate (10 nM) and protein concentrations of 0, 20, 30, 40, 50, 60, 70 and 80 nM were performed in triplicate. Results were quantified and the data plotted as in (D).

(F) Rif2 binds to dsDNA but not to ssDNA. 5 nM ^{32}P-labeled ssDNA (50 nt) or dsDNA (50 bp) was titrated with full-length Rif2 (50, 200, 800, 1600 nM) on ice for 30 min and analyzed by 1.2% agarose gel electrophoresis and autoradiography. Protein-DNA bands were only observed at high protein concentration (>200 nM) with dsDNA, not with ssDNA.

(G-J) Rif1 and Rif2 bind to DNA in a sequence-independent manner. (G) Binding of Rif1_N (10, 20, 40 nM) to ^{32}P-labled dsDNA (1 nM) was abolished in the presence of 20 ng unspecific competitor polyd(I-C)). (H) Binding of Rap1 (80 nM) to Cy5-labled Tel31 (150 nM) was efficiently competed by unlabeled Tel31 but not by an unlabeled 31 bp duplex with random sequence unrelated to TG$_{1-3}$ repeats (each at 1-, 2- and 3-fold molar excess), indicative of sequence-specific DNA-binding. Reactions were analyzed after 30 min incubation by 6% polyacrylamide gel electrophoresis. (I) Rif2

(160 nM) and (J) Rif1_C (160 nM) in EMSA experiments as described for (H). Tel31 and the random duplex displaced Rif2 and Rif1_C from Cy5-labeled Tel31, demonstrating that these proteins bind DNA in a sequence-independent manner.

Figure S6. Potential dimerization interfaces of Rif2. Related to Figure 6

(A and B) Two potential Rif2-dimer interfaces have been found in the Rif2-Rap1$_{RCT}$ crystal lattice with two molecules of Rif2-Rap1$_{RCT}$ present in the asymmetric unit of the crystal. (A) One possible interface comprises residues Phe330, Val333, and Phe334 located in helix α8 of the α-bundle domain and V256 from α5 of the ASCE domain. This interface covers 323 Å^2 and was classified as a non-physiological interface by PDBePISA (Krissinel and Henrick, 2007). (B) The alternative complex-dimer interface contains residues from α3' and α4 of the ASCE domain (Met191, Met195, Lys241 and Val238). It encompasses 726 Å^2 and was estimated to be potentially physiologically relevant by PDBePISA.

(C and D) *In vivo* assessment of Rif2-Rap1$_{RCT}$ complex-dimer interface mutants. Crystal packing interactions are often indicative of *in vivo* oligomerization or protein-protein binding interfaces. The two possible dimer interfaces shown in (A) and (B) were examined for telomere length (C) and G2/M arrest (D) phenotypes in yeast. Different mutants in the Phe330-Val333-Phe334 interface did not show deficiencies in either telomere length or G2/M checkpoint activation. The M191K-M195K-K241D mutation, however, showed no G2/M checkpoint defect whilst exhibiting a slight telomere elongation. The indicated strains are listed in **Table S2**.

(E) Higher-order fold-up driven by the molecular Rap1-Rif1-Rif2 "*Velcro*" at telomeres. Surface representations of the Rif1 RBM domain (in blue) and the Rif2 RBM domain (in red). All the other protein domains are shown as ribbon: the Rap1 Myb domain (orange), the Rap1 RCT domain (yellow), the Rif2 AAA+ domain (green) and the Rif1 CTD domain (blue). The DNA strands are presented as surface view in grey. Distal Rap1-Rif1-Rif2 complexes from the same telomere (*cis*-telomere) or neighboring telomeres (*trans*-telomere) can be interlinked *via* the multivalent binding interfaces present in Rif1 and Rif2, resulting in telomere fold-back or telomere clustering.

12 SUPPLEMENTAL TABLES

Table S1. Data collection, refinement statistics and crystallization conditions. Related to Experimental Procedures

Data collection	Rif2(66-395)	SeMet Rif2(66-395)	Rif2-Rap1$_{RCT}$	Rif2$_{35-395}$ -Rap1$_{RCT}$	SeMet Rif2$_{L42M}$ -Rap1$_{RCT}$	Rif1$_{RBM}$ -Rap1$_{RCT}$	Rif1$_{CTD}$
Beamline	SLS X10SA	SLS X10SA	SLS X10SA	SLS X10SA	SLS X10SA	SLS X10SA	SLS X10SA
Wavelength (Å)	1.0000	0.9600	1.0000	1.0000	0.9600	1.0000	1.0000
Space Group	$P\,6_522$	$P6_522$	$P2_12_12_1$	$P2_12_12_1$	$P2_12_12_1$	$C2$	$P1$
Cell parameters							
a, b, c (Å)	78.0, 78.0, 236.3	78.3, 78.3, 234.8	108.3, 113.7, 140.9	108.2, 112.7, 140.8	108.8, 112.8, 140.1	164.0, 88.9, 57.6	34.8, 34.8, 46.2
α, β, γ (°)	90, 90, 120	90, 90, 120	90, 90, 90	90, 90, 90	90, 90, 90	90, 90.1, 90	87.4, 79.9, 82.3
Resolution (Å)	44.5-2.55 (2.66-2.55)	44.4-3.6 (4.03-3.6)	68.5-3.1 (3.27-3.1)	48.8-2.95 (3.08-2.95)	46.25-3.5 (3.78-3.5)	47-1.6 (1.63-1.60)	45.5-1.94 (1.95-1.94)
Completeness (%)	99.6 (99.1)	99.8 (100)	99.0 (99.1)	99.4 (97.6)	99.9 (99.9)	96.5 (84.0)	96.4 (73.6)
Unique reflections	14816 (1743)	5447 (1480)	32266 (4630)	36846 (4503)	22309 (4508)	103829 (4435)	15001 (109)
Multiplicity	7.8 (6.4)	20.2 (21)	7.3 (7.5)	4.1 (4.2)	8.1 (8.2)	3.1 (2.7)	2.2 (2.1)
Rsym (%)	6.1 (193.3)	8.9 (22.5)	7.1 (125.2)	5.5 (123.6)	8.4 (34.5)	5.8 (57.9)	7.8 (35.7)
$\langle I/\sigma I \rangle$	16.2 (0.9)	34 (15.6)	12.2 (2.2)	16.5 (1.2)	23.2 (6.6)	12.7 (2.2)	11.2 (3.8)
Refinement							
PDB code	XXXX		XXXX	XXXX		XXXX	XXXX
Rwork/Rfree (%)	22.9/24.4		18.1/19.9	18.3/20.4		16.6/18.7	20.2/22.8
Reflections (working set)	14071		30666	34947		98669	14250
Reflections (test set)	745		1600	1899		5133	751
Number of Atoms							
Protein	2085		7242	7242		7864	3437
Water	2		0	0		646	162
Ligand	1		25	25			0

R.m.s. deviations							
Bond lengths (Å)	0.008		0.010	0.010		0.010	0.008
Bond Angles (°)	0.97		1.3	1.10		0.95	0.89
Ramachandran							
favoured	98		97.8	97.8		99.4	99
disallowed	0		0.1	0.1		0	0
Avg. B-factor (Å2)	102.0		117.8	114.2		31.0	22.2
Crystallization							
Reservoir	14-20% 1, 4-Butandiol, 100mM Na-Acetate pH 5.1	14-20% 1, 4-Butandiol, 100mM Na-Acetate pH 5.1	100 mM Tris pH 8.0, 500 mM Li_2SO_4, 22-25% PEG 6K	100 mM Tris pH 8.0, 500 mM Li_2SO_4, 22-25% PEG 6K	100 mM Tris pH 8.0, 500 mM Li_2SO_4, 22-25% PEG 6K	100 mM Na-citrate pH 5.0, 2.4-2.5M $(NH_4)_2SO_4$,	100 mM HEPES pH 7.5, 200 mM NaCl, 20% PEG 3K
Protein Concentration (mg/ml)	10	10	10	12	12	11	3.8
Cryoprotectant	Paratone-N	Paratone-N	Paratone-N	Reservoir + 25% Ethylene glycol	Reservoir + 25% Ethylene glycol	Reservoir	Reservoir + 10% Ethylene glycol

Table S2. Yeast strains used in this study. Related to Figure 2-5 and Figure S2-S6

Strain	Genotype	Source
W303-1A	*HMLa MATa HMRa ade2-1 can1-100 his3-11, 15 leu2-3, 112 trp1-1 ura3-1*	D. Shore
PJ69-4A	*MATa trp1-901 leu2-3,112 ura3-52 his3-200 gal4Δ gal8OΔ LYS2::GAL1-HIS3 GAL2-ADE2 met2::GAL7-lacZ*	D. Shore
Y87	pJ69-4A *rif1::KanMX6*	This study
Y88	pJ69-4A *rif2::KanMX6*	This study
Y92	W303-1A *rif1-I1762R/I1764R*	This study
YG16	W303-1A *hmrΔA::TRP1 telVII::ADE2/URA3*	D. Shore
Y96	YG16 *MATa rif1-I1762R/I1764R*	This study
Y98	YG16 MATa *rif2-L42K/L44R/V45E*	This study
Y102	YG16 MATa *rif1-I1762R/I1764R rif2-L42K/L44R/V45E*	This study
Y103	YG16 *rif1::KanMX6*	This study
Y104	YG16 *rif2::KanMX6*	This study
Y105	YG16 *rif1::KanMX6 rif2::HIS3*	This study
YCR34	*mnt2::TG80-HO-CA250-ADE2*	Ribeyre and Shore, 2011
YCR55	*mnt2::TG250-HO-CA250-ADE2*	Ribeyre and Shore, 2011
YCR120	*mnt2::TG250-HO-CA250-ADE2 rif2::KanMX4*	Ribeyre and Shore, 2011
YCR175	*mnt2::TG250-HO-CA250-ADE2 rif1::KanMX4*	Ribeyre and Shore, 2011
YCR116	*mnt2::TG80-HO-CA80-ADE2 rif2::KanMX4*	Ribeyre and Shore, 2011
YCR272	*mnt2::TG80-HO-CA80-ADE2 rif1::NatMX4*	Ribeyre and Shore, 2011
YCR307	*mnt2::TG80-HO-CA80-ADE2 rif2-E213A*	This study
YCR359	*mnt2::TG80-HO-CA80-ADE2 rif2-E213K*	This study
YCR303	*mnt2::TG80-HO-CA80-ADE2 rif2-F334A*	This study
YCR330	*mnt2::TG80-HO-CA80-ADE2 rif2-V256A*	This study
YCR361	*mnt2::TG80-HO-CA80-ADE2 rif2-F334A/V256A*	This study
YCR410	*mnt2::TG80-HO-CA80-ADE2 rif2-F3330A/V334A/F334A*	This study
YCR428	*mnt2::TG80-HO-CA80-ADE2 rif2-M191K/M195K/K241D*	This study

YCR304	*mnt2::TG80-HO-CA80-ADE2 rif2-F342A*	This study
YCR305	*mnt2::TG80-HO-CA80-ADE2 rif2-T346A*	This study
YCR306	*mnt2::TG80-HO-CA80-ADE2 rif2-E347R*	This study
YCR494	*mnt2::TG80-HO-CA80-ADE2 rif2-L44R/V45E*	This study
YCR495	*mnt2::TG80-HO-CA80-ADE2 rif2-44R/V45E*	This study
YCR532	*mnt2::TG80-HO-CA80-ADE2 rif1-I1762R/I1764R*	This study
YCR533	*mnt2::TG80-HO-CA80-ADE2 rif1-I1762R/I1764R*	This study
YCR263	*mnt2::TG80-HO-CA80-ADE2 RIF1-13MYC-HIS3MX6*	This study
YCR201	*mnt2::TG80-HO-CA80-ADE2 rif1::NatMX4*	This study
YSM53-2	*W303-1A Δbar1 RIF1-13MYC-HIS3MX6*	This study
YSM54-2	Y92 *rif1-I1762R/I1764R-13MYC-HIS3MX6*	This study
YSM52-2	YCR532 *rif1-I1762R/I1764R-13MYC-HIS3MX6*	This study

Table S3. Sequences of the oligonucleotides used for the EMSA assays. Related to Experimental Procedures

Oligo	Sequence (5' – 3')
1	CCGCACACCCACACACCAG
2	*CCTGGTGTGTGGGTGTGCG
3	*CGCACACCCACACACCACACCCACACACCAG
4	CCTGGTGTGTGGGTGTGGTGTGTGGGTGTGC
5	ATGCTCTCATGTACATCGATTACCATGACGC
6	GCGTCATGGTAATCGATGTACATGAGAGCAT
7	**ACGCTGCCGAATTCTACCAGTGCCTTGCTAGGACATCTTTGCCCACCTGCAGGTTCACCC
8	GGGTGAACCTGCAGGTGGGCAAAGATGTCCATCTGTTGTAATCGTCAAGCTTTATGCCGT
9	ACGGCATAAAGCTTGACGATTACAACAGATCATGGAGCTGTCTAGAGGATCCGACTATCG
10	CGATAGTCGGATCCTCTAGACAGCTCCATGTAGCAAGGCACTGGTAGAATTCGGCAGCGT
11	GGGTGAACCTGCAGGTGGGCAAAGATGTCCTAGCAAGGCACTGGTAGAATTCGGCAGCGT
12	CATGGAGCTGTCTAGAGGATCCGACTATCG
13	GGGTGAACCTGCAGGTGGGCAAAGATGTCC
14	*CTGCCACCACACCCACAC

15	GATTAAGTTGGGTAACGC
16	**ACGCTGCCGAATTCTACCAGTGCCTTGCTAGGACATCTTTGCCCACCTGC
17	GCAGGTGGGCAAAGATGTCCTAGCAAGGCACTGGTAGAATTCGGCAGCGT
18	**ACGCTGCCGAATTCTACCAGTGCCTTGCTAGGACATCTTT
19	AAAGATGTCCTAGCAAGGCACTGGTAGAATTCGGCAGCGT
20	**ACGCTGCCGAATTCTACCAGTGCCTTGCTA
21	TAGCAAGGCACTGGTAGAATTCGGCAGCGT

* Cy5-labeled oligonucleotides; ** ^{32}P-labeled oligonucleotides

13 SUPPLEMENTAL EXPERIMENTAL PROCEDURES

General crystallographic methods

All diffraction data were collected at the Swiss Light Source, Villigen, Switzerland and were processed with XDS (Kabsch, 2010). Models were built with COOT (Emsley et al., 2010) and refined initially with PHENIX (Adams et al., 2010) and/or autoBUSTER (Bricogne, 1993). The final protein structural models were produced using autoBUSTER. Structural figures were generated with PyMOL (Schrödinger; http://www.pymol.org). A summary of the crystallization conditions, data processing statistics and refinement statistics is provided in **Table S1**. A detailed description of the methods concerning each crystal structure are given in the following sections

Structure of Rif2 and the Rif2-Rap1$_{RCT}$ complex

Protein expression and purification

Saccharomyces cerevisiae Rif2 (residues 66-380) was cloned into a pGEX-derived vector with a TEV-cleavable N-terminal GST tag. The resulting plasmid was transformed into *Escherichia coli* BL21 (DE3) pLysS cells for expression. Full-length Rif2 and Rap1 (residues 672-827) were cloned into a pAD-derived plasmid (BD biosciences). Recombinant Rif2 and Rap1 baculoviruses were prepared according to the manufacturer's protocol (Invitrogen). Proteins were expressed either as N-terminally (His)$_6$ tagged or Strep tagged fusion proteins in High Five insect cells (Invitrogen).

For Rif2 (66-380) and Rif2-Rap1 complex purification, cells were resuspended in lysis buffer (50 mM Tris, pH 8.0, 300 mM NaCl, 5 mM β-ME, 1 mM PMSF) and lysed by sonication. Rif2 (66-380) was purified using Glutathion-Sepharose (Sigma), and full-length Rif2-Rap1 (672-827) by Strep-Tactin affinity chromatography (IBA). All N-terminal tags were cleaved with TEV protease at 4°C overnight. Proteins were further purified by ion exchange chromatography (GE Healthcare), using cation-exchange (Source15S) for Rif2 and anion-exchange (Source15Q) for Rap1. The purification was completed by performing size exclusion chromatography (SEC) (Superdex 200; GE Healthcare) in 50 mM HEPES, pH 7.4, 200 mM NaCl, and 1 mM TCEP. Proteins were stored at -80°C until further use. Selenomethionine-substituted Rif2 (66-380) and full-length Rif2 L42M were expressed in M9 medium supplemented with 50 mg/l selenomethionine and purified using a protocol identical to that for native Rif2.

Crystallization of Rif2 (66-380)

Crystals of native and SeMet Rif2 (66-380) were grown at 20-25°C using the sitting drop diffusion method. The proteins crystallized in the gel filtration buffer (50 mM HEPES, pH 7.4; 200 mM NaCl; 1 mM TCEP) without mixing with the reservoir solution (14-20% 1,4-Butandiol, 100 mM Na-acetate, pH 5.1). Crystals were transferred into Paratone-N as cryoprotectant (Hampton) and flash frozen in liquid N_2 prior to data collection.

Crystallization of Rif2-Rap1 complex

Crystals of the native full-length Rif2-Rap1 complex, Rif2 (35-395)-Rap1 complex and the SeMet Rif2$_{L42M}$-Rap1 complex were grown at 20-25°C using sitting drop vapor diffusion methodology. For the crystallization of the Rif2-Rap1 complex, a 1.2 molar excess of Rif2 was added. Crystals were obtained by mixing the protein solution in the gel filtration buffer in a 1:1 ratio with a reservoir solution containing 100 mM Tris, pH 8.0; 500 mM Li$_2$SO$_4$; 22-25% PEG 6K and flash frozen in liquid N_2 following transfer into the cryoprotectant consisting of mother liquor and 25% ethylene glycol.

Structure determination

Crystals of Rif2 (66-380) belonged to space group $P6_522$ containing one molecule per asymmetric unit. The structure was solved by the single-wavelength anomalous dispersion method. Initial selenium sites were localized using SHELXD (Sheldrick, 2008). Phases were calculated with the program SHARP (delaFortelle and Bricogne, 1997) and were improved using solvent flattening and the program DM (Collaborative Computational Project, Number 4, 1994). The structure of the Rif2-Rap1 crystals was solved by molecular replacement using PHASER (McCoy et al., 2007) with Rif2 (66-380) and Rap1 (PDB code 3CZ6) as search models. The Rif2-Rap1 crystals belonged to space group $P2_12_12_1$ and contained two complexes per asymmetric unit. Sequence assignment for Rif2$_{RBM}$ in the Rif2-Rap1 structure was confirmed using the Rif2$_{35-395}$-Rap1 data set and anomalous signal from full-length SeMet-Rif2$_{L42M}$-Rap1 crystals.

Structure of Rif1$_{RBM}$-Rap1$_{RCT}$

Crystallization and structure determination

The Rif1$_{RBM}$ (residues 1752-1772) peptide with the sequence ADISVLPEIRIPIFNSLKMQ (synthesized by PSL GMBH, >95% purity) was dissolved in 100% DMSO at a concentration of 0.18 mg/µl. For the Rif1$_{RBM}$-Rap1$_{RCT}$ complex formation, a 5-fold molar excess of the peptide was added to Rap1, with the final DMSO concentration below 5% (v/v), and the mixture was incubated on ice overnight. After centrifugation at 1770g for 10 minutes, the protein in the supernatant was used for crystallization. The Rif1$_{RBM}$-Rap1$_{RCT}$ complex crystallized at 4°C

using the sitting drop diffusion method in 100 mM Na-citrate, pH 5.0, 2.4-2.5 M $(NH_4)_2SO_4$. Crystals were transferred into cryoprotectant (mother liquor) and flash frozen in liquid N_2 for data collection.

Crystals of Rif1-Rap1 belonged to the space group *C*2 containing three complexes per asymmetric unit. The Rif1$_{RBM}$-Rap1$_{RCT}$ crystal structure was solved by MR using Rap1 (PDB code 3CZ6) as a probe. Unequivocal electron density was found in the initial m*F*o-D*F*c map for the bound Rif1 peptide, which was manually built into the density using COOT.

Structure of Rif1$_{CTD}$

<u>Purification, crystallization and structure determination</u>

Rif1 (residues 1709-1916) was expressed as (His)$_6$-tagged protein in BL21 (DE3) pLysS cells with 0.5 mM IPTG induction at 18°C overnight. Cells were resuspended in lysis buffer (50 mM Tris, pH 8.0; 500 mM NaCl; 5 mM β-ME; 1 mM PMSF) and lysed by sonication. Rif1$_{CTD}$ was purified by NiNTA affinity chromatography (Sigma) followed by Source15S ion exchange chromatography (GE Healthcare) and SEC (Superdex 200; GE Healthcare). The protein was stored in 50 mM HEPES, pH 7.4, 500 mM NaCl, and 1 mM TCEP at -80°C until use.

Rif1$_{CTD}$ crystals were grown at 20°C using the sitting drop vapor diffusion method. The protein (3.5 mg/ml) was supplemented with 0.003% trypsin prior to set-up. Crystals were obtained after 10 days by mixing the protein solution in a 1:1 ratio with reservoir containing 100 mM HEPES, pH 7.5, 200 mM NaCl, 20% PEG 3000, and flash frozen in liquid N_2 after transfer into the cryoprotectant (mother liquor + 10% ethylene glycol). The protein boundary in the crystals was determined by mass spectrometry analysis of dissolved crystals.

The crystal structure of Rif1$_{CTD}$ was determined using the ARCIMBOLDO ab initio phasing protocol (Rodriguez et al., 2009) by PHASER (McCoy et al., 2007) for molecular replacement calculations and SHELXE (Sheldrick, 2008) for density modification, poly-Ala chain extension, and scoring. Models containing one to five idealized (Ala)$_{14}$ α-helical fragments were generated by MR. The majority of solutions produced from five α-helical fragments by SHELXE were correct as indicated by a correlation coefficient (CC) between the data and the poly-Ala model of greater than 25%. The poly-Ala model from the best solution (with a CC of 34%) was rebuilt by ARP/wARP, which provided an initial, sequence-assigned model.

Silencing assay

Rap1 peptide-binding groove mutants of endogenous Rif1 (I1762R-I1764R, *rif1*_{RBM} allele, strain Y96) and Rif2 (L44R-V45E, *rif2*_{RBM} allele, strain Y98) were examined in respect to silencing at telomeres and mating type locus, either individually or in combination (*rif1*_{RBM} *rif2*_{RBM} double mutant, strain Y102). Silencing at the *HMR* was assayed in derivatives of strain YG16 with a *TRP1* reporter located at HMR silencer containing the origin recognition complex (ORC) binding site mutation (*HMRΔA::TRP1*). In context of this weakened silencer (Sussel and Shore, 1991), mutations in *RAP1* and *RIF1* led to de-repression, indicated by growth on SC-Trp medium. Telomeric silencing assays were performed with the same strains, but using a telomeric *URA3* reporter on chromosome VII (*telVII::URA3*). Expression of *URA3* was tested on medium containing 5-FOA, which is lethal to cells expressing *URA3*. The inability to grow on SC+5-FOA indicates a loss of telomeric silencing. Cells from overnight cultures were spotted in 10-fold serial dilutions (starting with 10^7 cells) on the test medium and synthetic complete medium as growth control.

SEC-MALS

To determine the average mass of protein complexes, SEC using a Superdex 200 column (GE Healthcare) was coupled to MALS using an Optilab T-rEX refractive index detector and a miniDAWN TREOS 3 angle MALS detector (Wyatt Technology). Runs were done with 50 µl samples containing 5 mg/ml or 3 mg/ml Rif1 (residues 1709-1916) or 10 mg/ml full-length Rif2 in 50 mM HEPES pH 7.4, 500 mM NaCl, and 1 mM TCEP. The weight-averaged molecular mass of material contained in chromatographic peaks was determined using ASTRA V software version 5.3 (Wyatt Technology Corp., Santa Barbara, CA).

14 SUPPLEMENTAL REFERENCES

Adams, I.R., and McLaren, A. (2004). Identification and characterisation of mRif1: a mouse telomere-associated protein highly expressed in germ cells and embryo-derived pluripotent stem cells. Dev Dyn *229*, 733-744.

Adams, P.D., Afonine, P.V., Bunkoczi, G., Chen, V.B., Davis, I.W., Echols, N., Headd, J.J., Hung, L.W., Kapral, G.J., Grosse-Kunstleve, R.W.*, et al.* (2010). PHENIX: a comprehensive Python-based system for macromolecular structure solution. Acta Crystallogr D Biol Crystallogr *66*, 213-221.

Addinall, S.G., Holstein, E.M., Lawless, C., Yu, M., Chapman, K., Banks, A.P., Ngo, H.P., Maringele, L., Taschuk, M., Young, A.*, et al.* (2011). Quantitative fitness analysis shows that NMD proteins and many other protein complexes suppress or enhance distinct telomere cap defects. PLoS Genet *7*, e1001362.

Anbalagan, S., Bonetti, D., Lucchini, G., and Longhese, M.P. (2011). Rif1 supports the function of the CST complex in yeast telomere capping. PLoS Genet *7*, e1002024.

Aparicio, O.M., Billington, B.L., and Gottschling, D.E. (1991). Modifiers of position effect are shared between telomeric and silent mating-type loci in S. cerevisiae. Cell *66*, 1279-1287.

Arneric, M., and Lingner, J. (2007). Tel1 kinase and subtelomere-bound Tbf1 mediate preferential elongation of short telomeres by telomerase in yeast. EMBO Rep *8*, 1080-1085.

Atrazhev, A., Zhang, S., and Grosse, F. (1992). Single-stranded DNA binding protein from calf thymus. Purification, properties, and stimulation of the homologous DNA-polymerase-alpha-primase complex. Eur J Biochem *210*, 855-865.

Azzalin, C.M., Reichenbach, P., Khoriauli, L., Giulotto, E., and Lingner, J. (2007). Telomeric repeat containing RNA and RNA surveillance factors at mammalian chromosome ends. Science *318*, 798-801.

Baker, H.V. (1991). GCR1 of Saccharomyces cerevisiae encodes a DNA binding protein whose binding is abolished by mutations in the CTTCC sequence motif. Proc Natl Acad Sci U S A *88*, 9443-9447.

Bazzi, M., Mantiero, D., Trovesi, C., Lucchini, G., and Longhese, M.P. (2010). Dephosphorylation of gamma H2A by Glc7/protein phosphatase 1 promotes recovery from inhibition of DNA replication. Mol Cell Biol *30*, 131-145.

Berthiau, A.S., Yankulov, K., Bah, A., Revardel, E., Luciano, P., Wellinger, R.J., Geli, V., and Gilson, E. (2006). Subtelomeric proteins negatively regulate telomere elongation in budding yeast. Embo J *25*, 846-856.

Bianchi, A., and Shore, D. (2007). Increased association of telomerase with short telomeres in yeast. Genes & Development *21*, 1726-1730.

Bianchi, A., and Shore, D. (2008). Molecular biology. Refined view of the ends. Science *320*, 1301-1302.

Biessmann, H., and Mason, J.M. (1997). Telomere maintenance without telomerase. Chromosoma *106*, 63-69.

Blackwell, L.J., and Borowiec, J.A. (1994). Human replication protein A binds single-stranded DNA in two distinct complexes. Mol Cell Biol *14*, 3993-4001.

Bonetti, D., Clerici, M., Manfrini, N., Lucchini, G., and Longhese, M.P. (2010). The MRX complex plays multiple functions in resection of Yku- and Rif2-protected DNA ends. PLoS One *5*, e14142.

Bonetti, D., Martina, M., Clerici, M., Lucchini, G., and Longhese, M.P. (2009). Multiple pathways regulate 3' overhang generation at S. cerevisiae telomeres. Mol Cell *35*, 70-81.

Boule, J.B., Vega, L.R., and Zakian, V.A. (2005). The yeast Pif1p helicase removes telomerase from telomeric DNA. Nature *438*, 57-61.

Boulton, S.J., and Jackson, S.P. (1996). Identification of a Saccharomyces cerevisiae Ku80 homologue: roles in DNA double strand break rejoining and in telomeric maintenance. Nucleic Acids Res *24*, 4639-4648.

Bourns, B.D., Alexander, M.K., Smith, A.M., and Zakian, V.A. (1998). Sir proteins, Rif proteins, and Cdc13p bind Saccharomyces telomeres in vivo. Mol Cell Biol *18*, 5600-5608.

Brand, A.H., Micklem, G., and Nasmyth, K. (1987). A yeast silencer contains sequences that can promote autonomous plasmid replication and transcriptional activation. Cell *51*, 709-719.

Breitkreutz, A., Choi, H., Sharom, J.R., Boucher, L., Neduva, V., Larsen, B., Lin, Z.Y., Breitkreutz, B.J., Stark, C., Liu, G*., et al.* (2010). A global protein kinase and phosphatase interaction network in yeast. Science *328*, 1043-1046.

Bricogne, G. (1993). Direct phase determination by entropy maximization and likelihood ranking: status report and perspectives. Acta Crystallogr D Biol Crystallogr *49*, 37-60.

Brill, S.J., and Stillman, B. (1991). Replication factor-A from Saccharomyces cerevisiae is encoded by three essential genes coordinately expressed at S phase. Genes & Development *5*, 1589-1600.

Bryan, T.M., Englezou, A., Dalla-Pozza, L., Dunham, M.A., and Reddel, R.R. (1997). Evidence for an alternative mechanism for maintaining telomere length in human tumors and tumor-derived cell lines. Nat Med *3*, 1271-1274.

Bryan, T.M., Englezou, A., Gupta, J., Bacchetti, S., and Reddel, R.R. (1995). Telomere elongation in immortal human cells without detectable telomerase activity. Embo J *14*, 4240-4248.

Buchman, A.R., Lue, N.F., and Kornberg, R.D. (1988). Connections between transcriptional activators, silencers, and telomeres as revealed by functional analysis of a yeast DNA-binding protein. Mol Cell Biol *8*, 5086-5099.

Buck, S.W., and Shore, D. (1995). Action of a RAP1 carboxy-terminal silencing domain reveals an underlying competition between HMR and telomeres in yeast. Genes & Development *9*, 370-384.

Buonomo, S.B., Wu, Y., Ferguson, D., and de Lange, T. (2009). Mammalian Rif1 contributes to replication stress survival and homology-directed repair. J Cell Biol *187*, 385-398.

Ceulemans, H., and Bollen, M. (2006). A tighter RVxF motif makes a finer Sift. Chem Biol *13*, 6-8.

Chan, C.S., and Tye, B.K. (1983). Organization of DNA sequences and replication origins at yeast telomeres. Cell *33*, 563-573.

Chan, S.W., Chang, J., Prescott, J., and Blackburn, E.H. (2001). Altering telomere structure allows telomerase to act in yeast lacking ATM kinases. Curr Biol *11*, 1240-1250.

Chandra, A., Hughes, T.R., Nugent, C.I., and Lundblad, V. (2001). Cdc13 both positively and negatively regulates telomere replication. Genes & Development *15*, 404-414.

Chen, Y., Rai, R., Zhou, Z.R., Kanoh, J., Ribeyre, C., Yang, Y., Zheng, H., Damay, P., Wang, F., Tsujii, H*., et al.* (2011). A conserved motif within RAP1 has diversified roles in telomere protection and regulation in different organisms. Nat Struct Mol Biol *18*, 213-221.

Chien, C.T., Buck, S., Sternglanz, R., and Shore, D. (1993). Targeting of SIR1 protein establishes transcriptional silencing at HM loci and telomeres in yeast. Cell *75*, 531-541.

Cohn, M., McEachern, M.J., and Blackburn, E.H. (1998). Telomeric sequence diversity within the genus Saccharomyces. Curr Genet *33*, 83-91.

Cong, Y.S., Wright, W.E., and Shay, J.W. (2002). Human telomerase and its regulation. Microbiol Mol Biol Rev *66*, 407-425, table of contents.

Conrad, M.N., Wright, J.H., Wolf, A.J., and Zakian, V.A. (1990). RAP1 protein interacts with yeast telomeres in vivo: overproduction alters telomere structure and decreases chromosome stability. Cell *63*, 739-750.

Conti, E., Uy, M., Leighton, L., Blobel, G., and Kuriyan, J. (1998). Crystallographic analysis of the recognition of a nuclear localization signal by the nuclear import factor karyopherin alpha. Cell *94*, 193-204.

de Lange, T. (2005). Shelterin: the protein complex that shapes and safeguards human telomeres. Genes & Development *19*, 2100-2110.

de Lange, T. (2009). How telomeres solve the end-protection problem. Science *326*, 948-952.

Dewar, J.M., and Lydall, D. (2010). Pif1- and Exo1-dependent nucleases coordinate checkpoint activation following telomere uncapping. Embo J *29*, 4020-4034.

Dewar, J.M., and Lydall, D. (2012). Similarities and differences between "uncapped" telomeres and DNA double-strand breaks. Chromosoma *121*, 117-130.

Dickson, A.M., Krasikova, Y., Pestryakov, P., Lavrik, O., and Wold, M.S. (2009). Essential functions of the 32 kDa subunit of yeast replication protein A. Nucleic Acids Res *37*, 2313-2326.

DuBois, M.L., Haimberger, Z.W., McIntosh, M.W., and Gottschling, D.E. (2002). A quantitative assay for telomere protection in Saccharomyces cerevisiae. Genetics *161*, 995-1013.

Duderstadt, K.E., Chuang, K., and Berger, J.M. (2011). DNA stretching by bacterial initiators promotes replication origin opening. Nature *478*, 209-213.

Dueber, E.L., Corn, J.E., Bell, S.D., and Berger, J.M. (2007). Replication origin recognition and deformation by a heterodimeric archaeal Orc1 complex. Science *317*, 1210-1213.

Egloff, M.P., Johnson, D.F., Moorhead, G., Cohen, P.T., Cohen, P., and Barford, D. (1997). Structural basis for the recognition of regulatory subunits by the catalytic subunit of protein phosphatase 1. Embo J *16*, 1876-1887.

Emsley, P., Lohkamp, B., Scott, W.G., and Cowtan, K. (2010). Features and development of Coot. Acta Crystallogr D Biol Crystallogr *66*, 486-501.

Enomoto, S., Glowczewski, L., and Berman, J. (2002). MEC3, MEC1, and DDC2 are essential components of a telomere checkpoint pathway required for cell cycle arrest during senescence in Saccharomyces cerevisiae. Mol Biol Cell *13*, 2626-2638.

Esteves, S.L., Domingues, S.C., da Cruz e Silva, O.A., Fardilha, M., and da Cruz e Silva, E.F. (2012). Protein phosphatase 1alpha interacting proteins in the human brain. Omics *16*, 3-17.

Evans, S.K., and Lundblad, V. (1999). Est1 and Cdc13 as comediators of telomerase access. Science *286*, 117-120.

Feeser, E.A., and Wolberger, C. (2008). Structural and functional studies of the Rap1 C-terminus reveal novel separation-of-function mutants. J Mol Biol *380*, 520-531.

Fisher, T.S., Taggart, A.K., and Zakian, V.A. (2004). Cell cycle-dependent regulation of yeast telomerase by Ku. Nat Struct Mol Biol *11*, 1198-1205.

Forstemann, K., and Lingner, J. (2001). Molecular basis for telomere repeat divergence in budding yeast. Mol Cell Biol *21*, 7277-7286.

Foster, S.S., Zubko, M.K., Guillard, S., and Lydall, D. (2006). MRX protects telomeric DNA at uncapped telomeres of budding yeast cdc13-1 mutants. DNA Repair (Amst) *5*, 840-851.

Freeman, K., Gwadz, M., and Shore, D. (1995). Molecular and genetic analysis of the toxic effect of RAP1 overexpression in yeast. Genetics *141*, 1253-1262.

Gallardo, F., Laterreur, N., Cusanelli, E., Ouenzar, F., Querido, E., Wellinger, R.J., and Chartrand, P. (2011). Live cell imaging of telomerase RNA dynamics reveals cell cycle-dependent clustering of telomerase at elongating telomeres. Mol Cell *44*, 819-827.

Gao, H., Cervantes, R.B., Mandell, E.K., Otero, J.H., and Lundblad, V. (2007). RPA-like proteins mediate yeast telomere function. Nat Struct Mol Biol *14*, 208-214.

Gao, H., Toro, T.B., Paschini, M., Braunstein-Ballew, B., Cervantes, R.B., and Lundblad, V. (2010). Telomerase recruitment in Saccharomyces cerevisiae is not dependent on Tel1-mediated phosphorylation of Cdc13. Genetics *186*, 1147-1159.

Garces, R.G., Gillon, W., and Pai, E.F. (2007). Atomic model of human Rcd-1 reveals an armadillo-like-repeat protein with in vitro nucleic acid binding properties. Protein Sci *16*, 176-188.

Garvik, B., Carson, M., and Hartwell, L. (1995). Single-stranded DNA arising at telomeres in cdc13 mutants may constitute a specific signal for the RAD9 checkpoint. Mol Cell Biol *15*, 6128-6138.

Gaudier, M., Schuwirth, B.S., Westcott, S.L., and Wigley, D.B. (2007). Structural basis of DNA replication origin recognition by an ORC protein. Science *317*, 1213-1216.

Gilson, E., Roberge, M., Giraldo, R., Rhodes, D., and Gasser, S.M. (1993). Distortion of the DNA double helix by RAP1 at silencers and multiple telomeric binding sites. J Mol Biol *231*, 293-310.

Gottschling, D.E. (1992). Telomere-proximal DNA in Saccharomyces cerevisiae is refractory to methyltransferase activity in vivo. Proc Natl Acad Sci U S A *89*, 4062-4065.

Gottschling, D.E., Aparicio, O.M., Billington, B.L., and Zakian, V.A. (1990). Position effect at S. cerevisiae telomeres: reversible repression of Pol II transcription. Cell *63*, 751-762.

Graham, I.R., Haw, R.A., Spink, K.G., Halden, K.A., and Chambers, A. (1999). In vivo analysis of functional regions within yeast Rap1p. Mol Cell Biol *19*, 7481-7490.

Grandin, N., Damon, C., and Charbonneau, M. (2001). Ten1 functions in telomere end protection and length regulation in association with Stn1 and Cdc13. Embo J *20*, 1173-1183.

Grandin, N., Reed, S.I., and Charbonneau, M. (1997). Stn1, a new Saccharomyces cerevisiae protein, is implicated in telomere size regulation in association with Cdc13. Genes & Development *11*, 512-527.

Gravel, S., Chapman, J.R., Magill, C., and Jackson, S.P. (2008). DNA helicases Sgs1 and BLM promote DNA double-strand break resection. Genes & Development *22*, 2767-2772.

Gravel, S., Larrivee, M., Labrecque, P., and Wellinger, R.J. (1998). Yeast Ku as a regulator of chromosomal DNA end structure. Science *280*, 741-744.

Greenwell, P.W., Kronmal, S.L., Porter, S.E., Gassenhuber, J., Obermaier, B., and Petes, T.D. (1995). TEL1, a gene involved in controlling telomere length in S. cerevisiae, is homologous to the human ataxia telangiectasia gene. Cell *82*, 823-829.

Greider, C.W., and Blackburn, E.H. (1987). The telomere terminal transferase of Tetrahymena is a ribonucleoprotein enzyme with two kinds of primer specificity. Cell *51*, 887-898.

Greider, C.W., and Blackburn, E.H. (1989). A telomeric sequence in the RNA of Tetrahymena telomerase required for telomere repeat synthesis. Nature *337*, 331-337.

Grossi, S., Puglisi, A., Dmitriev, P.V., Lopes, M., and Shore, D. (2004). Pol12, the B subunit of DNA polymerase alpha, functions in both telomere capping and length regulation. Genes & Development *18*, 992-1006.

Haber, J.E. (1998). The many interfaces of Mre11. Cell *95*, 583-586.

Hahn, W.C., Counter, C.M., Lundberg, A.S., Beijersbergen, R.L., Brooks, M.W., and Weinberg, R.A. (1999). Creation of human tumour cells with defined genetic elements. Nature *400*, 464-468.

Hammet, A., Magill, C., Heierhorst, J., and Jackson, S.P. (2007). Rad9 BRCT domain interaction with phosphorylated H2AX regulates the G1 checkpoint in budding yeast. EMBO Rep *8*, 851-857.

Hang, L.E., Liu, X., Cheung, I., Yang, Y., and Zhao, X. (2011). SUMOylation regulates telomere length homeostasis by targeting Cdc13. Nat Struct Mol Biol *18*, 920-926.

Hardy, C.F., Sussel, L., and Shore, D. (1992). A RAP1-interacting protein involved in transcriptional silencing and telomere length regulation. Genes & Development *6*, 801-814.

Harley, C.B., Futcher, A.B., and Greider, C.W. (1990). Telomeres shorten during ageing of human fibroblasts. Nature *345*, 458-460.

Harrison, J.C., and Haber, J.E. (2006). Surviving the breakup: the DNA damage checkpoint. Annu Rev Genet *40*, 209-235.

Hecht, A., Laroche, T., Strahl-Bolsinger, S., Gasser, S.M., and Grunstein, M. (1995). Histone H3 and H4 N-termini interact with SIR3 and SIR4 proteins: a molecular model for the formation of heterochromatin in yeast. Cell *80*, 583-592.

Hecht, A., Strahl-Bolsinger, S., and Grunstein, M. (1996). Spreading of transcriptional repressor SIR3 from telomeric heterochromatin. Nature *383*, 92-96.

Hendrickx, A., Beullens, M., Ceulemans, H., Den Abt, T., Van Eynde, A., Nicolaescu, E., Lesage, B., and Bollen, M. (2009). Docking motif-guided mapping of the interactome of protein phosphatase-1. Chem Biol *16*, 365-371.

Henry, Y.A., Chambers, A., Tsang, J.S., Kingsman, A.J., and Kingsman, S.M. (1990). Characterisation of the DNA binding domain of the yeast RAP1 protein. Nucleic Acids Res *18*, 2617-2623.

Heyer, W.D., Rao, M.R., Erdile, L.F., Kelly, T.J., and Kolodner, R.D. (1990). An essential Saccharomyces cerevisiae single-stranded DNA binding protein is homologous to the large subunit of human RP-A. Embo J *9*, 2321-2329.

Higashiyama, T., Noutoshi, Y., Fujie, M., and Yamada, T. (1997). Zepp, a LINE-like retrotransposon accumulated in the Chlorella telomeric region. Embo J *16*, 3715-3723.

Hirano, Y., Fukunaga, K., and Sugimoto, K. (2009). Rif1 and rif2 inhibit localization of tel1 to DNA ends. Mol Cell *33*, 312-322.

Hiyama, E., Hiyama, K., Yokoyama, T., Matsuura, Y., Piatyszek, M.A., and Shay, J.W. (1995). Correlating telomerase activity levels with human neuroblastoma outcomes. Nat Med *1*, 249-255.

Holm, L., and Rosenstrom, P. (2010). Dali server: conservation mapping in 3D. Nucleic Acids Res *38*, W545-549.

Howarth, K.D., Blood, K.A., Ng, B.L., Beavis, J.C., Chua, Y., Cooke, S.L., Raby, S., Ichimura, K., Collins, V.P., Carter, N.P.*, et al.* (2008). Array painting reveals a high frequency of balanced translocations in breast cancer cell lines that break in cancer-relevant genes. Oncogene *27*, 3345-3359.

Huber, A.H., Nelson, W.J., and Weis, W.I. (1997). Three-dimensional structure of the armadillo repeat region of beta-catenin. Cell *90*, 871-882.

Hughes, T.R., Weilbaecher, R.G., Walterscheid, M., and Lundblad, V. (2000). Identification of the single-strand telomeric DNA binding domain of the Saccharomyces cerevisiae Cdc13 protein. Proc Natl Acad Sci U S A *97*, 6457-6462.

Hurley, T.D., Yang, J., Zhang, L., Goodwin, K.D., Zou, Q., Cortese, M., Dunker, A.K., and DePaoli-Roach, A.A. (2007). Structural basis for regulation of protein phosphatase 1 by inhibitor-2. J Biol Chem *282*, 28874-28883.

Idrissi, F.Z., Fernandez-Larrea, J.B., and Pina, B. (1998). Structural and functional heterogeneity of Rap1p complexes with telomeric and UASrpg-like DNA sequences. J Mol Biol *284*, 925-935.

Iglesias, N., Redon, S., Pfeiffer, V., Dees, M., Lingner, J., and Luke, B. (2011). Subtelomeric repetitive elements determine TERRA regulation by Rap1/Rif and Rap1/Sir complexes in yeast. EMBO Rep *12*, 587-593.

Ivanov, E.L., Sugawara, N., White, C.I., Fabre, F., and Haber, J.E. (1994). Mutations in XRS2 and RAD50 delay but do not prevent mating-type switching in Saccharomyces cerevisiae. Mol Cell Biol *14*, 3414-3425.

Jia, X., Weinert, T., and Lydall, D. (2004). Mec1 and Rad53 inhibit formation of single-stranded DNA at telomeres of Saccharomyces cerevisiae cdc13-1 mutants. Genetics *166*, 753-764.

Kabsch, W. (2010). Xds. Acta Crystallogr D Biol Crystallogr *66*, 125-132.

Kanoh, J., and Ishikawa, F. (2001). spRap1 and spRif1, recruited to telomeres by Taz1, are essential for telomere function in fission yeast. Curr Biol *11*, 1624-1630.

Keogh, M.C., Kim, J.A., Downey, M., Fillingham, J., Chowdhury, D., Harrison, J.C., Onishi, M., Datta, N., Galicia, S., Emili, A., *et al.* (2006). A phosphatase complex that dephosphorylates gammaH2AX regulates DNA damage checkpoint recovery. Nature *439*, 497-501.

Kim, C., Snyder, R.O., and Wold, M.S. (1992). Binding properties of replication protein A from human and yeast cells. Mol Cell Biol *12*, 3050-3059.

Kim, S.T., Lim, D.S., Canman, C.E., and Kastan, M.B. (1999). Substrate specificities and identification of putative substrates of ATM kinase family members. J Biol Chem *274*, 37538-37543.

Konig, P., Giraldo, R., Chapman, L., and Rhodes, D. (1996). The crystal structure of the DNA-binding domain of yeast RAP1 in complex with telomeric DNA. Cell *85*, 125-136.

Krissinel, E., and Henrick, K. (2007). Inference of macromolecular assemblies from crystalline state. J Mol Biol *372*, 774-797.

Kurtz, S., and Shore, D. (1991). RAP1 protein activates and silences transcription of mating-type genes in yeast. Genes & Development *5*, 616-628.

Kyrion, G., Liu, K., Liu, C., and Lustig, A.J. (1993). RAP1 and telomere structure regulate telomere position effects in Saccharomyces cerevisiae. Genes & Development *7*, 1146-1159.

Landry, J., Slama, J.T., and Sternglanz, R. (2000). Role of NAD(+) in the deacetylase activity of the SIR2-like proteins. Biochem Biophys Res Commun *278*, 685-690.

Larrivee, M., LeBel, C., and Wellinger, R.J. (2004). The generation of proper constitutive G-tails on yeast telomeres is dependent on the MRX complex. Genes & Development *18*, 1391-1396.

Laurenson, P., and Rine, J. (1992). Silencers, silencing, and heritable transcriptional states. Microbiol Rev *56*, 543-560.

Lazzaro, F., Sapountzi, V., Granata, M., Pellicioli, A., Vaze, M., Haber, J.E., Plevani, P., Lydall, D., and Muzi-Falconi, M. (2008). Histone methyltransferase Dot1 and Rad9 inhibit single-stranded DNA accumulation at DSBs and uncapped telomeres. Embo J *27*, 1502-1512.

Lee, S.E., Moore, J.K., Holmes, A., Umezu, K., Kolodner, R.D., and Haber, J.E. (1998). Saccharomyces Ku70, mre11/rad50 and RPA proteins regulate adaptation to G2/M arrest after DNA damage. Cell *94*, 399-409.

Lendvay, T.S., Morris, D.K., Sah, J., Balasubramanian, B., and Lundblad, V. (1996). Senescence mutants of Saccharomyces cerevisiae with a defect in telomere replication identify three additional EST genes. Genetics *144*, 1399-1412.

Levis, R.W., Ganesan, R., Houtchens, K., Tolar, L.A., and Sheen, F.M. (1993). Transposons in place of telomeric repeats at a Drosophila telomere. Cell *75*, 1083-1093.

Levy, D.L., and Blackburn, E.H. (2004). Counting of Rif1p and Rif2p on Saccharomyces cerevisiae telomeres regulates telomere length. Mol Cell Biol *24*, 10857-10867.

Li, S., Makovets, S., Matsuguchi, T., Blethrow, J.D., Shokat, K.M., and Blackburn, E.H. (2009). Cdk1-dependent phosphorylation of Cdc13 coordinates telomere elongation during cell-cycle progression. Cell *136*, 50-61.

Lieb, J.D., Liu, X., Botstein, D., and Brown, P.O. (2001). Promoter-specific binding of Rap1 revealed by genome-wide maps of protein-DNA association. Nat Genet *28*, 327-334.

Lin, J.J., and Zakian, V.A. (1996). The Saccharomyces CDC13 protein is a single-strand TG1-3 telomeric DNA-binding protein in vitro that affects telomere behavior in vivo. Proc Natl Acad Sci U S A *93*, 13760-13765.

Lingner, J., Cech, T.R., Hughes, T.R., and Lundblad, V. (1997a). Three Ever Shorter Telomere (EST) genes are dispensable for in vitro yeast telomerase activity. Proc Natl Acad Sci U S A *94*, 11190-11195.

Lingner, J., Hughes, T.R., Shevchenko, A., Mann, M., Lundblad, V., and Cech, T.R. (1997b). Reverse transcriptase motifs in the catalytic subunit of telomerase. Science *276*, 561-567.

Lisby, M., Barlow, J.H., Burgess, R.C., and Rothstein, R. (2004). Choreography of the DNA damage response: spatiotemporal relationships among checkpoint and repair proteins. Cell *118*, 699-713.

Lisby, M., and Rothstein, R. (2004). DNA damage checkpoint and repair centers. Curr Opin Cell Biol *16*, 328-334.

Longhese, M.P., Mantiero, D., and Clerici, M. (2006). The cellular response to chromosome breakage. Mol Microbiol *60*, 1099-1108.

Lu, X., Nannenga, B., and Donehower, L.A. (2005). PPM1D dephosphorylates Chk1 and p53 and abrogates cell cycle checkpoints. Genes & Development *19*, 1162-1174.

Luciano, P., Coulon, S., Faure, V., Corda, Y., Bos, J., Brill, S.J., Gilson, E., Simon, M.N., and Geli, V. (2012). RPA facilitates telomerase activity at chromosome ends in budding and fission yeasts. Embo J *31*, 2034-2046.

Luke, B., Panza, A., Redon, S., Iglesias, N., Li, Z., and Lingner, J. (2008). The Rat1p 5' to 3' exonuclease degrades telomeric repeat-containing RNA and promotes telomere elongation in Saccharomyces cerevisiae. Mol Cell *32*, 465-477.

Lundblad, V., and Blackburn, E.H. (1993). An alternative pathway for yeast telomere maintenance rescues est1- senescence. Cell *73*, 347-360.

Lundblad, V., and Szostak, J.W. (1989). A mutant with a defect in telomere elongation leads to senescence in yeast. Cell *57*, 633-643.

Lustig, A.J., Kurtz, S., and Shore, D. (1990). Involvement of the silencer and UAS binding protein RAP1 in regulation of telomere length. Science *250*, 549-553.

Lydall, D., and Weinert, T. (1995). Yeast checkpoint genes in DNA damage processing: implications for repair and arrest. Science *270*, 1488-1491.

Lydeard, J.R., Jain, S., Yamaguchi, M., and Haber, J.E. (2007). Break-induced replication and telomerase-independent telomere maintenance require Pol32. Nature *448*, 820-823.

Mak, H.C., Pillus, L., and Ideker, T. (2009). Dynamic reprogramming of transcription factors to and from the subtelomere. Genome Res *19*, 1014-1025.

Makarov, V.L., Hirose, Y., and Langmore, J.P. (1997). Long G tails at both ends of human chromosomes suggest a C strand degradation mechanism for telomere shortening. Cell *88*, 657-666.

Mallory, J.C., Bashkirov, V.I., Trujillo, K.M., Solinger, J.A., Dominska, M., Sung, P., Heyer, W.D., and Petes, T.D. (2003). Amino acid changes in Xrs2p, Dun1p, and Rfa2p that remove the preferred targets of the ATM family of protein kinases do not affect DNA repair or telomere length in Saccharomyces cerevisiae. DNA Repair (Amst) *2*, 1041-1064.

Manning, G., Whyte, D.B., Martinez, R., Hunter, T., and Sudarsanam, S. (2002). The protein kinase complement of the human genome. Science *298*, 1912-1934.

Marcand, S., Brevet, V., and Gilson, E. (1999). Progressive cis-inhibition of telomerase upon telomere elongation. Embo J *18*, 3509-3519.

Marcand, S., Gilson, E., and Shore, D. (1997). A protein-counting mechanism for telomere length regulation in yeast. Science *275*, 986-990.

Marcand, S., Pardo, B., Gratias, A., Cahun, S., and Callebaut, I. (2008). Multiple pathways inhibit NHEJ at telomeres. Genes & Development *22*, 1153-1158.

Maringele, L., and Lydall, D. (2002). EXO1-dependent single-stranded DNA at telomeres activates subsets of DNA damage and spindle checkpoint pathways in budding yeast yku70Delta mutants. Genes & Development *16*, 1919-1933.

Martina, M., Clerici, M., Baldo, V., Bonetti, D., Lucchini, G., and Longhese, M.P. (2012). A balance between Tel1 and Rif2 activities regulates nucleolytic processing and elongation at telomeres. Mol Cell Biol *32*, 1604-1617.

Matot, B., Le Bihan, Y.V., Lescasse, R., Perez, J., Miron, S., David, G., Castaing, B., Weber, P., Raynal, B., Zinn-Justin, S*., et al.* (2012). The orientation of the C-terminal domain of the

Saccharomyces cerevisiae Rap1 protein is determined by its binding to DNA. Nucleic Acids Res *40*, 3197-3207.

Matsuoka, S., Ballif, B.A., Smogorzewska, A., McDonald, E.R., 3rd, Hurov, K.E., Luo, J., Bakalarski, C.E., Zhao, Z., Solimini, N., Lerenthal, Y.*, et al.* (2007). ATM and ATR substrate analysis reveals extensive protein networks responsive to DNA damage. Science *316*, 1160-1166.

McCoy, A.J., Grosse-Kunstleve, R.W., Adams, P.D., Winn, M.D., Storoni, L.C., and Read, R.J. (2007). Phaser crystallographic software. J Appl Crystallogr *40*, 658-674.

McEachern, M.J., and Blackburn, E.H. (1996). Cap-prevented recombination between terminal telomeric repeat arrays (telomere CPR) maintains telomeres in Kluyveromyces lactis lacking telomerase. Genes & Development *10*, 1822-1834.

McElligott, R., and Wellinger, R.J. (1997). The terminal DNA structure of mammalian chromosomes. Embo J *16*, 3705-3714.

McGee, J.S., Phillips, J.A., Chan, A., Sabourin, M., Paeschke, K., and Zakian, V.A. (2010). Reduced Rif2 and lack of Mec1 target short telomeres for elongation rather than double-strand break repair. Nat Struct Mol Biol *17*, 1438-1445.

Michelson, R.J., Rosenstein, S., and Weinert, T. (2005). A telomeric repeat sequence adjacent to a DNA double-stranded break produces an anticheckpoint. Genes & Development *19*, 2546-2559.

Miller, W.G., and Goebel, C.V. (1968). Dimensions of protein random coils. Biochemistry *7*, 3925-3935.

Mimitou, E.P., and Symington, L.S. (2008). Sae2, Exo1 and Sgs1 collaborate in DNA double-strand break processing. Nature *455*, 770-774.

Mitton-Fry, R.M., Anderson, E.M., Hughes, T.R., Lundblad, V., and Wuttke, D.S. (2002). Conserved structure for single-stranded telomeric DNA recognition. Science *296*, 145-147.

Moazed, D., Kistler, A., Axelrod, A., Rine, J., and Johnson, A.D. (1997). Silent information regulator protein complexes in Saccharomyces cerevisiae: a SIR2/SIR4 complex and evidence for a regulatory domain in SIR4 that inhibits its interaction with SIR3. Proc Natl Acad Sci U S A *94*, 2186-2191.

Moorhead, G.B., Trinkle-Mulcahy, L., Nimick, M., De Wever, V., Campbell, D.G., Gourlay, R., Lam, Y.W., and Lamond, A.I. (2008). Displacement affinity chromatography of protein phosphatase one (PP1) complexes. BMC Biochem *9*, 28.

Moorhead, G.B., Trinkle-Mulcahy, L., and Ulke-Lemee, A. (2007). Emerging roles of nuclear protein phosphatases. Nat Rev Mol Cell Biol *8*, 234-244.

Morales, C.P., Holt, S.E., Ouellette, M., Kaur, K.J., Yan, Y., Wilson, K.S., White, M.A., Wright, W.E., and Shay, J.W. (1999). Absence of cancer-associated changes in human fibroblasts immortalized with telomerase. Nat Genet *21*, 115-118.

Morcillo, G., Barettino, D., Carmona, M.J., Carretero, M.T., and Diez, J.L. (1988). Telomeric DNA sequences differentially activated by heat shock in two Chironomus subspecies. Chromosoma *96*, 139-144.

Moretti, P., Freeman, K., Coodly, L., and Shore, D. (1994). Evidence that a complex of SIR proteins interacts with the silencer and telomere-binding protein RAP1. Genes & Development *8*, 2257-2269.

Moretti, P., and Shore, D. (2001). Multiple interactions in Sir protein recruitment by Rap1p at silencers and telomeres in yeast. Mol Cell Biol *21*, 8082-8094.

Nakada, D., Matsumoto, K., and Sugimoto, K. (2003). ATM-related Tel1 associates with double-strand breaks through an Xrs2-dependent mechanism. Genes & Development *17*, 1957-1962.

Nakamura, T.M., Morin, G.B., Chapman, K.B., Weinrich, S.L., Andrews, W.H., Lingner, J., Harley, C.B., and Cech, T.R. (1997). Telomerase catalytic subunit homologs from fission yeast and human. Science *277*, 955-959.

Nazarov, I.B., Smirnova, A.N., Krutilina, R.I., Svetlova, M.P., Solovjeva, L.V., Nikiforov, A.A., Oei, S.L., Zalenskaya, I.A., Yau, P.M., Bradbury, E.M., *et al.* (2003). Dephosphorylation of histone gamma-H2AX during repair of DNA double-strand breaks in mammalian cells and its inhibition by calyculin A. Radiat Res *160*, 309-317.

Negrini, S., Ribaud, V., Bianchi, A., and Shore, D. (2007). DNA breaks are masked by multiple Rap1 binding in yeast: implications for telomere capping and telomerase regulation. Genes & Development *21*, 292-302.

Ngo, H.P., and Lydall, D. (2010). Survival and growth of yeast without telomere capping by Cdc13 in the absence of Sgs1, Exo1, and Rad9. PLoS Genet *6*, e1001072.

Niida, H., Matsumoto, T., Satoh, H., Shiwa, M., Tokutake, Y., Furuichi, Y., and Shinkai, Y. (1998). Severe growth defect in mouse cells lacking the telomerase RNA component. Nat Genet *19*, 203-206.

Nugent, C.I., Bosco, G., Ross, L.O., Evans, S.K., Salinger, A.P., Moore, J.K., Haber, J.E., and Lundblad, V. (1998). Telomere maintenance is dependent on activities required for end repair of double-strand breaks. Curr Biol *8*, 657-660.

Olovnikov, A.M. (1973). A theory of marginotomy. The incomplete copying of template margin in enzymic synthesis of polynucleotides and biological significance of the phenomenon. J Theor Biol *41*, 181-190.

Ono, Y., Tomita, K., Matsuura, A., Nakagawa, T., Masukata, H., Uritani, M., Ushimaru, T., and Ueno, M. (2003). A novel allele of fission yeast rad11 that causes defects in DNA repair and telomere length regulation. Nucleic Acids Res *31*, 7141-7149.

Palm, W., and de Lange, T. (2008). How shelterin protects mammalian telomeres. Annu Rev Genet *42*, 301-334.

Papai, G., Tripathi, M.K., Ruhlmann, C., Layer, J.H., Weil, P.A., and Schultz, P. (2010). TFIIA and the transactivator Rap1 cooperate to commit TFIID for transcription initiation. Nature *465*, 956-960.

Peifer, M., Berg, S., and Reynolds, A.B. (1994). A repeating amino acid motif shared by proteins with diverse cellular roles. Cell *76*, 789-791.

Pennock, E., Buckley, K., and Lundblad, V. (2001). Cdc13 delivers separate complexes to the telomere for end protection and replication. Cell *104*, 387-396.

Peterson, S.E., Stellwagen, A.E., Diede, S.J., Singer, M.S., Haimberger, Z.W., Johnson, C.O., Tzoneva, M., and Gottschling, D.E. (2001). The function of a stem-loop in telomerase RNA is linked to the DNA repair protein Ku. Nat Genet *27*, 64-67.

Pfingsten, J.S., Goodrich, K.J., Taabazuing, C., Ouenzar, F., Chartrand, P., and Cech, T.R. (2012). Mutually exclusive binding of telomerase RNA and DNA by Ku alters telomerase recruitment model. Cell *148*, 922-932.

Philipova, D., Mullen, J.R., Maniar, H.S., Lu, J., Gu, C., and Brill, S.J. (1996). A hierarchy of SSB protomers in replication protein A. Genes & Development *10*, 2222-2233.

Polotnianka, R.M., Li, J., and Lustig, A.J. (1998). The yeast Ku heterodimer is essential for protection of the telomere against nucleolytic and recombinational activities. Curr Biol *8*, 831-834.

Puglisi, A., Bianchi, A., Lemmens, L., Damay, P., and Shore, D. (2008). Distinct roles for yeast Stn1 in telomere capping and telomerase inhibition. Embo J *27*, 2328-2339.

Qi, H., and Zakian, V.A. (2000). The Saccharomyces telomere-binding protein Cdc13p interacts with both the catalytic subunit of DNA polymerase alpha and the telomerase-associated est1 protein. Genes & Development *14*, 1777-1788.

Rass, U., Compton, S.A., Matos, J., Singleton, M.R., Ip, S.C., Blanco, M.G., Griffith, J.D., and West, S.C. (2010). Mechanism of Holliday junction resolution by the human GEN1 protein. Genes & Development *24*, 1559-1569.

Ray, A., and Runge, K.W. (1999). The yeast telomere length counting machinery is sensitive to sequences at the telomere-nontelomere junction. Mol Cell Biol *19*, 31-45.

Ribes-Zamora, A., Mihalek, I., Lichtarge, O., and Bertuch, A.A. (2007). Distinct faces of the Ku heterodimer mediate DNA repair and telomeric functions. Nat Struct Mol Biol *14*, 301-307.

Ribeyre, C., and Shore, D. (2012). Anticheckpoint pathways at telomeres in yeast. Nat Struct Mol Biol *19*, 307-313.

Ritchie, K.B., Mallory, J.C., and Petes, T.D. (1999). Interactions of TLC1 (which encodes the RNA subunit of telomerase), TEL1, and MEC1 in regulating telomere length in the yeast Saccharomyces cerevisiae. Mol Cell Biol *19*, 6065-6075.

Ritchie, K.B., and Petes, T.D. (2000). The Mre11p/Rad50p/Xrs2p complex and the Tel1p function in a single pathway for telomere maintenance in yeast. Genetics *155*, 475-479.

Rodriguez, D.D., Grosse, C., Himmel, S., Gonzalez, C., de Ilarduya, I.M., Becker, S., Sheldrick, G.M., and Uson, I. (2009). Crystallographic ab initio protein structure solution below atomic resolution. Nat Methods *6*, 651-653.

Rouse, J., and Jackson, S.P. (2002). Lcd1p recruits Mec1p to DNA lesions in vitro and in vivo. Mol Cell *9*, 857-869.

Rusche, L.N., Kirchmaier, A.L., and Rine, J. (2002). Ordered nucleation and spreading of silenced chromatin in Saccharomyces cerevisiae. Mol Biol Cell *13*, 2207-2222.

Sabourin, M., Tuzon, C.T., and Zakian, V.A. (2007). Telomerase and Tel1p preferentially associate with short telomeres in S. cerevisiae. Mol Cell *27*, 550-561.

Sanchez, Y., Bachant, J., Wang, H., Hu, F., Liu, D., Tetzlaff, M., and Elledge, S.J. (1999). Control of the DNA damage checkpoint by chk1 and rad53 protein kinases through distinct mechanisms. Science *286*, 1166-1171.

Sandell, L.L., and Zakian, V.A. (1993). Loss of a yeast telomere: arrest, recovery, and chromosome loss. Cell *75*, 729-739.

Schoeftner, S., and Blasco, M.A. (2008). Developmentally regulated transcription of mammalian telomeres by DNA-dependent RNA polymerase II. Nat Cell Biol *10*, 228-236.

Schramke, V., Luciano, P., Brevet, V., Guillot, S., Corda, Y., Longhese, M.P., Gilson, E., and Geli, V. (2004). RPA regulates telomerase action by providing Est1p access to chromosome ends. Nat Genet *36*, 46-54.

Sharan, S.K., Morimatsu, M., Albrecht, U., Lim, D.S., Regel, E., Dinh, C., Sands, A., Eichele, G., Hasty, P., and Bradley, A. (1997). Embryonic lethality and radiation hypersensitivity mediated by Rad51 in mice lacking Brca2. Nature *386*, 804-810.

Sheldrick, G.M. (2008). A short history of SHELX. Acta Crystallogr A *64*, 112-122.

Shore, D. (1994). RAP1: a protean regulator in yeast. Trends Genet *10*, 408-412.

Shore, D., and Nasmyth, K. (1987). Purification and cloning of a DNA binding protein from yeast that binds to both silencer and activator elements. Cell *51*, 721-732.

Silverman, J., Takai, H., Buonomo, S.B., Eisenhaber, F., and de Lange, T. (2004). Human Rif1, ortholog of a yeast telomeric protein, is regulated by ATM and 53BP1 and functions in the S-phase checkpoint. Genes & Development *18*, 2108-2119.

Singer, M.S., and Gottschling, D.E. (1994). TLC1: template RNA component of Saccharomyces cerevisiae telomerase. Science *266*, 404-409.

Singh, J., and Klar, A.J. (1992). Active genes in budding yeast display enhanced in vivo accessibility to foreign DNA methylases: a novel in vivo probe for chromatin structure of yeast. Genes & Development *6*, 186-196.

Sinha, M., Watanabe, S., Johnson, A., Moazed, D., and Peterson, C.L. (2009). Recombinational repair within heterochromatin requires ATP-dependent chromatin remodeling. Cell *138*, 1109-1121.

Sjoblom, T., Jones, S., Wood, L.D., Parsons, D.W., Lin, J., Barber, T.D., Mandelker, D., Leary, R.J., Ptak, J., Silliman, N., *et al.* (2006). The consensus coding sequences of human breast and colorectal cancers. Science *314*, 268-274.

Smith, C.D., Smith, D.L., DeRisi, J.L., and Blackburn, E.H. (2003). Telomeric protein distributions and remodeling through the cell cycle in Saccharomyces cerevisiae. Mol Biol Cell *14*, 556-570.

Smolka, M.B., Albuquerque, C.P., Chen, S.H., and Zhou, H. (2007). Proteome-wide identification of in vivo targets of DNA damage checkpoint kinases. Proc Natl Acad Sci U S A *104*, 10364-10369.

Solovei, I., Gaginskaya, E.R., and Macgregor, H.C. (1994). The arrangement and transcription of telomere DNA sequences at the ends of lampbrush chromosomes of birds. Chromosome Res *2*, 460-470.

Sreesankar, E., Senthilkumar, R., Bharathi, V., Mishra, R.K., and Mishra, K. (2012). Functional diversification of yeast telomere associated protein, Rif1, in higher eukaryotes. BMC Genomics *13*, 255.

Stellwagen, A.E., Haimberger, Z.W., Veatch, J.R., and Gottschling, D.E. (2003). Ku interacts with telomerase RNA to promote telomere addition at native and broken chromosome ends. Genes & Development *17*, 2384-2395.

Sun, Z., Hsiao, J., Fay, D.S., and Stern, D.F. (1998). Rad53 FHA domain associated with phosphorylated Rad9 in the DNA damage checkpoint. Science *281*, 272-274.

Sussel, L., and Shore, D. (1991). Separation of transcriptional activation and silencing functions of the RAP1-encoded repressor/activator protein 1: isolation of viable mutants affecting both silencing and telomere length. Proc Natl Acad Sci U S A *88*, 7749-7753.

Taggart, A.K., Teng, S.C., and Zakian, V.A. (2002). Est1p as a cell cycle-regulated activator of telomere-bound telomerase. Science *297*, 1023-1026.

Taylor, H.O., O'Reilly, M., Leslie, A.G., and Rhodes, D. (2000). How the multifunctional yeast Rap1p discriminates between DNA target sites: a crystallographic analysis. J Mol Biol *303*, 693-707.

Teixeira, M.T., Arneric, M., Sperisen, P., and Lingner, J. (2004). Telomere length homeostasis is achieved via a switch between telomerase- extendible and -nonextendible states. Cell *117*, 323-335.

Teng, S.C., Chang, J., McCowan, B., and Zakian, V.A. (2000). Telomerase-independent lengthening of yeast telomeres occurs by an abrupt Rad50p-dependent, Rif-inhibited recombinational process. Mol Cell *6*, 947-952.

Teng, S.C., and Zakian, V.A. (1999). Telomere-telomere recombination is an efficient bypass pathway for telomere maintenance in Saccharomyces cerevisiae. Mol Cell Biol *19*, 8083-8093.

Terrak, M., Kerff, F., Langsetmo, K., Tao, T., and Dominguez, R. (2004). Structural basis of protein phosphatase 1 regulation. Nature *429*, 780-784.

Terwilliger, T.C. (2000). Maximum-likelihood density modification. Acta Crystallogr D Biol Crystallogr *56*, 965-972.

Trinkle-Mulcahy, L., Andersen, J., Lam, Y.W., Moorhead, G., Mann, M., and Lamond, A.I. (2006). Repo-Man recruits PP1 gamma to chromatin and is essential for cell viability. J Cell Biol *172*, 679-692.

Triolo, T., and Sternglanz, R. (1996). Role of interactions between the origin recognition complex and SIR1 in transcriptional silencing. Nature *381*, 251-253.

Tsai, H.J., Huang, W.H., Li, T.K., Tsai, Y.L., Wu, K.J., Tseng, S.F., and Teng, S.C. (2006). Involvement of topoisomerase III in telomere-telomere recombination. J Biol Chem *281*, 13717-13723.

Tseng, S.F., Lin, J.J., and Teng, S.C. (2006). The telomerase-recruitment domain of the telomere binding protein Cdc13 is regulated by Mec1p/Tel1p-dependent phosphorylation. Nucleic Acids Res *34*, 6327-6336.

Vignais, M.L., Huet, J., Buhler, J.M., and Sentenac, A. (1990). Contacts between the factor TUF and RPG sequences. J Biol Chem *265*, 14669-14674.

Vodenicharov, M.D., Laterreur, N., and Wellinger, R.J. (2010). Telomere capping in non-dividing yeast cells requires Yku and Rap1. Embo J *29*, 3007-3019.

Vodenicharov, M.D., and Wellinger, R.J. (2006). DNA degradation at unprotected telomeres in yeast is regulated by the CDK1 (Cdc28/Clb) cell-cycle kinase. Mol Cell *24*, 127-137.

Vonrhein, C., Blanc, E., Roversi, P., and Bricogne, G. (2007). Automated structure solution with autoSHARP. Methods Mol Biol *364*, 215-230.

Walker, J.R., Corpina, R.A., and Goldberg, J. (2001). Structure of the Ku heterodimer bound to DNA and its implications for double-strand break repair. Nature *412*, 607-614.

Walter, M.F., Bozorgnia, L., Maheshwari, A., and Biessmann, H. (2001). The rate of terminal nucleotide loss from a telomere of the mosquito Anopheles gambiae. Insect Mol Biol *10*, 105-110.

Wang, H., Zhao, A., Chen, L., Zhong, X., Liao, J., Gao, M., Cai, M., Lee, D.H., Li, J., Chowdhury, D*., et al.* (2009). Human RIF1 encodes an anti-apoptotic factor required for DNA repair. Carcinogenesis *30*, 1314-1319.

Wang, S.S., and Zakian, V.A. (1990). Sequencing of Saccharomyces telomeres cloned using T4 DNA polymerase reveals two domains. Mol Cell Biol *10*, 4415-4419.

Watson, J.D. (1972). Origin of concatemeric T7 DNA. Nat New Biol *239*, 197-201.

Watson, J.D., and Crick, F.H. (1953). The structure of DNA. Cold Spring Harb Symp Quant Biol *18*, 123-131.

Wellinger, R.J., Ethier, K., Labrecque, P., and Zakian, V.A. (1996). Evidence for a new step in telomere maintenance. Cell *85*, 423-433.

Wellinger, R.J., Wolf, A.J., and Zakian, V.A. (1993a). Origin activation and formation of single-strand TG1-3 tails occur sequentially in late S phase on a yeast linear plasmid. Mol Cell Biol *13*, 4057-4065.

Wellinger, R.J., Wolf, A.J., and Zakian, V.A. (1993b). Saccharomyces telomeres acquire single-strand TG1-3 tails late in S phase. Cell *72*, 51-60.

Williams, T.L., Levy, D.L., Maki-Yonekura, S., Yonekura, K., and Blackburn, E.H. (2010). Characterization of the yeast telomere nucleoprotein core: Rap1 binds independently to each recognition site. J Biol Chem *285*, 35814-35824.

Wotton, D., and Shore, D. (1997). A novel Rap1p-interacting factor, Rif2p, cooperates with Rif1p to regulate telomere length in Saccharomyces cerevisiae. Genes & Development *11*, 748-760.

Wu, Y., and Zakian, V.A. (2011). The telomeric Cdc13 protein interacts directly with the telomerase subunit Est1 to bring it to telomeric DNA ends in vitro. Proc Natl Acad Sci U S A *108*, 20362-20369.

Xu, D., Muniandy, P., Leo, E., Yin, J., Thangavel, S., Shen, X., Ii, M., Agama, K., Guo, R., Fox, D., 3rd*, et al.* (2010). Rif1 provides a new DNA-binding interface for the Bloom syndrome complex to maintain normal replication. Embo J *29*, 3140-3155.

Xu, L., and Blackburn, E.H. (2004). Human Rif1 protein binds aberrant telomeres and aligns along anaphase midzone microtubules. J Cell Biol *167*, 819-830.

Xu, L., Petreaca, R.C., Gasparyan, H.J., Vu, S., and Nugent, C.I. (2009). TEN1 is essential for CDC13-mediated telomere capping. Genetics *183*, 793-810.

Xue, Y., Rushton, M.D., and Maringele, L. (2011). A novel checkpoint and RPA inhibitory pathway regulated by Rif1. PLoS Genet *7*, e1002417.

Yarragudi, A., Parfrey, L.W., and Morse, R.H. (2007). Genome-wide analysis of transcriptional dependence and probable target sites for Abf1 and Rap1 in Saccharomyces cerevisiae. Nucleic Acids Res *35*, 193-202.

Yu, E.Y., Steinberg-Neifach, O., Dandjinou, A.T., Kang, F., Morrison, A.J., Shen, X., and Lue, N.F. (2007). Regulation of telomere structure and functions by subunits of the INO80 chromatin remodeling complex. Mol Cell Biol *27*, 5639-5649.

Yuan, S.S., Lee, S.Y., Chen, G., Song, M., Tomlinson, G.E., and Lee, E.Y. (1999). BRCA2 is required for ionizing radiation-induced assembly of Rad51 complex in vivo. Cancer Res *59*, 3547-3551.

Zhang, W., and Durocher, D. (2010). De novo telomere formation is suppressed by the Mec1-dependent inhibition of Cdc13 accumulation at DNA breaks. Genes & Development *24*, 502-515.

Zhou, J., Monson, E.K., Teng, S.C., Schulz, V.P., and Zakian, V.A. (2000). Pif1p helicase, a catalytic inhibitor of telomerase in yeast. Science *289*, 771-774.

Zou, L., and Elledge, S.J. (2003). Sensing DNA damage through ATRIP recognition of RPA-ssDNA complexes. Science *300*, 1542-1548.

Zubko, M.K., Guillard, S., and Lydall, D. (2004). Exo1 and Rad24 differentially regulate generation of ssDNA at telomeres of Saccharomyces cerevisiae cdc13-1 mutants. Genetics *168*, 103-115.

15 Supplemental figures
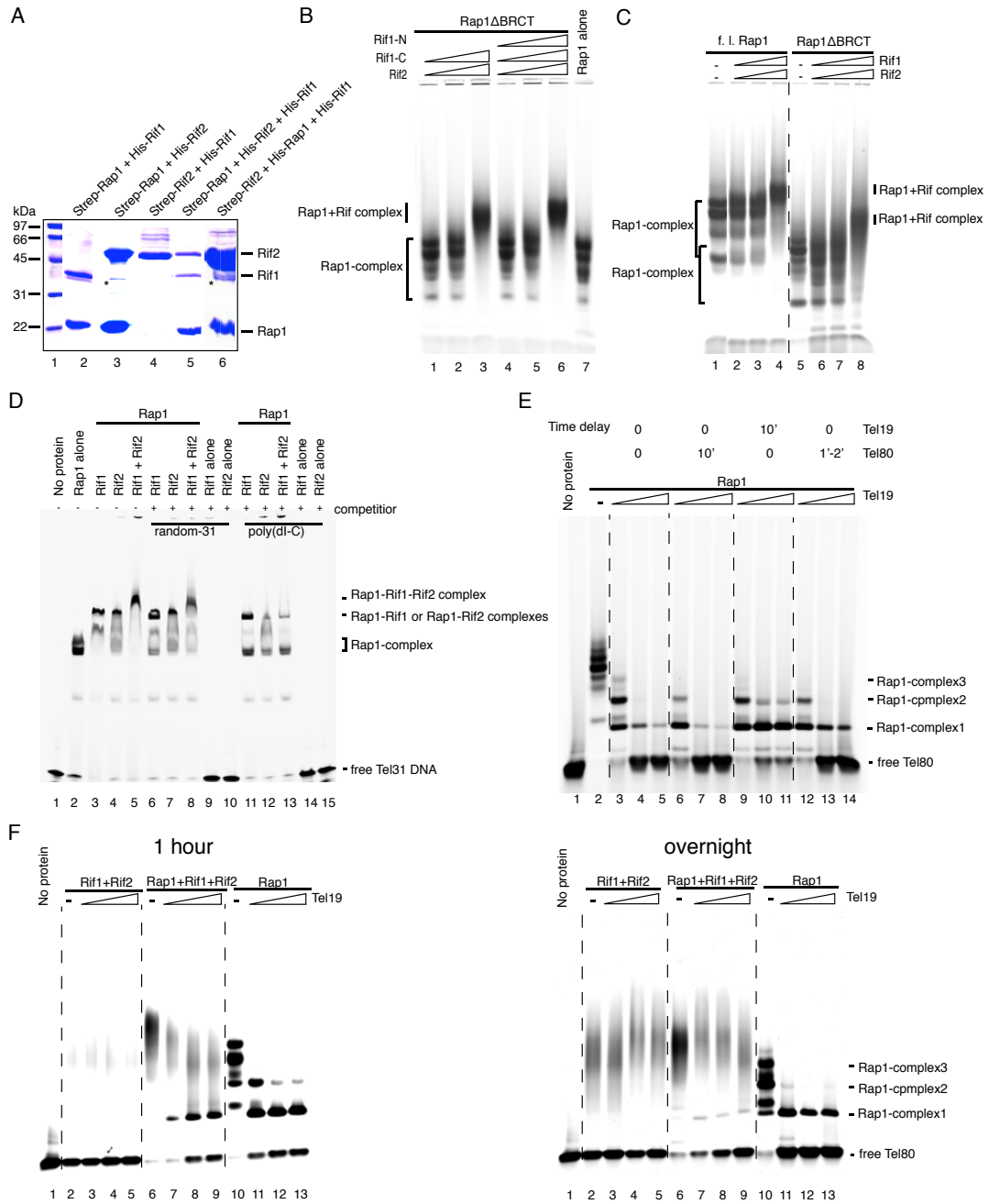
Figure S2, related to Figure 2
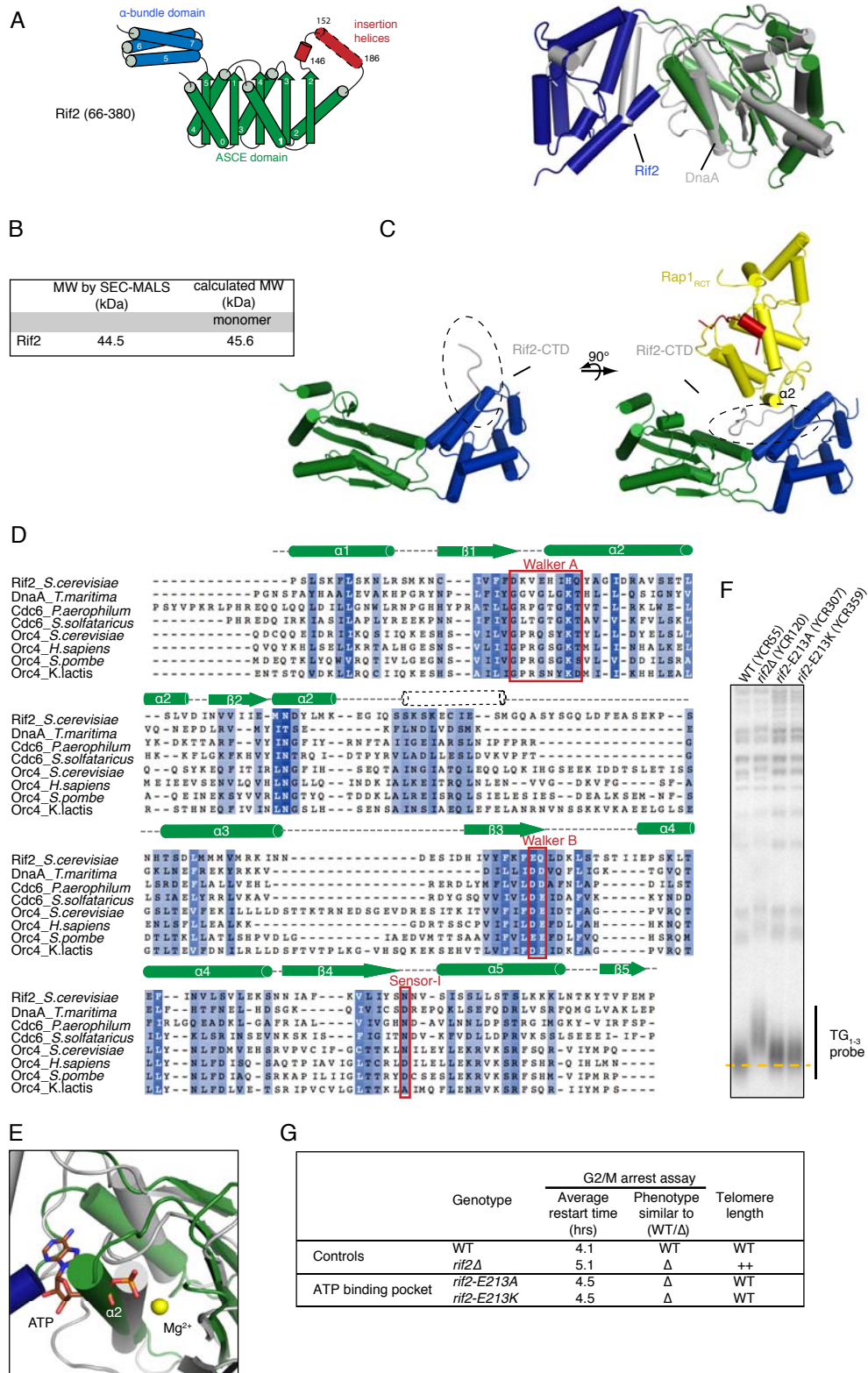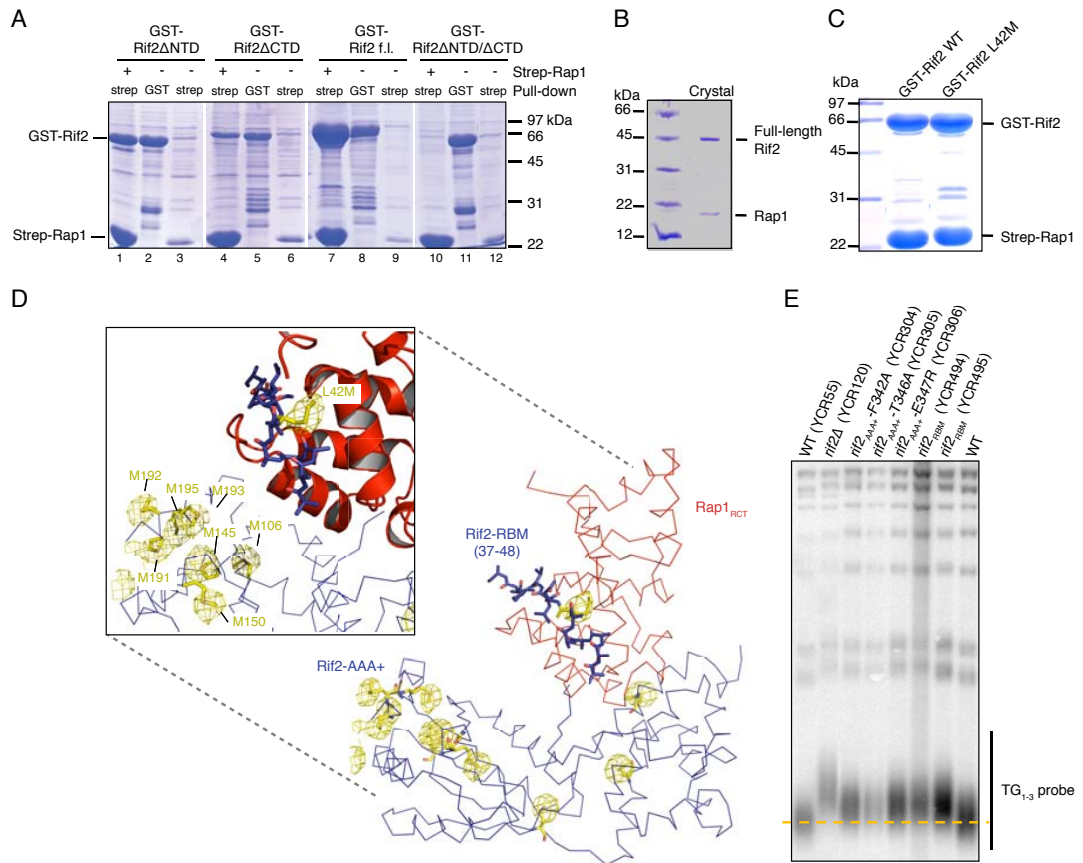
Figure S4, related to Figure 3
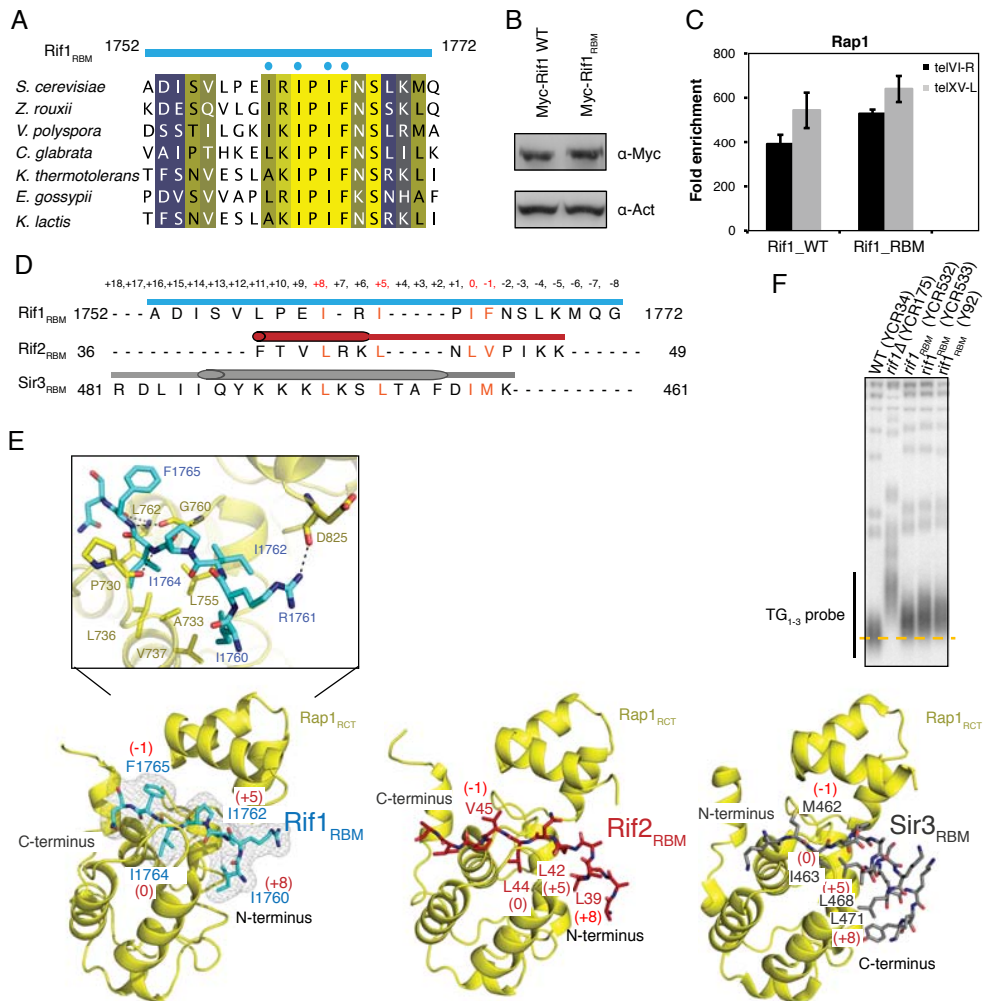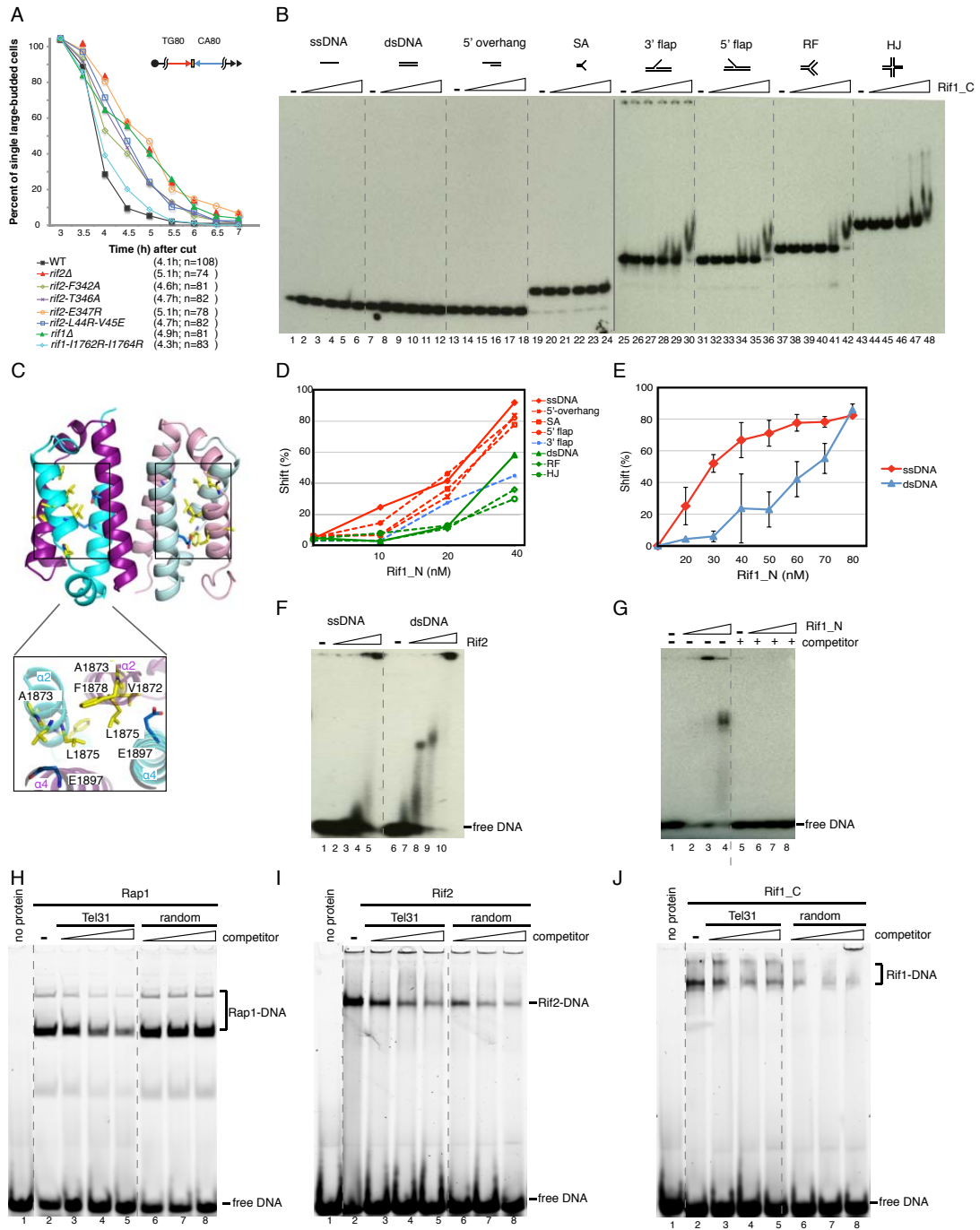
Figure S6, related to Figure 6

<table>
<thead>
<tr><th></th><th></th><th colspan="3">G2/M arrest assay</th></tr>
<tr><th></th><th>Genotype</th><th>Average restart time (hrs)</th><th>Phenotype similar to (WT/Δ)</th><th>Telomere length</th></tr>
</thead>
<tbody>
<tr><td rowspan="2">Controls</td><td>WT</td><td>4.1</td><td>WT</td><td>WT</td></tr>
<tr><td>rif2Δ</td><td>5.1</td><td>Δ</td><td>++</td></tr>
<tr><td rowspan="4">Rif2-dimer (A)</td><td>rif2-F334A</td><td>4.2</td><td>WT</td><td>WT</td></tr>
<tr><td>rif2-V256A</td><td>4.1</td><td>WT</td><td>WT</td></tr>
<tr><td>rif2-V256A-F334A</td><td>4.1</td><td>WT</td><td>WT</td></tr>
<tr><td>rif2-F330A-V333A-F334A</td><td>4.2</td><td>WT</td><td>WT</td></tr>
<tr><td>Rif2-dimer (B)</td><td>rif2-M191K-M195K-K241D</td><td>4.3</td><td>WT</td><td>+</td></tr>
</tbody>
</table>
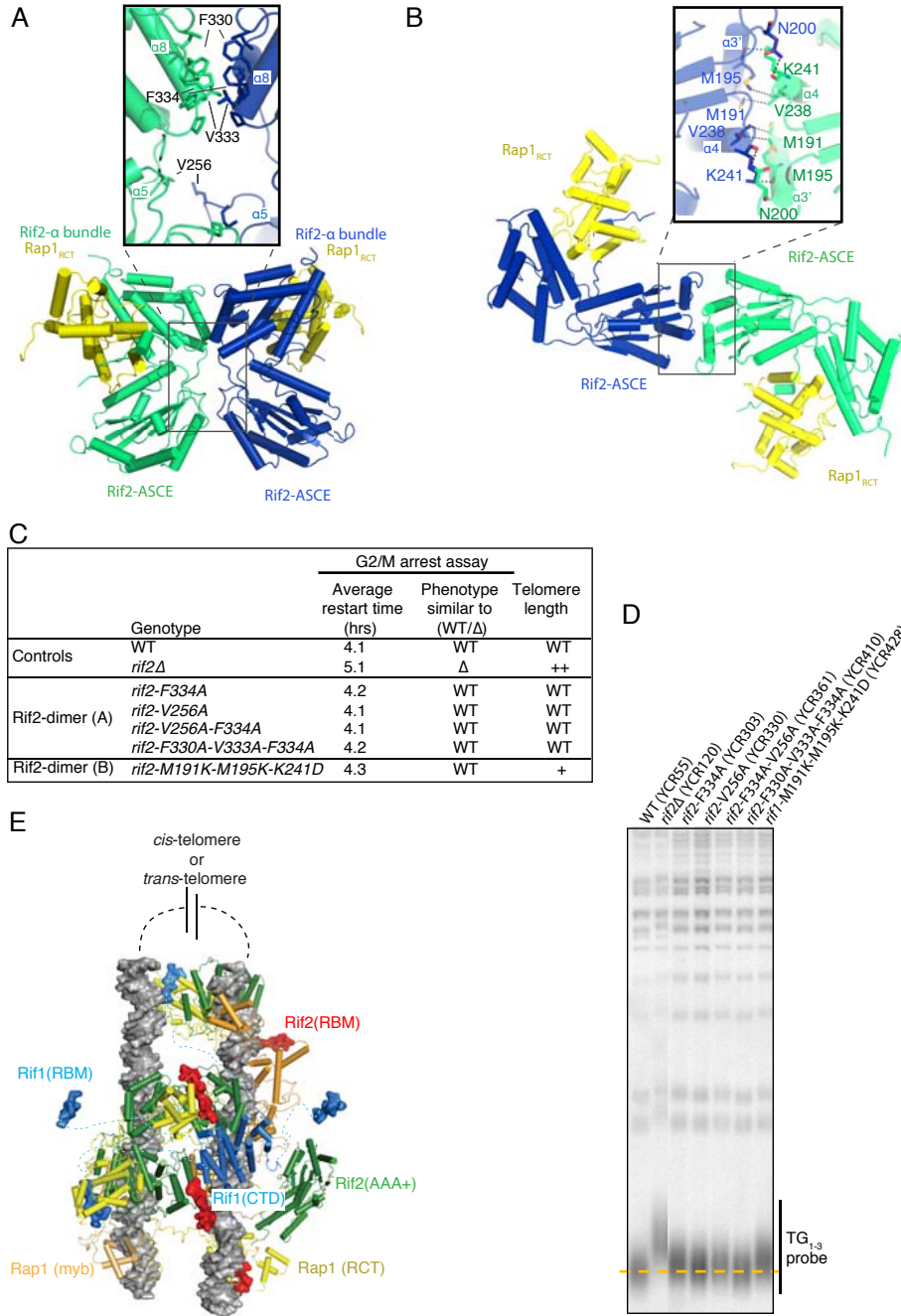
Chapter 2

Structure-function studies of

S. cerevisiae Rif1 N-terminus

1 Materials and methods

1.1 Cloning, protein expression and purification

Saccharomyces cerevisiae Rif1 (residues 100-1322) and Rif1 (residues 177-1283) constructs were cloned into a pAC-derived plasmid with an N-terminal Strep-tag. Recombinant Rif1 baculoviruses were prepared according to the supplier's manufacturer instructions (Invitrogen). Proteins were expressed in High Five insect cells (Invitrogen).

For purification of recombinant proteins, cells were resuspended in lysis buffer (50 mM Tris, pH 8.0, 500mM NaCl, 5 mM β-ME, 1 mM PMSF) and lysed by sonication. Proteins were then purified using Strep-Tactin affinity chromatography (IBA). After N-terminal Strep-tags were cleaved with 2% (w/w) TEV protease at 4°C overnight, proteins were further purified by size exclusion chromatography (SEC) (Superose 6 or Superdex 200; GE Healthcare) in 50 mM HEPES, pH 7.4, 500 mM NaCl, and 1 mM TCEP, and stored at -80°C until further use. Selenomethionine-substituted Rif1 (177-1283) were expressed in Sf900 II minimal media with 80 mg/L selenomethionine, 2 mM cysteine and 2 mM glutamine.

1.2 Limited proteolysis

For trypsin digestion, 10 μg of purified protein was incubated with increasing amount of trypsin in 10-fold steps from 0.001% (w/w) to 3%. Reactions were performed in the same buffer used for gel filtration in 10 μl volume for 10 min on ice. To stop the reactions, 5 μl SDS loading buffer was added and the mixture was boiled at 95°C for 5 min. The digested fragments were analyzed on 12% SDS gel and stained by Coomassie blue.

1.3 Crystallization of Rif1 (100-1322) trypsin digested protein

The purified protein (6.8 mg/ml) was supplemented with 0.01% trypsin prior to set-up of crystallization experiments. Crystals were obtained after 3-5 days by mixing the protein solution equally with reservoir solution at 20°C using sitting drop vapor diffusion methodology. The reservoir solution contained 100 mM Glycine, pH 10.5, 200 mM Li_2SO_4, 1.2 M NaH_2PO_4 and 800 mM K_2HPO_4.

1.4 Crystallization of Rif1 (177-1283)

Crystals of both native and SeMet Rif1 (177-1283) were grown at 20-25°C using sitting drop vapor diffusion methodology. Protein drop (3.8 mg/ml) was mixed in a 1:1 ration with the reservoir solution containing 100 mM Tris pH 7.0, 360 mM Li_2SO_4 and 810 mM Na/K tartrate. Crystals were transferred into cryoprotectant (mother liquor plus 25% ethylene glycol) and flash frozen in liquid nitrogen.

1.5 Hevy-atom soaking of Rif1 (177-1283) crystals

A stabilising solution was made up to replicate the crystal-growth: 100 M Tris-HCl, 820 mM Na/K tartrate, 310 mM Li_2SO_4 supplemented with 50 mM HEPES, 150 mM NaCl (final pH 7.3). A soaking solution was prepared with stabilizing solution supplemented with 1 mM $KAu(CN)_2$. Three crystals were transferred from their growth to a new vapor diffusion well containing a 4 μl drop of soaking solution above a 600 μl reservoir of stabilising solution. The crystals were soaked for 1.5 hr at 20°C prior to being transferred to a fresh 10 μl drop of stabilizing solution and back-soaked for 5 min. The crystals were then transferred into cryo-protectant solution (mother liquor plus 25% ethylene glycol) and flash-cooled in liquid nitrogen.

1.6 Data collection and structure determination

All diffraction data were collected at the Swiss Light Source, Villigen, Switzerland. The diffraction data were processed with XDS (Kabsch, 2010) followed by final scaling and merging with AIMLESS (P. Evans, unpublished work 2011). Integrated intensities were converted to structure factor amplitudes using TRUNCATE (French and Wilson, 1978).

An initial set of selenium positions was determined with SHELXD (Sheldrick, 2008) from anomalous difference data. The initial selenium sites were provided to autoSHARP (Vonrhein et al., 2007) for refinement and phasing, using a dual-wavelength anomalous dispersion (DAD) approach. Molecular replacement searches to determine cross-crystal relationships and single-wavelength anomalous dispersion (SAD) phasing calculations were conducted with PHASER (McCoy et al., 2007). DMMULTI (Cowtan, 1994) was used to extend the phases and improve the electron density maps using cross-crystal averaging. The model was built

with COOT (Emsley et al., 2010) into electron density maps from DMMULTI and refined using PHENIX.REFINE (Adams et al., 2010). The electron density maps used in the later stages of model building were produced from the refined partial model phases after improvement by statistical density modification with RESOLVE (Terwilliger, 2000) with regularized map sharpening.

1.7 Electrophoretic mobility shift assay

Oligo 1 listed in **Table 1** was 5'-end-labeled using T4 polynucleotide kinase (New England Biolabs) and γ-^{32}P ATP (Hartmann Analytics). Labeled oligo was subsequently purified by spin column purification using a MicroSpin G-25 column (GE Healthcare). Purified oligo 1 was then annealed with different complementary oligonucleotide listed in **Table 1**. 30 nt-overhang was assembled from oligos 1 and 2, 60 nt-overhang from oligos 1 and 3, 90 nt-overhang from oligos 1 and 4. Annealed substrates were purified from 12% native Polyacrylamide gel and stored in 50 mM Tris-HCl, pH 8.0.

EMSA reactions (10 μl) were performed in 20 mM Tris-HCl pH 7.5, 5 mM MgCl2, 100 mM NaCl, 100 μg/ml BSA, 5% glycerol with 1 nM labeled DNA and the indicated amounts of protein. In the competitive binding assay, the first protein was pre-incubated with DNA substrates on ice for 30 min prior to addition of the competitive protein. After another 30 min incubation on ice, the protein-DNA complexes were resolved on a 1.2% agarose gel run in 0.5x TBE at 4°C at 150 V for 2.5 hours. For the protein supershift, polyclonal anti-serum against yeast RPA complex (antibodies-online, ABIN190714) was supplied to the reactions and incubated on ice for another 15 min, before the result was analyzed on a 1.2% agarose gel. Signal of ^{32}P-labeled DNA was analyzed by autoradiography and phosphorimaging.

Table1. Sequences of the oligonucleotides used for the EMSA assays.

| Oligo	Sequence (5'-3')
1	GCGTCATGGTAATCGATGTACATGAGAGCA
2	TGCTCTCATGTACATCGATTACCATGACGCACGCTGCCGAATTCTACCAGTGCCTTGCTA
3	TGCTCTCATGTACATCGATTACCATGACGCACGCTGCCGAATTCTACCAGTGCCTTGCTA GGACATCTTTGCCCACCTGCAGGTTCACCC
4	TGCTCTCATGTACATCGATTACCATGACGCACGCTGCCGAATTCTACCAGTGCCTTGCTA GGACATCTTTGCCCACCTGCAGGTTCACCCATCTGGCACCTATGCGGATACTGCTACACT

2   Results

2.1   Rif1 N-terminal domain can outcompete RPA from 3'-overhang with different length

In chapter 1, Rif1_N (residues 100-1322) was shown to actively dissociate RPA from ssDNA when a 3'-overhang was used as substrate (chapter 1, **Figure 5F**). In that experiment, incubation of Rif1_N with pre-formed RPA-DNA complex results in disappearance of the RPA-DNA complex accompanied with the formation of Rif1-DNA complex, which migrates slower on the gel than the RPA-DNA complex.

To examine whether the slow migrating protein-DNA complex contains only Rif1_N, or whether both Rif1_N and RPA could co-exist on the same DNA substrate, supershifts with RPA antibody were applied with the result shown in **Figure 1A**. To distinguish the two senarios above, the specificity of the antibody was examined first (lanes 1-6). While the RPA-DNA complex was significantly supershifted by the polyclonal antibody (lanes 3-4), migration of neither DNA substrate alone nor the Rif1_N-DNA complex was affected in the presence of this antibody (lanes 1-2 and 5-6). This indicates that the antibody specifically recognizes RPA, and there is no cross reactions with DNA or Rif1_N.

If Rif1 and RPA would coexist on the same DNA substrate, the addition of RPA to the pre-formed Rif1-DNA complex would be expected to result in a supershift of the Rif1-RPA-DNA complex through RPA antibody. In contrast, no Rif1-DNA complex supershift in the presence of RPA and the RPA antibody would suggest a mutually exclusive interplay between Rif1 and RPA on the same DNA substrate. Indeed, addition of increasing RPA amounts to the Rif1-DNA complex did not lead to any further shift of the Rif1-DNA-complex through the RPA antibody (compare lanes 13-15 with lane 12), suggesting that the protein-DNA complex contains only Rif1. Consistently, adding Rif1_N to the RPA-DNA complex led to the formation of protein-DNA complex that migrates in the same manner as that of Rif1_N-DNA (compare lanes 5-6 and 9-11), implying that the interaction between RPA and DNA is disrupted by Rif1. In general, the Rif1_N-DNA complex migrates slower than the RPA-supershift (compare lane 4 and 5). This is likely due to the elongated protein shape of Rif1_N as shown in the crystal structure (see **Figure 3A**), or the presence of multi Rif1_N molecules on one DNA substrate. Together, these results confirm that Rif1 can outcompete RPA from 3'-overhangs. In addition, the binding of Rif1 and RPA on the ssDNA moiety next to the ssDNA/dsDNA junctions is mutually exclusive.

The *S. cerevisiae* RPA complex has been shown to have different binding modes dependent on the ssDNA length. Rfa1 processes a major 30 nt binding mode (Atrazhev et al., 1992; Kim et al., 1992). A much smaller 8- to 10-nucleotide binding mode is created together by RPA1 and Rfa2 (Blackwell and Borowiec, 1994). Given a sufficiently long ssDNA substrate, a larger, 90 nt binding mode is observed through the wrapping of ssDNA around the heterotrimer RPA with all the three components participating in the protein-DNA interaction (Philipova et al., 1996). To assess whether various RPA ssDNA-binding modes play a role in the competition between Rif1 and RPA for the ssDNA moiety next to the ssDNA/dsDNA junction, 3'-overhang substrates with different length of the ssDNA region were examined using the competitive EMSAs (**Figure 1B**). The subsequent addition of RPA to the preformed Rif1-DNA complex with 30 nt overhang (lanes 7-9), 60 nt overhang (lanes 16-18) or 90 nt overhang (lanes 25-27) did not lead to the RPA-DNA complex, suggesting that the interaction between Rif1 and DNA is not affected by RPA. In contrast, the increasing presence of Rif1_N in addition to preformed RPA-DNA complex resulted in the clear formation of Rif1-DNA complex (lanes 3-5, lanes 12-14 and lanes 21-23). With increasing length of the ssDNA moiety, the Rif1-DNA complex appears to form gradually (compare lanes 12-14 and 21-23 with 3-5). These *in vitro* results indicate that Rif1 can dissociate RPA from 3'-overhangs regardless of the binding modes used by RPA. In addition, the protective zone created by Rif1 on the 3'-overhang appears to span from 30 nt to 90 nt.
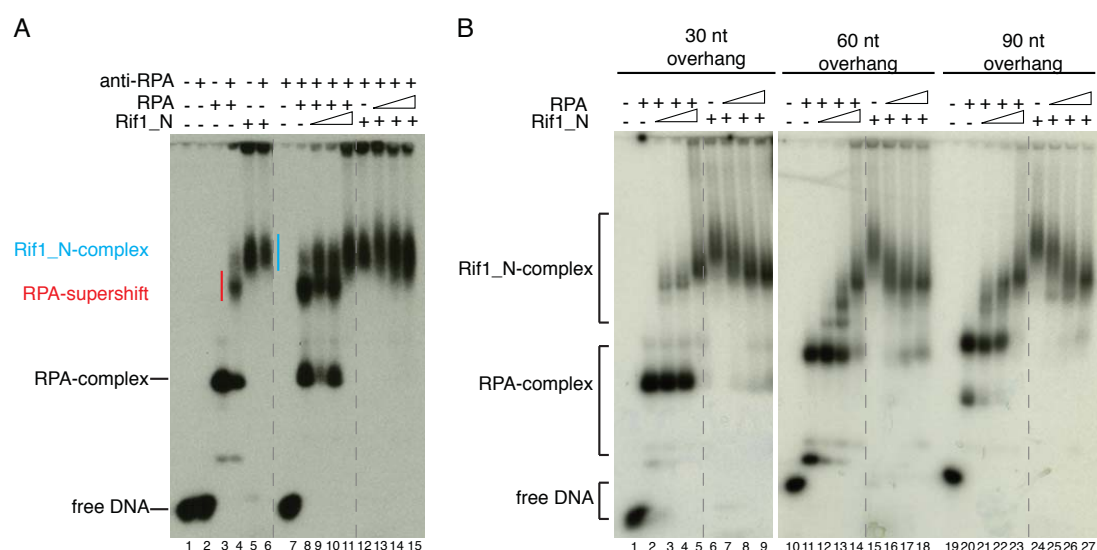
Figure 1. Electromobility shift assays (EMSAs) of Rif1 and RPA.

(A) The binding of Rif1_N and RPA on 3'-overhangs is mutually exclusive. EMSA reactions were performed with 1 nM 3'-overhang consisting of a 30 nt and a 30 bp component, purified Rif1_N (100-1322), and the *S. cerevisiae* RPA complex. The DNA substrate was pre-incubated with 80 nM RPA (lanes 8-11) or 80 nM Rif1_N (lanes 12-15) on ice for 30 min, before the competitor proteins Rif1_N (20, 40, 80 nM) or RPA (20, 40, 80 nM) were added. After another 30 min incubation on ice, anti-RPA antibody (1:80 dilution of the anti-serum) was supplied to the protein-DNA complex for 15 min on ice. Lanes 1-6 serve as controls to exclude cross-reactions of anti-RPA antibody with DNA or Rif1_N. The Rif1_N-DNA complex is highlighted with a blue line, supershifted RPA-antibody-DNA complex is indicated with a red line.

(B) Competition EMSAs of Rif1 and RPA with different DNA substrates. A 3'-overhang substrate consisting of a 30 bp dsDNA and a 30 nt, 60 nt or 90 nt ssDNA component (1 nM) was pre-incubated with 80 nM RPA (lanes 2-5, 11-14 and 20-23) or 80 nM Rif1_N (lanes 6-9, 15-18 and 24-27) on ice for 30 min. Increasing amounts of Rif1_N (20, 40, 80 nM) or RPA (20, 40, 80 nM) were subsequently added to pre-formed RPA-DNA or Rif1_N-DNA complexes, respectively. The incubation was continued for 30 min before the protein-DNA complexes were resolved on a neutral agarose gel. The results originate from the same agarose gel.

2.2 Optimization of crystallization boundary for Rif1 N-terminal domain

After the identification of the novel DNA-binding function of Rif1 N-terminus, structural study was carried out, aiming to understand the molecular details of this domain. A soluble fragment of the yeast *Saccharomyces cerevisiae* Rif1 N-terminus (**Figure 2A**), comprising residues 100-1322 could be expressed and purified by Strep-Tactin affinity chromatography, followed by a gel filtration step. Although the protein exhibits homogenous behavior during gel filtration (**Figure 2B**), crystallization trial with this purified fragment did not yield crystals. In order to optimize the construct boundary for crystallization, limited proteolysis of Rif1 (100-1322) with a wide range of trypsin amounts was performed, revealing two major protein fragments (**Figure 2C**). The stability of these two fragments at the presence of high trypsin concentration (>1% trypsin) suggests that Rif1 (100-1322) contains two major structured domains. Indeed, Rif1 (100-1322) crystallized in the presence of 0.01% trypsin over a time interval of 3-5 days, giving rise to rod-like crystals with both ends strongly split

(**Figure 2D**). The diffraction quality of these crystals was not suitable for the structure determination with resolution limited to ca. 10 Å. The low diffraction quality might be due to the heterogeneity of the digested and undigested protein present in the crystallization drop. In order to obtain homogeneous fragments suitable for crystallization, mass spectrometry of trypsin digested Rif1 (100-1322) coupled to liquid chromatography was performed, which revealed the boundaries for the major fragments (see **Figure 2A)**.

A variant containing the shortest obtained boundary (residues 177-1283) was expressed and purified (**Figure 2E**). Although the new construct crystallized under different crystallization conditions, the resulting crystals exhibited similar crystal morphology as those of Rif1 (100-1322) (**Figure 2F**). The Rif1 (177-1283) crystals showed improved diffraction to a resolution of < 5.0 Å. Two related hexagonal crystal forms of Rif1 (177-1283) were obtained. Crystals of Form-I, with unit cell parameters a=b= 203 Å, c= 197 Å were the most common. On three occasions, however, native crystals of Form-II (unit cell parameters a=b= 208 Å, c= 167 Å) were found in conditions that would usually give rise to Form-I. Experimental phasing experiments were conducted with Form-I crystals. A summary of the data collection and phasing statistics is given in **Table 2.**

The crystal structure was subsequently determined using a multiwavelength anomalous diffraction approach with the selenomethionine-substituted Rif1 (177-1283). The initial selenium substructure was determined using the Se1 absorption peak data SAD phasing, with both Se1 data sets producing a preliminary electron density map at 5.36 Å resolution. One Rif1 molecule was present in the asymmetric unit, resulting in crystals with 76% solvent for Form-I and 74% solvent for Form-II. SAD phases were then calculated for two data sets (data sets $KAu(CN)_2$ and Se2). They were improved and extended to a resolution of 3.8 Å using cross-crystal averaging in combination with an unphased native data set from a different crystal form (crystal Form-II, data set Native). The most detailed electron density maps were obtained with data set Se2, using the refined partial model phases after all of the helical fragments and selenium sites were included in the model (described in the Material and methods section 1.6). The structure of Rif1 (177-1283) is currently undergoing building and refinement at 3.8 Å resolution.
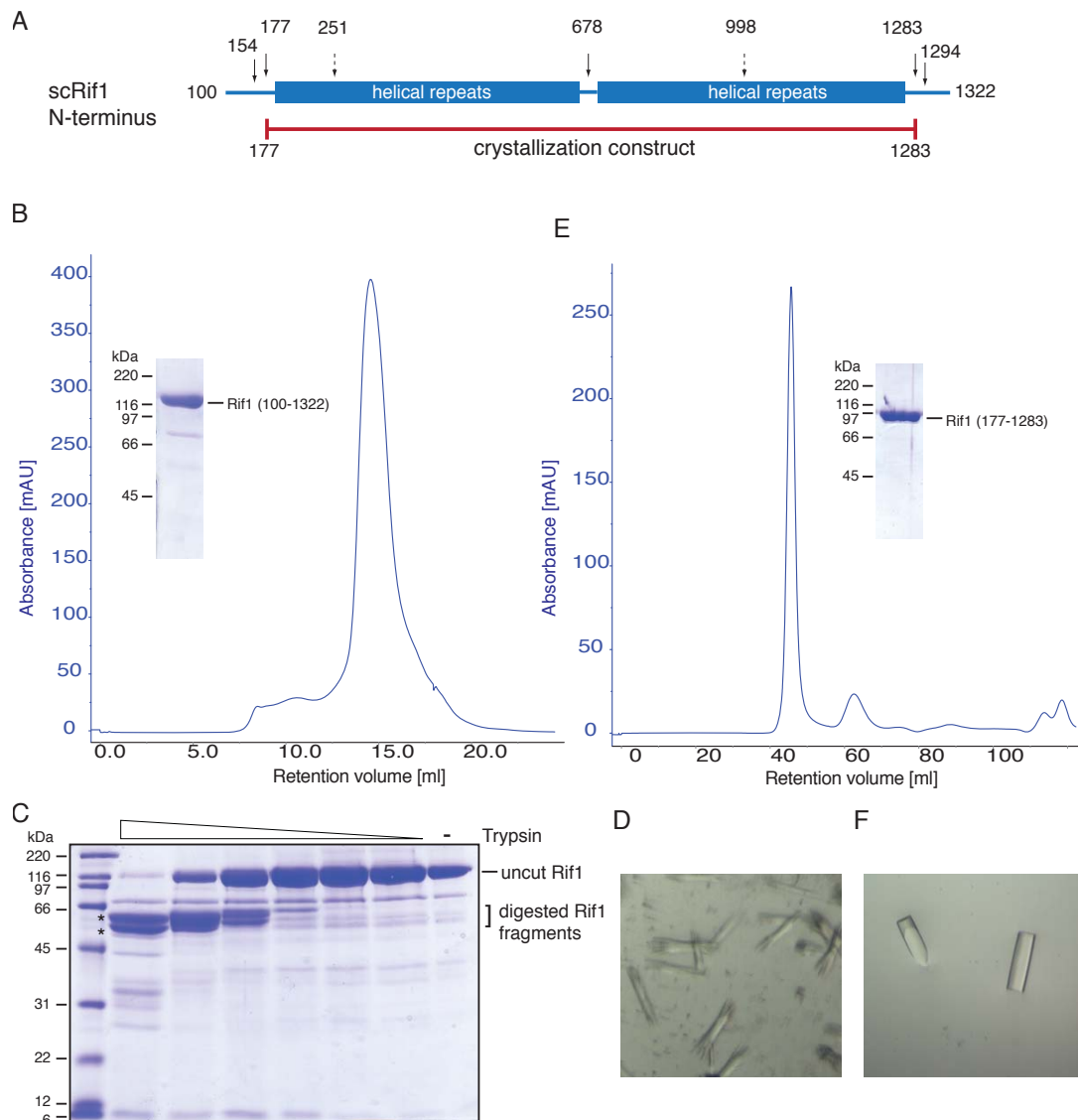
Figure 2. Purification and crystallization of Rif1 N-terminus.

(A) Optimization of the *S. cerevisiae* Rif1 N-terminal construct for crystallization. Structured regions with predicted helical folds are denoted by the two helical-repeats domains. The identified fragment boundaries from (C) are depicted with arrows. Fragment boundaries that originate from weak signals in the LC-MS analysis are indicated with dashed arrows. The optimized protein variant used for crystallization is indicated with a red line.

(B) Purification of Rif1 (100-1322) by the size exclusive chromatography. The fraction corresponding to the absorption A260 peak of the chromatogram is shown on the 12% SDS-polyacrylamide gel.

(C) Trypsin digestion of purified Rif1 (100-1322) for optimizing crystallization construct. Protease amounts used were 0.001% (w/w), 0.01%, 0.1%, 1%, 1.5% and 3%. At 1% trypsin, Rif1 (100-1322) began to be digested into two main fragments of similar size. The boundaries of the resulting fragments are summarized in (A).

(D) Crystallization of trypsin digested Rif1 (100-1322). Crystals were obtained in the presence of 0.01% (w/w) trypsin in 100 mM Glycine, pH 10.5, 200 mM Li_2SO_4, 1.2 M NaH_2PO_4 and 800 mM K_2HPO_4.

(E) Purification of Rif1 (177-1322) by the size exclusive chromatography. The fraction corresponding to the absorption A260 peak of the chromatogram is shown on the accompanying 12% SDS-polyacrylamide gel.

(F) Crystallization of Rif1 (177-1322). Rod-shaped crystals were obtained in 100 mM Tris pH 7.0, 360 mM Li_2SO_4 and 810 mM Na/K tartrate.

Table 2. Rif1 (177-1283) data collection and MAD phasing statistics.

| Data collection	Se1 peak	Se1 inflection point	KAu(CN)$_2$	Se2 peak	Native
Crystal form	form-I	form-I	form-I	form-I	form-II
Space group	$P6_522$	$P6_522$	$P6_522$	$P6_522$	$P6_522$
Wavelength (Å)	0.97944	0.97967	1.03679	0.97902	0.9946
Cell dimensions (Å)	a=b=203.44, c=197.64	a=b=203.32, c=197.94	a=b=203.6, c=194.62	a=b=203.58, c=197.74	a=b=208.7, c=167.32
Resolution (Å)	49.40-5.36 (5.65-5.36)	49.20-6.60 (6.92-6.60)	130.65-7.00 (7.83-7.00)	49.43-3.80 (4.06-3.80)	50.13-3.80 (4.10-3.80)
Rsym (%)	14.2 (135.2)	7.3 (54.9)	14.6 (206.5)	33.0 (711.1)	21.1 (533.0)
Rmeas[1] (%)	15.6 (148.9)	8.0 (60.4)	15.1 (212.7)	33.8 (739.2)	21.6 (549.6)
CC*	0.997 (0.393)	0.999 (0.952)	0.999 (0.901)	0.999 (0.144)	0.999 (0.258)
Observed reflections	94410 (12690)	58039 (16402)	126396 (35755)	960534 (108839)	455161 (79010)
Unique reflectifons	8891 (1235)	4964 (1363)	4099 (1133)	24285 (4202)	21616 (4274)
Completeness	99.5 (98.0)	99.6 (99.4)	100.0 (100.0)	99.6 (97.9)	99.5 (97.8)
Multiplicity[2]	10.6 (10.3)	11.7 (12.0)	30.8 (31.6)	39.6 (25.9)	21.1 (18.5)
$\langle I/\sigma I\rangle$	13.1 (1.5)	25.8 (5.3)	21.7 (2.0)	15.7 (0.6)	13.7 (0.7)
Phasing statistics					
Number of sites	20				
Figure of merit[3]	0.363	0.208			
Phasing power[4]					
Anomalous acentric	0.9	0.651			
Isomorphous acentric / centric		0.454 / 0.366			

[1]Multiplicity-independent merging R factor $R_{mes} = \sum_{hkl}(n_{hkl}/[n_{hkl}-l]^{1/2})\sum_i|I_i(hkl)-\langle I(hkl)\rangle|/\sum_{hkl}\sum_i I_i(hkl)$ where n is multiplicity $I_i(hkl)$ is the ith observation of reflection *hkl* and $\langle I(hkl)\rangle$ is the weighted mean of all observations. [2]Friedel mates separate. [3]Combined value from *SHARP*. The figure of merit for a given reflection *hkl* is calculated as $\text{FOM} = |F(hkl)_{best}|/|F(hkl)|$. [4]Phasing power= $\langle |F_H(calc)|/\text{phase-integrated lack of closure}\rangle$, where $F_H(calc)$ is the calculated anomalous difference and phase-integrated lack of closure is $|F_{PH}|_{obs} - |F_{PH}|_{calc}$ distribution.

2.3 Overall structure of the Rif1 N-terminal domain

The structure reported herein contains the Rif1 N-terminal domain comprising residues 177-1283 (hereafter referred to as Rif1$_{NTD}$). Rif1$_{NTD}$ crystallized in the space group $P6_522$ with one molecule found in each asymmetric unit. Rif1$_{NTD}$ has an extraordinarily elongated structure, spanning approximately 235 Å from its N-terminus to its C-terminus (**Figure 3A**). The structure reveals an all-helical fold that contains 24 helical repeats. Each of these repeats consists of two anti-parallel α-helices. Based on the curvature formed by these helical repeats, the structure of Rif1$_{NTD}$ can be divided into two regions: an N-terminal curved region (repeats 1-12), which resembles a horseshoe, and a significantly less bent C-terminal region (repeats 13-24). The entire Rif1$_{NTD}$ structure resembles the overall shape of a question mark.

Due to the low sequence similarity between Rif1 and other proteins with known structures, homology models cannot be reliably applied to guide building of Rif1$_{NTD}$ structure. This necessitates manual placement of all the helices with poly-Ser sequence at the initial stages of the structure determination. Based on the anomalous signal originating from SeMet-substituted protein, all 22 selenium sites of Rif1$_{NTD}$ (corresponding to Met-sites in the native protein) were identified in log-likelihood gradient maps by PHASER. The positions of SeMet-sites along the structure of Rif1$_{NTD}$ are illustrated by the anomalous difference map (**Figure 3B).** Subsequent investigation successfully assigned 21 out of 22 Met-sites with their corresponding residue numbers. The remaining one is located in an insertion loop, whose electron density is mainly disconnected from the rest of the protein. The defined methonine residue number allows the subsequent assignment of residue ranges for each individual helix including some of the loop regions.
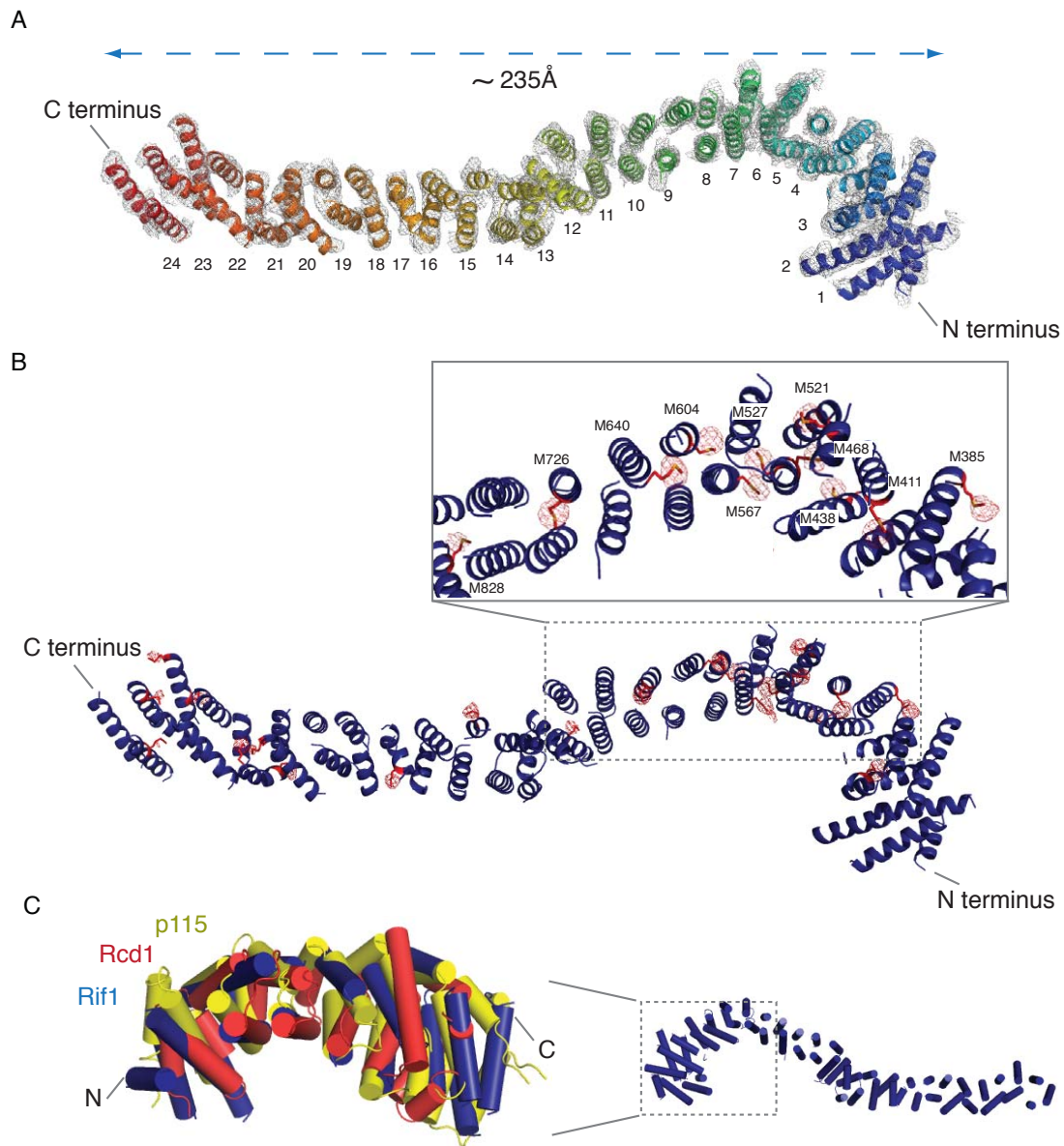
Figure 3 Crystal structure of *S. cerevisiae* Rif1 N-terminal domain.

(A) Ribbon illustration of the overall structure of Rif1 (177-1283). The peptide chain is colored from blue at the N-terminus to red at the C-terminus. The protein comprises 24 anti-parallel helical repeats. The repeat numbers are indicated next to the repeats. Most of the helices in the model are so far disconnected. The electron density (the $2F_0$-F_c density countered at 1.0σ) of the structure is shown as grey mesh. The distance spanning from the N- to C-terminus is indicated above the structure.

(B) Ribbon representation of the Rif1 (177-1283) structure highlighting experimental SeMet sites. An anomalous difference map contoured at 4.0σ is shown as red mesh. Rif1 is colored

in blue with all the assigned methionine residues represented as red sticks. The protein region containing methionine residues 385-828 is shown with a close view.

(C) A structure superposition of Rif1 (blue) with two armadillo-like proteins human Rcd1 (red) and human p115 (yellow). The superimposed region is indicated with a dashed box in the overall structure of Rif1 on the right side.

3   Discussion and outlook

Despite the lack of sequence similarity, comparison of the Cα traced Rif1$_{NTD}$ structure with other known structures reveals that the N-terminal region of Rif1$_{NTD}$ largely resembles the structure of human Rcd-1 (PDB code: 2fv2) and human p115 (PDB code: 2w3c) (**Figure 3C**). The structural comparison server DALI reported a Z-score of 12.5 with a root-mean-square deviation (rmsd) of 3.7 Å for Rif1$_{NTD}$ and Rcd-1 (over 227 aligned residues), a Z-score of 13.3 with rmsd of 4.9 Å for Rif1$_{NTD}$ and p115 (over 352 aligned residues). Both Rcd-1 and p115 have conserved armadillo (ARM)-like folds. ARM-repeats have been found in many functionally unrelated proteins from β-catenin to karyopherin α (Conti et al., 1998; Peifer et al., 1994). Sequence conservation of ARM-motifs between different proteins or even within ARM-repeats of the same protein is typically low. The structural hallmark of ARM-motifs is a three-α-helix pattern that consists of two anti-parallel α-helices connected by a short helix. The three helices pack in a clockwise spiraling fashion and thereby give rise to a curving C-shaped appearance of the overall ARM-repeat region (**Figure 3C**). Recently, the ARM-repeat domain of human Rcd-1 was reported to interact with ssDNA and dsDNA in a sequence specific manner (Garces et al., 2007). Moreover, a single residue mutation within the ARM-repeat domain of Rcd-1 abolished its binding to dsDNA. Currently, a detailed comparison of Rif1$_{NTD}$ helical repeats and ARM-repeats is not possible, as the majority of the loop regions remain to be modeled. Based on the well-aligned helix arrangement between the Rif1$_{NTD}$ N-terminal region and Rcd-1 or p115, in addition to the DNA-binding feature of Rif1$_{NTD}$ and Rcd-1, it is likely that at least the N-terminal region of Rif1$_{NTD}$ prossesses an armadillo-repeat fold.

In general, ARM-repeat folds or other helical-repeats (like HEAT-repeat) containing domains provide a possible surface for protein-protein interactions (Conti et al., 1998; Huber et al., 1997). In accordance with that, using the Rif1 N-terminal fragment (residues 1-1322) as bait in the Y2H, Red1, Gip1 and Ysw1 were identified as Rif1 interaction partners (data not

shown). Interestingly, Red1 is a direct target of the protein phosphatase 1 PP1 (Glc7 in *S. cerevisiae*). A recent study revealed a conserved PP1-binding site in all the 92 identified Rif1 proteins from yeast to human (Sreesankar et al., 2012). This consensus sequence RVxF is located at residues 114-118 in scRif1, closely positioned to the Rif1$_{NTD}$ helical-repeat domain. It is possible that Rif1 functions as a conserved PP1 regulator (see **Discussion and Perspectives** for detailed discussion) through the consensus RVxF motif and the Rif1$_{NTD}$ domain as a docking interface for PP1.

In this study, the novel DNA-binding function of Rif1 N-terminus is identified. Using 3'-overhang DNA substrates carring different lengths of the ssDNA moiety, Rif1 was shown to exclude RPA from ssDNA next to a junction up to 90 nt. It is likely that the intrinsic elongated structure of Rif1 itself, which is ca. 235 Å and corresponds to the length of 72 bp of B-form dsDNA, provides the basis for this large exclusion zone on DNA. Another possibility could be that once nucleation at the ssDNA/dsDNA junction is completed, Rif1 can spread along the ssDNA and thus removes RPA over a long range. Further biochemical or structural studies addressing the molecular mechanism of Rif1 interaction with 3'-overhangs are necessary to distinguish the two possibilities. In summary, Rif1 can provide a large exclusion zone up to 90 nt on a 3'-overhang. Importantly, the binding of Rif1 and RPA on ssDNA next to ssDNA/dsDNA junctions is mutually exclusive. The feteaure of this DNA substrate resembles the resected DNA ends of dysfunctional telomeres. These properties bestow Rif1 the principal ability to prevent checkpoint activation, should telomeres be uncapped.

DISCUSSION AND PERSPECTIVES

The structural, biochemical, and cellular data presented here provide molecular details of the major proteins Rif1 and Rif2 at the double-strand telomeric region. Based on the knowledge gained from this work and previous data, I will discuss: (i) how the major telomere binding proteins Rap1, Rif1, and Rif2 participate in telomere length regulation; (ii) what determines the partner choice of Rap1 at different places in the genome; (iii) the dependence of Rif1/Rif2-mediated telomere functions on their interactions with Rap1; (iv) a proposed molecular model of how Rif1 functions in the DNA-damage response; and (v) the evolutionary conservation of Rif1 in structure and functions.

Telomere length homeostasis by Rap1, Rif1, and Rif2

Dynamic higher-order telomere chromatin structure

In this study, I showed that Rif1 and Rif2 utilize multivalent long- and short-range interactions with the Rap1 RCT domain to facilitate Rap1-Rif1-Rif2 assemblies. The presence of Rif1 and Rif2 provides essential interconnections for juxtaposed Rap1 molecules, driving higher-order telomere structure. In late S and G2 phases, telomerase is known to be active. ChIP analysis has shown that the association of Rif2 with telomeric DNA is lowest during the S and G2 phases (Smith et al., 2003). One interpretation is that dissociation of one of the components from the Rap1-Rif1-Rif2 complex would reduce the stability of these assemblies, thus "opening" the telomeric chromatin structure. As a result, telomeres would be more accessible for telomerase. Consistently, fusion of the mammalian oligomerization PDZ domain to Rap1 can confer control of telomere length in the absence of Rif1 and Rif2 proteins (Levy and Blackburn, 2004). The observation that telomeric association of only Rif2 decreases during the S phase, while that of Rif1 increases (Smith et al., 2003), sounds paradoxical to the telomeric chromatin structure remodeling proposed above. However, this may be reconciled by the high binding affinity of Rif1 to ssDNA identified in this study. Temporary extended G-overhangs in S phase could serve as a substrate to recruit Rif1, leading to elevated association of Rif1 with telomeric DNA in a Rap1-independent fashion. Therefore, the increased Rif1 levels at telomeres in S phase likely do not contribute to the formation of Rap1-Rif1-Rif2 assembly, but rather participate in preventing DNA-damage checkpoint responses at the G-tail. Consistently, Rif1 has been shown to functionally assist Cdc13 in telomere capping (Anbalagan et al., 2011). In summary, the stability of Rap1-Rif1-

Rif2 assembly provides the dynamics of the telomeric chromatin structure. This in turn regulates the access of telomerase to its substrates and influences the overall telomere length homeostasis.

Rap1-independent telomere length regulation by Rif1 and Rif2

The roles of Rif1 and Rif2 as negative regulators of telomere length have long been established. The classical "counting model" suggests that the telomere lengthening machinery senses the number of telomere-bound Rif proteins. However, overexpression of either Rif1 or Rif2 protein in a Rap1ΔRCT strain can substantially regulate telomere length (Levy and Blackburn, 2004), suggesting that Rif1 and Rif2 might affect telomerase activity regardless of their telomeric localization. Given that Rif1 and Rif2 can only act on telomere length homeostasis when bound to Rap1, Rap1 interface mutants of Rif1 or Rif2 are expected to result in similar telomere length phenotypes as the deletion of *rif1* or *rif2*. Conversely, a Rif1$_{RBM}$ mutant that does not bind to Rap1 and is not associated at functional telomeres by ChIP, shows only moderated telomere elongation compared to the *rif1Δ* mutant. The amount of the Rif2$_{AAA+}$ mutant at telomeres is much lower than that of Rif2$_{RBM}$ mutant using ChIP (data not shown). Nevertheless, telomeres are elongated to the same level in Rif2$_{AAA+}$ and Rif2$_{RBM}$ mutant strains. These results indicate that Rif1 and Rif2 can participate in inhibiting telomerase in a Rap1-independent manner. They most likely do this by affecting positive telomerase regulators.

Both the MRX complex and Tel1 are required for telomere elongation. MRX generates a 3'-overhang for telomerase to act on (Bonetti et al., 2009), and Tel1 enhances MRX activity (Martina et al., 2012). Telomere elongation processes and DSB repair pathways have similar initiation events, as both require MRX and Tel1. Rif2 is thought to negatively regulate telomere length and inhibit DSB-induced checkpoint activation by counteracting MRX/Tel1-mediated nucleolytic processing. The interaction between Rif2 and the C-terminus of Xrs2 (Xrs2-C) that binds Tel1 further supports this model (Hirano et al., 2009). In this study, Rif2$_{AAA+}$ and Rif2$_{RBM}$ mutants, having partially lost their interaction with Rap1, showed only moderate telomere lengthening. A plausible explanation for this phenomenon is that preventing Tel1 recruitment to telomeres by Rif2 is independent of the protein interaction between Rif2 and Rap1. This would explain the much stronger telomere elongation phenotype caused by deletion of *RIF2* when compared with the mutations in the Rif2$_{AAA+}$ or Rif2$_{RBM}$ domains. Surprisingly, the same Rif2$_{AAA+}$ and Rif2$_{RBM}$ mutants showed significant anti-

checkpoint deficiency, comparable to that of the Rif2 deletion mutant, suggesting that impaired Rap1 binding no longer allows Rif2 to inhibit resection by MRX/Tel1 at telomeres. At present, it is unclear how the same event controlled by Rif2 (inhibition of MRX/Tel1 mediated telomere end resection) has differential effects on telomere homeostasis and DSB response. Further studies exploring potential Rif2 interaction proteins might offer new insight into the functional link between end resection, telomere homeostasis, and the telomeric DSB checkpoint response.

Although Rif1 has also been shown to prevent Tel1 localization to telomeres, the inhibitory effect is much smaller than that of Rif2 (Hirano et al., 2009). In addition, no interaction between Rif1 and MRX has been reported. These results suggest that, unlike Rif2, Rif1 might interfere with other positive regulators of telomere length control. The understanding of a Rap1-independent telomere length regulation through Rif1 gained further support from a recent report from Luciano *et al*. They showed that RPA transiently localizes at telomeres during the late S-phase through interactions with Ku, Cdc13, and telomerase. Moreover, mutations that abolish the interaction between RPA, yKu, and telomerase partially reduce the increase in telomere length found in the *rif1Δrif2Δ* double mutant. Thus, RPA appears to facilitate telomerase activity in S-phase (Luciano et al., 2012). In this study, the intrinsic DNA-binding properties of Rif1 and its ability to outcompete RPA from ssDNA next to ssDNA/dsDNA junctions were identified. It is conceivable that Rif1 blocks RPA binding to G-overhangs in late S-phase, thereby inhibiting RPA-facilitated telomerase activity. Loss of *RIF1* would favor RPA binding to the telomeric ssDNA, which in turn can promote telomerase recruitment. In accordance with this hypothesis, the Rif1$_{RBM}$ mutant that remains functional in DNA binding exhibits moderate telomere elongation, while the deletion of *RIF1* causes severe telomere lengthening. Future studies to identify a DNA-binding deficient Rif1 mutant, or additional Rif1 interaction proteins other than Rap1, may allow the clarification of how Rif1 controls telomere length.

In summary, telomere length homeostasis is the result of effects on multiple levels: Rap1, Rif1, and Rif2 utilize multivalent interactions to create a dynamic higher-order telomeric chromatin structure, which prevents telomerase access during most of the cell cycle. In late S-phase, the controlled dissociation of Rif1 and Rif2 from Rap1 allows the telomeric chromatin to "open" for telomerase. How this dynamic process is regulated is still unclear. Once the telomere can be accessed by telomerase, Rif1 and Rif2 likely further influence the elongation events independently of Rap1, providing fine-tuning for telomere length

regulation. Rif1 is equipped to reduce telomerase activity by blocking RPA at temporally extended G-overhangs. Rif2 can limit telomere end resection by competing with Tel1 for interaction with Xrs2. In the absence of Tel1, Rap1 can promote dissociation of MRX from the ends (Hirano et al., 2009). Thus the major telomere duplex binding proteins Rap1, Rif1, and Rif2 act in concert to keep telomeres within a broad size range.

How does Rap1 recruit different sets of proteins at HM silencers, promoters and telomeres?

Rap1 is an essential multifunctional protein in budding yeast. At promoters, it acts as a transcriptional activator or as a repressor according to the DNA sequence context. Rap1 is also an important component of the telomere proteinaceous cap. Moreover, Rap1 contributes to transcriptional gene silencing at silencers. If the label *factotum* (meaning "do everything") were assigned to a protein, Rap1 would deserve it. Interestingly, Rap1 itself does not exhibit any enzymatic activity. Early results suggested that the functions of Rap1 are not only due to its property of DNA binding, but rather due to its ability to interact with different sets of factors at promoters, silencers, and telomeres. For example, a promoter-specific Rap1-binding site functions as a Sir protein recruiter when placed at silencer, and vice versa (Shore and Nasmyth 1987; Buchman et al., 1988). At the same time, these results also pose the question: how does Rap1 select which factors should be recruited to each site?

Rap1 has to interact with different sets of proteins to fulfill different roles in cells, which leads to general weak interactions between Rap1 and all its interaction proteins. For example, the two Rap1 telomere interaction partners Rif1 and Rif2 both bind to Rap1 so weakly that no binding of these proteins to Rap1 was detectable in the size-exclusive chromatography analysis (data not shown). Another interaction partner, Sir3, also binds to Rap1 with a low affinity (Kd=2.5 μM) (Chen et al., 2011). Apparently, the cost of weak protein interaction is compensated by the multi protein-protein or protein-DNA context at different Rap1-binding sites, as illustrated below.

As the most studied silencer element, *HMR-E* comprises juxtaposed binding sites of three different factors (ORC, Rap1, ABF1), all with independent roles in the cells. It has been shown that Orc1 binds to Sir1 directly (Triolo and Sternglanz, 1996); Sir3 likely interacts with ABF1; and Rap1 binds to both Sir3 and Sir4 (Moretti et al., 1994). Each of these three factors has a certain binding affinity for one or more Sir proteins, but no single factor by itself can

create a sufficiently high local concentration of Sir proteins to exert silencng. However, in the specialized context of *HMR-E* loci, the affinity of ORC and ABF1 towards Sir proteins not only helps Rap1 to recruit Sir proteins, but also precludes the binding of transcription factors or Rif proteins to Rap1.

At promoter regions, the multi-protein interaction environment is replaced by specific protein-DNA interactions. For example: Rap1 regulates the transcription of genes for the glycolytic pathway. One of the coactivators, GCR1, is itself a sequence-specific DNA binding protein (Baker, 1991). In general, glycolytic Rap1-binding sites are accompanied by one or two GCR1 binding sites (Shore, 1994). The main role of Rap1 in these promoter regions is to recruit GCR1 to its cognate sequence. Thus the presence of the binding sites for Rap1-interaction proteins likely constitutes an alternative way of providing specificity.

At telomeres, binding sites for ORC or ABF1 are absent, and no specific binding sites for Sir or Rif proteins have been reported at telomeric DNA. Determining which protein sets will be recruited relies largely on the presence of multiple copies of adjacent Rap1-binding sites. This explains the observed shift in the Rap1-Rif and Rap1-Sir balance at telomeres. As demonstrated in this study, the multivalent protein interactions within Rap1-Rif1-Rif2 assembly, the tetramerization module of Rif1$_{CTD}$, and the *trans* Rap1-Rif2 units provide a protein interaction network that resembles a molecular Velcro. In addition, the stability of this molecular Velcro increases with an increasing number of Rap1-binding sites. Thus, single or double Rap1-binding sites are not sufficient to provide the stable assembly of the Rap-Rif complexes. In addition, Rif1 and Rif2 do not have any known interaction partners at promoters or silencers next to the Rap1-binding sites. All these contribute to the restricted presence of Rif proteins bound to Rap1 at telomeres, as compared to any other regions of the genome.

In conclusion, Rap1 functions as a one-for-all plug to recruit various factors. The complexity of protein-protein or protein-DNA networks at diverse Rap1-binding sites allows the fine-tuning of biological events while using the same Rap1 docking platform.

Functional dissection of Rif1- and Rif2-mediated telomere regulation

Previous genetic studies addressing the telomere functions of Rif1 and Rif2 used either Rap1 RCT domain deletion, or *rif1/rif2* deletion strains. As both Rif proteins bind to the Rap1 RCT domain, depletion of this domain simultaneously affects the telomere association of Rif1 and Rif2. Deletion of either *rif1* or *rif2*, instead of the Rap1 RCT domain, allowed us to address their individual roles at telomeres. However, by doing so, it was not possible to understand to what degree their telomeric roles were Rap1-dependent. Based on the structural information, I addressed the effect of Rap1-binding deficient Rif1 and Rif2 mutants on their regulation of telomeres. This allowed me to examine the interplay of their telomere functions with their Rap1 interactions.

I identified a separation-of-function Rif1$_{RBM}$ mutant that affects only silencing, but not other Rif1-mediated functions at telomeres. Besides its C-terminal domain (Rif1$_{CTD}$), the Rif1 RBM-module is the major binding domain for the interaction with Rap1. Mutations of the RBM domain exhibit a strong modulation effect on Sir-mediated silencing. The strength of the Rif1$_{RBM}$ mutant silencing phenotype is highly comparable to that observed by deletion of *RIF1*. Surprisingly, the same RBM-module is completely dispensable for Rif1-regulated checkpoint response, and is apparently necessary, but not sufficient, for Rif1 control of telomere length. Taken together, Rif1 silencing modulation is dependent on its interaction with Rap1, while the role of Rif1 in preventing DNA-damage response is independent of its association with Rap1.

In Rif2 mutational studies, mutations in the individual Rap1 binding interfaces (AAA+ and RBM domains) impaired Rif2-mediated anti-checkpoint responses at telomeres. The Rap1-binding deficient Rif2$_{RBM}$ mutant shows the same silencing effect as the *rif2Δ* strain. However, the impaired Rap1 interaction seen in the Rif2$_{AAA+}$ and Rif2$_{RBM}$ mutants is largely dispensable for Rif2-regulated telomere length homeostasis. These results suggest that, with the exception of telomere length regulation, most of the Rif2 telomeric functions are dependent on its association with Rap1.

In summary, the *RIF1* and *RIF2* point mutants from this study provided important tools to discover Rap1-independent telomere functions of Rif1 and Rif2, and allowed the determination of individual contributions of Rif1 and Rif2 to different aspects of telomere homeostasis.

Rif1 as a potential protein phosphatase 1 (PP1) regulator

In *S. cerevisiae*, 129 genes encode Ser/Thr kinases (in humans there are 400 genes), but only about 30 genes (40 in humans) are responsible for Ser/Thr protein phosphatases (www.yeastkinome.org; Manning et al., 2002; Moorhead et al., 2007). This strikingly unbalanced difference in gene number is strategically compensated through a number of different Ser/Thr phosphatase regulatory subunits. In cells, these Ser/Thr phosphatases are multimeric enzymes, assembled from a handful of catalytic subunits and a wide range of regulatory subunits. Despite the high cellular abundance of the protein phosphatase 1 (PP1) catalytic subunit, it does not exist in an isolated form, but is always bound to different helper proteins. In fact, PP1 interactors determine the enzyme subcellular localization, phosphatase activity, and substrate specificity.

The catalytic subunit of PP1 is conserved from yeast to human. However, PP1 regulatory proteins have not been shown to share extensive sequence conservation or structural similarities. To date, all recognition motifs identified for human PP1 are short and degenerate (Hurley et al., 2007; Terrak et al., 2004). A common PP1-binding motif with the consensus sequence [R/K]-X(0,1)-[V/I]-(P)-[F/W], where X is any residue and (P) is any residue except proline, often referred to as the "RVxF" motif, is found in 143 known regulators of PP1 (Egloff et al., 1997; Hendrickx et al., 2009). However, this conserved RVxF motif has a low specificity by itself, as it presents randomly in about fourth quarter of all proteins (Ceulemans and Bollen, 2006). A recent study showed that additional common sequence motifs also play a key role for PP1 binding. For example, six mammalian PP1 interactors contain the "SILK" motifs N-terminal to the consensus RVxF motifs (Hendrickx et al., 2009).

Sequence alignment of 92 Rif1 proteins across species from yeast to human revealed that both the SILK and the RVxF motifs are conserved in all Rif1 orthologs, including *S. cerevisiae* Rif1 (Sreesankar et al., 2012), hinting that Rif1 could be a potential PP1 regulatory protein. Interestingly, while the SILK motifs in all the mammalian PP1 interactors are found N-terminally to their RVxF motifs ("SILK-RVxF"), the SILK motifs of Rif1 in fungi or other single-cell organisms are located C-terminally of the RVxF sequence ("RVxF-SILK"). Further sequence comparison of PP1 interaction proteins in yeast, *Drosophila*, and human showed that the reversed motif location (from "SILK-RVxF" to "RVxF-SILK") is not restricted to Rif1 (Sreesankar et al., 2012). For example, Gip1, the known meiosis-specific regulatory subunit of the PP1 ortholog in *S. cerevisiae*, also contains the SILK motif 76 residues downstream of

its RVxF motif. Importantly, it is known that the essential PP1 binding motif RVxF is located in a flexible loop that adapts a β-strand conformation upon binding to PP1 (Egloff et al., 1997). Indeed, both the RVxF motif (corresponding to KSVAF at residues 114-118) and the SILK motif of scRif1 (corresponding to SILR at residues 146-149) are located in a flexible loop region, N-terminal to the structured armadillo/HEAT repeats rich domain. The presence of conserved PP1 binding motifs, together with their correct localizations in Rif1, offer for a clear indication that Rif1 is a potential PP1 regulator.

It has been demonstrated by different laboratories that a DNA DSB near internal telomeric sequences results in an abridged DNA-damage checkpoint response, which involves the Rad9-Mec1-Rad53 checkpoint pathway (Michelson et al., 2005; Ribeyre and Shore, 2012). However, this abridged arrest is not the result of DNA repair. The presence of telomeric sequences inhibits the phosphorylation of Rad9 and Rad53, and thereby results in an abridged DNA-damage checkpoint response (Michelson et al. 2005). The inhibition of the two central convergence factors (Rad9 and Rad53) in the checkpoint cascade hints that telomere-associated proteins actively impact on the checkpoint phosphorylation cascade. Rif1, as one of the major telomeric proteins, is thus a possible candidate for influencing the checkpoint cascade and affecting cell cycle arrest. Indeed, upon telomere deprotection, Rad53 phosphorylation is clearly detectable once *RIF1* is lost in a *cdc13-1* mutant background, whereas no Rad53 phosphorylation was detectable in the *cdc13-1* mutant alone or in *RIF1* deletion strains (Anbalagan et al., 2011). Additionally, during induced expression of Rif1, the timing of cells escaping from cell cycle arrest correlates well with a progressive reduction in Rad53 phosphorylation and the gradual increase in Rif1 expression levels (Xue et al., 2011). If Rif1 is the "sensor" and phosphorylated DDR factors like Rad53 and Rad9 are the effectors, then the transducer bridging the cascade could be Glc7, the yeast ortholog of PP1. Indeed, a proteome-wide high-throughput mass spectrometry analysis of yeast kinases and phosphatases identified Rif1 as an interactor of Glc7, besides other phosphatases (Cdc14, Ptp1 and Psr2) (Breitkreutz et al., 2010). Glc7 was found to promote replication recovery after HU-induced fork stalling, and shown to participate in cell cycle restart after DSB-induced checkpoint activation. In both events, Glc7 inactivates the hyperphosphorylated Rad53 and γ-H2AX (Bazzi et al., 2010), whose hyperphosphorylations are hallmarks of checkpoint activation upon DNA damage, or stalling of DNA replication. Furthermore, Glc7 counteracts not only phosphorylation of Rad53 and γ-H2AX, but also of Ddc2, Rad9, and Mre11, after DSB-induced checkpoint activation (Bazzi et al., 2010). Rif1 efficiently prevented the recruitment of all these proteins at telomeric DSB (Rebeyre and

Shore, 2012; Xue et al., 2011), implying a functional interaction between Rif1 and Glc7 in the checkpoint response.

Taken together, based on the presence of conserved PP1 motifs in combination with the functional relationship between Glc7 and Rif1, I propose that Rif1 is a Glc7 regulatory protein for the DNA-damage response at telomeres. Future experiments addressing this attractive but untested hypothesis might yield insight into the regulatory role of Rif1 in telomere homeostasis, as well as its role in the DNA-damage response.

Posttranslational control of Rif1 by phosphorylation

Based on the knowledge of the phosphorylation consensus S/T-Q sites of ATM/Tel1 and ATR/MEC1 (Kim et al., 1999), another proteome-wide screen identified that the SQ site of scRif1 Ser1351 is phosphorylated in a Mec1/Tel1-dependent and Rad53-independent manner following methyl methane sulfonate (MMS)-induced DNA damage (Smolka et al., 2007). Three S/T-Q sites in hRif1 (T1518, S1851, and S1542) have also been found to be phosphorylated by ATM/ATR in response to DNA damage (Matsuoka et al., 2007). Interestingly, the same kinases, Mec1 and Tel1, are also responsible for phosphorylating the central effector kinases (Rad53 and Chk1) upon checkpoint activation. These then transfer the arrest signal to downstream proteins (reviewed in Longhese et al., 2006). Is there a correlation between Mec1/Tel1-dependent phosphorylation of Rif1 and the ability of Rif1 to counteract Rad53 phosphorylation?

So far, little is known about the mechanism by which Rif1 prevents the checkpoint response following telomeric DSB, allowing cells to escape the G2/M arrest. One possible simplified hypothesis could be the following: damage to telomeric DNA induces the phosphorylation of Rif1 by Mec1/Tel1, the modification then triggers the assembly of Rif1 and Glc7, and thereby targets the phosphatase specifically to the dissected telomeric DSB. The subsequent dephosphorylation of Rad53 by Glc7 would allow the downstream signal cascade to be inactivated, and thus promote cell cycle restart. Many protein phosphatase regulators are phosphorylated *in vivo*, allowing for cellular signaling to control their functions. Thus, it is conceivable that the assembly of Rif1 and Glc7 is transient and occurs only under certain conditions (upon telomeric DNA damage induced phosphorylation, for example). This would explain why Glc7 has escaped detection in Y2H as a Rif1 interaction partner. However,

further studies are necessary to address whether the Mec1/Tel1 phosphorylation site on Rif1 functions as a regulatory signal for the assembly of Rif1 and Glc7.

Rif1 serves dual purpose at uncapped telomeres

In examining cell cycle-dependent protein associations at telomeres using ChIP, a notably higher level of Rif1 than of Rap1 was found throughout the entire S and G2 phases (Smith et al., 2003). This posed the question: what allows a higher telomeric level of Rif1, given that the Rif1 telomeric localization is thought to be solely Rap1-dependent? In this study, I demonstrated that the N-terminus of Rif1, by itself, has an exceptionally high DNA-binding affinity towards ssDNA and ssDNA/dsDNA junctions, which are both present during transient G-strand extension in late S phase. As a consequence, Rif1 is attracted to telomeric DNA in a Rap1-independnt fashion. Such DNA-binding affinity would be also facilitated once uncapped or damaged telomeres are present. In agreement with this scenario, different experimental systems demonstrated an increased recruitment of Rif1 to dysfunctional telomeres, regardless of its interaction with Rap1. For example: in this study, I demonstrated that the $Rif1_{RBM}$ mutant is not found at natural telomeres, while being efficiently associated at telomeric DSB after HO-cut induction. In the temperature-sensitive *cdc13-1* strain, a Rif1 mutant carrying a deletion of the Rap1 interaction domain (Rif1ΔC) is recruited to uncapped telomeres at the same level as the wildtype Rif1 (Xue et al., 2011). Moreover, in the heteroallelic *tlc1-476A/TLC1* strain, normal telomerase activity is preserved, yet newly synthesized telomeric DNA lacks Rap1 binding sites due to a C-to-A mutation in the RNA template. As a consequence, a 34% decrease in Rap1 telomeric association is observed in the *tlc1-476A/TLC1* strain compared to the wild-type strain. Surprisingly, binding of Rif1 in this strain is increased rather than decreased (Smith et al., 2003).

In addition to the intrinsic DNA-binding property of Rif1, I also presented the remarkable ability of Rif1 to actively outcompete RPA from ssDNA/dsDNA junctions, which resemble uncapped or resected telomeric DNA. Taken together, this result offers a new perspective for Rif1 action in the DNA-damage checkpoint response, as discussed below.

Deletion of *RIF1* in the *cdc13-1* strain leads to a significantly reduced cell viability, whereas no such effect is observed in strains with a dysfunctional Ku complex. This indicates that a lack of *RIF1* causes a severe defect in telomere protection and subsequent checkpoint activation only when Cdc13, but not Ku, function is compromised (Anbalagan et al, 2011).

However, the role of Rif1 in assisting CST-mediated telomere capping cannot be attributed to a suppression of ssDNA formation at telomeres, as several independent reports have shown that *RIF1* deletion has only a very mild effect in preventing ssDNA generation at telomeric DSBs (Ribeyre and Shore, 2012; Xue et al., 2011). Moreover, Rif2 is a more efficient inhibitor of telomere resection through MRX, while *RIF2* deletion does not reduce viability in *cdc13-1/rif2Δ* cells (Anbalagan et al., 2011). Together, these results imply that Rif1 can prevent the DNA-damage response without affecting the level of ssDNA in cells. Xue et al., 2011 therefore suggested that Rif1 affects the ssDNA tolerance threshold *in vivo*. While *RIF1* deletion leads to impaired cell viability at low levels of ssDNA, overexpression of *RIF1* tolerates cell growth at much higher ssDNA levels (Xue et al., 2011). The mechanism underlining this effect remains unclear. The *in vitro* assays in this study show that Rif1 has a DNA-binding affinity comparable to RPA, and that Rif1 is able to effectively outcompete RPA from ssDNA at junctions. In addition, the much higher local concentrations of Rif1, compared to RPA, at telomeres would also favor binding of Rif1 to resected telomeres. Generally, the short telomeric overhang (11-14 nt) is covered by the CST complex in a sequence-specific manner throughout the cell cycle. In case of accidental telomere uncapping or telomeric DSBs, Rif1, as an abundant major double-stranded protein, can efficiently mobilize to damaged telomere sites. Rif1 either occupies the ssDNA generated after telomere uncapping before RPA arrives, or actively outcompetes telomere-bound RPA. In both cases, the presence of Rif1 protects telomeres from associating with DNA-damage response (DDR) factors. Due to the high abundance of RPA, and its extraordinary affinity towards ssDNA on one hand, and the general high DNA-binding affinity of Rif1 for various DNA substrates with different structures *in vitro* on the other hand, Rif1 likely can also physically outcompete other DDR factors (like Rad9, Ddc1) at telomeres.

Taken together, I propose that Rif1 can prevent checkpoint activation at telomeric DSB at two levels. (i) The intrinsic DNA-specific binding activity of Rif1 drives it to dysfunctional telomeres. Through physically outcompeting various DDR factors, Rif1 then dampens further activation of the DNA damage pathway. (ii) Rif1 simultaneously recruits Glc7, which antagonizes the phosphorylation cascade and thereby extinguishes the ongoing DNA-damage response pathway.

Given that the DNA-binding activity of Rif1 is not sequence-dependent, as presented in this study, and that its recruitment to DNA damage sites does not require any interaction with Rap1, the question emerges: would Rif1 associate with non-telomeric DSBs in the genome,

and does it affect the checkpoint response in general? Xue et al. have shown that Rif1 does not influence the DNA damage response outside of telomeres, as it is not recruited to a DSB without having a telomeric sequence nearby (Xue et al., 2011). It is worth noting that these experiments were performed in the wild-type Rif1 strain, where most of the Rif1 proteins are probably trapped by Rap1 at telomeres. The lack of free Rif1 protein in cells could mask its potential role in inhibiting checkpoint activation outside telomeres. Thus, it would be interesting to investigate the response of the Rif1$_{RBM}$ mutant to a DSB in the genome. No constitutive telomeric interaction partner comparable to Rap1 in *S. cerevisiae* has been reported for human Rif1, which may explain the observed accumulation of Rif1 at DNA damage foci in response to both general and telomere-specific chromosomal aberrancies (Silverman et al., 2004; Wang et al., 2009; Xu and Blackburn, 2004). On the other hand, the telomere-specific function of Rif1 in *S. cerevisiae*, instead of a global anti-checkpoint function, is biologically relevant. Telomere capping proteins ensure that natural chromosome ends are not inappropriately processed by the DNA repair machinery, while genome-wide DNA repair pathways are dedicated to capturing all DSBs. Since Rif1 has been demonstrated to elevate the cellular ssDNA tolerance and, therefore, facilitate cell proliferation in the presence of dysfunctional telomeres, a global anti-checkpoint response by Rif1 would exclude cells from undergoing repair. This would lead to an accumulation of unrepaired DNA damage, which is a requisite for chromosomal instability and toxic for long-term cell survival.

A novel DNA-binding activity of Rif1 is demonstrated in this study, which opens new possibilities to consider how Rif1 could impact on telomere maintenance. Therefore, it is important to perform structural studies of the Rif1 N-terminus in complex with DNA in the future. This would allow us to separate Rif1 telomere functions which rely on its DNA-binding activity from its protein-protein interaction.

Evolutional conservation of Rif1

Rif1 was first discovered as a Rap1 interaction partner in *S. cerevisiae* twenty years ago (Hardy et al., 1992). Almost a decade later, a Rif1 ortholog in *S. pombe* and murine Rif1 were identified based on low sequence similarity to scRif1 (Adams and McLaren, 2004; Kanoh and Ishikawa, 2001). Human Rif1 was discovered by two independent groups in parallel through sequence alignment to scRif1 (Silverman et al., 2004; Xu and Blackburn, 2004). Up to now,

functions of Rif1 from yeast, mouse, human, frog, and fruit fly have been reported. A recent bioinformatic study has expanded our knowledge to 92 Rif1 orthologs across species (Sreesankar et al., 2012).

Structural conservation

Rif1 proteins have extraordinarily large primary sequences (scRif1: 1916 residues, hRif1: 2446 residues), with general low protein sequence similarities between fungal Rif1 and that of higher eukaryotes. Together with the overall low sequence conservation, domain fold prediction for Rif1 turns out to be very challenging. As a consequence, it has been reported that Rif1 contains a conserved N-terminal domain of HEAT-like or Armadillo-type fold, with between 8 and 21 repeats (Silverman et al., 2004; Xu et al., 2010). In addition, the C-terminal domain of Rif1 is thought to be conserved only in vertebrates, and is completely absent in yeast (Xu et al., 2010). In this study, I provide the first structure of the $Rif1_{CTD}$ domain, depicting the outmost C-terminal domain of *S. cerevisiae*. However, structure-based sequence alignment of $Rif1_{CTD}$ with the C-terminal domain II of vertebrate Rif1 (Rif1 C-II) demonstrated a striking sequence conservation. This implies that Rif1 does preserve a conserved C-terminal domain. Furthermore, structural and biochemical studies of *S. cerevisiae* $Rif1_{CTD}$ reveal that the function of this domain is oligomerization, which has been also previously suggested for the hRif1 C-terminal domain (Xu et al., 2010). Interestingly, overexpression of hRif1 in budding yeast influenced telomere length regulation in a scRif1-dependent manner, although hRif1 does not contribute to telomere length regulation in vertebrates (Xu and Blackburn, 2004). The authors observed significant telomere elongation (telomeres were 500 bp longer) upon hRif1 overexpression in wildtype *S. cerevisiae* cells. Based on the oligomerization feature of $Rif1_{CTD}$ and the sequence conservation of this domain, I propose an attractive but untested possibility that endogenous scRif1 forms a heterotetramer with hRif1. Due to the lack of Rap1 interaction domains in hRif1, the heterotetramer could titrate scRif1 away from telomeres and lead to the observed telomere elongation phenotype. It is worth noting that the scRif1 C-terminal domain and the hRif1 C-II domain share similar DNA-binding affinities, in addition to their preferential association with forks and HJ DNA substrates (results from this study; Xu et al., 2010). Therefore, I conclude that evidence for Rif1 C-terminus conservation from yeast to human is not only found in their sequences and likely in structures, but also in their DNA-binding activities.

In addition to the Rif1$_{CTD}$ structure, in this study I also provide the first structure of the Rif1 N-terminus. Despite low sequence conservation in the N-terminal domain, all Rif1 proteins are predicted to contain an N-terminal domain that spans ca. 1000 residues comprised of HEAT-like or Armadillo-type folds. The structure of the scRif1 N-terminus reveals an all-helical domain, containing 24 helical repeats. Given that Rif1 has an N-terminus conserved from yeast to human, the novel DNA-binding activity of the scRif1 N-terminus and its associated ability to outcompete RPA from resected telomeric DNA can be extended to higher eukaryotes, including humans. This feature would offer a new perspective on how Rif1 functions in the DNA-damage response in mammals.

Functional conservation

Historically, budding yeast Rif1 was first assigned to a role in telomere length homeostasis, in addition to having a second effect on modulating Sir-mediated silencing through competitive binding to Rap1. In *S. pombe*, besides the spRif1 function in telomere length regulation, spRif1 is more efficiently associated with dysfunctional telomeres, playing a role in the DNA-damage response (Kanoh and Ishikawa 2001). Fission yeast spRif1 was thought to be functionally more similar to vertebrate Rif1. However, human Rif1 does not accumulate at telomeres unless they are dysfunctional. hRif1 has been shown to localize at general DSB foci, and to function in the intra S-phase checkpoint in an ATM- and 53BP1-dependent manner (Silverman et al., 2004; Xu and Blackburn 2004). Murine Rif1 has been demonstrated to be involved in the DNA replication checkpoint. Moreover, it is essential for embryonic development and normal DNA replication (Buonomo et al., 2009). Until recently, there had been little indication of a conserved role for yeast and mammalian Rif1 orthologs.

Nevertheless, recent publications have reported a novel function of budding yeast Rif1 in the DNA-damage checkpoint response by inhibiting the association of various DDR factors with resected telomeres (Xue et al., 2011; Ribeyre and Shore, 2012). The *in vitro* demonstration from this study additionally identified Rif1 as being the first protein to sufficiently outcompete RPA from ssDNA/dsDNA junctions. While yeast Rif1 performs this function regionally at telomeres in addition to its role in telomere maintenance, mammalian Rif1 does not participate in telomere homeostasis, but has extended its function in the general DNA-damage response pathway. This evolutionary change further underscores the close relationship between the DNA-damage response and telomere maintenance. These

results suggest that inhibiting the checkpoint-dependent response to DNA damage (for example DSBs or DNA replication stalling) is a conserved role of yeast and human Rif1.

As discussed above, the presence of PP1 binding motifs across species suggests an additional conserved function of Rif1: being a PP1 regulator in the checkpoint-dependent DNA-damage response. Yeast PP1/Glc7 is involved in checkpoint termination through dephosphorylation of Rad53 and γ-H2AX redundantly to PP4/pph3 (Bazzi et al., 2010). Deletion of *RIF1* in the *cdc13-1* background causes a significant increase in phosphorylated Rad53 (Xue et al., 2011). In accordance with the hypothesis that Rif1 is a conserved PP1 regulator through evolution, human Rif1 was identified in three different screens directly interacting with PP1 (Esteves et al., 2012; Moorhead et al., 2008; Trinkle-Mulcahy et al., 2006). The lack of γ-H2AX has been shown to contribute to recovery from a DSB-induced checkpoint arrest in budding yeast (Keogh et al., 2006). In addition, both PP1 and histone components, including H2AX, are highly conserved. It is possible that dephosphorylation of γ-H2AX also serves as a conserved signal for checkpoint termination in mammals. Consistently, deletion of human Rif1 has been shown to cause a significant increase in γ-H2AX upon DSB induction (Wang et al., 2009), while having no effect on the Chk2 phosphorylation level (Silverman et al., 2004). Deletion of Rif1 in mouse cells without any additional treatment is enough to elicit a low level of phosphorylated Chk1, but not of Chk2 (Buonomo et al., 2009). This finding correlates well with the previous report that mammalian PP1, along with other phosphatases, directly participates in the elimination of γ-H2AX after IR (Nazarov et al., 2003), and is involved in Chk1 but not Chk2 dephosphorylation (Lu et al., 2005).

Modulating Rad51-dependent HR by affecting the heterochromatin state could be another conserved function of Rif1. Budding yeast Rif1 is important in HR-dependent telomere maintenance by promoting Rad51-mediated type I survivors (Teng et al., 2000). It has been shown that Rad51-dependent recombination requires the SWI/SNF chromatin-remodeling complex in the context of the Sir3-bound heterochromatin region (Sinha et al., 2009). These results suggest a functional interaction between Rif1 and the chromatin-remodeling complex in regulating telomeric chromatin. In this study, I presented the molecular basis for Rif1-modulated TPE and *HMR* silencing. Rif1 competes with Sir3 for the same Rap1 RBM-binding groove. However, how this dynamic process is regulated still remains to be elucidated. The indicated functional relation between Rif1 and the chromatin-remodeling complex could offer a new perspective for considering how Rif1 modulates TPE or exerts other telomere functions. Interestingly, deletion of the subunits *IES3* or *ARP8* from the

INO80 complex leads to reduced TPE, and deletion of the same subunits results in moderate telomere elongation (Yu et al., 2007). Murine Rif1 is involved in regulating Rad51-dependent HR when replication forks stall at regions of the genome that are difficult to replicate. For example, the localization of mRif1 was observed at phericentromeric heterochromatin, which consists of a highly repetitive sequence and resembles telomeres (Buonomo et al., 2009). Finally, the hypothesis of Rif1 modulating Rad51-mediated HR can likely be applied to humans, since hRif1 is required for HR-mediated DNA repair, in addition to its role in the S-phase checkpoint (Wang et al., 2009; Silverman et al., 2004). So far, all the identified *RIF1* mutations (two point mutations and a translocation) come exclusively from human breast cancer samples, where defects in HR and DNA repair are common features (Howarth et al., 2008; Sjoblom et al., 2006). Impaired Rad51-mediated HR due to inactivation of Rif1 in breast cancer is of particular interest with regard to BRCA2, a well-characterized breast cancer gene that is implicated in the Rad51 pathway (Sharan et al., 1997; Yuan et al., 1999). To a certain extent, it is possible that mammalian Rif1 influences the DNA damage response like stalled replication forks or DSBs by modulating Rad51-mediated HR.

Comparing results from this work on *S. cerevisiae* Rif1 to those from other model organisms, Rif1 appears to share evolutionary conservation both in its structure and functions. The ability of Rif1 to outcompete DNA-damage response factors at 3' overhangs, being a PP1 regulator, and modulating Rad51-dependent HR could be the common roles of Rif1 from yeast and human. The correlation between Rif1 activities or expression alterations and cancer genesis highlights the importance of understanding the molecular mechanism of Rif1 functions in the DNA-damage response or DNA replication.

References

Adams, I.R., and McLaren, A. (2004). Identification and characterisation of mRif1: a mouse telomere-associated protein highly expressed in germ cells and embryo-derived pluripotent stem cells. Dev Dyn *229*, 733-744.

Adams, P.D., Afonine, P.V., Bunkoczi, G., Chen, V.B., Davis, I.W., Echols, N., Headd, J.J., Hung, L.W., Kapral, G.J., Grosse-Kunstleve, R.W.*, et al.* (2010). PHENIX: a comprehensive Python-based system for macromolecular structure solution. Acta Crystallogr D Biol Crystallogr *66*, 213-221.

Anbalagan, S., Bonetti, D., Lucchini, G., and Longhese, M.P. (2011). Rif1 supports the function of the CST complex in yeast telomere capping. PLoS Genet *7*, e1002024.

Aparicio, O.M., Billington, B.L., and Gottschling, D.E. (1991). Modifiers of position effect are shared between telomeric and silent mating-type loci in S. cerevisiae. Cell *66*, 1279-1287.

Arneric, M., and Lingner, J. (2007). Tel1 kinase and subtelomere-bound Tbf1 mediate preferential elongation of short telomeres by telomerase in yeast. EMBO Rep *8*, 1080-1085.

Atrazhev, A., Zhang, S., and Grosse, F. (1992). Single-stranded DNA binding protein from calf thymus. Purification, properties, and stimulation of the homologous DNA-polymerase-alpha-primase complex. Eur J Biochem *210*, 855-865.

Azzalin, C.M., Reichenbach, P., Khoriauli, L., Giulotto, E., and Lingner, J. (2007). Telomeric repeat containing RNA and RNA surveillance factors at mammalian chromosome ends. Science *318*, 798-801.

Baker, H.V. (1991). GCR1 of Saccharomyces cerevisiae encodes a DNA binding protein whose binding is abolished by mutations in the CTTCC sequence motif. Proc Natl Acad Sci U S A *88*, 9443-9447.

Bazzi, M., Mantiero, D., Trovesi, C., Lucchini, G., and Longhese, M.P. (2010). Dephosphorylation of gamma H2A by Glc7/protein phosphatase 1 promotes recovery from inhibition of DNA replication. Mol Cell Biol *30*, 131-145.

Berthiau, A.S., Yankulov, K., Bah, A., Revardel, E., Luciano, P., Wellinger, R.J., Geli, V., and Gilson, E. (2006). Subtelomeric proteins negatively regulate telomere elongation in budding yeast. Embo J *25*, 846-856.

Bianchi, A., and Shore, D. (2007). Increased association of telomerase with short telomeres in yeast. Genes & Development *21*, 1726-1730.

Biessmann, H., and Mason, J.M. (1997). Telomere maintenance without telomerase. Chromosoma *106*, 63-69.

Blackwell, L.J., and Borowiec, J.A. (1994). Human replication protein A binds single-stranded DNA in two distinct complexes. Mol Cell Biol *14*, 3993-4001.

Bonetti, D., Clerici, M., Manfrini, N., Lucchini, G., and Longhese, M.P. (2010). The MRX complex plays multiple functions in resection of Yku- and Rif2-protected DNA ends. PLoS One *5*, e14142.

Bonetti, D., Martina, M., Clerici, M., Lucchini, G., and Longhese, M.P. (2009). Multiple pathways regulate 3' overhang generation at S. cerevisiae telomeres. Mol Cell *35*, 70-81.

Boule, J.B., Vega, L.R., and Zakian, V.A. (2005). The yeast Pif1p helicase removes telomerase from telomeric DNA. Nature *438*, 57-61.

Boulton, S.J., and Jackson, S.P. (1996). Identification of a Saccharomyces cerevisiae Ku80 homologue: roles in DNA double strand break rejoining and in telomeric maintenance. Nucleic Acids Res *24*, 4639-4648.

Bourns, B.D., Alexander, M.K., Smith, A.M., and Zakian, V.A. (1998). Sir proteins, Rif proteins, and Cdc13p bind Saccharomyces telomeres in vivo. Mol Cell Biol *18*, 5600-5608.

Brand, A.H., Micklem, G., and Nasmyth, K. (1987). A yeast silencer contains sequences that can promote autonomous plasmid replication and transcriptional activation. Cell *51*, 709-719.

Breitkreutz, A., Choi, H., Sharom, J.R., Boucher, L., Neduva, V., Larsen, B., Lin, Z.Y., Breitkreutz, B.J., Stark, C., Liu, G.*, et al.* (2010). A global protein kinase and phosphatase interaction network in yeast. Science *328*, 1043-1046.

Brill, S.J., and Stillman, B. (1991). Replication factor-A from Saccharomyces cerevisiae is encoded by three essential genes coordinately expressed at S phase. Genes & Development *5*, 1589-1600.

Bryan, T.M., Englezou, A., Dalla-Pozza, L., Dunham, M.A., and Reddel, R.R. (1997). Evidence for an alternative mechanism for maintaining telomere length in human tumors and tumor-derived cell lines. Nat Med *3*, 1271-1274.

Bryan, T.M., Englezou, A., Gupta, J., Bacchetti, S., and Reddel, R.R. (1995). Telomere elongation in immortal human cells without detectable telomerase activity. Embo J *14*, 4240-4248.

Buchman, A.R., Lue, N.F., and Kornberg, R.D. (1988). Connections between transcriptional activators, silencers, and telomeres as revealed by functional analysis of a yeast DNA-binding protein. Mol Cell Biol *8*, 5086-5099.

Buck, S.W., and Shore, D. (1995). Action of a RAP1 carboxy-terminal silencing domain reveals an underlying competition between HMR and telomeres in yeast. Genes & Development *9*, 370-384.

Buonomo, S.B., Wu, Y., Ferguson, D., and de Lange, T. (2009). Mammalian Rif1 contributes to replication stress survival and homology-directed repair. J Cell Biol *187*, 385-398.

Ceulemans, H., and Bollen, M. (2006). A tighter RVxF motif makes a finer Sift. Chem Biol *13*, 6-8.

Chan, C.S., and Tye, B.K. (1983). Organization of DNA sequences and replication origins at yeast telomeres. Cell *33*, 563-573.

Chan, S.W., Chang, J., Prescott, J., and Blackburn, E.H. (2001). Altering telomere structure allows telomerase to act in yeast lacking ATM kinases. Curr Biol *11*, 1240-1250.

Chandra, A., Hughes, T.R., Nugent, C.I., and Lundblad, V. (2001). Cdc13 both positively and negatively regulates telomere replication. Genes & Development *15*, 404-414.

Chen, Y., Rai, R., Zhou, Z.R., Kanoh, J., Ribeyre, C., Yang, Y., Zheng, H., Damay, P., Wang, F., Tsujii, H.*, et al.* (2011). A conserved motif within RAP1 has diversified roles in telomere protection and regulation in different organisms. Nat Struct Mol Biol *18*, 213-221.

Chien, C.T., Buck, S., Sternglanz, R., and Shore, D. (1993). Targeting of SIR1 protein establishes transcriptional silencing at HM loci and telomeres in yeast. Cell *75*, 531-541.

Cohn, M., McEachern, M.J., and Blackburn, E.H. (1998). Telomeric sequence diversity within the genus Saccharomyces. Curr Genet *33*, 83-91.

Cong, Y.S., Wright, W.E., and Shay, J.W. (2002). Human telomerase and its regulation. Microbiol Mol Biol Rev *66*, 407-425, table of contents.

Conrad, M.N., Wright, J.H., Wolf, A.J., and Zakian, V.A. (1990). RAP1 protein interacts with yeast telomeres in vivo: overproduction alters telomere structure and decreases chromosome stability. Cell *63*, 739-750.

Conti, E., Uy, M., Leighton, L., Blobel, G., and Kuriyan, J. (1998). Crystallographic analysis of the recognition of a nuclear localization signal by the nuclear import factor karyopherin alpha. Cell *94*, 193-204.

de Lange, T. (2005). Shelterin: the protein complex that shapes and safeguards human telomeres. Genes & Development *19*, 2100-2110.

Dewar, J.M., and Lydall, D. (2010). Pif1- and Exo1-dependent nucleases coordinate checkpoint activation following telomere uncapping. Embo J *29*, 4020-4034.

Dewar, J.M., and Lydall, D. (2012). Similarities and differences between "uncapped" telomeres and DNA double-strand breaks. Chromosoma *121*, 117-130.

DuBois, M.L., Haimberger, Z.W., McIntosh, M.W., and Gottschling, D.E. (2002). A quantitative assay for telomere protection in Saccharomyces cerevisiae. Genetics *161*, 995-1013.

Egloff, M.P., Johnson, D.F., Moorhead, G., Cohen, P.T., Cohen, P., and Barford, D. (1997). Structural basis for the recognition of regulatory subunits by the catalytic subunit of protein phosphatase 1. Embo J *16*, 1876-1887.

Emsley, P., Lohkamp, B., Scott, W.G., and Cowtan, K. (2010). Features and development of Coot. Acta Crystallogr D Biol Crystallogr *66*, 486-501.

Esteves, S.L., Domingues, S.C., da Cruz e Silva, O.A., Fardilha, M., and da Cruz e Silva, E.F. (2012). Protein phosphatase 1alpha interacting proteins in the human brain. Omics *16*, 3-17.

Eugster, A., Lanzuolo, C., Bonneton, M., Luciano, P., Pollice, A., Pulitzer, J.F., Stegberg, E., Berthiau, A.S., Forstemann, K., Corda, Y.*, et al.* (2006). The finger subdomain of yeast telomerase cooperates with Pif1p to limit telomere elongation. Nat Struct Mol Biol *13*, 734-739.

Evans, S.K., and Lundblad, V. (1999). Est1 and Cdc13 as comediators of telomerase access. Science *286*, 117-120.

Fisher, T.S., Taggart, A.K., and Zakian, V.A. (2004). Cell cycle-dependent regulation of yeast telomerase by Ku. Nat Struct Mol Biol *11*, 1198-1205.

Forstemann, K., and Lingner, J. (2001). Molecular basis for telomere repeat divergence in budding yeast. Mol Cell Biol *21*, 7277-7286.

Foster, S.S., Zubko, M.K., Guillard, S., and Lydall, D. (2006). MRX protects telomeric DNA at uncapped telomeres of budding yeast cdc13-1 mutants. DNA Repair (Amst) *5*, 840-851.

Freeman, K., Gwadz, M., and Shore, D. (1995). Molecular and genetic analysis of the toxic effect of RAP1 overexpression in yeast. Genetics *141*, 1253-1262.

Gallardo, F., Laterreur, N., Cusanelli, E., Ouenzar, F., Querido, E., Wellinger, R.J., and Chartrand, P. (2011). Live cell imaging of telomerase RNA dynamics reveals cell cycle-dependent clustering of telomerase at elongating telomeres. Mol Cell *44*, 819-827.

Gao, H., Cervantes, R.B., Mandell, E.K., Otero, J.H., and Lundblad, V. (2007). RPA-like proteins mediate yeast telomere function. Nat Struct Mol Biol *14*, 208-214.

References

Gao, H., Toro, T.B., Paschini, M., Braunstein-Ballew, B., Cervantes, R.B., and Lundblad, V. (2010). Telomerase recruitment in Saccharomyces cerevisiae is not dependent on Tel1-mediated phosphorylation of Cdc13. Genetics *186*, 1147-1159.

Garces, R.G., Gillon, W., and Pai, E.F. (2007). Atomic model of human Rcd-1 reveals an armadillo-like-repeat protein with in vitro nucleic acid binding properties. Protein Sci *16*, 176-188.

Garvik, B., Carson, M., and Hartwell, L. (1995). Single-stranded DNA arising at telomeres in cdc13 mutants may constitute a specific signal for the RAD9 checkpoint. Mol Cell Biol *15*, 6128-6138.

Gilson, E., Roberge, M., Giraldo, R., Rhodes, D., and Gasser, S.M. (1993). Distortion of the DNA double helix by RAP1 at silencers and multiple telomeric binding sites. J Mol Biol *231*, 293-310.

Gottschling, D.E. (1992). Telomere-proximal DNA in Saccharomyces cerevisiae is refractory to methyltransferase activity in vivo. Proc Natl Acad Sci U S A *89*, 4062-4065.

Graham, I.R., Haw, R.A., Spink, K.G., Halden, K.A., and Chambers, A. (1999). In vivo analysis of functional regions within yeast Rap1p. Mol Cell Biol *19*, 7481-7490.

Grandin, N., Damon, C., and Charbonneau, M. (2001). Ten1 functions in telomere end protection and length regulation in association with Stn1 and Cdc13. Embo J *20*, 1173-1183.

Grandin, N., Reed, S.I., and Charbonneau, M. (1997). Stn1, a new Saccharomyces cerevisiae protein, is implicated in telomere size regulation in association with Cdc13. Genes & Development *11*, 512-527.

Gravel, S., Chapman, J.R., Magill, C., and Jackson, S.P. (2008). DNA helicases Sgs1 and BLM promote DNA double-strand break resection. Genes & Development *22*, 2767-2772.

Gravel, S., Larrivee, M., Labrecque, P., and Wellinger, R.J. (1998). Yeast Ku as a regulator of chromosomal DNA end structure. Science *280*, 741-744.

Greenwell, P.W., Kronmal, S.L., Porter, S.E., Gassenhuber, J., Obermaier, B., and Petes, T.D. (1995). TEL1, a gene involved in controlling telomere length in S. cerevisiae, is homologous to the human ataxia telangiectasia gene. Cell *82*, 823-829.

Greider, C.W., and Blackburn, E.H. (1987). The telomere terminal transferase of Tetrahymena is a ribonucleoprotein enzyme with two kinds of primer specificity. Cell *51*, 887-898.

Greider, C.W., and Blackburn, E.H. (1989). A telomeric sequence in the RNA of Tetrahymena telomerase required for telomere repeat synthesis. Nature *337*, 331-337.

Grossi, S., Puglisi, A., Dmitriev, P.V., Lopes, M., and Shore, D. (2004). Pol12, the B subunit of DNA polymerase alpha, functions in both telomere capping and length regulation. Genes & Development *18*, 992-1006.

Haber, J.E. (1998). The many interfaces of Mre11. Cell *95*, 583-586.

Hahn, W.C., Counter, C.M., Lundberg, A.S., Beijersbergen, R.L., Brooks, M.W., and Weinberg, R.A. (1999). Creation of human tumour cells with defined genetic elements. Nature *400*, 464-468.

Hammet, A., Magill, C., Heierhorst, J., and Jackson, S.P. (2007). Rad9 BRCT domain interaction with phosphorylated H2AX regulates the G1 checkpoint in budding yeast. EMBO Rep *8*, 851-857.

Hang, L.E., Liu, X., Cheung, I., Yang, Y., and Zhao, X. (2011). SUMOylation regulates telomere length homeostasis by targeting Cdc13. Nat Struct Mol Biol *18*, 920-926.

Hardy, C.F., Sussel, L., and Shore, D. (1992). A RAP1-interacting protein involved in transcriptional silencing and telomere length regulation. Genes & Development *6*, 801-814.

Harley, C.B., Futcher, A.B., and Greider, C.W. (1990). Telomeres shorten during ageing of human fibroblasts. Nature *345*, 458-460.

Harrison, J.C., and Haber, J.E. (2006). Surviving the breakup: the DNA-damage checkpoint. Annu Rev Genet *40*, 209-235.

Hecht, A., Laroche, T., Strahl-Bolsinger, S., Gasser, S.M., and Grunstein, M. (1995). Histone H3 and H4 N-termini interact with SIR3 and SIR4 proteins: a molecular model for the formation of heterochromatin in yeast. Cell *80*, 583-592.

Hecht, A., Strahl-Bolsinger, S., and Grunstein, M. (1996). Spreading of transcriptional repressor SIR3 from telomeric heterochromatin. Nature *383*, 92-96.

Hendrickx, A., Beullens, M., Ceulemans, H., Den Abt, T., Van Eynde, A., Nicolaescu, E., Lesage, B., and Bollen, M. (2009). Docking motif-guided mapping of the interactome of protein phosphatase-1. Chem Biol *16*, 365-371.

Henry, Y.A., Chambers, A., Tsang, J.S., Kingsman, A.J., and Kingsman, S.M. (1990). Characterisation of the DNA binding domain of the yeast RAP1 protein. Nucleic Acids Res *18*, 2617-2623.

Heyer, W.D., Rao, M.R., Erdile, L.F., Kelly, T.J., and Kolodner, R.D. (1990). An essential Saccharomyces cerevisiae single-stranded DNA binding protein is homologous to the large subunit of human RP-A. Embo J *9*, 2321-2329.

Higashiyama, T., Noutoshi, Y., Fujie, M., and Yamada, T. (1997). Zepp, a LINE-like retrotransposon accumulated in the Chlorella telomeric region. Embo J *16*, 3715-3723.

Hiyama, E., Hiyama, K., Yokoyama, T., Matsuura, Y., Piatyszek, M.A., and Shay, J.W. (1995). Correlating telomerase activity levels with human neuroblastoma outcomes. Nat Med *1*, 249-255.

Howarth, K.D., Blood, K.A., Ng, B.L., Beavis, J.C., Chua, Y., Cooke, S.L., Raby, S., Ichimura, K., Collins, V.P., Carter, N.P.*, et al.* (2008). Array painting reveals a high frequency of balanced translocations in breast cancer cell lines that break in cancer-relevant genes. Oncogene *27*, 3345-3359.

Huber, A.H., Nelson, W.J., and Weis, W.I. (1997). Three-dimensional structure of the armadillo repeat region of beta-catenin. Cell *90*, 871-882.

Hughes, T.R., Weilbaecher, R.G., Walterscheid, M., and Lundblad, V. (2000). Identification of the single-strand telomeric DNA binding domain of the Saccharomyces cerevisiae Cdc13 protein. Proc Natl Acad Sci U S A *97*, 6457-6462.

Hurley, T.D., Yang, J., Zhang, L., Goodwin, K.D., Zou, Q., Cortese, M., Dunker, A.K., and DePaoli-Roach, A.A. (2007). Structural basis for regulation of protein phosphatase 1 by inhibitor-2. J Biol Chem *282*, 28874-28883.

Idrissi, F.Z., Fernandez-Larrea, J.B., and Pina, B. (1998). Structural and functional heterogeneity of Rap1p complexes with telomeric and UASrpg-like DNA sequences. J Mol Biol *284*, 925-935.

Iglesias, N., Redon, S., Pfeiffer, V., Dees, M., Lingner, J., and Luke, B. (2011). Subtelomeric repetitive elements determine TERRA regulation by Rap1/Rif and Rap1/Sir complexes in yeast. EMBO Rep *12*, 587-593.

Ivanov, E.L., Sugawara, N., White, C.I., Fabre, F., and Haber, J.E. (1994). Mutations in XRS2 and RAD50 delay but do not prevent mating-type switching in Saccharomyces cerevisiae. Mol Cell Biol *14*, 3414-3425.

Jia, X., Weinert, T., and Lydall, D. (2004). Mec1 and Rad53 inhibit formation of single-stranded DNA at telomeres of Saccharomyces cerevisiae cdc13-1 mutants. Genetics *166*, 753-764.

Kabsch, W. (2010). Xds. Acta Crystallogr D Biol Crystallogr *66*, 125-132.

Kanoh, J., and Ishikawa, F. (2001). spRap1 and spRif1, recruited to telomeres by Taz1, are essential for telomere function in fission yeast. Curr Biol *11*, 1624-1630.

Keogh, M.C., Kim, J.A., Downey, M., Fillingham, J., Chowdhury, D., Harrison, J.C., Onishi, M., Datta, N., Galicia, S., Emili, A.*, et al.* (2006). A phosphatase complex that dephosphorylates gammaH2AX regulates DNA-damage checkpoint recovery. Nature *439*, 497-501.

Kim, C., Snyder, R.O., and Wold, M.S. (1992). Binding properties of replication protein A from human and yeast cells. Mol Cell Biol *12*, 3050-3059.

Kim, S.T., Lim, D.S., Canman, C.E., and Kastan, M.B. (1999). Substrate specificities and identification of putative substrates of ATM kinase family members. J Biol Chem *274*, 37538-37543.

Konig, P., Giraldo, R., Chapman, L., and Rhodes, D. (1996). The crystal structure of the DNA-binding domain of yeast RAP1 in complex with telomeric DNA. Cell *85*, 125-136.

Kurtz, S., and Shore, D. (1991). RAP1 protein activates and silences transcription of mating-type genes in yeast. Genes & Development *5*, 616-628.

Kyrion, G., Liu, K., Liu, C., and Lustig, A.J. (1993). RAP1 and telomere structure regulate telomere position effects in Saccharomyces cerevisiae. Genes & Development *7*, 1146-1159.

Landry, J., Slama, J.T., and Sternglanz, R. (2000). Role of NAD(+) in the deacetylase activity of the SIR2-like proteins. Biochem Biophys Res Commun *278*, 685-690.

Larrivee, M., LeBel, C., and Wellinger, R.J. (2004). The generation of proper constitutive G-tails on yeast telomeres is dependent on the MRX complex. Genes & Development *18*, 1391-1396.

Laurenson, P., and Rine, J. (1992). Silencers, silencing, and heritable transcriptional states. Microbiol Rev *56*, 543-560.

Lazzaro, F., Sapountzi, V., Granata, M., Pellicioli, A., Vaze, M., Haber, J.E., Plevani, P., Lydall, D., and Muzi-Falconi, M. (2008). Histone methyltransferase Dot1 and Rad9 inhibit single-stranded DNA accumulation at DSBs and uncapped telomeres. Embo J *27*, 1502-1512.

Lee, S.E., Moore, J.K., Holmes, A., Umezu, K., Kolodner, R.D., and Haber, J.E. (1998). Saccharomyces Ku70, mre11/rad50 and RPA proteins regulate adaptation to G2/M arrest after DNA-damage. Cell *94*, 399-409.

Lendvay, T.S., Morris, D.K., Sah, J., Balasubramanian, B., and Lundblad, V. (1996). Senescence mutants of Saccharomyces cerevisiae with a defect in telomere replication identify three additional EST genes. Genetics *144*, 1399-1412.

Levis, R.W., Ganesan, R., Houtchens, K., Tolar, L.A., and Sheen, F.M. (1993). Transposons in place of telomeric repeats at a Drosophila telomere. Cell *75*, 1083-1093.

Levy, D.L., and Blackburn, E.H. (2004). Counting of Rif1p and Rif2p on Saccharomyces cerevisiae telomeres regulates telomere length. Mol Cell Biol *24*, 10857-10867.

Li, S., Makovets, S., Matsuguchi, T., Blethrow, J.D., Shokat, K.M., and Blackburn, E.H. (2009). Cdk1-dependent phosphorylation of Cdc13 coordinates telomere elongation during cell-cycle progression. Cell *136*, 50-61.

Lieb, J.D., Liu, X., Botstein, D., and Brown, P.O. (2001). Promoter-specific binding of Rap1 revealed by genome-wide maps of protein-DNA association. Nat Genet *28*, 327-334.

Lin, J.J., and Zakian, V.A. (1996). The Saccharomyces CDC13 protein is a single-strand TG1-3 telomeric DNA-binding protein in vitro that affects telomere behavior in vivo. Proc Natl Acad Sci U S A *93*, 13760-13765.

Lingner, J., Cech, T.R., Hughes, T.R., and Lundblad, V. (1997a). Three Ever Shorter Telomere (EST) genes are dispensable for in vitro yeast telomerase activity. Proc Natl Acad Sci U S A *94*, 11190-11195.

Lingner, J., Hughes, T.R., Shevchenko, A., Mann, M., Lundblad, V., and Cech, T.R. (1997b). Reverse transcriptase motifs in the catalytic subunit of telomerase. Science *276*, 561-567.

Lisby, M., Barlow, J.H., Burgess, R.C., and Rothstein, R. (2004). Choreography of the DNA-damage response: spatiotemporal relationships among checkpoint and repair proteins. Cell *118*, 699-713.

Longhese, M.P., Mantiero, D., and Clerici, M. (2006). The cellular response to chromosome breakage. Mol Microbiol *60*, 1099-1108.

Lu, X., Nannenga, B., and Donehower, L.A. (2005). PPM1D dephosphorylates Chk1 and p53 and abrogates cell cycle checkpoints. Genes & Development *19*, 1162-1174.

Luciano, P., Coulon, S., Faure, V., Corda, Y., Bos, J., Brill, S.J., Gilson, E., Simon, M.N., and Geli, V. (2012). RPA facilitates telomerase activity at chromosome ends in budding and fission yeasts. Embo J *31*, 2034-2046.

Luke, B., Panza, A., Redon, S., Iglesias, N., Li, Z., and Lingner, J. (2008). The Rat1p 5' to 3' exonuclease degrades telomeric repeat-containing RNA and promotes telomere elongation in Saccharomyces cerevisiae. Mol Cell *32*, 465-477.

Lundblad, V., and Blackburn, E.H. (1993). An alternative pathway for yeast telomere maintenance rescues est1- senescence. Cell *73*, 347-360.

Lundblad, V., and Szostak, J.W. (1989). A mutant with a defect in telomere elongation leads to senescence in yeast. Cell *57*, 633-643.

Lustig, A.J., Kurtz, S., and Shore, D. (1990). Involvement of the silencer and UAS binding protein RAP1 in regulation of telomere length. Science *250*, 549-553.

Lydall, D., and Weinert, T. (1995). Yeast checkpoint genes in DNA-damage processing: implications for repair and arrest. Science *270*, 1488-1491.

Lydeard, J.R., Jain, S., Yamaguchi, M., and Haber, J.E. (2007). Break-induced replication and telomerase-independent telomere maintenance require Pol32. Nature *448*, 820-823.

Mak, H.C., Pillus, L., and Ideker, T. (2009). Dynamic reprogramming of transcription factors to and from the subtelomere. Genome Res *19*, 1014-1025.

Makarov, V.L., Hirose, Y., and Langmore, J.P. (1997). Long G tails at both ends of human chromosomes suggest a C strand degradation mechanism for telomere shortening. Cell *88*, 657-666.

Mallory, J.C., Bashkirov, V.I., Trujillo, K.M., Solinger, J.A., Dominska, M., Sung, P., Heyer, W.D., and Petes, T.D. (2003). Amino acid changes in Xrs2p, Dun1p, and Rfa2p that remove the preferred targets of the ATM family of protein kinases do not affect DNA repair or telomere length in Saccharomyces cerevisiae. DNA Repair (Amst) *2*, 1041-1064.

Manning, G., Whyte, D.B., Martinez, R., Hunter, T., and Sudarsanam, S. (2002). The protein kinase complement of the human genome. Science *298*, 1912-1934.

Marcand, S., Gilson, E., and Shore, D. (1997). A protein-counting mechanism for telomere length regulation in yeast. Science *275*, 986-990.

Marcand, S., Pardo, B., Gratias, A., Cahun, S., and Callebaut, I. (2008). Multiple pathways inhibit NHEJ at telomeres. Genes & Development *22*, 1153-1158.

Maringele, L., and Lydall, D. (2002). EXO1-dependent single-stranded DNA at telomeres activates subsets of DNA-damage and spindle checkpoint pathways in budding yeast yku70Delta mutants. Genes & Development *16*, 1919-1933.

Martina, M., Clerici, M., Baldo, V., Bonetti, D., Lucchini, G., and Longhese, M.P. (2012). A balance between Tel1 and Rif2 activities regulates nucleolytic processing and elongation at telomeres. Mol Cell Biol *32*, 1604-1617.

Matsuoka, S., Ballif, B.A., Smogorzewska, A., McDonald, E.R., 3rd, Hurov, K.E., Luo, J., Bakalarski, C.E., Zhao, Z., Solimini, N., Lerenthal, Y*., et al.* (2007). ATM and ATR substrate analysis reveals extensive protein networks responsive to DNA-damage. Science *316*, 1160-1166.

McCoy, A.J., Grosse-Kunstleve, R.W., Adams, P.D., Winn, M.D., Storoni, L.C., and Read, R.J. (2007). Phaser crystallographic software. J Appl Crystallogr *40*, 658-674.

McEachern, M.J., and Blackburn, E.H. (1996). Cap-prevented recombination between terminal telomeric repeat arrays (telomere CPR) maintains telomeres in Kluyveromyces lactis lacking telomerase. Genes & Development *10*, 1822-1834.

McElligott, R., and Wellinger, R.J. (1997). The terminal DNA structure of mammalian chromosomes. Embo J *16*, 3705-3714.

McGee, J.S., Phillips, J.A., Chan, A., Sabourin, M., Paeschke, K., and Zakian, V.A. (2010). Reduced Rif2 and lack of Mec1 target short telomeres for elongation rather than double-strand break repair. Nat Struct Mol Biol *17*, 1438-1445.

Michelson, R.J., Rosenstein, S., and Weinert, T. (2005). A telomeric repeat sequence adjacent to a DNA double-stranded break produces an anticheckpoint. Genes & Development *19*, 2546-2559.

Mimitou, E.P., and Symington, L.S. (2008). Sae2, Exo1 and Sgs1 collaborate in DNA double-strand break processing. Nature *455*, 770-774.

Mishra, K., and Shore, D. (1999). Yeast Ku protein plays a direct role in telomeric silencing and counteracts inhibition by rif proteins. Curr. Biol. *9*, 1123–1126.

Mitton-Fry, R.M., Anderson, E.M., Hughes, T.R., Lundblad, V., and Wuttke, D.S. (2002). Conserved structure for single-stranded telomeric DNA recognition. Science *296*, 145-147.

Moazed, D., Kistler, A., Axelrod, A., Rine, J., and Johnson, A.D. (1997). Silent information regulator protein complexes in Saccharomyces cerevisiae: a SIR2/SIR4 complex and evidence for a regulatory domain in SIR4 that inhibits its interaction with SIR3. Proc Natl Acad Sci U S A *94*, 2186-2191.

Moorhead, G.B., Trinkle-Mulcahy, L., Nimick, M., De Wever, V., Campbell, D.G., Gourlay, R., Lam, Y.W., and Lamond, A.I. (2008). Displacement affinity chromatography of protein phosphatase one (PP1) complexes. BMC Biochem *9*, 28.

Moorhead, G.B., Trinkle-Mulcahy, L., and Ulke-Lemee, A. (2007). Emerging roles of nuclear protein phosphatases. Nat Rev Mol Cell Biol *8*, 234-244.

Morales, C.P., Holt, S.E., Ouellette, M., Kaur, K.J., Yan, Y., Wilson, K.S., White, M.A., Wright, W.E., and Shay, J.W. (1999). Absence of cancer-associated changes in human fibroblasts immortalized with telomerase. Nat Genet *21*, 115-118.

Morcillo, G., Barettino, D., Carmona, M.J., Carretero, M.T., and Diez, J.L. (1988). Telomeric DNA sequences differentially activated by heat shock in two Chironomus subspecies. Chromosoma *96*, 139-144.

Moretti, P., Freeman, K., Coodly, L., and Shore, D. (1994). Evidence that a complex of SIR proteins interacts with the silencer and telomere-binding protein RAP1. Genes & Development *8*, 2257-2269.

Nakada, D., Matsumoto, K., and Sugimoto, K. (2003). ATM-related Tel1 associates with double-strand breaks through an Xrs2-dependent mechanism. Genes & Development *17*, 1957-1962.

Nakamura, T.M., Morin, G.B., Chapman, K.B., Weinrich, S.L., Andrews, W.H., Lingner, J., Harley, C.B., and Cech, T.R. (1997). Telomerase catalytic subunit homologs from fission yeast and human. Science *277*, 955-959.

Nazarov, I.B., Smirnova, A.N., Krutilina, R.I., Svetlova, M.P., Solovjeva, L.V., Nikiforov, A.A., Oei, S.L., Zalenskaya, I.A., Yau, P.M., Bradbury, E.M.*, et al.* (2003). Dephosphorylation of histone gamma-H2AX during repair of DNA double-strand breaks in mammalian cells and its inhibition by calyculin A. Radiat Res *160*, 309-317.

Ngo, H.P., and Lydall, D. (2010). Survival and growth of yeast without telomere capping by Cdc13 in the absence of Sgs1, Exo1, and Rad9. PLoS Genet *6*, e1001072.

Niida, H., Matsumoto, T., Satoh, H., Shiwa, M., Tokutake, Y., Furuichi, Y., and Shinkai, Y. (1998). Severe growth defect in mouse cells lacking the telomerase RNA component. Nat Genet *19*, 203-206.

Nugent, C.I., Bosco, G., Ross, L.O., Evans, S.K., Salinger, A.P., Moore, J.K., Haber, J.E., and Lundblad, V. (1998). Telomere maintenance is dependent on activities required for end repair of double-strand breaks. Curr Biol *8*, 657-660.

Olovnikov, A.M. (1973). A theory of marginotomy. The incomplete copying of template margin in enzymic synthesis of polynucleotides and biological significance of the phenomenon. J Theor Biol *41*, 181-190.

Ono, Y., Tomita, K., Matsuura, A., Nakagawa, T., Masukata, H., Uritani, M., Ushimaru, T., and Ueno, M. (2003). A novel allele of fission yeast rad11 that causes defects in DNA repair and telomere length regulation. Nucleic Acids Res *31*, 7141-7149.

Palm, W., and de Lange, T. (2008). How shelterin protects mammalian telomeres. Annu Rev Genet *42*, 301-334.

Peifer, M., Berg, S., and Reynolds, A.B. (1994). A repeating amino acid motif shared by proteins with diverse cellular roles. Cell *76*, 789-791.

Pennock, E., Buckley, K., and Lundblad, V. (2001). Cdc13 delivers separate complexes to the telomere for end protection and replication. Cell *104*, 387-396.

Peterson, S.E., Stellwagen, A.E., Diede, S.J., Singer, M.S., Haimberger, Z.W., Johnson, C.O., Tzoneva, M., and Gottschling, D.E. (2001). The function of a stem-loop in telomerase RNA is linked to the DNA repair protein Ku. Nat Genet *27*, 64-67.

Pfingsten, J.S., Goodrich, K.J., Taabazuing, C., Ouenzar, F., Chartrand, P., and Cech, T.R. (2012). Mutually exclusive binding of telomerase RNA and DNA by Ku alters telomerase recruitment model. Cell *148*, 922-932.

Philipova, D., Mullen, J.R., Maniar, H.S., Lu, J., Gu, C., and Brill, S.J. (1996). A hierarchy of SSB protomers in replication protein A. Genes & Development *10*, 2222-2233.

Polotnianka, R.M., Li, J., and Lustig, A.J. (1998). The yeast Ku heterodimer is essential for protection of the telomere against nucleolytic and recombinational activities. Curr Biol *8*, 831-834.

Puglisi, A., Bianchi, A., Lemmens, L., Damay, P., and Shore, D. (2008). Distinct roles for yeast Stn1 in telomere capping and telomerase inhibition. Embo J *27*, 2328-2339.

Qi, H., and Zakian, V.A. (2000). The Saccharomyces telomere-binding protein Cdc13p interacts with both the catalytic subunit of DNA polymerase alpha and the telomerase-associated est1 protein. Genes & Development *14*, 1777-1788.

Ray, A., and Runge, K.W. (1999). The yeast telomere length counting machinery is sensitive to sequences at the telomere-nontelomere junction. Mol Cell Biol *19*, 31-45.

Ribes-Zamora, A., Mihalek, I., Lichtarge, O., and Bertuch, A.A. (2007). Distinct faces of the Ku heterodimer mediate DNA repair and telomeric functions. Nat Struct Mol Biol *14*, 301-307.

Ribeyre, C., and Shore, D. (2012). Anticheckpoint pathways at telomeres in yeast. Nat Struct Mol Biol *19*, 307-313.

Ritchie, K.B., Mallory, J.C., and Petes, T.D. (1999). Interactions of TLC1 (which encodes the RNA subunit of telomerase), TEL1, and MEC1 in regulating telomere length in the yeast Saccharomyces cerevisiae. Mol Cell Biol *19*, 6065-6075.

Ritchie, K.B., and Petes, T.D. (2000). The Mre11p/Rad50p/Xrs2p complex and the Tel1p function in a single pathway for telomere maintenance in yeast. Genetics *155*, 475-479.

Rouse, J., and Jackson, S.P. (2002). Lcd1p recruits Mec1p to DNA lesions in vitro and in vivo. Mol Cell *9*, 857-869.

Rusche, L.N., Kirchmaier, A.L., and Rine, J. (2002). Ordered nucleation and spreading of silenced chromatin in Saccharomyces cerevisiae. Mol Biol Cell *13*, 2207-2222.

Sabourin, M., Tuzon, C.T., and Zakian, V.A. (2007). Telomerase and Tel1p preferentially associate with short telomeres in S. cerevisiae. Mol Cell *27*, 550-561.

Sanchez, Y., Bachant, J., Wang, H., Hu, F., Liu, D., Tetzlaff, M., and Elledge, S.J. (1999). Control of the DNA-damage checkpoint by chk1 and rad53 protein kinases through distinct mechanisms. Science *286*, 1166-1171.

Sandell, L.L., and Zakian, V.A. (1993). Loss of a yeast telomere: arrest, recovery, and chromosome loss. Cell *75*, 729-739.

Scannell, D.R., Frank, A.C., Conant, G.C., Byrne, K.P., Woolfit, M., and Wolfe, K.H. (2007). Independent sorting-out of thousands of duplicated gene pairs in two yeast species descended from a whole-genome duplication. Proc. Natl. Acad. Sci. *104*, 8397–8402.

Schoeftner, S., and Blasco, M.A. (2008). Developmentally regulated transcription of mammalian telomeres by DNA-dependent RNA polymerase II. Nat Cell Biol *10*, 228-236.

Schramke, V., Luciano, P., Brevet, V., Guillot, S., Corda, Y., Longhese, M.P., Gilson, E., and Geli, V. (2004). RPA regulates telomerase action by providing Est1p access to chromosome ends. Nat Genet *36*, 46-54.

Sharan, S.K., Morimatsu, M., Albrecht, U., Lim, D.S., Regel, E., Dinh, C., Sands, A., Eichele, G., Hasty, P., and Bradley, A. (1997). Embryonic lethality and radiation hypersensitivity mediated by Rad51 in mice lacking Brca2. Nature *386*, 804-810.

Sheldrick, G.M. (2008). A short history of SHELX. Acta Crystallogr A *64*, 112-122.

Shore, D. (1994). RAP1: a protean regulator in yeast. Trends Genet *10*, 408-412.

Shore, D., and Nasmyth, K. (1987). Purification and cloning of a DNA binding protein from yeast that binds to both silencer and activator elements. Cell *51*, 721-732.

Silverman, J., Takai, H., Buonomo, S.B., Eisenhaber, F., and de Lange, T. (2004). Human Rif1, ortholog of a yeast telomeric protein, is regulated by ATM and 53BP1 and functions in the S-phase checkpoint. Genes & Development *18*, 2108-2119.

Singer, M.S., and Gottschling, D.E. (1994). TLC1: template RNA component of Saccharomyces cerevisiae telomerase. Science *266*, 404-409.

Singh, J., and Klar, A.J. (1992). Active genes in budding yeast display enhanced in vivo accessibility to foreign DNA methylases: a novel in vivo probe for chromatin structure of yeast. Genes & Development *6*, 186-196.

Sinha, M., Watanabe, S., Johnson, A., Moazed, D., and Peterson, C.L. (2009). Recombinational repair within heterochromatin requires ATP-dependent chromatin remodeling. Cell *138*, 1109-1121.

Sjoblom, T., Jones, S., Wood, L.D., Parsons, D.W., Lin, J., Barber, T.D., Mandelker, D., Leary, R.J., Ptak, J., Silliman, N., *et al.* (2006). The consensus coding sequences of human breast and colorectal cancers. Science *314*, 268-274.

Smith, C.D., Smith, D.L., DeRisi, J.L., and Blackburn, E.H. (2003). Telomeric protein distributions and remodeling through the cell cycle in Saccharomyces cerevisiae. Mol Biol Cell *14*, 556-570.

Smolka, M.B., Albuquerque, C.P., Chen, S.H., and Zhou, H. (2007). Proteome-wide identification of in vivo targets of DNA-damage checkpoint kinases. Proc Natl Acad Sci U S A *104*, 10364-10369.

Solovei, I., Gaginskaya, E.R., and Macgregor, H.C. (1994). The arrangement and transcription of telomere DNA sequences at the ends of lampbrush chromosomes of birds. Chromosome Res *2*, 460-470.

Sreesankar, E., Senthilkumar, R., Bharathi, V., Mishra, R.K., and Mishra, K. (2012). Functional diversification of yeast telomere associated protein, Rif1, in higher eukaryotes. BMC Genomics *13*, 255.

Stellwagen, A.E., Haimberger, Z.W., Veatch, J.R., and Gottschling, D.E. (2003). Ku interacts with telomerase RNA to promote telomere addition at native and broken chromosome ends. Genes & Development *17*, 2384-2395.

Sun, Z., Hsiao, J., Fay, D.S., and Stern, D.F. (1998). Rad53 FHA domain associated with phosphorylated Rad9 in the DNA-damage checkpoint. Science *281*, 272-274.

Sussel, L., and Shore, D. (1991). Separation of transcriptional activation and silencing functions of the RAP1-encoded repressor/activator protein 1: isolation of viable mutants affecting both silencing and telomere length. Proc Natl Acad Sci U S A *88*, 7749-7753.

Taggart, A.K., Teng, S.C., and Zakian, V.A. (2002). Est1p as a cell cycle-regulated activator of telomere-bound telomerase. Science *297*, 1023-1026.

Taylor, H.O., O'Reilly, M., Leslie, A.G., and Rhodes, D. (2000). How the multifunctional yeast Rap1p discriminates between DNA target sites: a crystallographic analysis. J Mol Biol *303*, 693-707.

Teng, S.C., Chang, J., McCowan, B., and Zakian, V.A. (2000). Telomerase-independent lengthening of yeast telomeres occurs by an abrupt Rad50p-dependent, Rif-inhibited recombinational process. Mol Cell *6*, 947-952.

Teng, S.C., and Zakian, V.A. (1999). Telomere-telomere recombination is an efficient bypass pathway for telomere maintenance in Saccharomyces cerevisiae. Mol Cell Biol *19*, 8083-8093.

Terrak, M., Kerff, F., Langsetmo, K., Tao, T., and Dominguez, R. (2004). Structural basis of protein phosphatase 1 regulation. Nature *429*, 780-784.

Terwilliger, T.C. (2000). Maximum-likelihood density modification. Acta Crystallogr D Biol Crystallogr *56*, 965-972.

Trinkle-Mulcahy, L., Andersen, J., Lam, Y.W., Moorhead, G., Mann, M., and Lamond, A.I. (2006). Repo-Man recruits PP1 gamma to chromatin and is essential for cell viability. J Cell Biol *172*, 679-692.

Triolo, T., and Sternglanz, R. (1996). Role of interactions between the origin recognition complex and SIR1 in transcriptional silencing. Nature *381*, 251-253.

Tsai, H.J., Huang, W.H., Li, T.K., Tsai, Y.L., Wu, K.J., Tseng, S.F., and Teng, S.C. (2006). Involvement of topoisomerase III in telomere-telomere recombination. J Biol Chem *281*, 13717-13723.

Tseng, S.F., Lin, J.J., and Teng, S.C. (2006). The telomerase-recruitment domain of the telomere binding protein Cdc13 is regulated by Mec1p/Tel1p-dependent phosphorylation. Nucleic Acids Res *34*, 6327-6336.

Vignais, M.L., Huet, J., Buhler, J.M., and Sentenac, A. (1990). Contacts between the factor TUF and RPG sequences. J Biol Chem *265*, 14669-14674.

Vodenicharov, M.D., Laterreur, N., and Wellinger, R.J. (2010). Telomere capping in non-dividing yeast cells requires Yku and Rap1. Embo J *29*, 3007-3019.

Vodenicharov, M.D., and Wellinger, R.J. (2006). DNA degradation at unprotected telomeres in yeast is regulated by the CDK1 (Cdc28/Clb) cell-cycle kinase. Mol Cell *24*, 127-137.

Vonrhein, C., Blanc, E., Roversi, P., and Bricogne, G. (2007). Automated structure solution with autoSHARP. Methods Mol Biol *364*, 215-230.

Walker, J.R., Corpina, R.A., and Goldberg, J. (2001). Structure of the Ku heterodimer bound to DNA and its implications for double-strand break repair. Nature *412*, 607-614.

Walter, M.F., Bozorgnia, L., Maheshwari, A., and Biessmann, H. (2001). The rate of terminal nucleotide loss from a telomere of the mosquito Anopheles gambiae. Insect Mol Biol *10*, 105-110.

Wang, H., Zhao, A., Chen, L., Zhong, X., Liao, J., Gao, M., Cai, M., Lee, D.H., Li, J., Chowdhury, D*., et al.* (2009). Human RIF1 encodes an anti-apoptotic factor required for DNA repair. Carcinogenesis *30*, 1314-1319.

Wang, S.S., and Zakian, V.A. (1990). Sequencing of Saccharomyces telomeres cloned using T4 DNA polymerase reveals two domains. Mol Cell Biol *10*, 4415-4419.

Watson, J.D. (1972). Origin of concatemeric T7 DNA. Nat New Biol *239*, 197-201.

Watson, J.D., and Crick, F.H. (1953). The structure of DNA. Cold Spring Harb Symp Quant Biol *18*, 123-131.

Wellinger, R.J., Ethier, K., Labrecque, P., and Zakian, V.A. (1996). Evidence for a new step in telomere maintenance. Cell *85*, 423-433.

Wellinger, R.J., Wolf, A.J., and Zakian, V.A. (1993). Origin activation and formation of single-strand TG1-3 tails occur sequentially in late S phase on a yeast linear plasmid. Mol Cell Biol *13*, 4057-4065.

Wotton, D., and Shore, D. (1997). A novel Rap1p-interacting factor, Rif2p, cooperates with Rif1p to regulate telomere length in Saccharomyces cerevisiae. Genes & Development *11*, 748-760.

Wu, Y., and Zakian, V.A. (2011). The telomeric Cdc13 protein interacts directly with the telomerase subunit Est1 to bring it to telomeric DNA ends in vitro. Proc Natl Acad Sci U S A *108*, 20362-20369.

Xu, D., Muniandy, P., Leo, E., Yin, J., Thangavel, S., Shen, X., Ii, M., Agama, K., Guo, R., Fox, D., 3rd*, et al.* (2010). Rif1 provides a new DNA-binding interface for the Bloom syndrome complex to maintain normal replication. Embo J *29*, 3140-3155.

Xu, L., and Blackburn, E.H. (2004). Human Rif1 protein binds aberrant telomeres and aligns along anaphase midzone microtubules. J Cell Biol *167*, 819-830.

Xu, L., Petreaca, R.C., Gasparyan, H.J., Vu, S., and Nugent, C.I. (2009). TEN1 is essential for CDC13-mediated telomere capping. Genetics *183*, 793-810.

Xue, Y., Rushton, M.D., and Maringele, L. (2011). A novel checkpoint and RPA inhibitory pathway regulated by Rif1. PLoS Genet *7*, e1002417.

Yu, E.Y., Steinberg-Neifach, O., Dandjinou, A.T., Kang, F., Morrison, A.J., Shen, X., and Lue, N.F. (2007). Regulation of telomere structure and functions by subunits of the INO80 chromatin remodeling complex. Mol Cell Biol *27*, 5639-5649.

Yuan, S.S., Lee, S.Y., Chen, G., Song, M., Tomlinson, G.E., and Lee, E.Y. (1999). BRCA2 is required for ionizing radiation-induced assembly of Rad51 complex in vivo. Cancer Res *59*, 3547-3551.

Zhang, W., and Durocher, D. (2010). De novo telomere formation is suppressed by the Mec1-dependent inhibition of Cdc13 accumulation at DNA breaks. Genes & Development *24*, 502-515.

Zhou, J., Monson, E.K., Teng, S.C., Schulz, V.P., and Zakian, V.A. (2000). Pif1p helicase, a catalytic inhibitor of telomerase in yeast. Science *289*, 771-774.

Zou, L., and Elledge, S.J. (2003). Sensing DNA-damage through ATRIP recognition of RPA-ssDNA complexes. Science *300*, 1542-1548.

Zubko, M.K., Guillard, S., and Lydall, D. (2004). Exo1 and Rad24 differentially regulate generation of ssDNA at telomeres of Saccharomyces cerevisiae cdc13-1 mutants. Genetics *168*, 103-115.

CURRICULUM VITAE
Tianlai Shi

PERSONAL INFORMATION

Nationality:	Chinese
Place of birth:	Shanghai
Address:	Riehenstrasse 43, 4058 Basel, Switzerland
Contact number:	+41-(0) 76-7215425
Email:	tianlaishi@yahoo.com
Language skills:	Chinese (native), English (fluent), German (fluent)

EDUCATION

10/2008 – present: **PhD (Biochemistry)**

Friedrich Miescher Institute (FMI), Basel, Switzerland.
Group "Structural Tumour Biology", Dr. N. Thomä

Project: *Structure-function studies of budding yeast telomeric complex Rap1-Rif1-Rif2"*

2003 – 2008: **Diplom (Biochemistry)**

University of Hannover, Germany
Subject: biochemistry, immunology and biophysical chemistry

- Grade average: 1.2 ("excellent")

Thesis: *"Characterisation of Protein Kinase MAK-2 in Caenoharbditis elegans"* (01/2008-07/2008)

05/2007 – 10/2007: ERASMUS internship

University of Cambridge, Gurdon Institute of the Wellcome Trust / Cancer Research UK
Group "Small regulatory RNA", Dr. E. Miska

09/2003-09/2005: Vordiplom (Equivalent to a B.S.)

- Grade average: 1.1 ("excellent")

04/2002-02/2003: **High school**

Niedersächsisches Studienkolleg, Hannover, Germany

- Grad average: 1.0 ("excellent"), best graduate of my year

EXPERIENCE

01/2007- 03/2007: Solvay Pharmaceutical Corp., Hannover

- Scientific Co-Worker in the study on kinetics of carbon anhydrase

09/2006-12/2006: Hannover Medical School, Department of Nephrology
(Formerly Max Planck Institute of Experimental Endocrinology)

- Research assistant in signal transduction of PKC/VEGF-receptor in mice cells

02/2005: Hannover Medical School, Department of Biochemistry

- Teaching assistant in biochemistry laboratory course (3 weeks)

04/2004- 08/2006: University of Hannover, Department of Inorganic Chemistry

- Research assistant in conducting laboratory experiments for doctoral students and the professor

HONOURS

2008: Cambridge Overseas Trusts

2007: Socrates-Erasmus scholarship

2006-2008: merit fellowship, Friedrich-Naumann-Foundation

2005-2006: merit fellowship, Cologne-Citizens-Foundation

2005-2006: merit fellowship, Richard-Winter-Foundation

2005: The German Academic Exchange Service "DAAD"-award
For the best foreign student at the University of Hannover

2005: Honeywell Chemicals Co. award
For the best "Vordiplom"-student

2004: Riedel-de-Haën Chemicals Co. award
For the best first-semester-student